ULTRA HIGH SPEED PROTECTIVE RELAYING SCHEMES FOR EHV/UHV TRANSMISSION LINES BASED ON TRAVELLING WAVE PHENOMENA

A Thesis Submitted
in Partial Fulfilment of the Requirements
for the Degree of

DOCTOR OF PHILOSOPHY

By

KANDALA VEDANTA DESIKACHAR

to the

DEPARTMENT OF ELECTRICAL ENGINEERING

INDIAN INSTITUTE OF TECHNOLOGY KANPUR
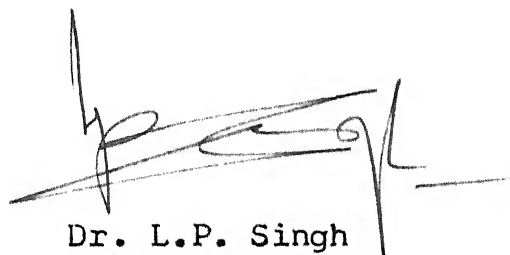
MAY, 1983

EE-1883-D-DES-ULT

DEDICATED   TO

LORD   SRI   VENKATESWARA

CERTIFICATE

It is certified that this work entitled 'Ultra High Speed Protective Relaying Schemes for EHV/UHV Transmission Lines Based on Travelling Wave Phenomena' by Kandala Vedanta Desikachar has been carried out under my supervision and that this work has not been submitted elsewhere for the award of a degree.

Dr. L.P. Singh
Professor
Department of Electrical Engineering
Indian Institute of Technology
Kanpur, India

9-1-1984

ACKNOWLEDGEMENTS

TABLE OF CONTENTS

LIST OF FIGURES

Fig.No.	Caption	Page

LIST OF TABLES

LIST OF PRINCIPAL SYMBOLS

v, V	voltage
i, I	current
R	resistance
G	conductance
L	inductance
C	capacitance
Z	impedance
Z_r	replica impedance
Z_o	surge impedance
Y	admittance
s	transform parameter
J	current source
φ_o	fault initiation angle
ω_o	nominal system angular frequency
ω	angular frequency as well as transform parameter
γ	propagation constant
u	velocity of the travelling waves
φ	Arg (V/I)
φ_r	Arg (Z_r)
ρ	voltage reflection coefficient
t	time
Ω	truncation frequency
σ	sigma factor

U	identity matrix
τ	travel time of the travelling waves
S,Q	voltage and current modal transformation matrices
Re	real part of
Im	imaginary part of
S.E.	sending end of a transmission line
R.E.	receiving end of a transmission line

Subscripts

S,R	sending and receiving-end quantities
pf,PF	prefault component
f	fault generated component
ff	fault generated component at the point of fault
pff	prefault component at the point of fault
m	modal component

Superscripts

a,b,c or A,B,C	phases
1,2,3	modal components
m	modal component
$-$	on the top of a variable indicates its transform value

SYNOPSIS

K.V. DESIKACHAR
Ph.D.
Department of Electrical Engineering
Indian Institute of Technology,Kanpur, INDIA
April, 1983

ULTRA HIGH SPEED PROTECTIVE RELAYING   SCHEMES
FOR EHV/UHV TRANSMISSION LINES
BASED   ON TRAVELLING WAVE PHENOMENA

It has long been recognized that the ultra high speed
(UHS) clearing of faults on a transmission line improves the
transient stability. The fault clearing time being dependent
on the speed of the protective relay as well as that of the
associated circuit breaker, and with the emergence of UHS
circuit breakers, the need for developing UHS protective
relays has become imperative. The realization of UHS
protective relays, for the protection of EHV/UHV transmission
lines, has been possible with the utilization of the
travelling wave characteristics.

The development of protective relays, based on
travelling wave phenomena, is of very recent origin. The
first travelling wave relay was developed by ASEA, Sweden,
and was installed on Bonneville Power Administration's (USA)
500 KV system in April 1976. Since then, a few other

travelling wave relay schemes have been proposed. Almost, all of these schemes necessitate the use of a fast communication channel for internal fault detection. And, two of these schemes possess the fault locating feature, but involve in cumbersome computational procedures. Therefore, there is a need for a travelling wave relay scheme, which can detect an internal fault without the aid of a carrier communication channel so that the operating time of the carrier communication equipment is eliminated, and which incorporates a simple fault locating feature.

For the development of high speed and UHS protective relay schemes, an accurate determination of the complex post-fault current and voltage waveforms is essential. For this purpose, accurate modelling of power systems and fault analysis techniques, suitable for digital simulation, are necessary. So far, only Johns and Aggarwal have developed techniques for the analysis of faulted power systems incorporating exact models of transmission lines. However, these techniques would be applicable, with ease, only to simple power systems.

It is well-known that the use of digital computers, for protective relaying purposes, offers several advantages. The digital distance algorithms, proposed for the protection of transmission lines, require the elimination of d.c. offset and also a wide spectrum of non-fundamental frequency

components with the help of digital filtering and data fitting techniques, a task that entails considerable time delay if adequate accuracy were to be achieved. On the other hand, the adoption of travelling wave techniques, for the digital protection of transmission lines, needs the elimination of only the prefault components, since the travelling wave relays use only the fault-generated components. Also, only a short data window is required, and this leads to a higher speed of fault detection. Very few papers have dealt with the development of digital travelling wave relay algorithms. Takagi et al. have proposed a digital travelling wave relay, which involves in the exchange of quantitative information between the ends of the protected line and consequently, imposes demanding requirements on the communication channel. Hence, there is a need for developing simpler digital travelling wave relay algorithms.

Accordingly, the primary objectives of this thesis have been as given below.

1. To generate a simple mathematical model for a long EHV/UHV transmission line and to develop fault analysis techniques, which are suitable for frequency domain methods of computing transients in complex multinode power systems.

2. To propose a new and simple travelling wave relaying scheme for the protection of EHV/UHV transmission lines.

3. To develop a new travelling wave relaying scheme, for the protection of EHV/UHV transmission lines, which can detect internal faults without the aid of a communication channel and which embodies a simple fault locating technique, and

4. To develop simple digital relaying algorithms, based on travelling wave phenomena.

An outline of the work reported in the thesis is given below.

Chapter 1 presents a brief and critical review of the important literature pertaining to the evolution of distance, travelling-wave and computer relaying schemes developed for the protection of transmission lines.

Chapter 2 starts with an overview of some important aspects of generating the distance relay characteristics, suitable for the protection of long and heavily-loaded EHV/UHV transmission lines, which are given in the literature. The theory, principles of operation, details of hardware implementation and test results of two new distance relaying schemes, fabricated with Integrated Circuits and capable of generating a suitable threshold characteristic, are also presented in this chapter.

In Chapter 3, an accurate frequency-domain Pi model of a transmission line and frequency-domain nodal analysis techniques, suitable for the analysis of faulted multinode power systems, are developed. An important feature of the fault analysis techniques is the use of frequency-domain bus admittance matrix. These form an important basis for the digital simulation of faulted EHV/UHV networks. The utility of the Pi model of the line and the application of the fault analysis techniques are illustrated by computing the voltages and currents at a chosen point in two sample power systems for symmetrical three-phase and also for one phase to ground faults.

Chapter 4 presents the development of, and test results pertaining to, two new travelling wave relay schemes. In one relay scheme, the amplitude comparison of each of the three pairs of modal relay input signals is utilized to distinguish between the reverse and forward faults. Tripping is initiated only if the fault is found to be forward at both the ends of the protected line.

In the other scheme, one relay input signal (for each mode) is used for detecting reverse faults. Under reverse fault conditions, tripping is blocked at the remote end, with the aid of a fast communication channel, and also at the local end directly. By making use of the first, and if necessary the second, time derivatives of the other input

signal, (for each mode), the instants of the first and second incidences of the backward travelling waves, at the relaying point, are determined. The time interval between these two instants is equal to twice the travel time of the waves between the fault and relaying points. Thus, the detection of an internal fault as well as its location are accomplished without the aid of exchanging information between the two ends of the protected line.

Both the relaying schemes cater to all types of faults and hence, can be regarded as a novel type of polyphase relays. The underlying principles of both the schemes are validated by the results obtained through digital simulation studies conducted on sample power systems for various conditions and two types of faults.

In Chapter 5, the algorithms for the digital computer application of the amplitude-comparison and fault-locating relay schemes, described in Chapter 4, are developed. The cycle-to-cycle comparison method, proposed by Mann and Morrison, is adapted as a simple digital filter for removing the prefault components. The viability of these algorithms is tested on the digital computer, DEC System 1090 at I.I.T., Kanpur, by using realistic fault data obtained from the digital simulation of sample power systems. The results of these tests have demonstrated the viability of the

proposed algorithms. In the beginning of the chapter, a brief overview of digital distance algorithms is presented in order to bring out their relative merits and demerits.

The thesis concludes with Chapter 6, wherein a brief review of the work carried out in this thesis and suggestions for further work are given.

CHAPTER 1

INTRODUCTION

1.1 MOTIVATION

The ever increasing size and interconnection of power systems, with resultant complexity, imposes a requirement for protective schemes that are not only highly reliable, sensitive and selective, but extremely fast as well. Being an important link, especially in interconnected systems, a transmission line needs special attention with regards to protection requirements. The sensitivity and selectivity of a protective scheme depend upon the type of the relay unit employed. Of the several electromagnetic measuring units, the induction cup unit proved to be the best in distance relaying applications inasmuch as it was faster (3-5 cycles) and more sensitive compared to the other types of electromechanical relays and also as it was easy to produce any type of conventional threshold characteristics. However, with the advent of solid state devices such as semiconductor diodes and transistors, a trend towards employing them for relays has emerged. The need for a faster measuring unit gave impetus to the development of solid state relays in the initial stages. The amplitude and phase comparison principles, developed in its wake, gave rise to much greater flexibility with which special threshold

characteristics, like conic and quadrilateral, could be
produced. In addition, the static relays possess other
valuable merits such as greater sensitivity, lower burden,
absence of contacts and mechanical motion, and immunity
from vibrations and shocks due to external causes. The
static relays are being used increasingly in recent years,
particularly on EHV/UHV systems where increased sensitivity,
reliability and speed are important. Recent advances, made
in the Integrated Circuit (IC) technology, have resulted in
the availability of cheap and reliable IC chips. Use of ICs,
in place of transistors and several discrete components,
leads to compact, simpler, more reliable and economical
relay units. Research and development work, in the field
of relays employing ICs, is in progress.

The selectivity, provided by a protective relaying
scheme, depends upon the type of threshold characteristics
obtained from the relay units employed in it. The
selectivity, between the internal and external faults, can be
achieved by the use of multi-zone directional distance
relaying schemes with or without carrier-current pilot
schemes. The selectivity, between internal faults and other
abnormal conditions such as power swings etc., depends upon
the shape of the threshold characteristic. So does the
change of balance point due to fault resistance. The
quadrilateral characteristic has proven to be the best in

fulfilling these selectivity requirements to the maximum extent. All these factors gave rise to the motivation for developing new distance relaying schemes, which employ ICs and yield a three-step quadrilateral pickup characteristic.

It has long been recognized that ultra high speed clearance of faults on interties in large power systems very effectively improves the transient stability limit (i.e. the power transfer capability for a given stability limit). The rotational kinetic energy introduced into a power system during a fault is proportional to the square of the fault clearance time. Therefore, high speed clearance of faults close to large sources of generation will reduce the system acceleration more than any other form of dynamic control which can be used only after the system is being accelerated. Also, it has been reported that significant savings in transmission investment would accrue from the application of high speed circuit breakers and relays capable of clearing faults in one-cycle primary time [1]. In the recent years, this aspect of improving transient stability has been drawing the attention of quite a few research engineers and organisations. The fault clearance time depends on the speed of the protective relay as well as on that of the associated circuit breaker. With the emergence of ultra high speed circuit breakers [1,2], the realization of ultra high speed protective relaying schemes

has become imperative.

An accurate computation of the relaying quantities during a very short interval of time immediately following fault occurrence is essential, in order to design and assess the performance of not only analog ultra high speed protective schemes but also digital computer relaying schemes. Modelling of the power system for this purpose needs consideration of the distributed nature of the transmission line parameters, the nature of the earth return, the frequency dependency of the line and earth parameters, and the effect of untransposed lines, on account of the fact that high frequency electromagnetic transients, in the form of travelling waves, exist in the post fault waveforms during this short interval of time. The frequency domain method of computing these electromagnetic transients, although cumbersome, is the most accurate one. So far, as it appears from the recent literature, only one paper [3] has dealt with the frequency domain analysis of power systems, with all these factors taken into consideration. However, the mathematical formulation, developed therein, is suitable only for the analysis of simple power systems. From this, it is evident that there is a need for a more generalized mathematical formulation, which would be suitable for the analysis of complex multinode power systems.

The quest for an ultra high speed protective scheme, which is unaffected by the electromagnetic transients, has culminated in the generation of a novel and strikingly simple relaying concept; a concept that makes use of the characteristics of these very electromagnetic transients, manifested as travelling waves, to distinguish faulted conditions from normal as well as all other abnormal conditions, and internal faults from external faults. Only a few ultra high speed relaying schemes, embodying the above concept, have been proposed so far. However, there is a need to search for better alternative schemes based on this concept and to examine their viability in order to provide the practising engineers with a wider, if not better, choice.

Digital computers have been applied to, or considered for, multifarious off-line and on-line tasks pertaining to power system analysis, control and operation. Their use for the protection of power system equipment is of recent origin, the first serious proposals appearing in late 1960's. Also, very recently, there has been a trend towards employing microprocessors and multiprocessors for power system protection purposes. Uptill now, quite a good number of computer-oriented real-time distance protection algorithms have been developed. Extraction of the fundamental components from the complex post fault waveforms with the aid of analog and/or digital filters is necessary with the above algorithms. But,

use of these filters entails time delay. Contrarily, the
algorithms based on travelling wave relaying concept,
need no elaborate filtering and consequently, they would
be both faster and accurate. It appears that only two
computer relaying schemes, employing an algorithm of the
latter type, have been proposed so far. Therefore, there
is certainly a need for better and simpler algorithms of
this type.

1.2 OBJECTIVES AND SCOPE

The objectives and scope of the work reported in this
thesis have been :

1. To present a critical review of the important solid-
state relaying schemes reported so far, to explore the
ability of the solid-state circuitry, in terms of simplicity,
reliability and flexibility, to generate any desired complex
pickup characteristics and to develop a faster and more
reliable digital relay which uses digital ICs, and which
generates a multizone quadrilateral pickup characteristic,
acknowledged to be the best for the protection of long and
heavily loaded EHV/UHV transmission lines.

2. To develop a simple mathematical model for a long
EHV/UHV transmission line and techniques of fault analysis
based on nodal formulation which are suitable for frequency
domain methods of computing transients in complex multinode

power systems.

3.   To present an overview of the digital computer relay-
ing algorithms developed uptill now as well as the philosophy
behind the existing and proposed new algorithms and
schemes.

4.   To develop new relaying principles based on travelling
wave phenomena, and computer relaying algorithms based on
these relaying principles;   to develop a travelling wave
relay which incorporates the fault locating capability and
which dispenses with the need for carrier or microwave
communication channels in the event of internal faults so
that the fault detection time is reduced.

1.3 LITERATURE SURVEY

In the early days of electric power transmission, over-
current relays were mostly used for the protection of
transmission lines. However, as higher and higher trans-
mission voltages, necessitated by the increasing size of the
power systems, were employed, these o.c. relays were found
unsuitable because of the following reasons. The balance
point of an overcurrent relay shifts with the type of fault,
and also with variation in generating capacity. There may
be a wrong tripping in the event of a fault on a parallel
line under certain conditions [4]. Also, they can be
used only on systems where the minimum fault current

exceeds the maximum load current. However, the directional
overcurrent relays are still used for ground fault relaying
at subtransmission and transmission levels [5]. On account
of the above-mentioned problems associated with the overcurrent
relays, the distance relays have been developed. In view of
the necessity for ultra high speed fault clearance for the
attainment of improved transient stability, protective
relays, whose operation is based upon the travelling wave
phenomena, are being developed. A brief and critical review
of the important literature pertaining to the evolution and
development of distance and travelling-wave relays and
computer relaying schemes for the protection of transmission
lines, is presented in the following sections.

1.3.1 Distance Relays

1.3.1.1 Electromechanical Relays

In the evolution of relays for the protection of trans-
mission lines, the electromechanical relays were developed
first, and in that of distance relays, the plain impedance
relay was the first one that was conceived and developed.
In 1923, Crichton [6] reported about an impedance relay which
employed an induction disc actuating structure and operated
in a time proportional to the impedance between the relay
and the fault point. In 1928, McLaughlin and Erickson [7]
reported about a directional impedance-time relay built with

an induction disc actuating structure. They presented
the constructional details, and described the principle
of operation, methods of obtaining proper voltage for the
restraining elements and methods of compensating for the
voltage drop in power transformers and for the secondary
neutral shift. In 1930, Crichton [8] reported about a high
speed impedance relay, the high speed of operation having
been obtained with a balanced beam structure. He described
a three-step directional impedance relaying scheme and
discussed about the effect of fault resistance on the
operating speed of the relay. The development of a high
speed impedance relay with a balanced beam structure was
also reported by Goldsborough and Lewis [9]. In 1944,
Goldsborough [10] reported about a modified impedance relay
built with a balanced beam structure and described how a
circular pickup characteristic of any desired radius and
with any desired location of the centre could be obtained with
a voltage proportional to the system current added to or sub-
tracted from the relay voltage and with a current proportional
to the system voltage added to or subtracted from the relay
current.

In 1928, Warrington [4] designed an induction disc type
reactance relay for an American Company. In 1931, George [11]
presented the performance records of normal speed as well as
high speed reactance relays installed at two hydroplants of

Tennesse Electric Power Company of America, and reported
that, although they had performed satisfactorily on long
lines with wide variations in short circuit conditions,
certain difficulties had arisen on interconnectors operating
near stability limit. In 1933, Warrington [12] reported
about a high speed reactance relay which was built with a
four-pole induction cup actuating structure carrying current
coils on one pair of opposite poles, and current and
voltage coils on each of other poles. Dewey and Mc Glynn [13]
as well as Warren C. New [14] have reported about three-step
directional reactance relaying schemes with zones 1 and 2
protected by the combination of reactance and mho units, and
zone 3, by mho units. Both the reactance and mho relays
had employed 4-pole induction cup structures.

Though the mho relay was first used in 1933 as the
directional unit for an early type reactance relay [12], its
independent use for the protection of heavily loaded and long
transmission lines was first recommended in 1943 by Warrington
[15] with its merits lucidly brought out. In 1944, Cordrey
and Warrington [16] described its actual use in a carrier
current scheme. Later, Hutchinson [17] described its use in
a three-step distance relaying scheme in which protection for
zones 1 and 2 was provided by normal mho units, and for
zone 3, by an offset mho unit. He presented also the test
results in the form of transient overreach of zone 1 unit,

and the operating time of each unit as a function of the ratio of the impedance to fault to the setting impedance.

In 1962, Skuderna [18] put forth the mathematical development of how offset conic and limacon characteristics could be produced with a four-pole induction cup structure. He presented also detailed circuitry needed to obtain the various winding inputs and described the setting procedure with a numerical example for getting an offset elliptical characteristic.

1.3.1.2 Electronic Relays

In 1934, Wideröe [19] presented electronic circuits, incorporating thyratron tubes, which were equivalent of many electromechanical relays in use at that time. In 1948, Mac Pherson and Warrington [20] described an electronic mho relay wherein instantaneous values of voltage and current inputs to the relay were compared at the instant of voltage input maximum. Barnes and Mac Pherson [21] recounted the field experience of this relay and reported that it was not adversely affected by unknown system or other disturbances. In 1949, Loving [22] published electronic circuits for many common protective functions, and presented experimental results. In 1954, Bergseth published a paper [23] describing an electronic directional distance relay which was insensitive to moderate waveform distortion and which was operated by comparing the phase angle between two derived voltages. Hodges

and Mac Pherson [24], Price et al. [25] and Seely and Koss [26] described the operating principles and performance of an all-electronic one-cycle carrier relaying system. However, with the advent of solid-state devices, the development of these relays has ceased.

1.3.1.3 Solid-State Relays

The first serious proposal, for the employment of transistorised circuits for power system protective relaying, came from Adamson and Wedepohl [27,28] in 1956. In the first paper [27], they presented the mathematical development of determining the inputs necessary to obtain the directional, ohm, offset impedance and mho characteristics with a two-input phase comparator, detailed circuitry of the prototype relays built by them, and dynamic test results for a mho relay. In the second [28], they presented the dual phase comparator technique with which the transient overreach, present in the coincidence-block average comparators, could be reduced, and substantiated its effectiveness with the results of dynamic tests conducted on a prototype mho relay incorporating this technique. In 1959, Adamson and Talkhan [29] described a phase-comparison carrier relaying scheme, that employed transistors, and presented the test results. In 1960, Dewey and Hodges [30] described a transistorised phase - comparison carrier relaying scheme in which transistor circuits were used for level detector, comparer and squaring and

tripping amplifiers. Dewey et al. [31] and Caleca et al.[32] described, in two companion papers, the design principles, typical circuits, application and test results of a directional-comparison pilot relaying scheme which employed solid-state mho distance units with offset impedance supervision for phase faults and which employed the block-spike phase comparison technique for producing the distance relay. characteristics. Hahn [33] described a three-step solid-state directional impedance relaying scheme employing transistors and printed circuit boards, and the coincidence-block average phase comparison technique.

In 1965, Wedepohl [34] reported about a polarised mho relay which surmounted the problem of nonoperation for close-in faults. In the same year, Humpage and Sabberwal [35] presented a mathematical basis for two-input phase comparators with angular limits of comparison other than $\pm 90^{\circ}$ and gave block schematic diagrams of symmetrical and unsymmetrical comparators, the inputs necessary for obtaining composite. characteristics and a plural comparator arrangement that generates a quadrilateral characteristic. In 1966, Parthasarathy [36,37] reported about a static three-zone quadrilateral distance relay incorporating transistor circuits for measuring, discriminating and logic functions, and employing the multi-signal block-spike phase comparison technique. The papers include the results of dynamic tests

conducted on prototype (laboratory model) relays. In the same year, Hans Hoel et al. [38] described how reduced-size third zone pickup characteristics could be produced by multi-signal phase comparison.

In 1967, Anil Kumar and Parthasarathy [39] presented a mathematical basis for multi-input sine phase comparators and synthesised the inputs required to obtain conventional as well as quadrilateral characteristics. In the same year, Anil Kumar et al. [40] reported about a three-step transistorised quadrilateral distance relay using the same inputs as in [36] and discussed the modifications necessary for using it with carrier-blocking and carrier-tripping schemes. In 1968, the optimum dynamic design aspects of static relay comparators were presented in a paper by Jackson et al. [41]. In the same year, Mc Laren [42] developed a sampling technique which permits a comparison of instantaneous values of relay inputs at different instants of time and dispenses with the need for phase-shifting and mixing circuits. The theory and design of a solid-state high speed phase comparison relay based on the zero-crossings of the line currents were published in two companion papers by Robertson and Norman Meikle [43,44]. Vitanov [45] reported about the production of quadrilateral characteristics with transistorised circuitry.

In 1970, Ramamoorty and Wani [46] reported about the fabrication and test results of a solid-state quadrilateral

distance relay. In 1970, Anil Kumar [47] published a paper describing a new sampling circuit that employed a combination of ferrite cores and semiconductor components and also a new technique that needed sampling of only one input, the other being converted to a d.c. level. The advantage of this new technique is that it does not require synchronisation of input signals. Khincha et al. [48] put forth a new amplitude comparison technique in which full-wave rectified, but unsmoothed, voltage and current combinations are compared at every instant during each half cycle, and derived the inputs necessary for generating conic and quadrilateral characteristics. They extended the above principle [49] to produce parallelogram, directional parallelogram and directional quadrilateral characteristics. Anil Kumar [50] described the production of quadrilateral characteristics with phase sequence detectors. He presented two types of phase sequence detectors; one uses ferrite core logic and the other, semiconductor flip-flops.

In 1972, Johns [51] presented a generalised phase comparison technique in which a comparison period of fixed duration and related to either positive-going or negative-going zero crossing is assigned to each relaying signal and the coincidence of these comparison periods of all the relaying signals provides the criterion for the relay operation. He described how settings for two-input comparators could be determined. He reported [52] extension of this

technique to multi-input comparators and described the
procedure to determine the settings, with an example
worked out for a 4-input comparator. He also described
how a quadrilateral characteristic could be generated with a
3-input comparator employing this technique. In 1973, he
[53] presented variable characteristic generalised techniques
for distance protection. These techniques involve in varying
the resistive reach of a replica impedance by adding an extra
current-derived component to the appropriate relay input.
This component is a linear function of all the line currents
and is arranged to be zero under all balanced conditions and
finite during unbalanced faults. He described how to get a
variable quadrilateral characteristic whose area will be
minimal under power swings and heavy load conditions. He
reported also [54,55] the extension of this principle to the
distance protection of double circuit lines and lines with
selective-pole autoreclosure facility.

In 1974, Jackson [56] presented a comparator with auto-
matically variable angular limits of phase comparison. The
automatic variation is accomplished by modifying the integra-
tor response during the anticoincidence period with pulses of
widths corresponding to anticoincidence periods. In this way,
shaped pickup characteristics, narrow along the power swing
locus, can be obtained. In the same year, Paithankar and
Ingole [57] reported the production of quadrilateral

characteristics with multi-input amplitude comparators incorporating new techniques. In 1979, Ramamoorty and Lall presented a paper [58] describing a versatile phase comparator that was built with digital circuits and which employed coincidence-block average principle. Another novel feature of this comparator is a digital up/down counter which does the same job as the capacitor in the integrating circuit of a conventional comparator. Also, asymmetrical angular limits of comparison can easily be obtained by having clocks of different frequencies during coincidence and anticoincidence periods.

In 1980, Parthasarathy et al. [59] presented a new distance relay with an adaptive pickup characteristic which has a narrow tripping area during power swing conditions, and which automatically expands to large area during unbalanced faults. The adaptive feature is realised by controlling the angular limits of phase comparison with negative or zero sequence voltages generated during unbalanced faults. The results of the dynamic tests conducted on a polarised mho relay employing this technique were also presented. In the same year, Ramamoorty and Lall [60] reported about a multi-input phase comparator using digital ICs. A 3-input comparator, yielding a quadrilateral characteristic and possessing the capability of generating any slope for the sides of the characteristic, was described in the paper. A solid-state

distance relay, employing an operational amplifier chip as an amplitude comparator and producing elliptical characteristic, was developed by Ramamoorty et al. [61]. Paithankar and Thoke [62] reported about an earth-fault quadrilateral distance relay, capable of producing an adaptable swivelling characteristic and suitable for the protection of double end infeed lines. In the same year, Weller et al. [63] put forth a new technique of phase comparison. The relay inputs are squarewaved, treated as binary and AND compounded. The states of the AND gate output will have a particular sequence over the operating angular range, which is entirely different from that over the blocking range. With the aid of a counter, the tripping sequence is determined. In 1982, Kellog et al. [64] presented a relaying scheme using digital circuits and CMOS logic. The phase comparator described by them can be used as either sine or cosine comparator. It can also be used, with minor modifications, as a polyphase distance relay.

Bräten and Hoël [65], Ryder et al. [66] and Gimoyan [67] described protective relays employing rectifier bridge phase comparators in conjunction with a sensitive output relay, usually of the polarised moving iron or moving coil type.

1.3.2 Travelling Wave Relays

For the purpose of designing, developing and assessing the performance of ultra high speed relays, especially those based on travelling wave phenomena, fault analysis of multinode power

systems, with such factors as the distributed and untransposed
nature of transmission lines and the frequency dependency of
the line and earth parameters taken into consideration and
suitable for digital simulation, is essential. Humpage
et al. [68] reported a digital simulation of detailed models
of synchronous generators, transmission lines, and power and
protective transformers. Kothari et al. described modelling
techniques for simulating the primary system and the trans-
ducers in one paper [69], and digital simulation of fault
currents and voltages in the other [70]. Johns and Aggarwal
[3] described the digital simulation of faulted lines with all
the factors mentioned above, taken into consideration. They
have also described fault analysis techniques.

Vitins [71] described a novel transmission line protective
scheme based on the travelling wave phenomena. Fault location
is identified as fault detection and the location of the fault
is determined by a time delay equal to twice the travel time of
travelling waves between the fault and relaying points. A
correlation technique is developed to determine this time delay.
Yee and Esztergalyos [72], Chamia and Liberman [73],
Esztergalyos et al. [74], Matele [75] and Carter [76] reported
about the development, design, application and operational
experience of an ultra high speed relaying scheme based on
travelling wave theory. This relaying scheme utilises the
deviations in the relaying-point voltages and currents

occurring as a result of a fault and compares the polarities of the voltage and current deviations to determine as to whether the fault is ahead of or behind the relaying point. By exchanging information between the ends through a communication channel, tripping is initiated in the event of an internal fault. Johns [77], and Johns and Aggarwal [78] described an ultra high speed relaying scheme in which the direction to fault is determined by the sequence in which relay input signals, related to the modal components of the relaying-point voltage and current deviations, exceed a preset level. This scheme is designed to operate in conjunction with a carrier communication channel and in a carrier blocking mode.

Dommel and Michels [79] described a new method of fault detection which utilizes travelling wave voltage and current transients. A discriminant is derived and used to distinguish internal faults from external faults. Takagi et al. [80,81] and Akimoto et al. [82,83] presented the theory, sensitivity analysis and test results of a differential relay scheme based on travelling wave theory. They defined a discriminant which is a function of surge impedance of the line and instantaneous terminal voltages and currents. The discriminant is zero for normal conditions and external faults, and finite for internal faults. Ramamoorty and Verma [84] described a relaying principle based on travelling wave

phenomena. A discriminant, which is a function of backward-wave voltage and current deviations and a setting resistance, is defined. If this discriminant exceeds a preset value, which is the case for internal faults, tripping is initiated. Vitins [85] defined two wave signals, formed from the current and voltage deviations, and described the determination of the direction to a fault by detecting which of these two signals first reaches a threshold constant. He presented a geometric approach for this purpose.

1.3.3 Digital Computer Relaying

The use of digital computers and microprocessors for protective relaying purposes has been engaging the attention of research and practising engineers since late 1960s. The first serious proposals for using digital computers came from Rockefeller [86]. The algorithms proposed till now can be classified into two categories; distance relay algorithms and travelling wave relay algorithms. The distance relay algorithms involve in the determination of the fundamental-frequency impedance to fault from the fundamental components of voltages and currents which are extracted from the complex post-fault waveforms by analogue and/or digital filters. Slemon et al. [87] described the determination of the fundamental components in phasor form from an ensemble of samples collected over one full cycle by using Fourier Analysis techniques. Ramamoorty [88] described the determination of the impedance from the peak

values of voltage and current and phase angle between them and from the fundamental phasor components of voltage and current, both these methods requiring samples collected over one full cycle. Mann and Morrison [89] described the predictive calculation of the peak values of and the phase angle between the voltage and current from a much fewer number of samples and their time derivatives and also discussed, in another paper [90], the relaying of a three-phase line using this technique. The predictive technique was presented also by Gilcrest et al. [91] who proposed the use of first and second time derivatives of the samples, and by Gilbert and Shovlin [92] who proposed the use of samples and the sampling interval. Carr and Jackson [93] described the use of two digital orthogonal notch filters with sine characteristics to determine the magnitude and phase angle of the fundamental components from samples taken at four equally spaced time intervals over the fundamental period, and the use of an analog low pass RC filter with a cutoff frequency of 85 Hz to band-limit the voltage and current signals prior to sampling.

The use of Fourier Analysis techniques for extracting the fundamental components in phasor form has been reported by several authors, besides Slemon et al. [87] and Ramamoorty [88]. Hope and Umamaheswaran [94] described the use of odd and even square waves, besides sine and cosine functions, for the

extraction of the fundamental components. Hope et al. [95] and Tirupathaiah et al. [96] have also employed Fourier Analysis techniques with one cycle data window, whilst Phadke et al. [97,98] and Wiszniewski [99] have employed these techniques with half a cycle data window. Horton [100] described the use of Walsh functions to extract the fundamental components.

Quite a few authors have proposed the modelling of the line by a series R-L circuit, and solving the resultant differential equations to obtain the values of R and L between the relaying and fault points. Mc Innes and Morrison [101] proposed the integration of the differential equations over two successive sampling intervals to generate adequate number of equations to solve for R and L, and used the trapezoidal rule to evaluate the integrals. Poncelet [102], and Bornard and Bastide [103] treated the deficiency in this modelling as an error and solved for R and L subject to the minimisation of the sum of squares of these errors over a certain number of successive sampling intervals. Smolinski [104] modelled the line by a single Pi section and solved the resultant differential equations by replacing them by finite differences and using four sample sets to obtain the values of R and L. Ranjbar and Cory [105] presented a novel digital harmonic filter in which the integration is carried out over a certain number of overlapping subintervals with

preset limits while the above differential equations are being solved by the numerical integration method. In this way, any unwanted harmonics and their multiples can be eliminated. Sakaguchi and Uemura [106] defined the inverse Laplace transform of 1/(sL+R) as a weighting function and discussed a numerical solution technique to determine it. They showed that the weighting function is greater than zero only for a fault ahead of the relaying point.

Sachdev and Baribeau [107] assumed the post-fault waveform to be comprising of a decaying d.c. offset, the fundamental and a certain number of harmonics and determined the unknown parameters of the fundamental by applying the least square error method. After expanding the exponential term associated with the d.c. offset in a series, they considered three terms of this series and only the third harmonic for elimination. Following the same method, Luckett et al. [108] considered the d.c. offset and two harmonics for elimination, whilst Brooks [109] represented the complex post-fault waveform by a constant plus the fundamental frequency term. Johns and Martin [110] presented a finite transform method by which the fundamental frequency impedance can be determined by carrying out the filtering process in the frequency domain. Girgis and Brown [111, 112] developed two-state and three-state Kalman filters to extract the fundamental voltage and current phasors respectively, and reported that

the error involved is less than 1 percent after half a
cycle. Sanderson and Wright [113] have dealt with series
compensated lines. They modelled the line by a series
RLC circuit and solved the resultant differential
equations by integrating them over three successive sampling
intervals.

Vitin's correlation method based on travelling wave
theory [71] is suitable for computer application also.
Takagi and Yamakosi [114] described the microcomputer
application of the differential current relay [80-83] whose
operation is based on the travelling wave theory.

1.4 SUMMARY OF THE WORK REPORTED IN THIS THESIS

The summary, of the work carried out and reported in
this thesis, is presented below chapterwise.

Chapter Two starts with an overview of some important
aspects of generating the distance relay characteristics for
protection of long and heavily-loaded EHV/UHV transmission
lines. Later, two new distance relays, capable of generating
a three-step quadrilateral pickup characteristic, are
developed. Each proposed relay consists of a forward fault
detector, which generates an open quadrilateral pickup cha-
racteristic, and a zone detector, which closes the open
quadrilateral characteristic at the appropriate zonal reach,
depending upon the location of the fault.

Both the relays are fabricated with the ICs. The first relay scheme demonstrates that the use of ICs greatly simplifies the circuitry, although the input signals used are the same as given in reference [36]. The second relay has been fabricated only with the digital ICs, a feature that enhances the accuracy of measurement. Also, its forward fault detector uses only three input signals, which results in enhanced reliability. Although, the manner, in which the open quadrilateral characteristic is produced in this scheme, is somewhat similar to that described in reference [60], the modifications incorporated herein render the measurement of coincidence period to be completed in exactly half a cycle as against more than half a cycle in their scheme. The relays have been fabricated and tested in the laboratory.

In Chapter Three, the development of an equivalent Pi circuit for an untransposed transmission line, without disregarding the effect of a host of frequencies present in the complex post-fault waveforms, is described. This model makes the frequency-domain nodal analysis of multinode power systems easy. Also, a detailed fault analysis of multinode power system networks, based on nodal formulation and suitable for frequency domain methods, is presented in the same chapter. This analysis forms an important basis for the digital simulation of faulted e.h.v. networks. The utility of the Pi model

of the line developed, and the application of the fault analysis presented, are illustrated by determining the voltages and currents at a chosen point in two sample power systems for symmetrical three phase and single line to ground faults. For this purpose, computer programmes are developed for determining the frequency-dependent parameters of the transmission line, and for determining the time domain values from the frequency domain values through modified Fourier transform techniques. In this connection, it is shown that, the application of fast Fourier transform techniques in the computation of power system transients provides only marginal relief in terms of computational speed.

In Chapter Four, two new ultra high speed relaying schemes, utilizing the characteristics of the travelling waves generated immediately after the occurrence of a fault and for the protection of three-phase transmission lines, are developed. In one scheme, amplitude comparison of each of the three pairs of relay inputs, formed from the modal components of the fault-generated components of the relaying-point phase voltages and line currents, yields positive information as to whether the fault is ahead of or behind the relaying point. Exchanging information between the two ends of the line through a fast communication channel, tripping is initiated if the fault is found to be ahead of the

relaying points at both the ends of the line. In the second scheme also, two relay inputs for each mode of propagation are used. But, in this scheme, the magnitude of one input is used only to determine whether the fault is behind the relaying point. If the fault is behind, operation of the relay scheme is blocked, directly at the local end, and through a communication channel, at the remote end. The first and, if necessary the second time derivatives of the other input are used not only to detect an internal fault, but also to determine its distance from the relaying point. The reflection properties of the travelling waves are made use of, and no communication between the ends is necessary, in the detection and location of an internal fault. Both the schemes cater to all types of faults and therefore, can be regarded as polyphase relays. The underlying principles, of both the relaying schemes, are validated by the results obtained through the digital simulation studies conducted on sample power systems for various conditions of faults.

Chapter Five commences with a brief overview of digital distance algorithms in order to bring out their merits and demerits. Next, new algorithms for the digital computer application of the amplitude-comparison and fault-locating relay schemes, described in Chapter 4, are developed. The cycle-to-cycle comparison method, proposed by Mann and Morrison [90], is adapted as a simple digital filter for eliminating the

prefault components. The viability of these algorithms is tested on the digital computer, DEC System 1090 at I.I.T., Kanpur. For this purpose, realistic fault data, obtained from the digital simulation of sample power systems, are used. The results of these tests have demonstrated the viability of the proposed algorithms.

Finally, the thesis concludes with Chapter 6, which highlights briefly the work reported in this thesis and also discusses the future scope of work in this field.

CHAPTER 2

PROTECTION SCHEMES FOR EHV/UHV TRANSMISSION LINES
USING SOLID STATE COMPONENTS

2.1 INTRODUCTION

The rapid growth in the size and complexity of
electrical power systems has given rise to increasing demands
for reliable, faster and more discriminative protective
schemes. The electro-mechanical relays, which have rendered
satisfactory service over several years, have not been able
to cope up with these demands. Consequently, there has been
a constant search for better alternatives. First, the
electronic relays, incorporating vacuum and gas-filled
tube circuits, have made their appearance as a possible
alternative. However, notwithstanding the absence of
contacts with ensuing ease of maintenance, lower burdens
on c.t.s and p.t.s and fast in operation even when close
to pickup level, their development was short-lived due to
the following reasons. They were not robust, they required
complex wiring and their filaments imposed a burden on the
station batteries. However, with the emergence of solid-
state components, the solid-state relays, which provide a
much better alternative to the electromechanical relays,
could be developed. Amongst the several advantages of
solid-state relays, ability to provide optimum operating
speeds, flexible control of the shape of the threshold

characteristics and reduced panel space requirement are worth mentioning. Recently, the development of micro-electronics has made available cheap and highly reliable integrated circuit (IC) chips. As is well known, a single chip integrates several complex circuits into a tiny component. Thus, the use of ICs eliminates the need for wiring complicated circuits, improves the reliability and at the same time, it greatly reduces the panel space requirements.

The development of distance relay characteristics, suitable for the protection of long heavily-loaded transmission lines, has been the concern of protection engineers since a long time. Of the various distance threshold characteristics developed for this purpose, the quadrilateral characteristic is considered to be the best since it encloses the fault area very compactly and consequently, possesses the valuable properties of least tendency to operate under power-swing and heavy-load conditions, and also greater immunity to the effects of fault resistance.

In the light of the above, an overview of some important techniques and methods, developed to generate distance relay characteristics intended for the protection of long heavily-loaded e.h.v. and u.h.v. transmission lines is presented first, in order to throw light on their limitations, merits and demerits. Next, the principle of operation, hardware implementation and test results of two new relaying schemes

using ICs and capable of generating a three-step
quadrilateral characteristic are presented.

2.2 OVERVIEW OF DISTANCE RELAY CHARACTERISTICS INTENDED
FOR THE PROTECTION OF EHV/UHV TRANSMISSION LINES

One of the chief requirements of the distance relay
characteristics, meant for the protection of long heavily
loaded e.h.v. and u.h.v. transmission lines, has been
that there shall be no encroachment into the tripping
area by heavy load and also during power swing conditions.
Basically, there have been five approaches which have aimed
at fulfilling this requirement. They are the use of
elliptical, composite, shaped, adaptive and quadrilateral
characteristics. An overview of a few important methods
and techniques developed to generate these characteristics
is presented in this section.

Bräten and Hoel [65] employed a three-input circulating-
current rectifier-bridge amplitude comparator to produce
normal and offset elliptical characteristics. Ramamoorty
et al. [61] used phase-splitting networks to rectify the
input signals and an operational amplifier (op amp) summing
circuit for amplitude comparison of these signals for
generating normal and offset elliptical characteristics with
three input signals. The   round nature of these characteri-
stics makes the response of the relay, to resistive faults
near a zonal reach, poor.

The generation of composite pickup characteristics, which are composed of circular arcs and straight line segments and which have a tripping area closely surrounding the fault area, has been reported by Humpage and Sabberwal [35], Hans Hoel et al. [38] and Johns [51,52]. Humpage and Sabberwal, and Hans Hoel et al. described the generation of a characteristic, composed of a mho circle and two blinders, with three signal phase comparison. Johns described the generation of a characteristic, which is a combination of restricted directional, restricted ohm and restricted mho characteristics, with three signal phase comparison embodying a new generalised phase comparison technique. With this technique, symmetrical angular limits other than $\pm$ 90° as well as asymmetrical angular limits can be obtained with greater facility. A pulse of fixed duration and displaced from the positive going (or negative going) zero crossing by a fixed time delay is assigned to each relaying signal. The coincidence of such pulses of all the relaying signals is measured to provide a trip signal. Then, the angular limits would be dependent both on the pulse widths and time delays. For example, in the case of a two-input comparator, the limits are given by $(\theta_2-\theta_1+\delta_2)$ and $(\theta_1-\theta_2+\delta_1)$ where δ_1 and θ_1 are, respectively, the pulse width and time delay associated with one input signal, and δ_2 and θ_2 are the corresponding quantities associated with the other input signal. Thus, it can be observed that this technique

provides greater flexibility in setting the angular limits, especially the asymmetrical ones. The composite characteristics, however, do not enclose the fault area as closely as desired.

Jackson [56] developed shaped mho and polarised mho characteristics, besides other shaped characteristics. These characteristics are shrunk along a direction perpendicular to the replica impedance complexor. He obtained these shaped characteristics with signal dependent phase angular limits. The signal dependency of the angular limits is accomplished by modifying the rate of fall of integrator output voltage with the application of an additional voltage. This additional voltage is a block corresponding to the anticoincidence of one of the normal relay inputs and an additional relay input. The additional relay input is proportional to the system current, if circular characteristics are to be shaped. Each additional input, along with the coincidence block of the normal relay inputs, is applied to a separate integrating circuit. Apart from the increase in the complexity of the circuitry, when this technique is employed, the shaped characteristics also do not enclose the fault area closely.

Johns [53], Parthasarathy et al. [59] and Paithankar and Thoke [62] developed adaptive or variable pickup

characteristics whose tripping area will be minimal under
all balanced conditions including heavy loads and power
swings, and automatically expand to a large area under
unbalanced-fault conditions. Johns obtained this
feature by adding an extra current-derived component
to one of the relay inputs. This component is so formed
that it is zero under all balanced conditions and
increases the resistive reach of the relay under
unbalanced-fault conditions. Using the generalised
phase comparison and the present techniques, he generated
a variable characteristic which comprises of segments of
restricted directional, restricted ohm and restricted mho
characteristics. Parthasarathy et al. realised the adaptive
feature by controlling the angular limits of phase comparison
with negative or zero sequence voltages, and generated an
adaptive polarised mho characteristic. Paithankar and Thoke
accomplished this feature by incorporating zero sequence
voltage polarisation and cross polarisation in two inputs
of a three-input double phase comparator relay, and obtained
a variable quadrilateral characteristic suitable for earth-
fault protection of double end infeed transmission lines.
This technique needs the derivation of additional sequence
components which are complex in some cases.

Several authors have reported about the generation
of a quadrilateral pickup characteristic. McLaren [42]
and Khincha et al. [48,49] have reported about its
generation with plural arrangement of two-input amplitude
comparators, whilst Paithankar and Ingole [57] reported
about its generation with a multiinput amplitude comparator.
McLaren developed a sampling technique using which any
pickup characteristic can be obtained by comparing instanta-
neous values of voltage and current derived at two different
instants of time. Using this technique, he described the
generation of parallelogram and restricted directional
characteristics, besides some others. He explained how a
quadrilateral characteristic could be obtained by compounding
these two characteristics. This technique dispenses with
the need for phase shifting and mixing circuits.

Khincha et al. developed an amplitude comparison
technique in which full-wave rectified, but unsmoothed,
voltage and current combinations are compared at every
instant during each half cycle to generate various characteri-
stics. This technique needs no sampling circuits, delay
circuits or amplitude-to-pulse-width converters as compared
to the sampling technique. They described how a quadri-
lateral characteristic could be obtained either by AND
compounding parallelogram and directional parallelogram
characteristics or by OR gating two directional parallelogram

characteristics. However, multicomparator arrangements, used to generate a compounded characteristic, are associated with time coordination problems.

Paithankar and Ingole described the generation of a quadrilateral characteristic with a five-input amplitude comparator. The comparator is very simple. It consists of a switching transistor, to the base of which the rectified restraining input, in series opposition to the parallel combination of the remaining four rectified inputs, is applied. Trip signal is obtained at the collector of the transistor only when one or more of the rectified operating inputs exceed the rectified restraining input. Each operating input, in conjunction with the restraining input, produces one side of the quadrilateral characteristic. However, this scheme requires as many as five inputs and their rectification. Consequently, elaborate circuitry is needed.

The simplest way of generating a quadrilateral characteristic is by AND compounding restricted directional and restricted ohm characteristics. Humpage and Sabberwal [35], Hans Hoel et al.[38], Anil Kumar [50] and Ramamoorty and Lall [58] described the generation of a quadrilateral characteristic in this way. Humpage and Sabberwal employed two-input phase comparators, with asymmetrical angular limits of comparison, for this purpose. They developed a technique

to obtain asymmetrical angular limits. The basic principle involved is the determination of the coincidence of the relay inputs' coincidence block and a pulse produced at a fixed time delay from the start of this block. The angular limits are a function of this time delay. The assymmetrical limits are obtained by providing a different time delay according to which input is leading the other. The demerit of this technique is the possibility of maloperation due to a spurious pulse.

Ramamoorty and Lall developed a new two-input phase comparator in which assymmetrical angular limits can easily be derived. The comparator uses digital circuits. A novel feature of this comparator is the use of a digital up/down counter. The counter, in conjunction with constant frequency pulses, counts up during the coincidence period and counts down during the anticoincidence period. The net count, if positive, at the end of one cycle time, is taken to indicate a trip condition. Angular limits other than $\pm 90^{\circ}$ are obtained by using pulses of different frequencies during coincidence and anticoincidence periods. And, the asymmetrical limits are obtained by providing a different ratio of coincidence to anticoincidence counting pulse frequencies according to which input is leading the other. This comparator is not affected by spurious spikes and has a uniform operating speed of one cycle for faults anywhere in the trip region. They

used this comparator to produce restricted directional
and restricted ohm characteristics, and a quadrilateral
characteristic by AND compounding these characteristics.

Anil Kumar [50] described the generation of restri-
cted directional and restricted ohm characteristics in a
novel way. Each of these characteristics was produced
with a phase sequence detector fed with three appropriate
inputs. He described two types of phase sequence detectors;
one uses a ferrite-core logic which needs no d.c. supply,
and the other, semiconductor flip-flops. However, use of
either two two-input phase comparators or two phase sequence
detectors, to generate a quadrilateral characteristic in this
manner, is involved with time coordination problems.

Ramamoorty and Lall [60] developed a completely novel
way of generating a quadrilateral characteristic with only
three input signals. The three inputs used are; IZ_R,(IZ_R-V)
and (IZ_3-V) where V and I are relay's input voltage and
current, and Z_R is the replica impedance. One side of the
quadrilateral is fixed, and is equal to Z_R. Starting from
the zero crossing of IZ_R, three pulses, with successive
ones adjacent to each other and of widths equal to the
desired angles between the successive adjacent sides of
the quadrilateral, are produced by monostable chips.
Complete coincidence of the first pulse and (IZ_R-V) as
well as that of the third pulse and (IZ_3-V) indicate a

tripping condition. Partial coincidence of either or both indicates a blocking condition. The coincidence of these two pairs is measured, through an AND gate by a digital counter, in conjunction with constant and high frequency counting pulses. The counter is set to give an output for a count corresponding to the full coincidence condition.

Parthasarathy [36] developed a three-step quadrilateral relay, which employed transistor circuits for measuring, discriminating and logic functions. It consists of a phase detector and a zone differentiation circuit. With four appropriate inputs, the phase detector generates a directional open quadrilateral characteristic. One of the inputs is a pulse and the detector's operation is based on the extension of block-spike technique to multisignal phase comparison. The zone differentiation circuit produces three plain impedance characteristics, corresponding to the three zones of distance protection, either by amplitude comparison or by phase comparison of two appropriate inputs. The outputs of the phase detector and zone differentiation circuits are compounded to yield a three-step closed quadrilateral characteristic.

2.3 PROPOSED RELAYING SCHEME I

This scheme, generates a three-step quadrilateral characteristic. The principle of operation, hardware

implementation and test results of this scheme are presented in this section. Although the principle of operation of this scheme is the same as that given in the reference [36], the hardware implementation is different. In the present proposed scheme, Op Amp, monostable and digital IC chips are employed for measuring, discriminating, logic and other functions, whereas transistor circuits were used in the scheme described in the above reference.

2.3.1 Principle of Operation

This relaying scheme consists of a forward fault detector (FFD) and a zone detector (ZD). The FFD produces a directional open quadrilateral characteristic on the complex impedance plane, whilst the ZD produces three plain impedance characteristics corresponding to the three zones of protection, as shown in Fig. 2.1.

The FFD is basically a multi-input phase comparator and operates on the block-spike principle. It is supplied with the following inputs.

$S_1 = IZ_r$ pulse (at negative-going zero crossing of IZ_r)

$S_2 = (IR-V)$

$S_3 = V \angle -90°$

$S_4 = V$

where V and I are the relay's input voltage and current, Z_r is the replica impedance and R is the maximum expected
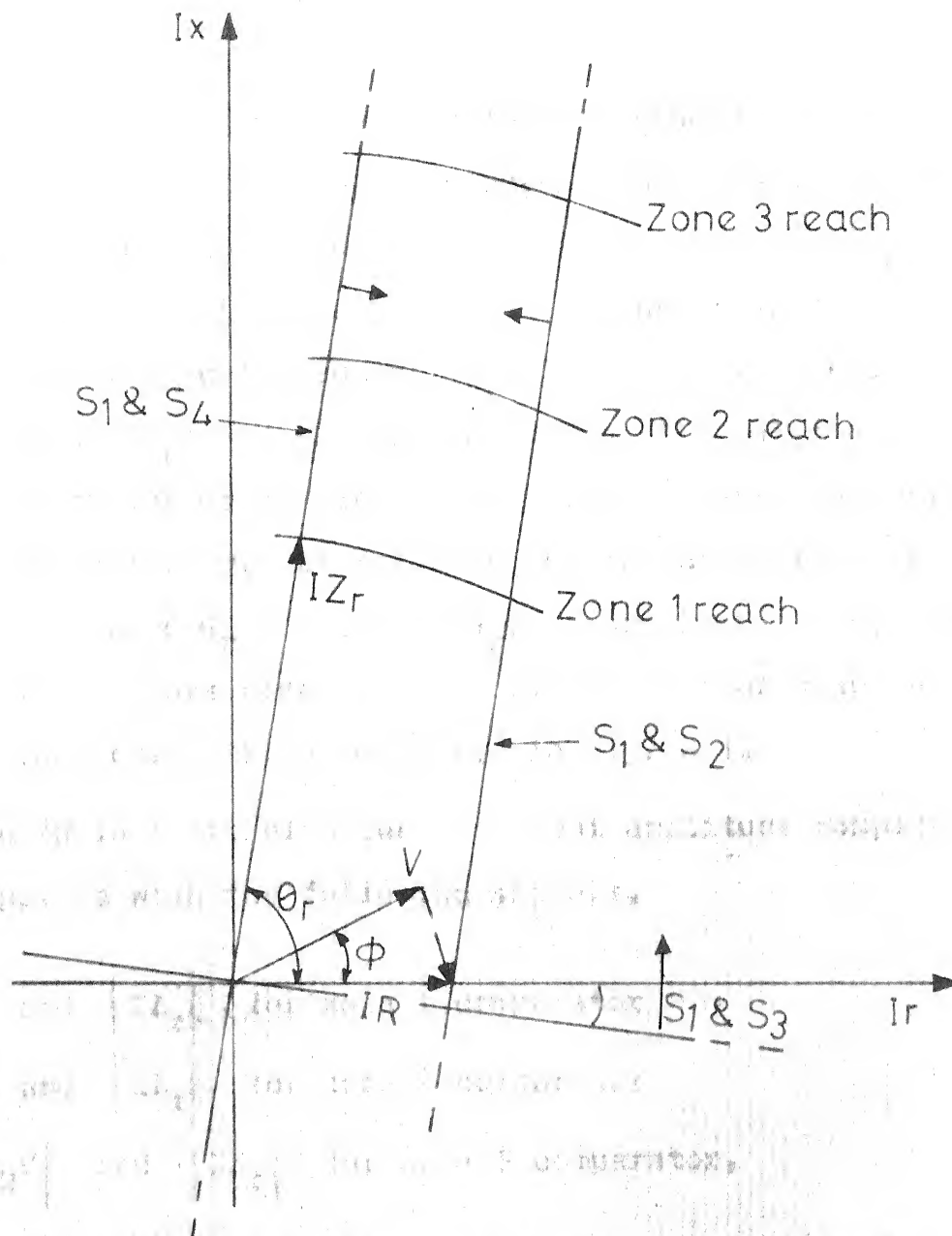
FIG.2·1 THRESHOLD CHARACTERISTICS OF
SCHEME I

fault resistance. That the resultant threshold characteristics generated by the FFD is an open quadrilateral characteristic can be explained as follows. The inputs; IZ_r pulse and $V\underline{/-90^o}$, give rise to a directional characteristic with an operating criterion of $(\Theta_r - 90^o) < \varphi < (\Theta_r + 90^o)$ where $\Theta_r = \arg(Z_r)$ and $\varphi = \arg(V/I)$. The IZ_r pulse with V and (IR-V) inputs gives rise to two blinder characteristics having, respectively, the following operating criteria :
$(-180^o + \Theta_r) < \varphi < \Theta_r$ and $(-180^o + \Theta_r) < \arg[IR-V] < \Theta_r$. The result of the above comparisons would be an open quadrilateral characteristic as depicted in Fig. 2.1.

The ZD is a set of three two-input amplitude comparators supplied with the following signals,

$|V|$ and $|IZ_r|$ for zone 1 comparator

$|k_1V|$ and $|IZ_r|$ for zone 2 comparator

and $|k_2V|$ and $|IZ_r|$ for zone 3 comparator,

where k_1 and k_2 are variable settings on a potentiometer. The three amplitude comparators produce three impedance circles of radii equal to $|Z_r|$, $|Z_r/k_1|$ and $|Z_r/k_2|$, as shown in Fig. 2.1.

2.3.2 Hardware Implementation

The FFD and ZD are built with ICs and a few discrete components. The hardware details of the FFD are given in

Figs. 2.2 and 2.3. Positive blocks, corresponding to the positive half cycles of the signals (IR-V), $V\underline{/-90^{\circ}}$ and V are produced at the points A,B and C respectively while positive blocks, corresponding to the negative half cycles of the same signals are produced at the points E,D and F respectively (vide Fig. 2.2). By means of a pulse shaping circuit, shown in Fig. 2.3, pulses at the negative going and positive going zero crossings of IZ_r are produced at G and H respectively. The positive coincidence of the blocks of (IR-V), $V\underline{/-90^{\circ}}$ and V, corresponding to a positive half cycle, and IZ_r pulse, produced at the negative going zero crossing, is measured by the combination of AND gates 1,2, and 5. Similarly, the negative coincidence of the blocks of (IR-V), $V\underline{/-90^{\circ}}$ and V, corresponding to a negative half cycle, and IZ_r pulse, produced at the positive going zero crossing, is measured by the combination of AND gates 3,4 and 6. The outputs of AND gates 5 and 6 are applied to an OR gate as shown. The output of this OR gate is the final output of the FFD.

The hardware details of the ZD are given in Fig. 2.4. The inputs, V and IZ_r, are phase split, full wave rectified and smoothed independently to obtain $\left|V\right|$ and $\left|IZ_r\right|$ respectively. $\left|V\right|$ is applied to a potential divider from which $\left|k_1V\right|$ and $\left|k_2V\right|$ are obtained. $\left|V\right|$ and $\left|IZ_r\right|$ are applied to a differential amplifier circuit to obtain $\left|IZ_r\right| - \left|V\right|$.
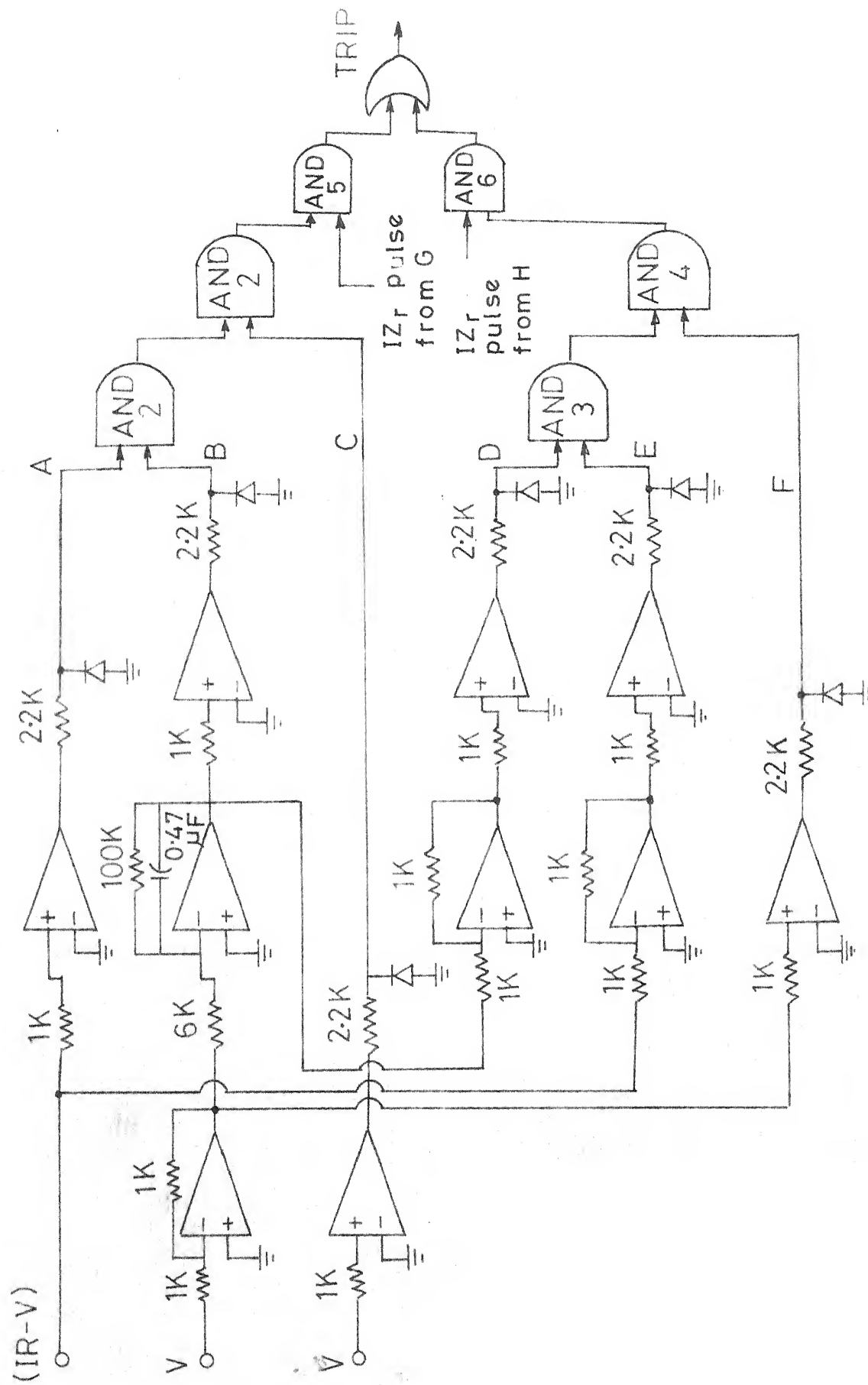
FIG. 2·2 FORWARD FAULT DETECTOR OF SCHEME I

With a diode clipper, only positive values of $\{|IZ_r| - |V|\}$ are made to appear at M. Non-zero positive values of this quantity represent a zone 1 fault. In a similar way, only the positive values of $\{|IZ_r| - |k_1V|\}$ and $\{|IZ_r| - |k_2V|\}$ are obtained at N and O respectively. Non-zero positive values of these quantities indicate that the fault is within zone 2 or within zone 3 reaches respectively. The last two quantities are delayed by T_2 and T_3 seconds respectively with mono chips. The delayed quantities appear at P and Q. The outputs available at M,P and Q are applied to an OR gate. The output from this OR gate is the output of the ZD, which is available immediately for zone 1 faults and after a time delay of T_2 or T_3 seconds for zone 2 or zone 3 faults.

The outputs of the FFD and ZD are applied to a final AND gate 7 to provide a trip signal. The block schematic of the entire scheme is given in Fig. 2.5.

2.3.3 Test Results

The relay has been fabricated and tested. Only zone 1 static pickup characteristics have been obtained. For the purpose of testing, IR is taken as reference. Signals V and IZ_r are obtained using phase-shifting networks. First, IZ_r is given the desired magnitude and phase shift. Next, V is given different phase shifts. For each phase shift, the magnitude of V is varied till the boundary of the trip region is identified by the operation of the relay. The

FIG. 2.5 BLOCK SCHEMATIC DIAGRAM OF THE ENTIRE
SCHEME I
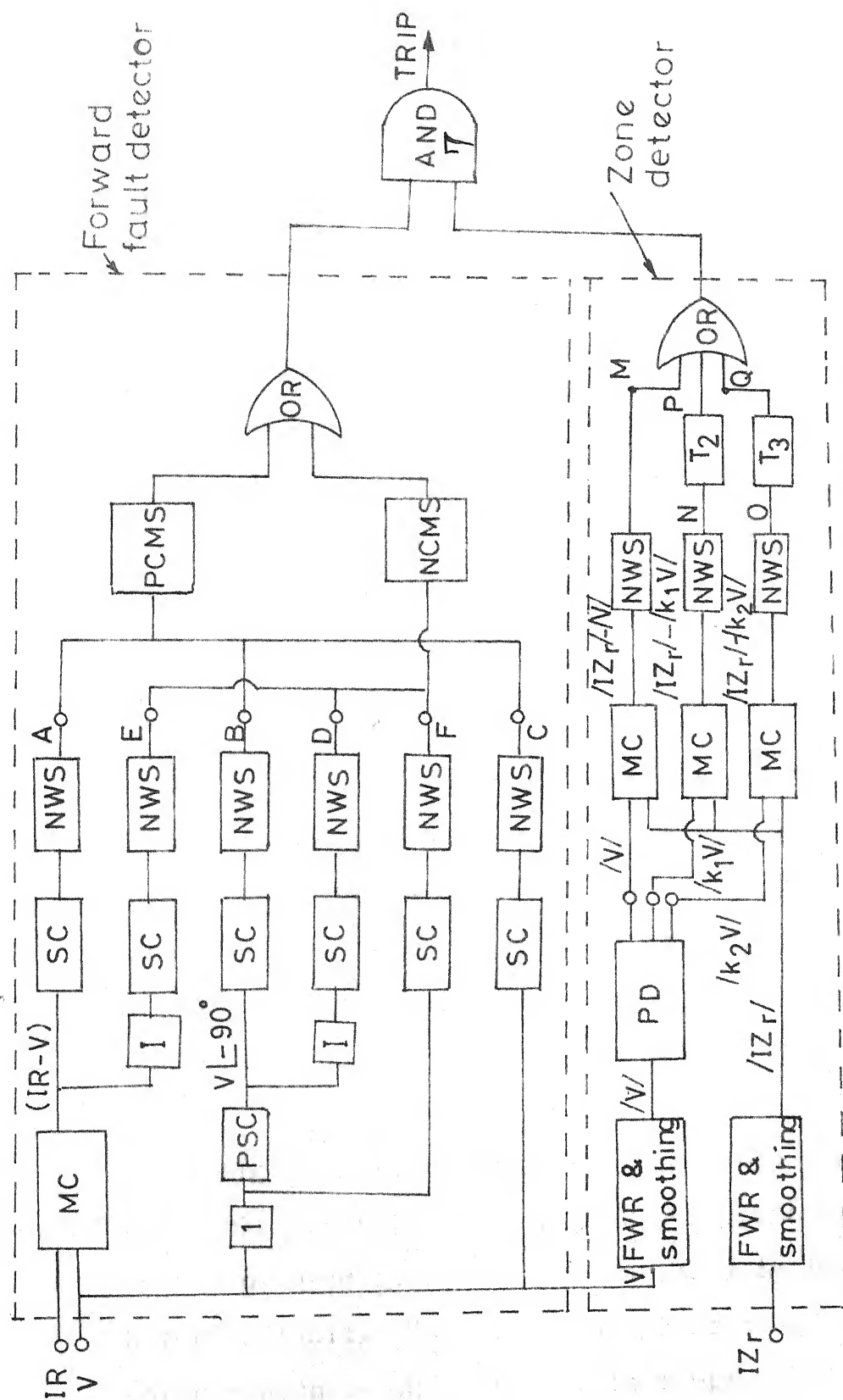
MC – Mixing circuit; SC – Squaring circuit; I – Inverter
PD – Potential divider; PSC – Phase shifting circuit; NWS – Negative
wave suppressor; PCMS & NCMS – Positive & Negative coincidence
measuring circuits; FWR – Full wave rectifier; T₂ & T₃ Delay circuits

relay characteristics are determined for two different values of Z_r at a constant value of R and also for two different values of R at a constant value of Z_r. In both the cases, θ_r is chosen to be 80°. The results obtained are given in Tables 2.1 and 2.2. The plots of the results, along with the theoretical curves, are given in Figs. 2.6 and 2.7. From the results obtained, it can be observed that there is a close agreement between the theoretical and experimental curves.

2.4 PROPOSED RELAYING SCHEME II

The principle of the operation of this relaying scheme is based on the extension of the technique reported in the reference [60]. This relaying scheme also consists of an FFD and a ZD. However, the FFD of this scheme needs only three inputs as against four in the previous scheme. Also, none of its inputs is a pulse. These modifications result in the enhancement of reliability and also in the elimination of the possibility of maloperation due to spurious spikes. In the present scheme, a pulse is used only for resetting a digital counter. Therefore, a spurious pulse will only reset the digital counter prematurely, resulting in the delayed operation of the relay in the event of an internal fault. The ZD of the present scheme generates three reactance characteristics corresponding to the three zones of distance protection. This modification leads to a

TABLE 2.1

The Pickup Characteristics of Scheme I

$\theta_r = 80^\circ$; $IZ_{r_1} = 4.0V$ and $IZ_{r_2} = 3.0V$

Phase Angle (Degrees)	Critical value of V for Z_{r_1} (volts)	Critical value of V for Z_{r_2}
0	1.5	1.5
10	1.6	1.5
20	1.7	1.6
30	1.9	1.8
40	2.3	2.2
50	2.9	2.8
60	4.0	3.0
70	4.0	3.0
80	4.0	3.0

TABLE 2.2

The Pickup Characteristics of Scheme I

$\theta_r = 80^\circ$; $IR_1 = 1.5V$ and $IR_2 = 2.0V$

Phase Angle (Degrees)	Critical value of V for R_1 (volts)	Critical value of V for R_2 (volts)
0	1.5	2.0
10	1.6	2.1
20	1.7	2.2
30	1.9	2.5
40	2.3	3.0
50	2.9	3.9
60	4.0	4.0
70	4.0	4.0
80	4.0	4.0
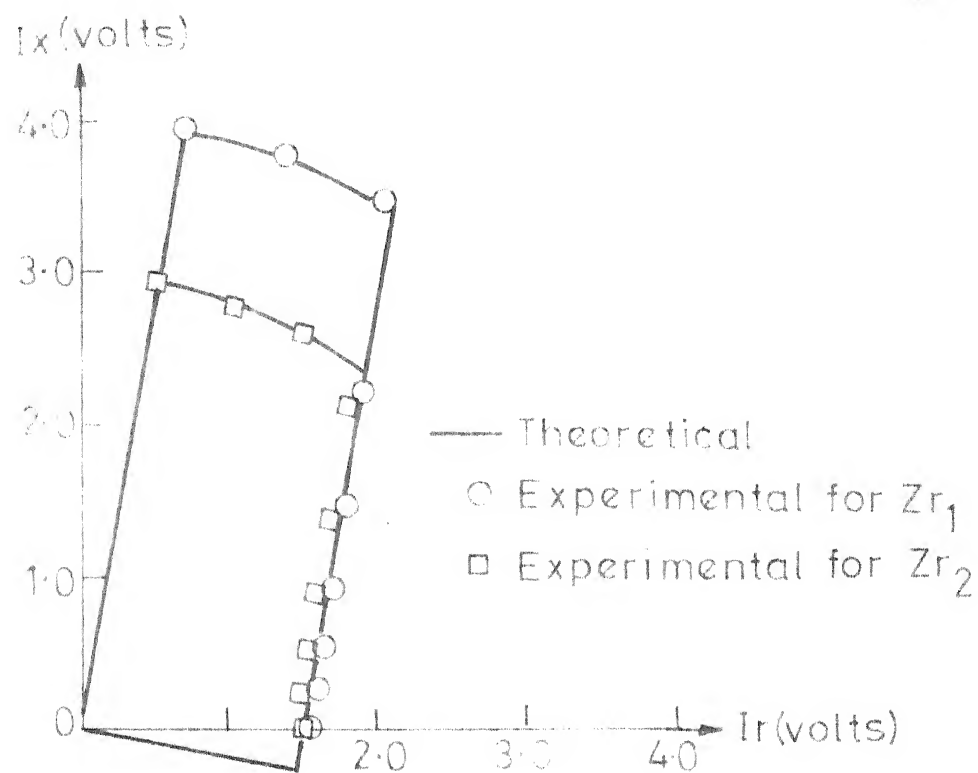
FIG. 2·6 PICKUP CHARACTERISTICS OF SCHEME I
FOR TWO VALUES OF Zr
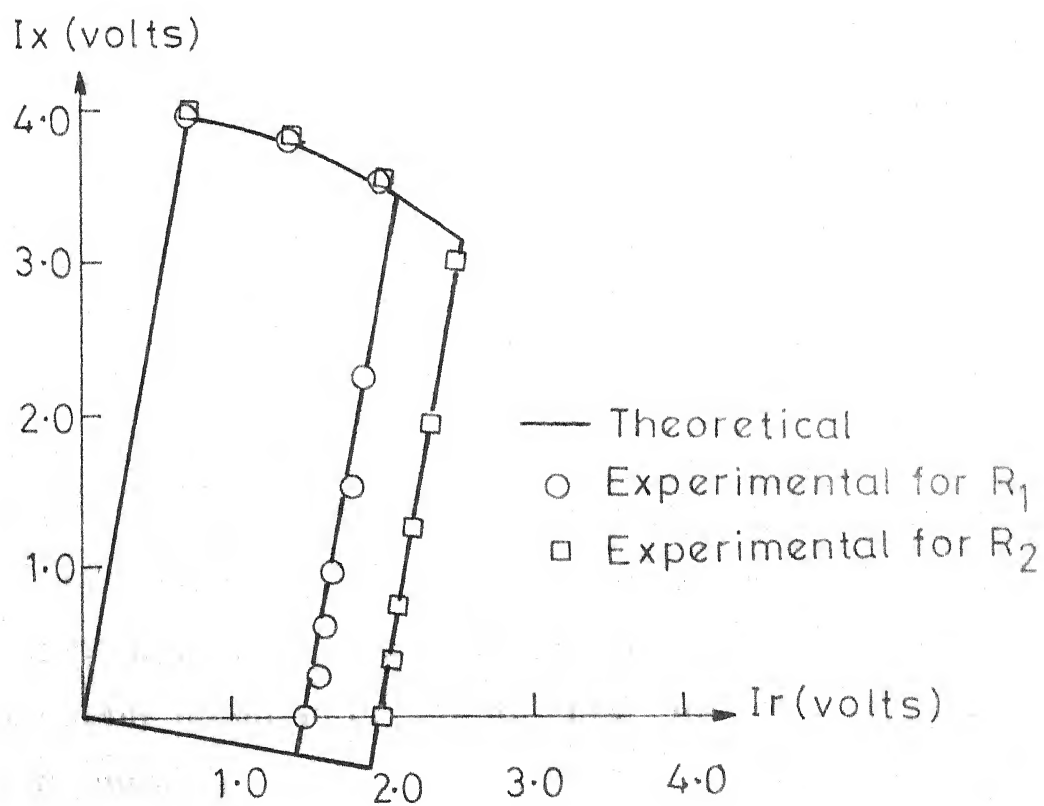
FIG. 2·7 PICKUP CHARACTERISTICS OF SCHEME I
FOR TWO VALUES OF R

better fault resistance coverage in the case of faults near
a zonal reach. The relay is built with digital ICs. This
results in a simpler circuitry, which is another factor
contributing to the enhancement of its reliability.

2.4.1 Principle of Operation

The FFD of the present scheme is supplied with the
following inputs.

$$S_1 = IR$$

$$S_2 = (IR-V)$$

$$S_3 = V$$

It yields a directional open quadrilateral characteri-
stic as explained below. The open quadrilateral characteri-
stic should enclose all those points, such as P shown in
Fig. 2.8, representing forward faults on the protected
transmission line and beyond. For P to fall within it, the
following two conditions must be fulfilled simultaneously :
(i) it should be above DOB and to the left of BC and (ii) it
should be to the right of EOA.

For the first condition to be fulfilled, the vector
$\overline{PB}$ = (IR-V) should be within the lagging angular range,
$0°$ to $(180°-\theta)$. This condition can be realised through
the circuitry shown in Fig. 2.9. The monostable multi-
vibrator, mono 1, produces a block of duration $(180°-\theta)$
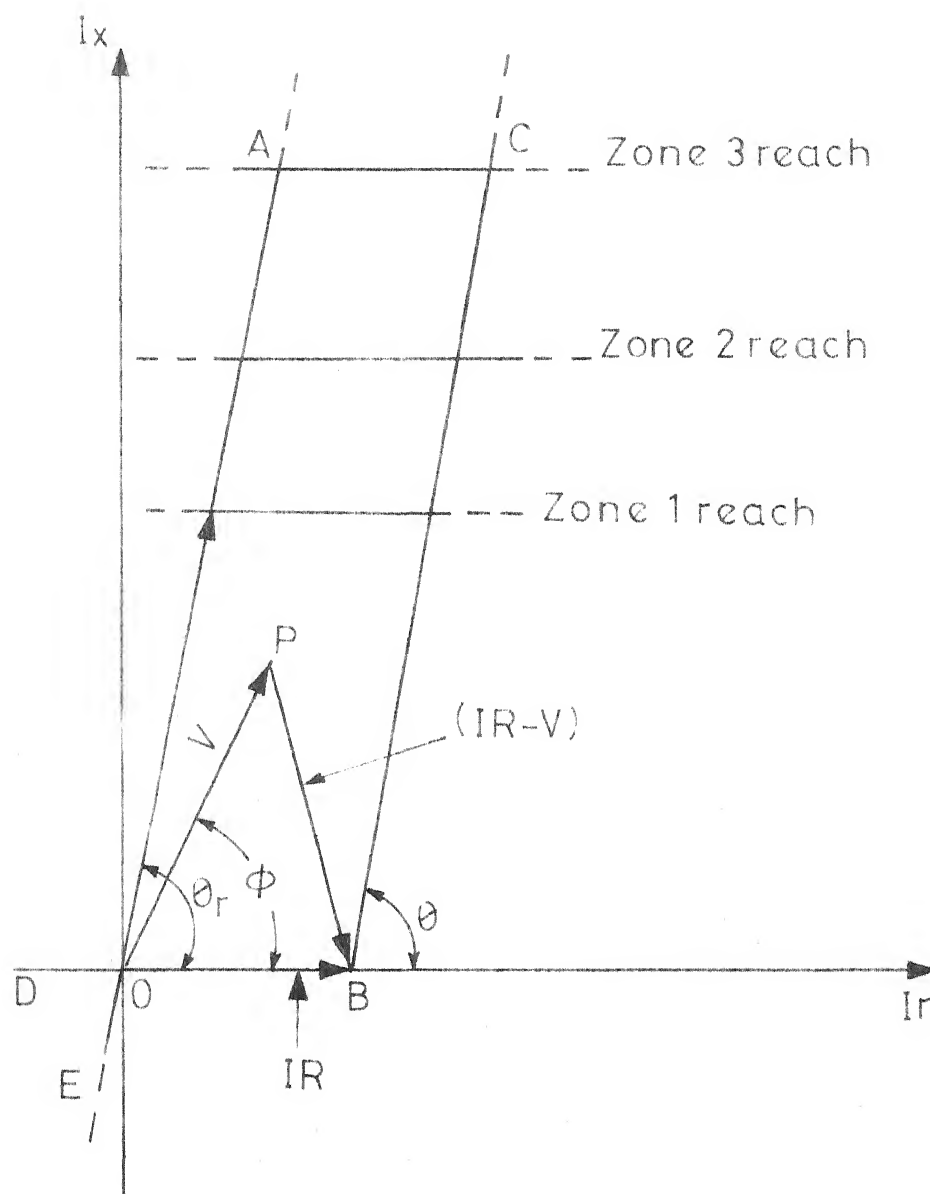
FIG·2·8 THRESHOLD CHARACTERISTICS
OF SCHEME II
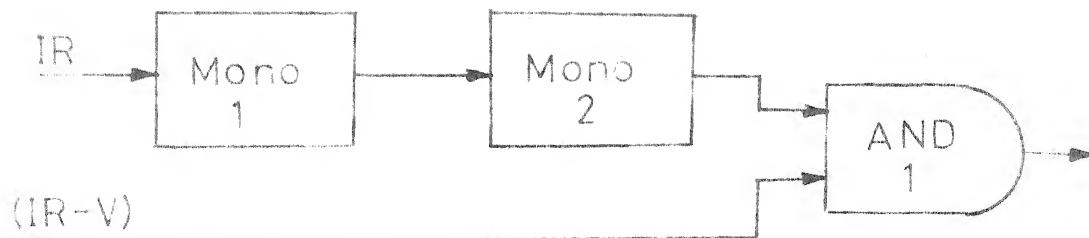
FIG. 2·9 CIRCUITRY FOR REALIZING CONDITION (i) OF
SCHEME II
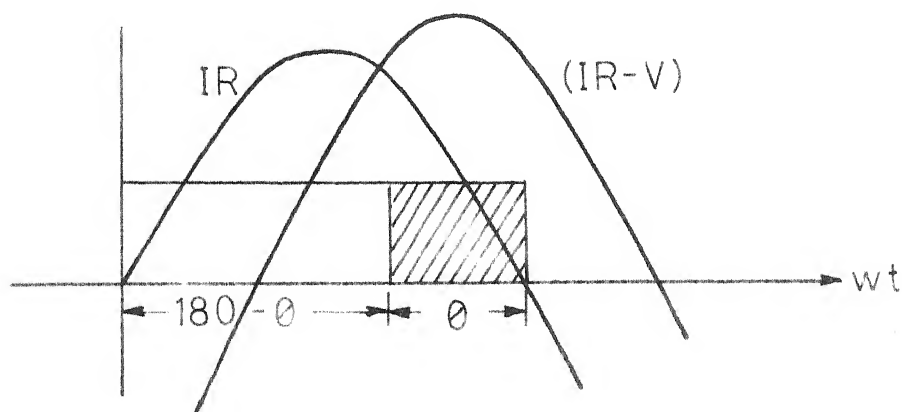
FIG. 2·10 WAVEFORMS PERTAINING TO REALIZATION
OF CONDITION (i) OF SCHEME II
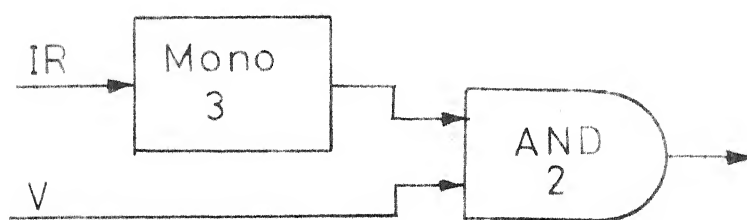
FIG. 2·11 CIRCUITRY FOR REALIZING CONDITION (ii)
OF SCHEME II
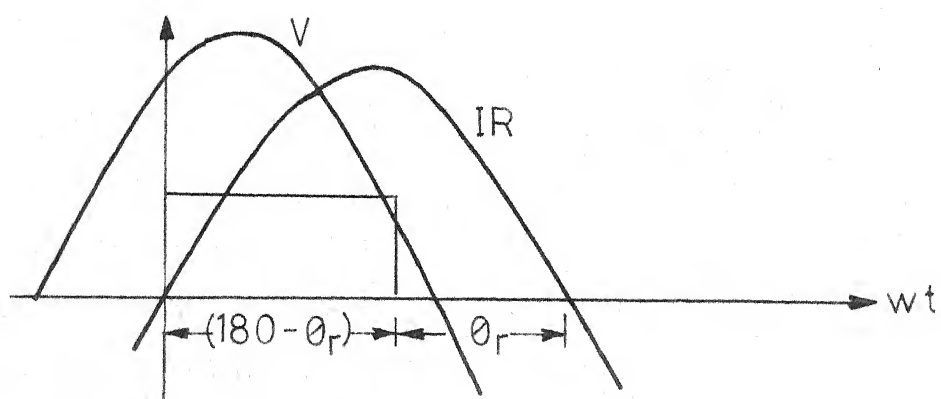
FIG. 2·12 WAVEFORMS PERTAINING TO REALIZATION
OF CONDITION (ii) OF SCHEME II

starting from the positive going zero crossing of IR.
Mono 2 produces a block of duration θ starting from
the instant when the previous block becomes zero. Only
if (IR-V) lags IR by not more than $(180^\circ-\theta)$, there will be
complete coincidence of (IR-V) and 'θ' block (the output
of mono 2) as shown in Fig. 2.10. Hence, the output
of AND 1 will be of full duration of θ only if P lies
above DOB and to the left of BC. It can be observed
that the slope of the line BC can be changed simply by
changing the widths of the two blocks.

For the second condition to be fulfilled, the angle
by which V leads IR should lie within the angular range
of 0° to θ_r. This condition is realised through the
circuitry shown in Fig. 2.11. Mono 3 produces a block
of duration $(180^\circ-\theta_r)$, starting at the positive going zero
crossing of IR. There will be a full coincidence of V and
the output of mono 3, only if V leads IR by not more than
θ_r. This is illustrated in Fig. 2.12. Hence, the output
of AND 2 will be of full duration of $(180^\circ-\theta_r)$, only if
this condition is fulfilled.

For fulfilling both the conditions simultaneously
and thus establishing the tripping criterion, an additional
circuitry is employed. This is shown in Fig. 2.13. The
outputs of AND gates 1 and 2 are applied to AND 3 through
an OR gate. The output of a clock (a standard oscillator),
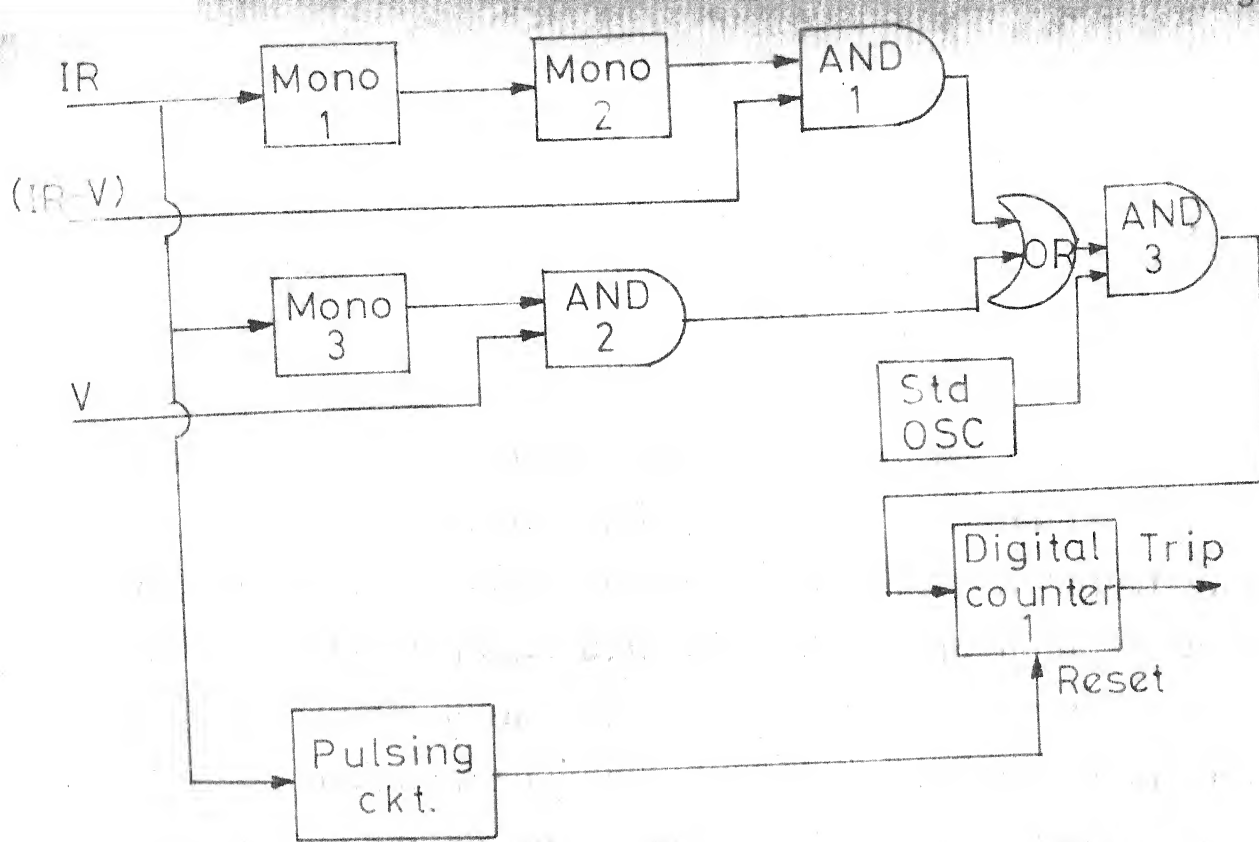
FIG. 2·13 BLOCK SCHEMATIC DIAGRAM OF THE FORWARD
FAULT DETECTOR OF SCHEME II
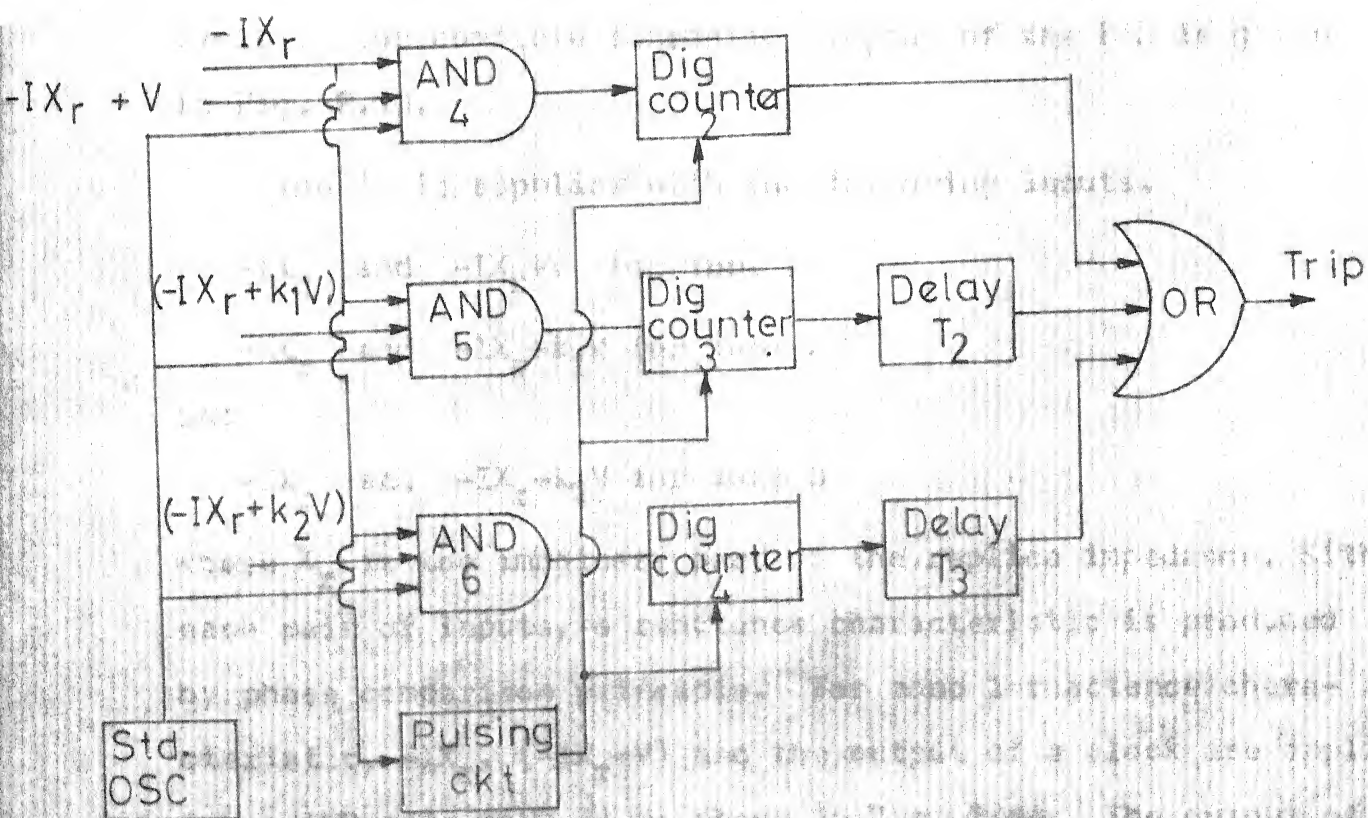
FIG. 2·14 BLOCK SCHEMATIC DIAGRAM OF THE ZONE
DETECTOR OF SCHEME II

which consists of train of pulses at a constant and high frequency, is also applied to AND 3. The output of AND 3 is fed to a digital counter which is set to give a trip signal only if the number of pulses from AND 3 corresponds to the full period of $(180^{\circ}-\Theta_r+\Theta)$, that is, only if P is within the open quadrilateral characteristic. Normally, Θ will be less than Θ_r. Consequently, the above measurement will be completed in half a cycle. Hence, with the above circuits duplicated for the negative coincidence measurement, the counter can be reset every half a cycle. Then, the maximum time of operation of the relay will be about one cycle. However, with only positive coincidence measurement, the time of operation of the relay will be between $\frac{1}{2}$ and $1\frac{1}{2}$ cycles. The complete schematic diagram of the FFD is given in Fig. 2.13.

The ZD is supplied with the following inputs,

$-IX_r$ and $-IX_r+V$ for zone 1

$-IX_r$ and $-IX_r+k_1V$ for zone 2

and

$-IX_r$ and $-IX_r+k_2V$ for zone 3

where X_r is the imaginary part of the replica impedance. With each pair of inputs, a reactance characteristic is produced by phase comparison principle. For zone 1 reactance characteristic, $-IX_r$, $(-IX_r+V)$ and the output of a clock are applied to an AND gate (AND 4) as shown in Fig. 2.14. The output of

AND 4 is applied to a digital counter (counter 2). The number of pulses applied to the counter depends upon the duration of the coincidence of $-IX_r$ and $(-IX_r+V)$. The level of the counter is set such that it gives a trip signal, only if the coincidence period of $-IX_r$ and $(-IX_r+V)$ equals or exceeds 90°. This results in the generation of a reactance characteristic. The counter is reset by $(-IX_r)$ pulse. Similar circuits are used for zones 2 and 3, and the necessary time delays are incorporated, as shown in the Fig. 2.14. The outputs of the circuits of all the zones are fed to an OR gate. Inputs $-IX_r$ and $(-IX_r+V)$, instead of the normal IX_r and (IX_r-V), are used to generate the reactance characteristic. This choice makes the outputs of the counter 1 of the FFD and counter 2 of the ZD to be available at the same instant, as shown in Fig. 2.15, and therefore, obviates the need for special time coordination measures. However, special time coordination measures are not necessary for zones 2 and 3 only when the time delays are integral multiples of full cycle time.

2.4.2 Hardware Implementation

The hardware details of the FFD of this relaying scheme are given in Fig. 2.16. The signals IR, (IR-V) and V are squarewaved by means of operational amplifier (Op Amp) chips. Timer 555 chips are used for building the monostables. The duration of the blocks, produced by the monostables, is
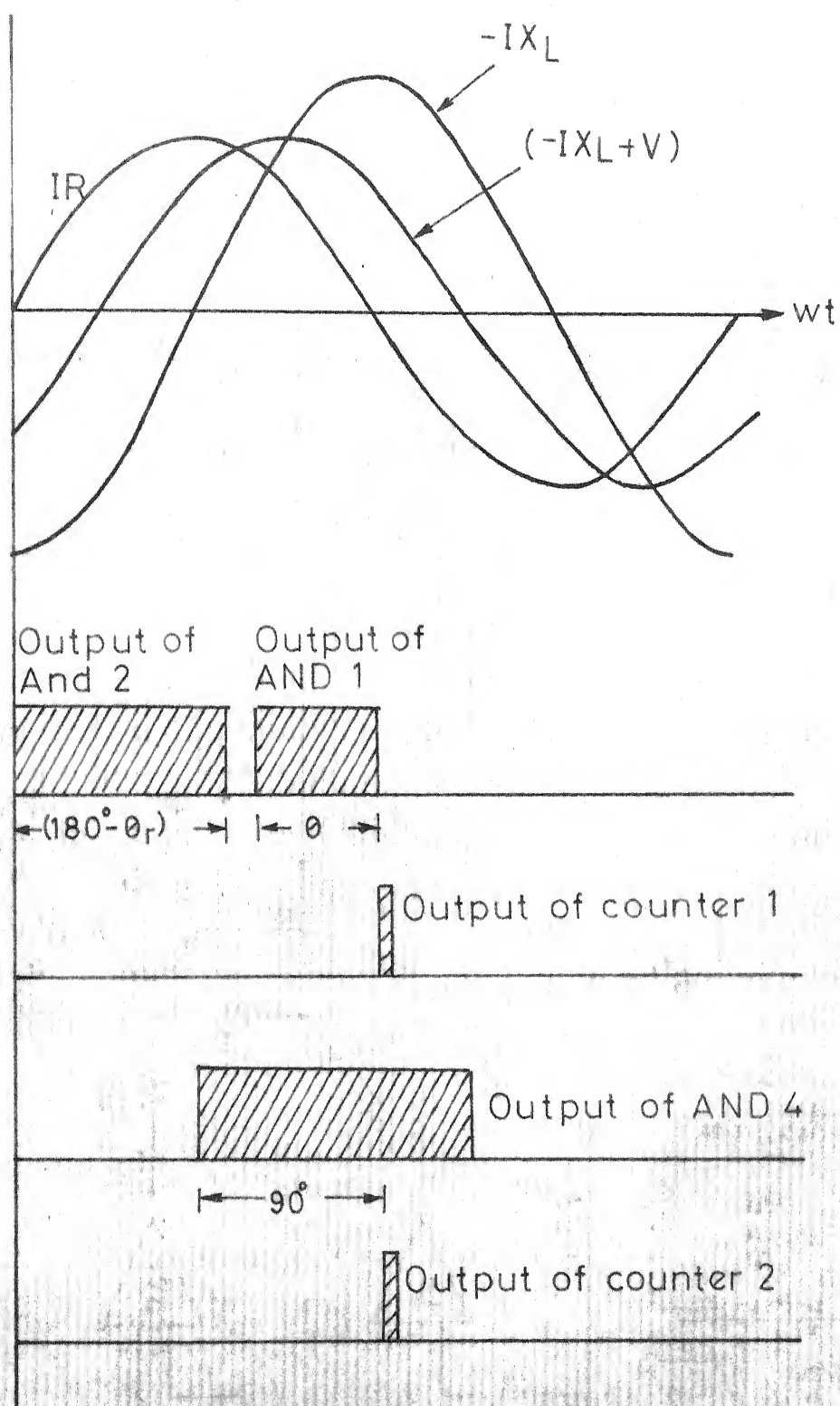
FIG. 2.15 ILLUSTRATION OF THE TIME CO-ORDINATION
BETWEEN OUTPUTS OF FORWARD FAULT
DETECTOR AND ZONE DETECTOR COUNTERS

FIG. 2·16 FORWARD FAULT DETECTOR OF SCHEME II

varied with the aid of (0-50 KΩ) potentiometers. The magnitudes of the outputs of the monostables and those of the squarewaved V and (IR-V) signals are limited to about +5 volts by means of zener diodes.

The hardware details of the ZD are given in Fig. 2.17 for zone 1. The circuitry is identical for other zones. The input signals -IX$_r$ and (V-IX$_r$) are squarewaved by means of Op Amp chips, and are limited to about +5 volts with the help of zener diodes.

The standard oscillator is built with the timer 555 chip as shown in Fig. 2.18. A train of pulses, with a constant frequency of 15 KHz, is generated by this oscillator (clock). It is used for both the FFD and ZD. The digital counter is built with a cascaded arrangement of 4-bit binary counters (7493) and magnitude comparators (7485), as depicted in Fig. 2.19. The clear pulses required for resetting the digital counters are generated, just before and terminating at the positive going zero crossing of the concerned signal, by the circuit shown in Fig. 2.20.

2.4.3 Test Results

The relay, whose hardware details are described in the previous section, has been fabricated and tested. The digital counter of the FFD is set to give a trip output if the number of input pulses exceeds 142 in a cycle. This corresponds to $\Theta_r = 70^\circ$ and $\Theta = 60^\circ$. The digital counter
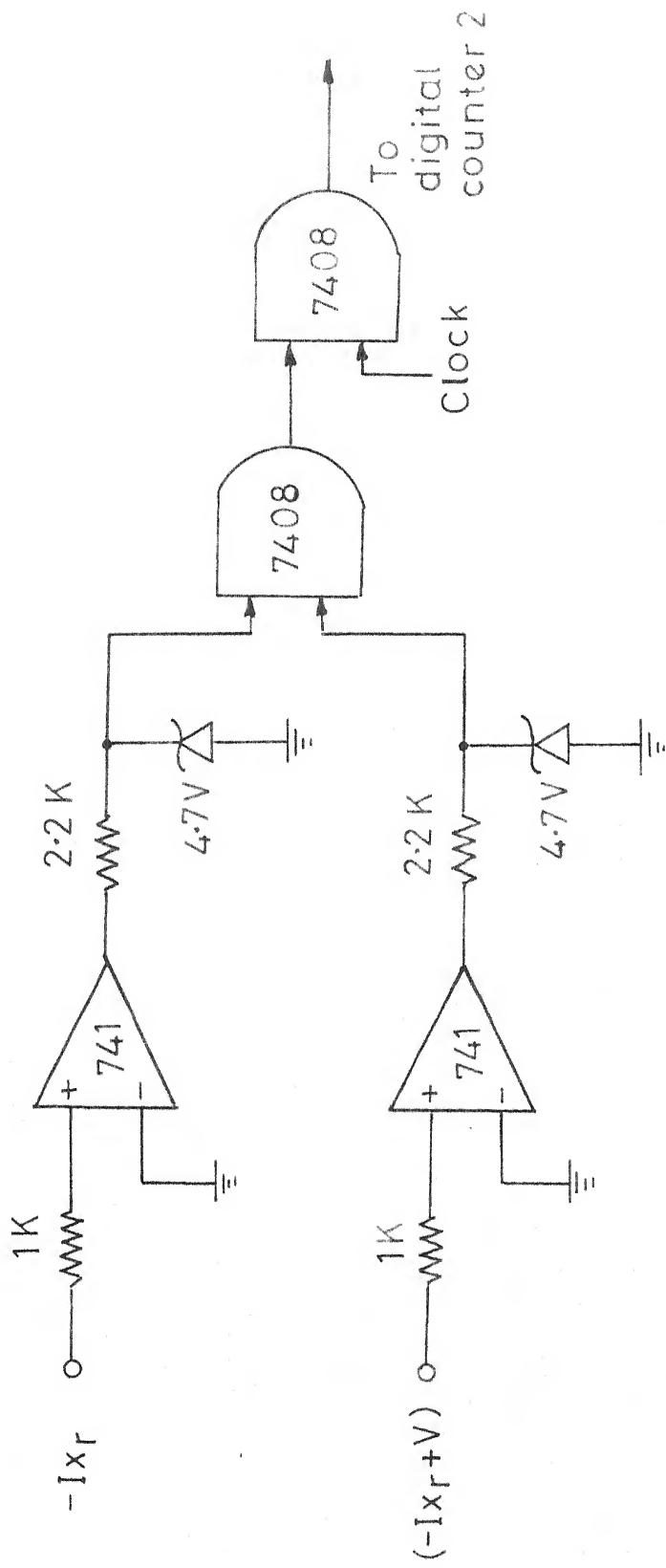
FIG. 2.17 ZONE 1 DETECTOR OF SCHEME II
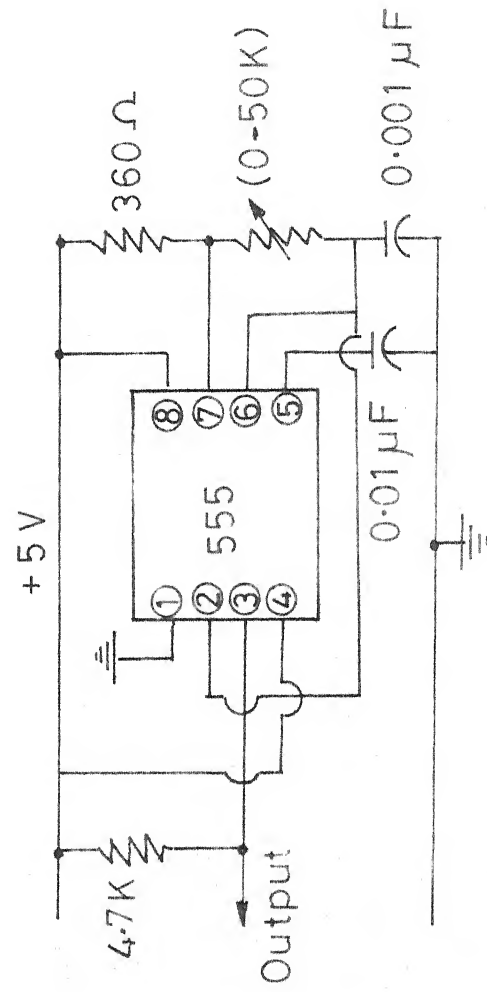
FIG. 2.18 STANDARD OSCILLATOR
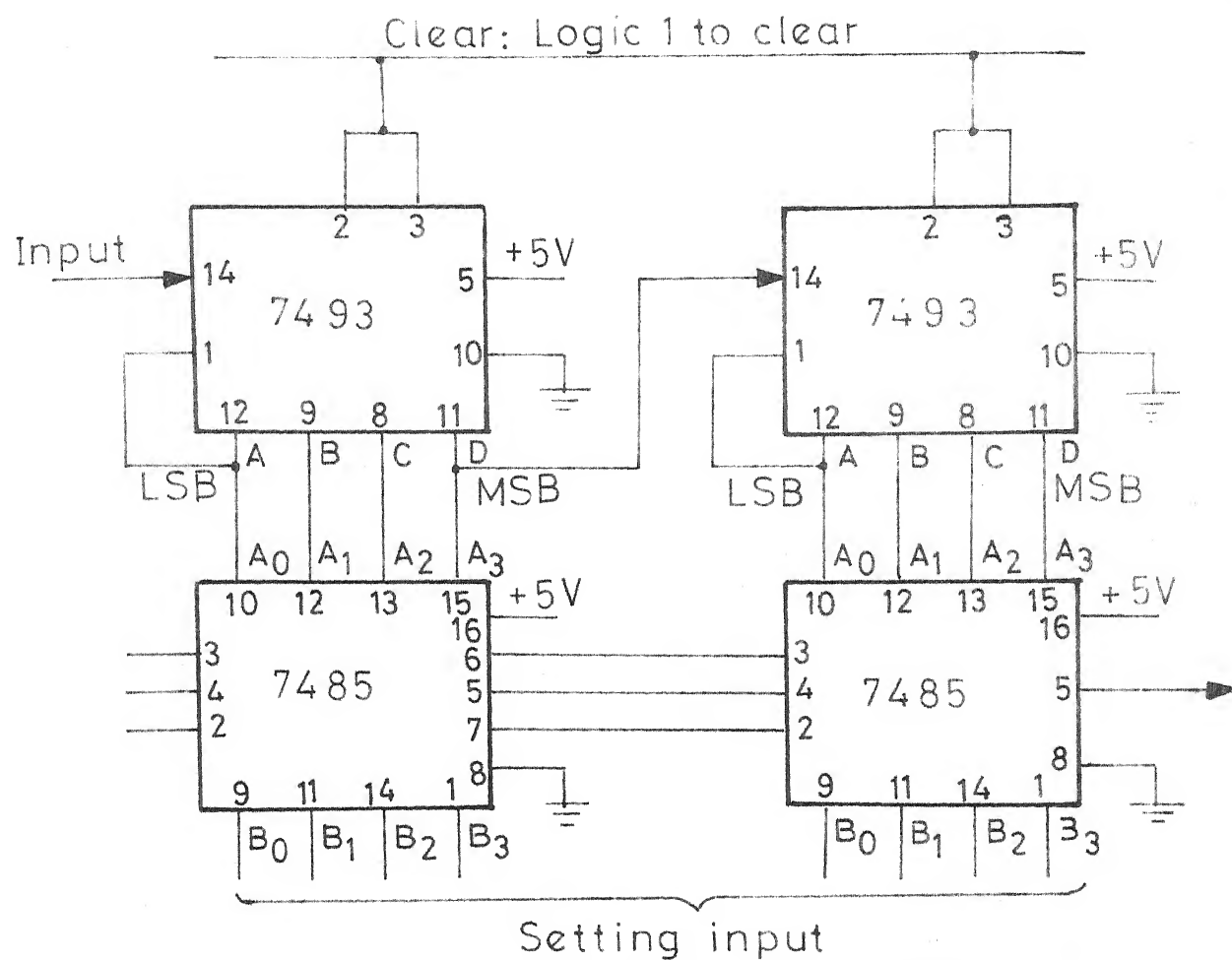
FIG. 2·19 DIGITAL COUNTER
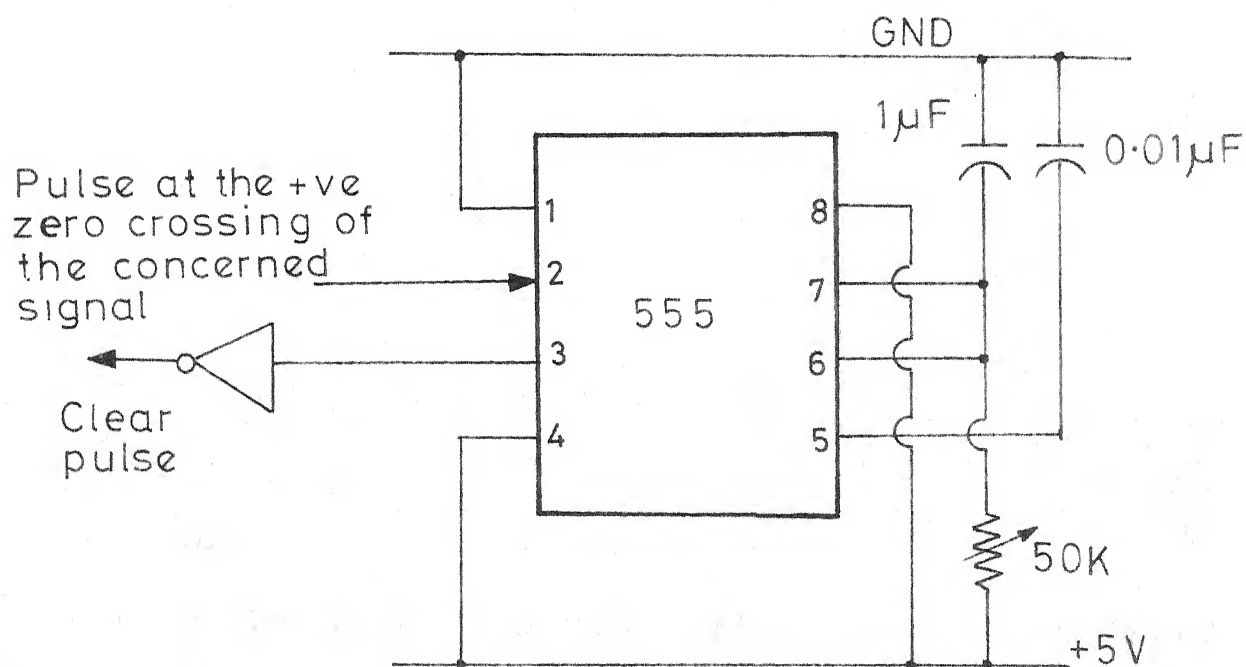
FIG. 2·20 CIRCUIT FOR PRODUCING THE CLEAR
PULSE

of the ZD is set to give a trip signal if the no. of input pulses exceeds 75. This corresponds to an angle of 90°. Both the settings are based on the input-signal and clock frequencies of 50 Hz and 15 KHz respectively.

Only the zone 1 pickup characteristic has been determined. The testing procedure adopted is as follows. First, the desired phase angle between V and I is obtained. Keeping this phase angle constant, the magnitude of V is decreased from a high value till the boundary of the trip region is identified by the operation of the relay. This procedure is repeated for different phase angles varying from 80° to 20° in steps of 5° each. Also, the nonoperation of the relay has been observed for a reverse fault at each angle, which is simulated by just reversing the direction of the current. A light emitting diode (LED) is used at the output terminals of the relay for indicating the operation of the relay. The results are given in Table 2.3. The experimentally-determined and theoretical pickup characteristics are given in Fig. 2.21. From these, it can be observed that there is a very close agreement between these characteristics.

2.5 CONCLUSIONS

The overview of some important distance relay characteristics, suitable for the protection of long and heavily-loaded EHV/UHV transmission lines presented in this chapter, leads

TABLE 2.3

The Pickup Characteristics of Scheme II

$$Z_S = 23\underline{/0^O} \text{ Ohms}$$

Phase Angle (Degrees)	IX_r (volts)	Critical value of V (volts)
20	1.50	4.7
25	2.25	5.3
30	3.00	6.1
35	4.00	7.1
40	5.50	8.7
45	7.00	9.8
50	7.00	9.2
55	7.00	8.6
60	7.00	8.0
65	7.00	7.8
70	7.00	7.5
70	5.00	5.3
70	3.00	3.2
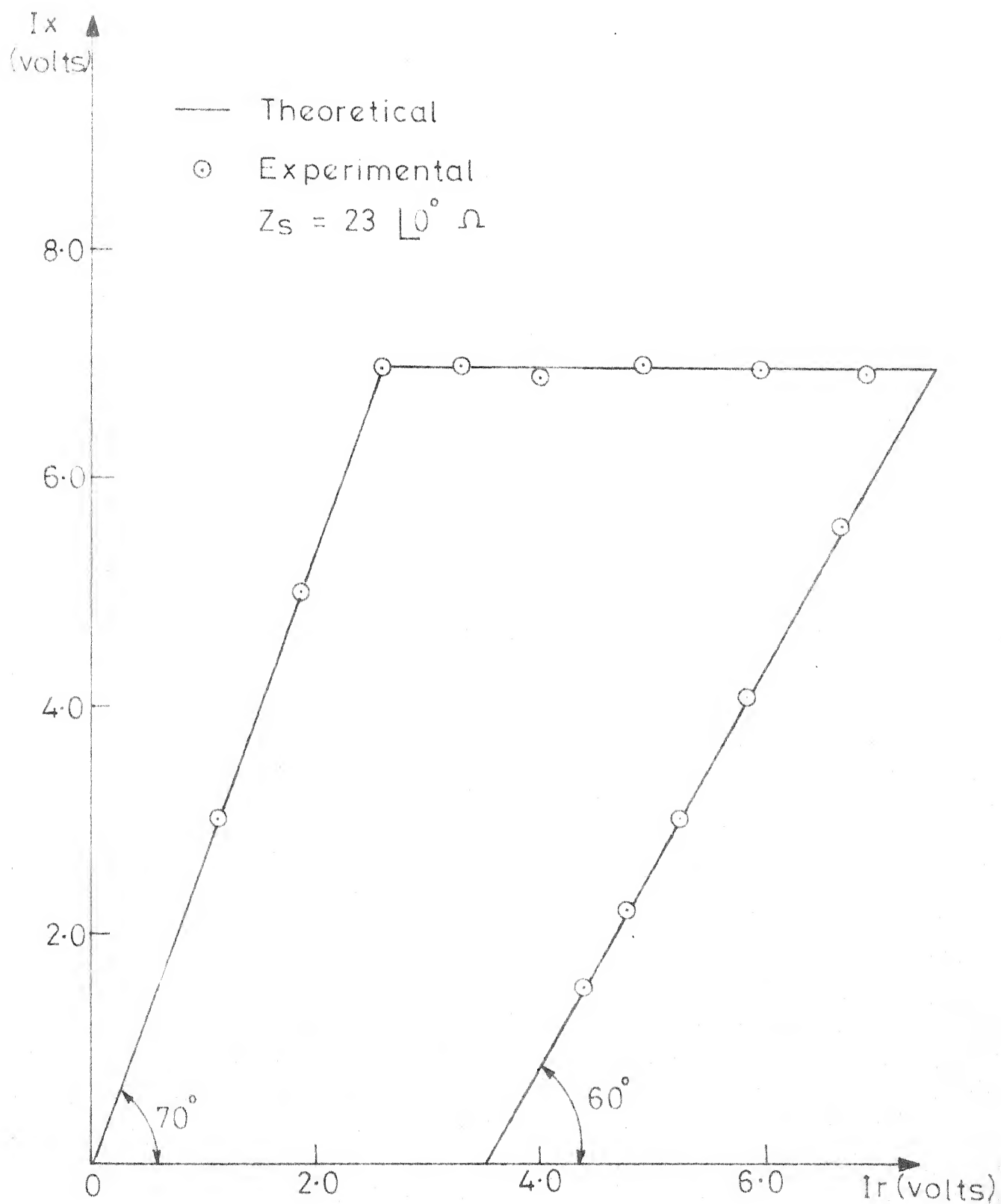
FIG.2·21 THE PICKUP CHARACTERISTICS OF
SCHEME II

one to the conclusion that the search for simpler techniques and circuitries is still necessary. Two new relays, employing ICs and yielding a three-step quadrilateral characteristics, have been developed, fabricated and tested. The hardware implementation of both the relays has demonstrated that the use of ICs results in great simplicity of the circuits. Also, the test results show that there is a close agreement between the theoretical and experimentally-determined threshold characteristics, in the case of both the relaying schemes.

CHAPTER 3

FREQUENCY DOMAIN FAULT ANALYSIS OF MULTINODE
POWER SYSTEMS

3.1 INTRODUCTION

Currently much interest is bestowed upon the development of ultra high speed protective relays. In order to design and develop such relays, an accurate determination/simulation of post-fault waveforms or of only the travelling wave components present in them, during a very short interval of time after fault inception, is essential. This necessitates an accurate modelling of power system components and also, the use of methods of computation, which are not only accurate but also amenable to digital computer application. The time-domain and frequency-domain methods are used for the computation of fault currents and voltages. However, the frequency-domain methods, though computationally cumbersome, are more accurate [115]. Four recent papers [3,68-70] have dealt with these aspects of modelling and fault analysis.

Humpage et al. [68] have described the digital simulation of models of synchronous generators, transmission lines, power transformers and transducers. But, they have considered only a simple lumped-parameter and frequency-

invariant series R-L model for the transmission lines.

Kothari et al. have presented modelling techniques for
simulating the primary system and transducers [69], and also
the digital simulation of fault voltages and currents [70].
Although, they have considered the distributed nature of the
line parameters, they have not incorporated the frequency
dependence of the line parameters and the untransposed
nature of the lines. They have derived detailed expressions
for voltages and currents for different types of faults
and recommended the use of bus impedance matrix for
frequency-domain fault analysis of complex power systems.
Johns and Aggarwal [3] have described the digital simulation
of faulted lines with an exact frequency-domain model for
transmission lines. That is, they have considered the
frequency dependency and distributed nature of the line
and earth parameters as well as the untransposed nature of
the lines. They have modelled the line by a two-port
[ABCD parameter] network in the frequency domain. They
have also developed techniques for the frequency-domain
fault analysis. However, these techniques would be appli-
cable, with ease, only to simple systems.

In the frequency-domain fault analysis of multinode
power systems, the use of bus impedance matrix may not
always be convenient in view of the fact that the bus
impedance matrix has to be formed for a large number of

frequencies, and stored. With this in view, frequency-domain fault analysis techniques, employing bus admittance matrix, are developed in this chapter. Also, a frequency-domain Pi model of a transmission line, which is suitable for bus admittance matrix formation, is developed. Application of these techniques to determine the relaying-point voltages and currents for all types of faults is outlined. The viability of these techniques is illustrated by determining the fault-generated components of the relaying-point voltages and currents for symmetrical three-phase and single-line-to-ground faults in two sample power systems.

3.2 FREQUENCY DOMAIN PI MODEL OF A TRANSMISSION LINE

Under transient conditions and in the frequency domain, the sending-end and receiving-end quantities, of a three-phase transmission line with distributed parameters, are related by the following equation [vide Appendix A]

$$
\begin{bmatrix} \overline{V}_S^{a,b,c} \\ \\ \overline{I}_S^{a,b,c} \end{bmatrix} = \begin{bmatrix} A & B \\ \\ C & D \end{bmatrix} \begin{bmatrix} \overline{V}_R^{a,b,c} \\ \\ \overline{I}_R^{a,b,c} \end{bmatrix} \tag{3.1}
$$

where

$\overline{V}^{a,b,c}$ − column vector of the transforms of the line to ground voltages of the phases a,b,c

$\overline{I}^{a,b,c}$ − column vector of the transforms of the line currents pertaining to the phases a,b,c

A,B,C,D — (3x3) matrices of frequency domain transmission-line constants

and, subscripts S and R refer to the sending and receiving ends of the line respectively.

Now, consider the Pi model of the line shown in Fig. 3.1. The following equations can be derived for this network .

$$\bar{V}_S^{a,b,c} = (U + \bar{Z}_P^{a,b,c}\ \bar{Y}_{2P}^{a,b,c})\ \bar{V}_R^{a,b,c} + \bar{Z}_P^{a,b,c}\ \bar{I}_R^{a,b,c}$$

and

$$\bar{I}_S^{a,b,c} = (\bar{Y}_{2P}^{a,b,c} + \bar{Y}_{1P}^{a,b,c} + \bar{Y}_{1P}^{a,b,c}\ \bar{Z}_P^{a,b,c}\ \bar{Y}_{2P}^{a,b,c})\ \bar{V}_R^{a,b,c}$$

$$+ (U + \bar{Y}_{1P}^{a,b,c}\ \bar{Z}_P^{a,b,c})\ \bar{I}_R^{a,b,c} \qquad (3.2)$$

where

$\bar{Z}_P^{a,b,c}$ — three-phase transform impedance matrix of the series branch of the Pi model

$\bar{Y}_{1P}^{a,b,c}$ and $\bar{Y}_{2P}^{a,b,c}$ — three-phase transform admittance matrices of the shunt branches of the Pi model at the two ends

and   U   — identity matrix of order 3.

Comparing equations (3.1) and (3.2), and solving, we get,

$$\bar{Z}_P^{a,b,c} = B$$

$$\bar{Y}_{1P}^{a,b,c} = (D - U)\ B^{-1}$$

and

$$\bar{Y}_{2P}^{a,b,c} = B^{-1}(A - U)$$
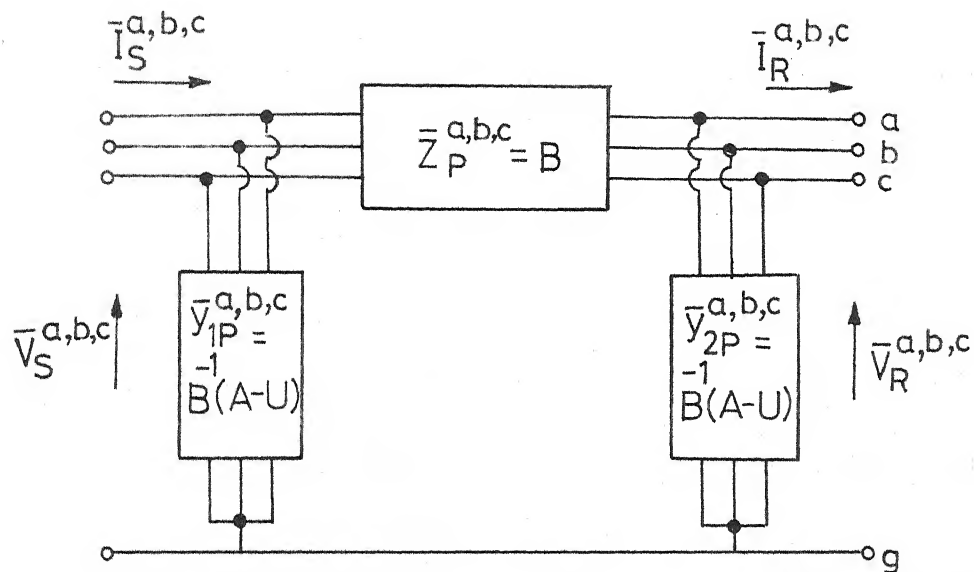
Fig. 3·1 FREQUENCY DOMAIN PI MODEL OF A
3-PHASE TRANSMISSION LINE

But,

$$(D-U)B^{-1} = (QD_m \ Q^{-1}-U)Q \ B_m^{-1} \ S^{-1}$$

$$= Q \ D_m \ B_m^{-1} \ S^{-1} - Q \ B_m^{-1} \ S^{-1}$$

$$= Q \ A_m \ B_m^{-1} \ S^{-1} - Q \ B_m^{-1} \ S^{-1} \ (\because D_m = A_m)$$

$$= Q \ B_m^{-1} \ A_m S^{-1} - QB_m^{-1} \ S^{-1}, \ \text{since } A_m \text{ and } B_m \text{ are}$$

diagonal matrices

$$= QB_m^{-1} \ S^{-1}S \ A_m \ S^{-1} - Q \ B_m^{-1} \ S^{-1}$$

$$= B^{-1} \ A - B^{-1} = B^{-1} \ (A - U)$$

where

S and Q — voltage and current modal transformation

matrices

and A_m, B_m, C_m, D_m — submatrices of modal line constants.

Therefore, finally we have

$$\bar{Z}_P^{a,b,c} = B$$

and

$$\bar{Y}_{1P}^{a,b,c} = \bar{Y}_{2P}^{a,b,c} = B^{-1} \ (A-U) \qquad\qquad (3.3)$$

Equation (3.3) defines the parameters of the Pi model in

terms of the A,B,C,D parameters of the line.

3.3 FREQUENCY DOMAIN FAULT ANALYSIS USING BUS ADMITTANCE MATRIX

The voltage or current at any point in a power system

network, after the occurrence of a fault, can be regarded as

the sum of the prefault and fault-generated components.
The fault analysis techniques, presented in this section,
enable the evaluation of the fault-generated components
in the frequency domain. The time-domain values of these
can be obtained by any standard numerical inverse transform
method . The prefault components can be determined in the
usual manner by load flow studies. The sum of the prefault
and fault-generated components gives the actual post-fault
values. In this connection, it may be stated that the deter-
mination of the fault-generated components separately is
quite useful for designing and developing ultra high speed
relays operated only with these components. As the above
procedure invokes superposition principle, it is valid only
for linear systems.

3.3.1 Application of the Superposition Principle [3]

The prefault three-phase power system transform network
is shown in Fig. 3.2(a), where only the fault node is shown in
detail. The open three-pole switch represents the unfaulted
condition. It can be replaced by a three-phase transform
voltage source $\bar{V}_{PF}^{a,b,c}$, having polarities as shown in Fig.
3.2(b). $\bar{V}_{PF}^{a,b,c}$ are the transforms of the three prefault
phase voltages at the fault point. A fault can be simulated
by connecting another three-phase transform voltage source
$\bar{V}_{FF}^{a,b,c}$ in series opposition to $\bar{V}_{PF}^{a,b,c}$ as shown in Fig. 3.3.
Choice of $\bar{V}_{FF}^{a,b,c}$ will depend upon the type of fault to be
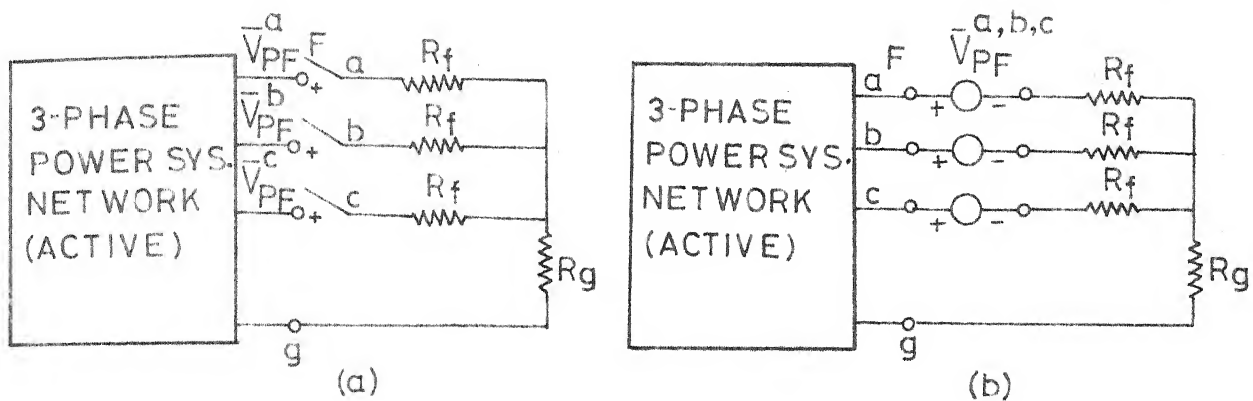
FIG·3·2 PREFAULT NETWORKS
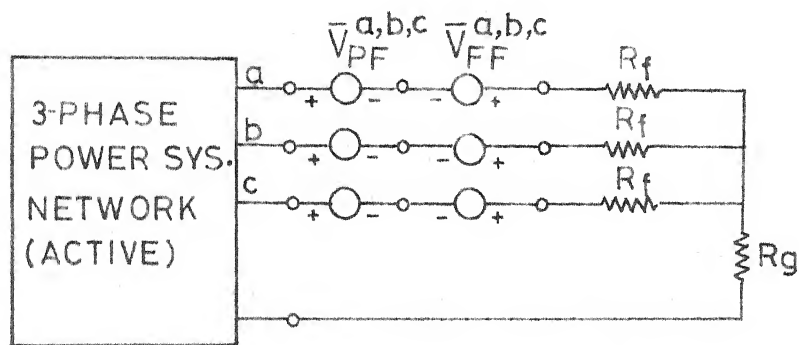
FIG·3·3 POST FAULT NETWORK
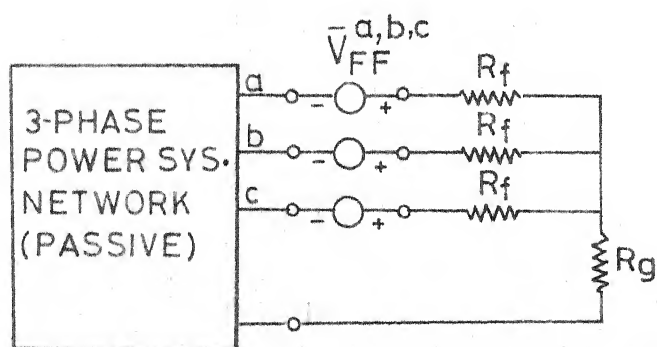
FIG·3·4 NETWORK FOR EVALUATING ONLY THE
FAULT GENERATED COMPONENTS

simulated. For example, $\bar{V}_{FF}^{a,b,c} = \bar{V}_{PF}^{a,b,c}$ for a symmetrical three-phase fault, and for one-phase-to-ground fault say on phase 'a' , $\bar{V}_{FF}^{a} = \bar{V}_{PF}^{a}$. The values of $\bar{V}_{FF}^{b}$ and $\bar{V}_{FF}^{c}$ in this case (i.e. one-phase-to-ground fault) are such that the fault currents in phases b and c are zero. Whatever the type of fault, the fault resistance network remains the same. The presence of unwanted resistances is rendered ineffective by setting the currents in them equal to zero. Application of Superposition theorem to the network of Fig. 3.3 yields the network of Fig. 3.4. The latter network is used for determining the fault-generated components.

3.3.2 Representation of the Fault Node

A fictitious bus, called fault bus hereafterwards, is created at the point of fault. At this bus, a series branch of the three-phase voltage source $\bar{V}_{FF}^{a,b,c}$ and the three-phase fault resistance $R_{F}^{a,b,c}$ exists to ground, as explained previously, where,

$$R_{F}^{a,b,c} = \begin{bmatrix} R_f + R_g & R_g & R_g \\ R_g & R_f + R_g & R_g \\ R_g & R_g & R_f + R_g \end{bmatrix} \qquad (3.4)$$

For the convenience of nodal analysis, it is replaced by an equivalent circuit consisting of a 3-phase current source $\bar{J}_{F}^{a,b,c}$ and a 3-phase conductance $G_{F}^{a,b,c}$ in parallel, as

shown in Fig. 3.5. For equivalence, it can be readily seen that,

$$\bar{J}_F^{a,b,c} = G_F^{a,b,c} \ \bar{V}_{FF}^{a,b,c}$$

and

$$G_F^{a,b,c} = \left[R_F^{a,b,c} \right]^{-1} \tag{3.5}$$

For the sake of generality, let

$$\bar{Z}_F^{a,b,c} = R_F^{a,b,c}$$

and

$$\bar{Y}_F^{a,b,c} = G_F^{a,b,c} \tag{3.6}$$

3.3.3 Nodal Equations and Bus Admittance Matrix

Assuming (N+1) number of buses, including the fault bus F, and with ground as the reference node, the following frequency-domain nodal matrix equation can be developed for a power system network to determine the fault-generated components (vide Fig. 3.4).

$$
\begin{bmatrix}
\bar{Y}_{11}^{a,b,c} & \bar{Y}_{12}^{a,b,c} & \cdots & \bar{Y}_{1N}^{a,b,c} & \bar{Y}_{1F}^{a,b,c} \\
\bar{Y}_{21}^{a,b,c} & \bar{Y}_{22}^{a,b,c} & \cdots & \bar{Y}_{2N}^{a,b,c} & \bar{Y}_{2F}^{a,b,c} \\
\vdots & \vdots & \vdots & \vdots \\
\bar{Y}_{N1}^{a,b,c} & \bar{Y}_{N2}^{a,b,c} & \cdots & \bar{Y}_{NN}^{a,b,c} & \bar{Y}_{NF}^{a,b,c} \\
\bar{Y}_{F1}^{a,b,c} & \bar{Y}_{F2}^{a,b,c} & & \bar{Y}_{FN}^{a,b,c} & \bar{Y}_{FF}^{a,b,c}
\end{bmatrix}
\begin{bmatrix}
\bar{V}_1^{a,b,c} \\
\bar{V}_2^{a,b,c} \\
\vdots \\
\bar{V}_N^{a,b,c} \\
\bar{V}_F^{a,b,c}
\end{bmatrix}
=
\begin{bmatrix}
0 \\
0 \\
\vdots \\
0 \\
-\bar{J}_F^{a,b,c}
\end{bmatrix}
\tag{3.7}
$$
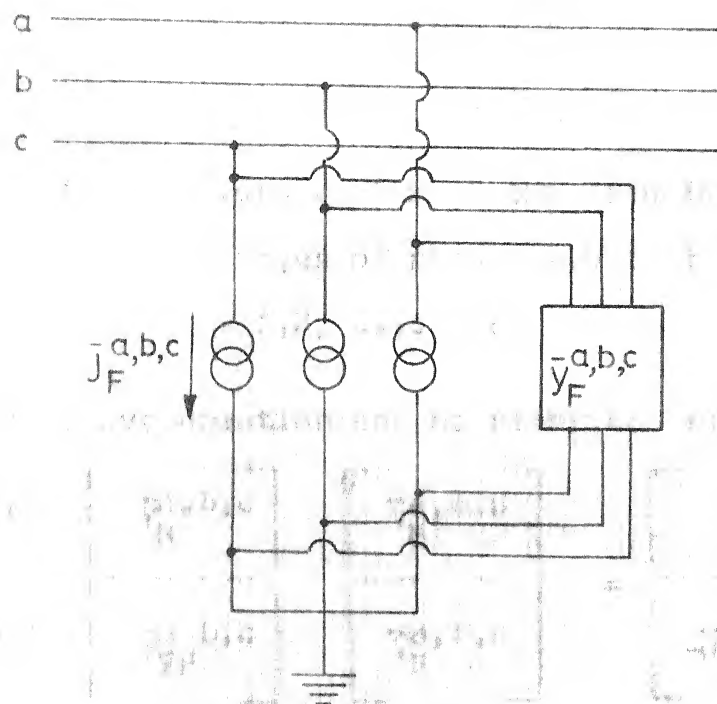
Fig.3·5 EQUIVALENT CURRENT SOURCE REPRESEN-
TATION AT THE FAULT BUS

200 km

R.P.

100 km   100 km
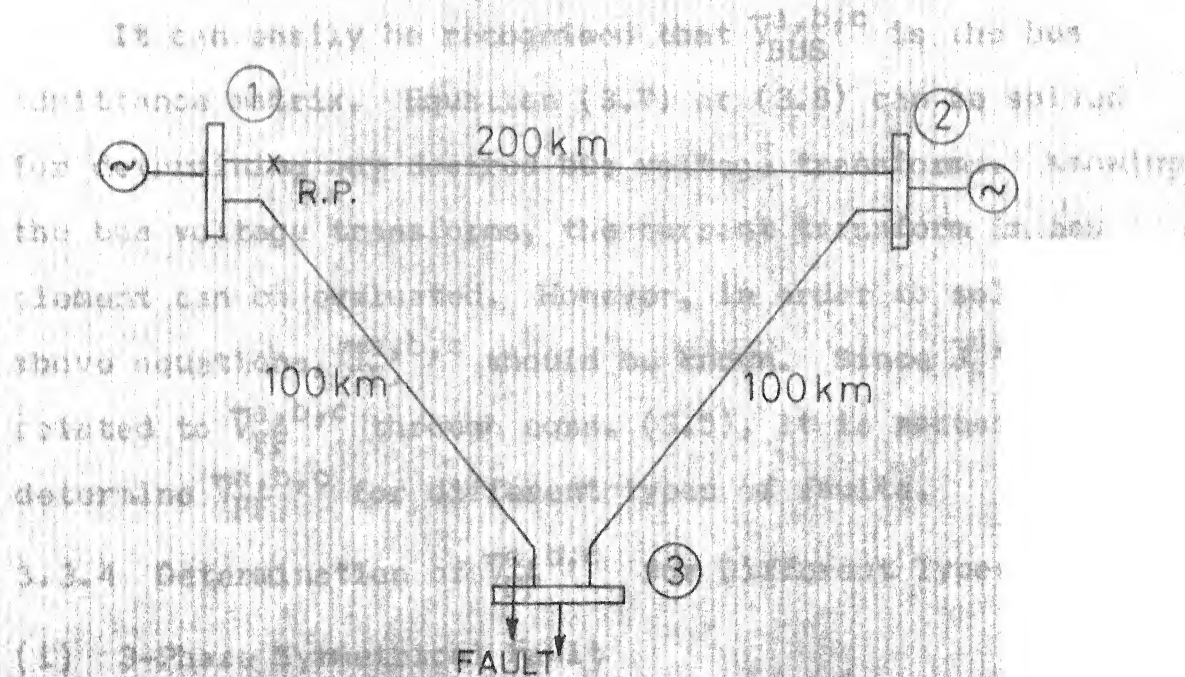
FAULT

R.P - Relay point

FIG.3·6 A SAMPLE 3-BUS POWER SYSTEM

where

$\bar{V}_i^{a,b,c}$ — column vector of the transforms of the

voltages of phases a,b,c at ith bus for all

i = 1,2, ..., N,F

The above equation can be rewritten as follows :

$$\left[\begin{array}{c|c} \bar{Y}_M^{a,b,c} & \bar{Y}_N^{a,b,c} \\ \hline \bar{Y}_P^{a,b,c} & \bar{Y}_{FF}^{a,b,c} \end{array}\right] \left[\begin{array}{c} \bar{V}_M^{a,b,c} \\ \hline \bar{V}_F^{a,b,c} \end{array}\right] = \left[\begin{array}{c} [0] \\ \hline -\bar{J}_F^{a,b,c} \end{array}\right] \qquad (3.8)$$

i.e., $\bar{Y}_{BUS}^{a,b,c} \cdot \bar{V}_{BUS}^{a,b,c} = \bar{I}_{BUS}^{a,b,c}$ (3.9)

It can easily be recognised that $\bar{Y}_{BUS}^{a,b,c}$ is the bus admittance matrix. Equation (3.7) or (3.8) can be solved for determining any desired bus voltage transforms. Knowing the bus voltage transforms, the current transform in any element can be evaluated. However, in order to solve the above equations, $\bar{J}_F^{a,b,c}$ should be known. Since $\bar{J}_F^{a,b,c}$ is related to $\bar{V}_{FF}^{a,b,c}$ through eqns. (3.5), it is necessary to determine $\bar{V}_{FF}^{a,b,c}$ for different types of faults.

3.3.4 Determination of $\bar{V}_{FF}^{a,b,c}$ for Different Types of Faults

(i) 3-Phase Symmetrical Fault

An examination of the post- fault power system network, shown in Fig. 3.3, reveals that $\bar{V}_{FF}^{a,b,c}$ should be equal to $\bar{V}_{PF}^{a,b,c}$, which is tantamount to closing the 3-pole switch

where

$$\bar{Z}^{a,b,c} = \bar{Z}_F^{a,b,c} - [\bar{Y}_F^{a,b,c} - \bar{Y}_{FF}^{a,b,c} + \bar{Y}_P^{a,b,c}(\bar{Y}_M^{a,b,c})^{-1} \bar{Y}_N^{a,b,c}]^{-1}$$

(3.14)

and

$$\bar{Z}_F^{a,b,c} = [\bar{Y}_F^{a,b,c}]^{-1}$$

Now, let

$$\bar{Z}^{a,b,c} = \begin{bmatrix} \bar{Z}^{aa} & \bar{Z}^{ab} & \bar{Z}^{ac} \\ \bar{Z}^{ba} & \bar{Z}^{bb} & \bar{Z}^{bc} \\ \bar{Z}^{ca} & \bar{Z}^{cb} & \bar{Z}^{cc} \end{bmatrix}$$

(3.15)

Solution of equation (3.13), with the condition $\bar{I}_F^b = \bar{I}_F^c = 0$, results in

$$\bar{V}_{FF}^{a,b,c} = \begin{bmatrix} \bar{Z}^{aa} \\ \bar{Z}^{ba} \\ \bar{Z}^{ca} \end{bmatrix} (\bar{V}_{PF}^a/\bar{Z}^{aa})$$

(3.16)

(iii) Phase-to-Phase Fault between Phases b and c

For the simulation of this fault, $\bar{V}_{FF}^{a,b,c}$ should be such that the following conditions are satisfied.

i.e., $\bar{V}_{FF}^b - \bar{V}_{FF}^c = \bar{V}_{PF}^b - \bar{V}_{PF}^c$

$\bar{I}_F^a = 0$ (3.17)

and $\bar{I}_F^b + \bar{I}_F^c = 0$

Solution of equations (3.13) and (3.17) yields,

$$\bar{V}_{FF}^{a,b,c} = \bar{Z}^{a,b,c} \begin{bmatrix} 0 \\ 1 \\ -1 \end{bmatrix} \frac{\bar{V}_{PF}^{b} - \bar{V}_{PF}^{c}}{(\bar{Z}^{bb} - \bar{Z}^{bc} - \bar{Z}^{cb} + \bar{Z}^{cc})} \qquad (3.18)$$

(iv) Double-Phase-to-Ground Fault Involving Phases b and c

This fault is simulated by letting $\bar{V}_{FF}^{b} = \bar{V}_{PF}^{b}$, $\bar{V}_{FF}^{c} = \bar{V}_{PF}^{c}$ and by letting $\bar{V}_{FF}^{a}$ to take up such a value that $\bar{I}_{F}^{a} = 0$.

Substitution of these in equation (3.13) leads to the solution,

$$\bar{V}_{FF}^{a} = [\bar{Z}^{ab} \ \bar{Z}^{ac}] \begin{bmatrix} \bar{Z}^{bb} & \bar{Z}^{bc} \\ \bar{Z}^{cb} & \bar{Z}^{cc} \end{bmatrix}^{-1} \begin{bmatrix} \bar{V}_{PF}^{b} \\ \bar{V}_{PF}^{c} \end{bmatrix} \qquad (3.19)$$

Bolted faults are simulated by assuming a very small value for R_f and by taking $R_g = 0$.

3.4 INVERSION TO THE TIME DOMAIN

After having determined the frequency-domain values of the relaying-point voltages and currents, it is necessary to determine their time-domain values. For this purpose, the modified Fourier transform techniques, described in [116], are employed. The inverse modified Fourier transform, given in equation (3.20) below, forms the basis of the method by which the wide frequency spectrum of the disturbance is used

to determine the corresponding time variation of any voltage or current of interest.

$$f(t) = \frac{\exp(at)}{2\pi} \int_{-\infty}^{+\infty} \overline{f}_+ (a+j\omega) \exp(j\omega t)d\omega \qquad (3.20)$$

where

ω - angular frequency as well as the transform parameter

a - frequency shift constant which is used to reduce aliasing errors when the integral is evaluated digitally

and $\overline{f}_+(a+j\omega)$ - modified Fourier transform of the function, $f(t)$.

For the numerical evaluation of the above integral, it is necessary to truncate the infinite range of the integral to some finite value, say $(-\Omega, \Omega)$. This truncation gives rise to Gibb's oscillations, which are suppressed by using the Lanczos Sigma factor, defined by

$$\sigma = \frac{\sin(\pi\omega/\Omega)}{(\pi\omega/\Omega)} \qquad (3.21)$$

With these modifications incorporated, and after some manipulation [116], equation (3.20) becomes

$$f(t) = \frac{2\exp(at)}{\pi} \int_{0}^{\Omega} \sigma P \cos\omega t \, d\omega \qquad (3.22)$$

where $P = Re[\overline{f}_+(a+j\omega)]$

Normally, the value of the function is required at several instants of time. In such a case, P_k^i s can be computed beforehand and stored.

3.5 EVALUATION OF THE TRANSMISSION LINE PARAMETERS

The capacitances and shunt conductance are voltage dependent, whilst the inductances and series resistance are frequency dependent. The general effect of corona discharge is to increase the capacitances and the conductance to earth. There is no quantitative information available at present to determine this effect in the case of multiconductor lines [116]. Accordingly, the capacitances are assumed to be independent of voltage in the present work. The conductance to earth is neglected. The self and mutual capacitances are determined by the potential coefficient method.

The frequency dependent series self and mutual impedances of the phase conductors and earth wires are determined by using the formulae given in reference [116]. Although these formulae permit the consideration of a stratified earth, the earth is considered only as a single layer in this work. The presence of earth wires in the final mathematical formulation is eliminated by mathematical manipulation with the assumption that the potential of the earth wires is zero. A computer programme is developed for the above. It is used as a subroutine in the main programme

which is used for the computation of relaying-point

voltages and currents.

3.6 NUMERICAL EXAMPLES

The application of the fault analysis techniques

developed is demonstrated by considering two sample power

systems, and by determining the relaying-point voltages and

currents for 3-phase and one-phase-to-ground faults.

3.6.1 Three-Bus Power System

The 3-bus power system, given in reference [117] and

reproduced in Fig. 3.6, is considered with the following

change. A 400 KV quad conductor three-phase single-circuit

transmisssion line, whose tower configuration and conductor

spacings are given in Fig. 3.7, is considered instead of

that given in the reference. An earth resistivity of

100 ohm-m is assumed. Other basic data of the line are

given in Appendix B. Identical (generator) sources are

considered at buses 1 and 2. The data of these sources

are given in Appendix C. The faults are simulated at bus 3.

Under these conditions, the one-line diagram of the equivalent

network of the system, suitable for computing the fault-

generated components, would be as shown in Fig. 3.8 where

A_1, B_1, C_1, D_1 are the matrices of the frequency-domain trans-

mission line constants for a length of 200 km and A_2 to D_2,

for a length of 100 Km. The bus admittance matrix can be

written by inspection as shown below.

EW – Earth wire
a,b,c – Phase conductors
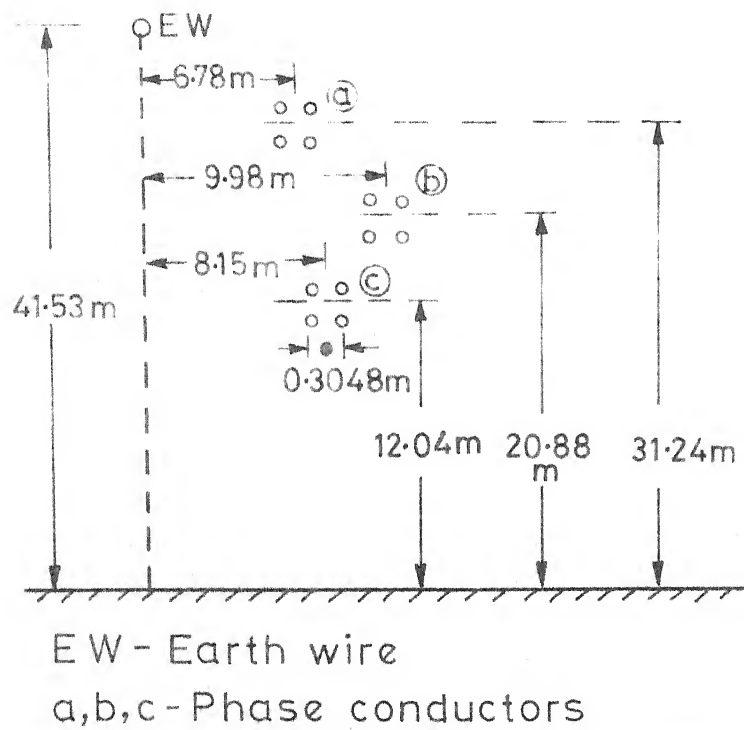
FIG.3·7. 400 KV TRANSMISSION LINE SPACINGS
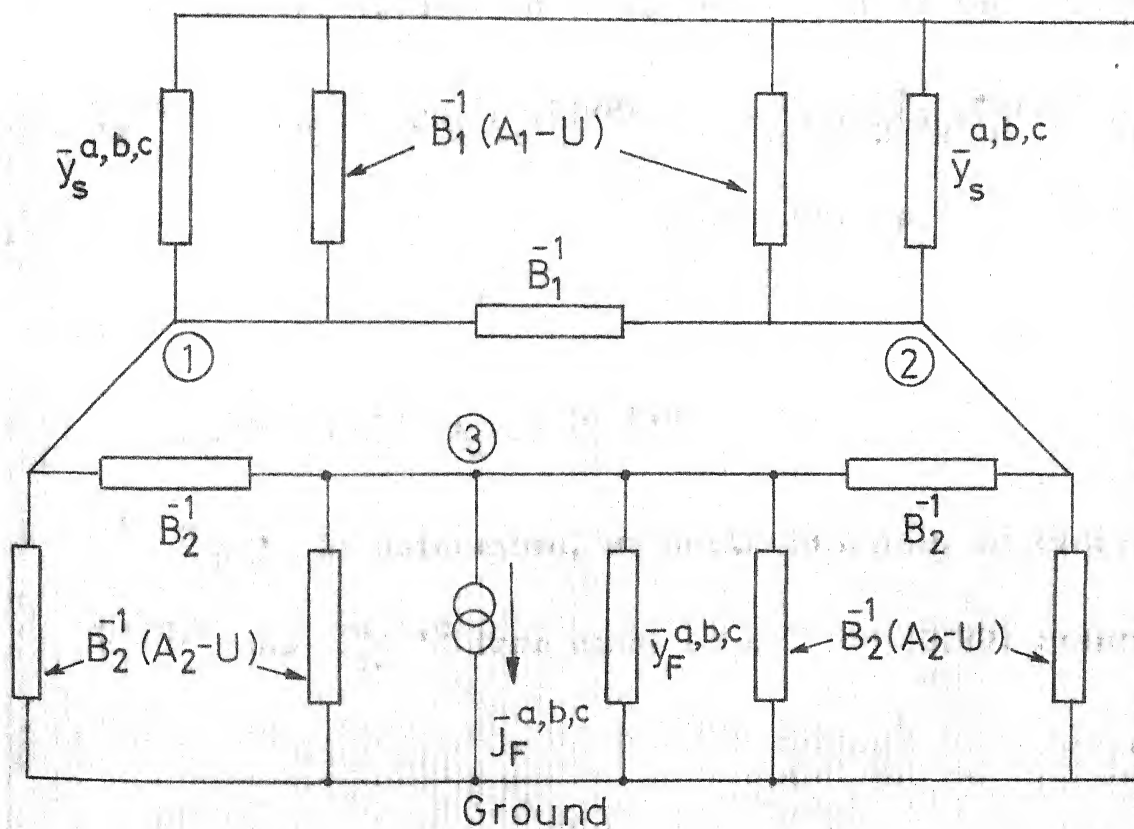
FIG.3·8 ONE-LINE DIAGRAM OF THE EQUIVALENT
NETWORK OF 3-BUS POWER SYSTEM

$$
\overline{Y}_{BUS}^{a,b,c} = \begin{array}{ccc} \quad\quad 1 & \quad\quad 2 & \quad\quad 3 \end{array}
$$

$$
\overline{Y}_{BUS}^{a,b,c} = \begin{array}{c} 1 \\ 2 \\ 3 \end{array}
\begin{bmatrix}
B_1^{-1}A_1+B_2^{-1}A_2+\overline{Y}_s^{a,b,c} & -B_1^{-1} & -B_2^{-1} \\
-B_1^{-1} & B_1^{-1}A_1+B_2^{-1}A_2+\overline{Y}_s^{a,b,c} & -B_2^{-1} \\
-B_2^{-1} & -B_2^{-1} & 2B_2^{-1}A_2+\overline{Y}_F^{a,b,c}
\end{bmatrix}
$$

(3.27)

The frequency-domain voltages and currents at the relaying point, considered at bus 1 on the line connecting buses 1 and 2, are determined from the following equations, which are obtained from the solution of the nodal equations of the system.

$$
\overline{V}_1^{a,b,c} = [2B_2^{-1}-(2B_2^{-1}A_2+\overline{Y}_F^{a,b,c})B_2(B_1^{-1}A_1+B_2^{-1}A_2+\overline{Y}_s^{a,b,c}-B_1^{-1})]^{-1} \times
$$

$$
\overline{Y}_F^{a,b,c}\; \overline{V}_{FF}^{a,b,c} \qquad\qquad (3.28)
$$

and

$$
\overline{I}_{12}^{a,b,c} = B_1^{-1}\,(A_1-U)\,\overline{V}_1^{a,b,c} \qquad\qquad (3.29)
$$

$\overline{V}_{FF}^{a,b,c}$ is determined, as outlined below, in order to compute $\overline{V}_1^{a,b,c}$ and $\overline{I}_{12}^{a,b,c}$ from eqns. (3.28) and (3.29) respectively.

(i) 3-phase symmetrical fault.

For this fault,

$$\overline{V}_{FF}^{a,b,c} = \overline{V}_{PF}^{a,b,c} \qquad [\text{vide, eqn. (3.10)}]$$

$$= \begin{bmatrix} V_m[s \, \sin\varphi_o + \omega_o \cos\varphi_o]/(s^2 + \omega_o^2) \\ V_m[s \, \sin(\varphi_o - 120^\circ) + \omega_o \cos(\varphi_o - 120^\circ)]/(s^2 + \omega_o^2) \\ V_m[s \, \sin(\varphi_o + 120^\circ) + \omega_o \cos(\varphi_o + 120^\circ)]/(s^2 + \omega_o^2) \end{bmatrix} \qquad (3.30)$$

where

V_m - peak value of the prefault voltage at the fault bus,

ω_o - nominal angular frequency of the system,

φ_o - fault initiation angle

and $s \rightarrow (a + j\omega)$, the modified Fourier transform parameter.

(ii) One-phase-to-ground fault on phase 'a'.

For the sample system, the matrix $\overline{Z}^{a,b,c}$, as defined by eqn. (3.14), is given by

$$\overline{Z}^{a,b,c} = \overline{Z}_F^{a,b,c} + [2B_2^{-1}A_2 - 2B_2^{-1}(B_1^{-1}A_1 + B_2^{-1}A_2 + \overline{Y}_s^{a,b,c} - B_1^{-1})B_2^{-1}]^{-1}$$

$$(3.31)$$

Using eqn. (3.16) in conjunction with the above matrix, $\overline{V}_{FF}^{a,b,c}$ is determined.

Assuming V_{max} as equal to 1.0 p.u. for both the types
of faults and employing inverse transform techniques, des-
cribed in Section 3.4, the time-domain values of the relaying-
point voltages and currents are evaluated. For this purpose,
the following values, for the parameters associated with the
inverse transformation, are chosen.

$$\Omega = 60,000, \quad a = 750, \quad n = 500 \quad \text{and time step} = 0.05 \text{ ms}$$

The results obtained, for $\varphi_0 = 0^\circ$ and $R_f = 100$ Ohms,
are plotted in Figs. 3.9 and 3.10, with the phase voltage and
line current bases chosen as equal to $400\sqrt{2}/\sqrt{3}$ KV and
600 KA respectively.

3.6.2 Four-Bus Power System

The 4-bus power system, given in reference [3] and
reproduced in Fig. 3.11, is considered without any modifica-
tion. The tower configuration, conductor spacings and other
basic data of the transmission lines of the present system
are the same as those of the previous system and also as
given in the above reference. All the lines are of 128 Km
length, and an earth resistivity of 100 Ohm-m is assumed.
In this case, the sources are represented by fault levels at
the corresponding buses [3]. The fault levels are converted
to equivalent circuits as explained in Appendix D. A ratio
of zero sequence impedance to positive sequence impedance,
equal to 0.5 at 50 Hz, is assumed for this purpose.
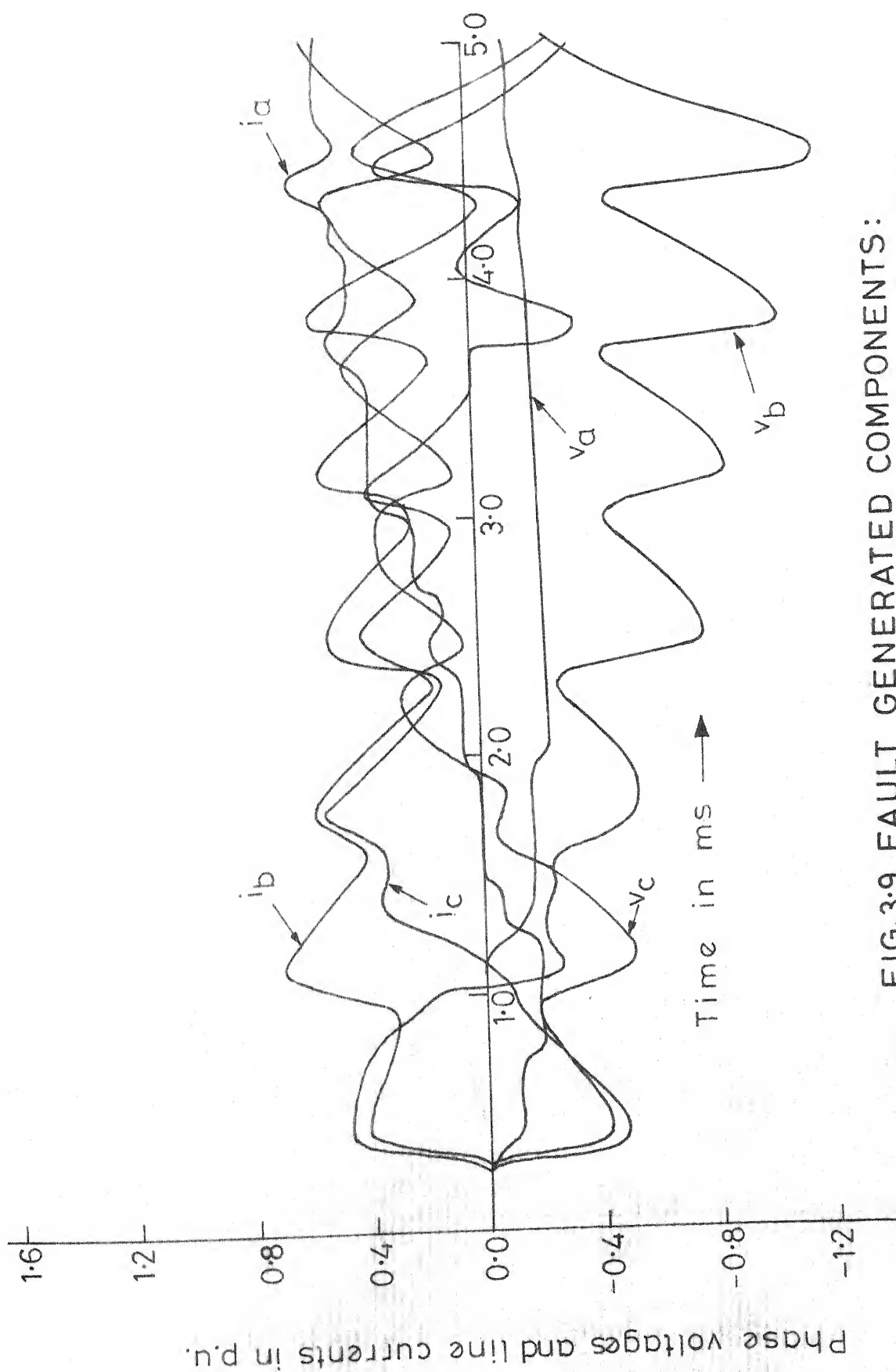
FIG.3·9 FAULT GENERATED COMPONENTS:
3-BUS POWER SYSTEM: 3-PHASE FAULT
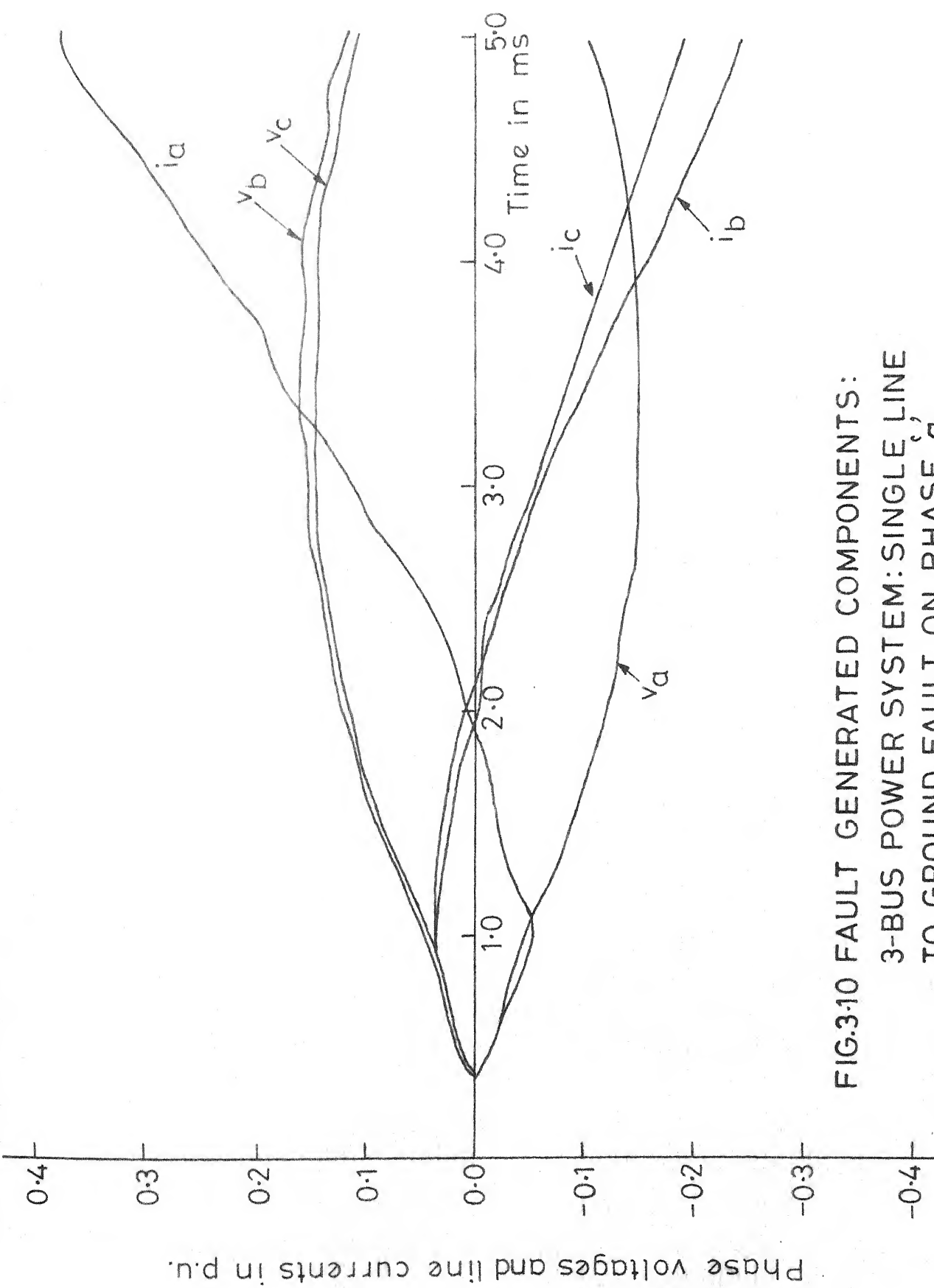
FIG.3·10 FAULT GENERATED COMPONENTS:
3-BUS POWER SYSTEM: SINGLE LINE
TO GROUND FAULT ON PHASE a
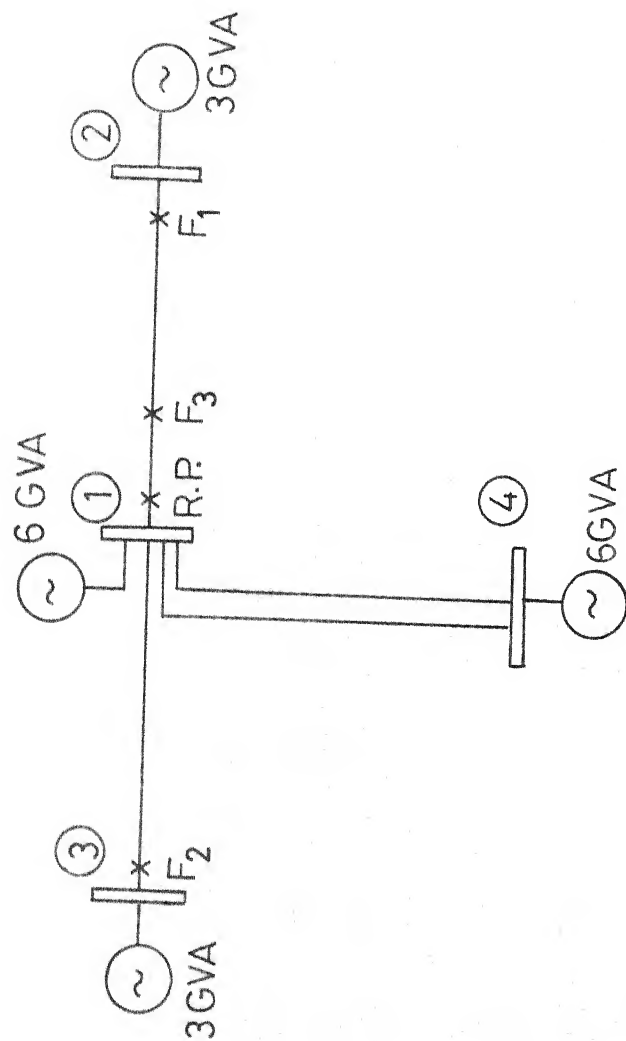
R.P.-Relaying point

Figures with GVA refer to short circuit levels

FIG. 3·11 A SAMPLE 4-BUS POWER SYSTEM

The faults are assumed to occur, at a distance of 25.6 Km from bus 1, on the line connected between buses 1 and 2. Under these conditions, the one-line diagram of the equivalent network of the system, suitable for computing the fault generated components, would be as given in Fig. 3.12, where A_1 to D_1, A_2 to D_2 and A to D are the matrices of the frequency domain line constants for lengths of 25.6 Km, 102.4 Km and 128.0 Km respectively. The bus admittance matrix can be written by inspection as shown, in eqn. (3.32), given on the next page.

Solution of the nodal equations of the system gives the voltage and current transforms at the relaying point which is considered at bus 1 on the line connected between buses 1 and 2. They are given below.

$$\overline{V}_1^{a,b,c} = M_5 B_1^{-1} M_4 \overline{Y}_F^{a,b,c} \, \overline{V}_{FF}^{a,b,c} \tag{3.33}$$

where

$$M_5 = [B^{-1}M_1 + 2B^{-1}M_2 - M_3 + B_1^{-1}M_4 B^{-1}]^{-1}$$

$$M_4 = [B_1^{-1}A_1 + B_2^{-1}A_2 + \overline{Y}_F^{a,b,c} - B_2^{-1}(A_2 + B_2 \overline{Y}_{s_1}^{a,b,c})^{-1}]^{-1}$$

$$M_1 = (A + B \, \overline{Y}_{s_1}^{a,b,c})^{-1}$$

$$M_2 = (A + 0.5B \, \overline{Y}_{s_2}^{a,b,c})^{-1}$$

and $M_3 = (3B^{-1}A + B_1^{-1}A_1 + \overline{Y}_{s_2}^{a,b,c})$

And, $\overline{I}_{12}^{a,b,c} = B_1^{-1} (A_1 \overline{V}_1^{a,b,c} - \overline{V}_5^{a,b,c})$ \hfill (3.34)
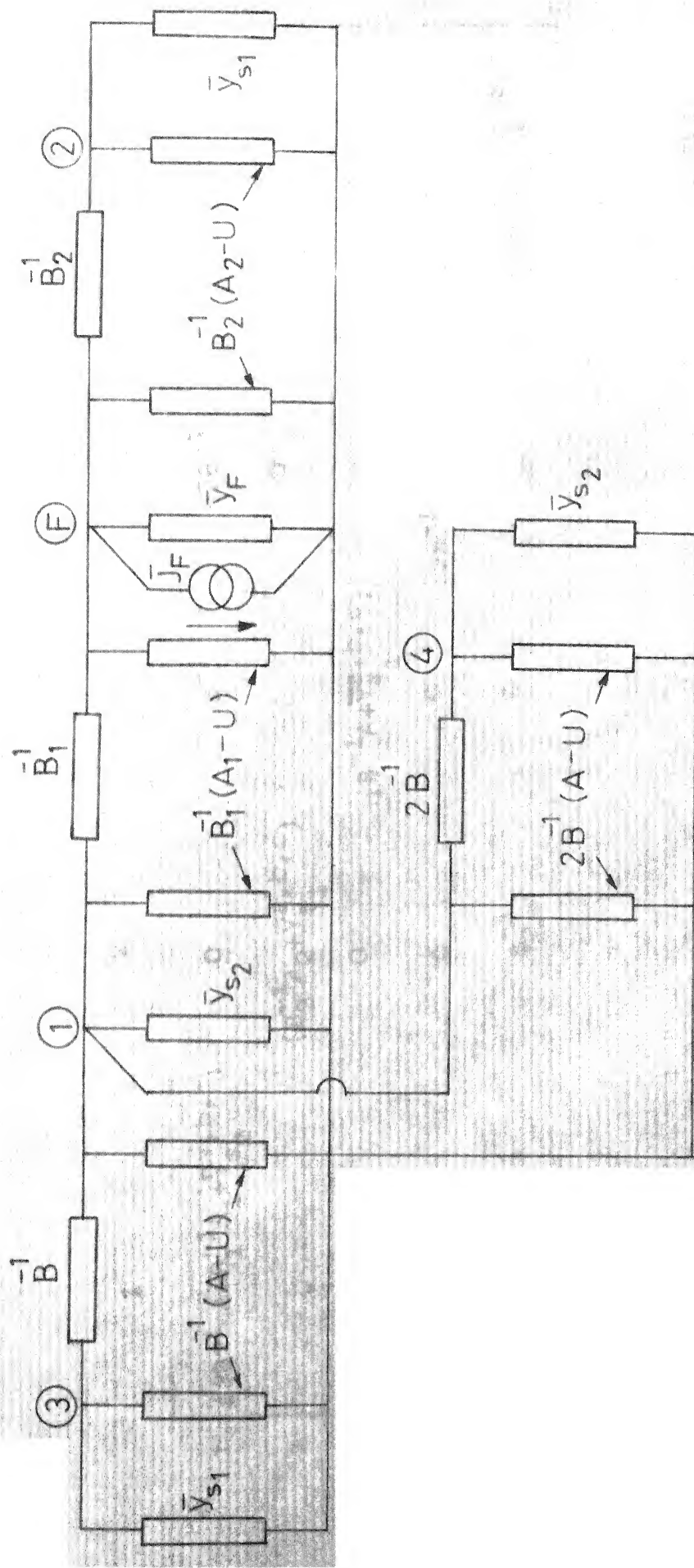
FIG.3.12 ONE-LINE DIAGRAM OF THE EQUIVALENT NETWORK
OF 4-BUS POWER SYSTEM

$$\overline{Y}^{a,b,c}_{BUS} = \begin{array}{c} \\ 1 \\ 2 \\ 3 \\ 4 \\ F \end{array}
\begin{array}{ccccc}
1 & 2 & 3 & 4 & F \\
(3B^{-1}A+B_1^{-1}A_1+\overline{Y}^{a,b,c}_{s_2}) & 0 & -B^{-1} & -2B^{-1} & -B_1^{-1} \\
0 & (B_2^{-1}A_2+\overline{Y}^{a,b,c}_{s_1}) & 0 & 0 & -B_2^{-1} \\
-B^{-1} & 0 & (B^{-1}A+\overline{Y}^{a,b,c}_{s_1}) & 0 & 0 \\
-2B^{-1} & 0 & 0 & (2B^{-1}A+\overline{Y}^{a,b,c}_{s_2}) & 0 \\
-B_1^{-1} & B_2^{-1} & 0 & 0 & (B_1^{-1}A_1+B_2^{-1}A_2+\overline{Y}^{a,b,c}_F)
\end{array}$$

(3.32)

where $\overline{V}_5^{a,b,c} = M_4(B_1^{-1} \overline{V}_1^{a,b,c} - \overline{Y}_F^{a,b,c} \overline{V}_{FF}^{a,b,c})$

$\overline{V}_{rr}^{a,b,c}$, required in the equations above, is determined as outlined below.

i)   3-phase Symmetrical fault

$\overline{V}_{FF}^{a,b,c}$ is given by eqn. (3.30)

ii)   One-phase-to-ground fault on phase 'a'.

The matrix $\overline{Z}^{a,b,c}$ is given by

$$\overline{Z}^{a,b,c} = \overline{Z}_F^{a,b,c} + [B_1^{-1}A_1 + B_2^{-1}A_2 - B_2^{-1}(A_2 + B_2\overline{Y}_{s_1}^{a,b,c})^{-1} - M_6]^{-1}$$

$$(3.35)$$

where

$$M_6 = [B_1(M_3 - B^{-1}M_1 - 2B^{-1}M_2)B_1]^{-1}$$

As in the previous case, $\overline{V}_{FF}^{a,b,c}$ is computed using eqn. (3.16) in conjunction with the above matrix, $\overline{Z}^{a,b,c}$.

For both the faults, V_{max} is assumed to be 1.0 p.u., R_f as 0.00001 and $\varphi_0 = 90^{\circ}$. The time-domain values are obtained by using the following values for the parameters associated with the inverse modified Fourier transformation.

$\Omega = 10^5$, $a = 1000.0$, $n = 500$ and $\Delta t = 0.05$ ms.

The results obtained are plotted in Figs. 3.13 and 3.14, with the bases chosen as given below

$$\text{Phase voltage} = \frac{400\sqrt{2}}{\sqrt{3}} \text{ KV}$$

$$\text{Line current} = 10 \text{ KA}$$
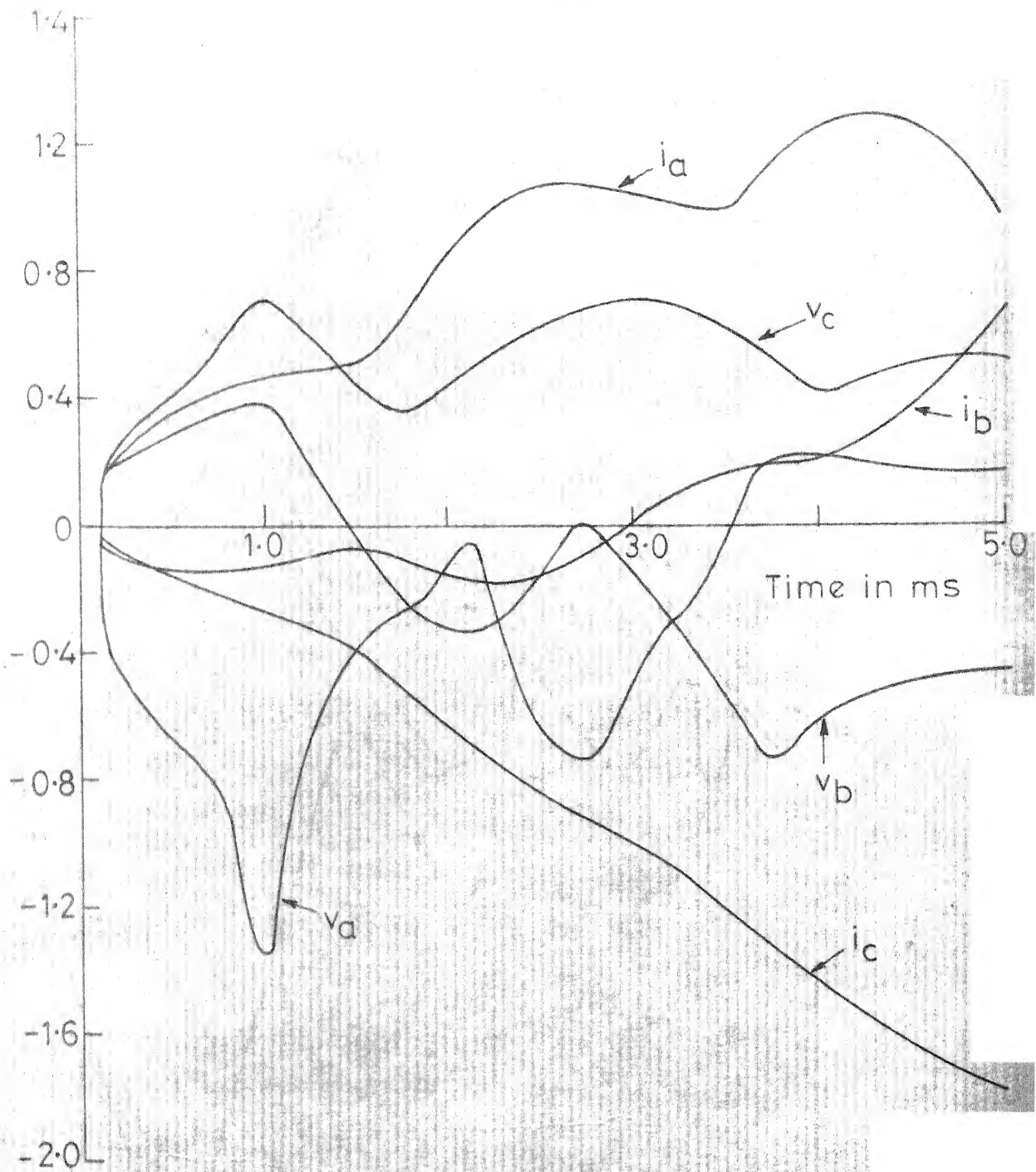
FIG.3·13 FAULT-GENERATED COMPONENTS:
4-BUS SYSTEM: 3-PHASE FAULT
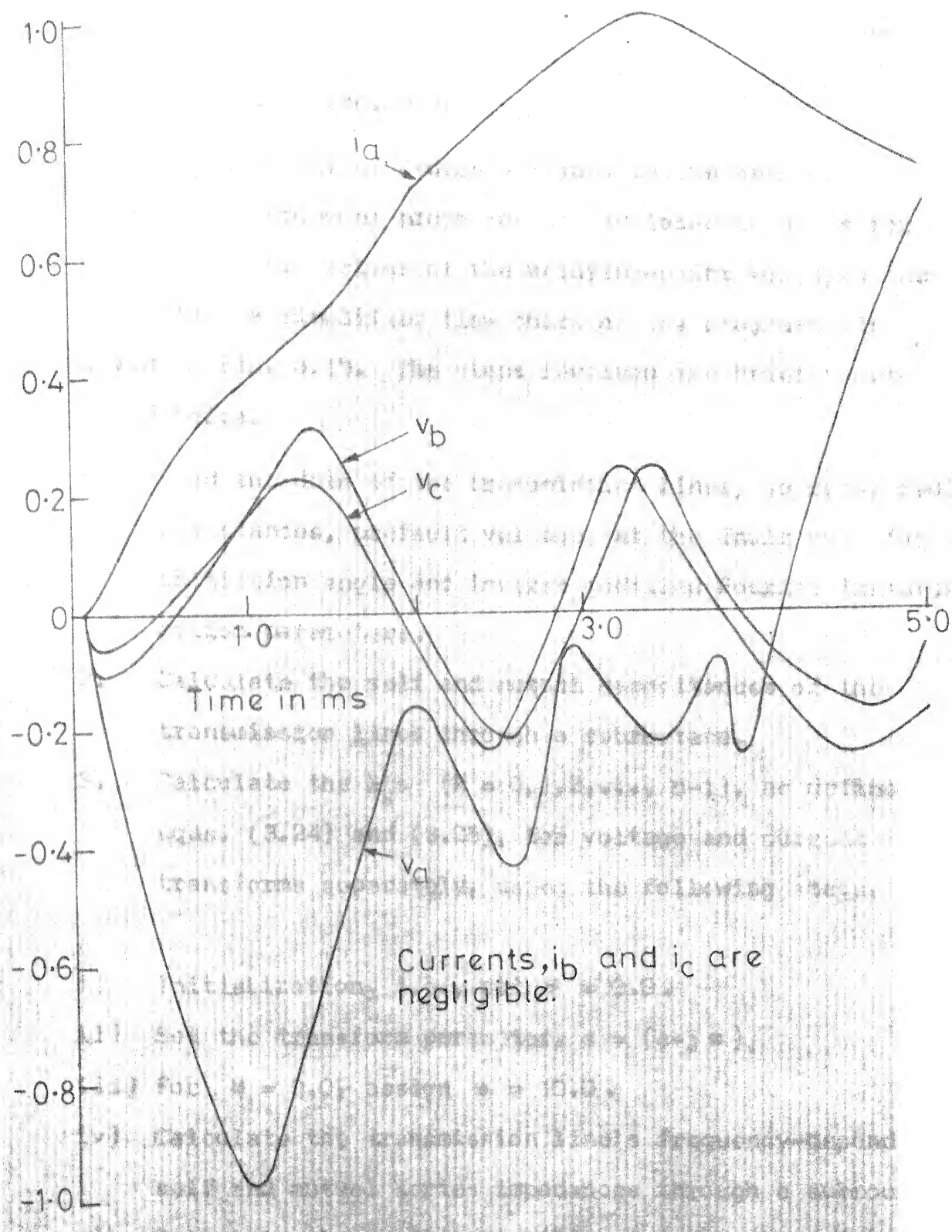
FIG.3.14 FAULT-GENERATED COMPONENTS:
4-BUS SYSTEM: SINGLE LINE TO
GROUND FAULT ON PHASE 'a'

3.6.3 Computer Programme

Based on the procedure outlined in the earlier sections, a computer programme is developed to solve for the time domain values of the relaying-point voltages and currents. A simplified flow chart of the programme is given in Fig. 3.15. The steps involved are briefly outlined below.

1. Read the data of the transmission lines, sources, fault resistances, prefault voltages at the fault bus, fault initiation angle and inverse modified Fourier transformation parameters.

2. Calculate the self and mutual capacitances of the transmission lines through a subroutine.

3. Calculate the P_k's ($k = 0, 1, 2, \ldots, n-1$), as defined in eqns. (3.24) and (3.25), for voltage and current transforms separately, using the following steps.

i) Initialization, i.e., set $\omega = 0.0$.

ii) Set the transform parameter, $s = (a+j\omega)$.

iii) For $\omega = 0.0$, assign $\omega = 10.0$.

iv) Calculate the transmission line's frequency-dependent self and mutual series impedances through a subroutine.

v) Calculate the resistances (R) and inductances (L) of the line from the above.

vi) When $\omega = 10.0$, take $\omega = 0.0$.

START

Read the data of transmission lines, sources, fault resistances, prefault voltages at the fault location, post fault initiation angle and inverse modified forced transform parameters.

Calculate the self and mutual capacitances of the transmission line

Set the iteration count k=1

Initialisation: ω=0·0

s=(a+jω)

Is k=1?
yes → ω=10·0
NO

Calculate self & mutual impedances of the line

Calculate self and mutual resistances and inductances of the line

Is k=1?
yes → ω=0·0
NO

Calculate Z_L and Y_L matrices as a function of s

Calculate eigenvalues and eigen vectors of ($\bar{Z}_L^{a,b,c}$, $\bar{Y}_L^{a,b,c}$)

Calculate S and Q

Calculate the A,B,C,D parameters of the line as a function of s

Calculate the source admittances as a function of s

Calculate the voltages and currents of interest using the appropriate equations

Calculate P_k's for all the voltages and currents of interest by using equations 3·24 & 325 and store them

Increment ω: ω=ω+Δω

Test k=n
NO → Advance iteration count,k=k+1
yes

Using eqn.(326), compute the time domain values of the voltages & currents at all the desired instants of time

Print results

STOP

FIG-3·15 FLOW CHART FOR COMPUTING VOLTAGES AND CURRENTS AT A DESIRED POINT IN A POWER SYSTEM

vii) Calculate the per unit length series impedance $\overline{Z}_L^{a,b,c}$ and shunt admittance $\overline{Y}_L^{a,b,c}$ of the line as a function of s.

viii) Calculate the eigenvalues and eigenvectors of the matrix $(\overline{Z}_L^{a,b,c}, \overline{Y}_L^{a,b,c})$ through a subroutine.

ix) Calculate the voltage and current modal transformation matrices, S and Q.

x) Calculate the frequency-domain A,B,C,D parameters of the line.

xi) Calculate the source admittances as a function of s.

xii) Calculate the relaying-point voltage and current transforms using appropriate equations.

xiii) Calculate P_k's for the above, using equations (3.24) and (3.25).

xiv) Increment ω by $\Delta\omega = \Omega/n$ and go to step 3 (ii).

4. Using eqn. (3.26), compute the time-domain values of the voltages and currents at all the desired instants of time.

The steps 3 (iii) and 3 (vi) are necessitated by the fact that the frequency-dependent series self and mutual impedances of the line cannot be evaluated at $\omega = 0.0$ by the formulae given in reference [116]. Hence, they are evaluated at an angular frequency close to zero. Subroutines have been employed also for complex matrix inversion as well as multiplication.

3.7 APPLICATION OF FAST FOURIER TRANSFORM

The fast Fourier transform (FFT) technique, which requires much less computation time, was first developed by Cooley and Tukey [121] and later, its applications were discussed by Cooley, Lewis and Welch [122]. Application of this technique to the computation of electrical transients was described by Ametani [123], who showed that considerable saving in computation time could be achieved in this way. However, it is shown that the application of FFT to the computation of power system transients, especially those under short-circuit conditions used for assessing or predicting the performance of high speed and ultra high speed protective relays, does not yield as much computational benefit as was reported [123]. It is also shown that the application of this technique imposes certain restrictions. Accordingly, this technique is not used in this work while the time-domain values are computed.

3.7.1 Problem Formulation

In order to apply the FFT algorithm, equation (3.26) has to be rewritten as given below.

$$f(r. \Delta t) = \frac{2 \Delta \omega}{\pi} \exp(a. \Delta t.r) \text{ Re } [\sum_{k=0}^{n-1} F_k \exp(j \frac{2\pi}{n} kr)];$$

$$r = 0,1,2 , ..., (m-1) \qquad (3.36)$$

where

$$F_k = (P'_k + j0)$$

n = number of frequency-domain samples

and   m = number of time-domain samples.

The above equation is modified as follows :

$$f(r. \Delta t) = \frac{2 \Delta \omega}{\pi} \exp(a. \Delta t.r).Re[\sum_{i=0}^{p-1} \left\{ \sum_{k=0}^{m-1} F_{pk+i} \cdot \right.$$

$$\left. \exp(j \frac{2\pi}{m} kr) \right\} \times \exp(j \frac{2\pi}{n} ir)]$$

$$= \frac{2 \Delta \omega}{\pi} \exp(a. \Delta t.r).Re[\sum_{i=0}^{p-1} B_r^{(i)} . \exp(j \frac{2\pi}{n} ir)] ;$$

$$r = 0,1, ..., (m-1). \hspace{2cm} (3.37)$$

where

$$B_r^{(i)} = \sum_{k=0}^{m-1} F_{pk+i} \exp(j \frac{2\pi}{m} kr) ; r = 0,1, ..., (m-1)$$

$$(3.38)$$

and p = n/m, an integer.

First, $B_r^{(i)}$'s are calculated by using the programme given by Ametani [123]. Next, f(r. Δt) is calculated for r = 0,1, ..., (m-1) by using equation (3.37). The following observations can be made with regard to the application of the FFT algorithm.

1. Complex arithmetic is involved because of the terms,

    $\exp(j \frac{2\pi}{m} kr)$ and $\exp(j \frac{2\pi}{n} ir)$.

2. For the most efficient utilization of the algorithm, m
    should be equal to 2^q where q is an integer. This
    imposes a restriction on the number of time steps,
    which can be chosen, if the algorithm were to be
    utilized most efficiently.

3. There is a blanket restriction on the choice of the time
    step Δt, as explained below.

    Comparing equations (3.26) and (3.36), we get

$$\Delta\omega \cdot \Delta t = \frac{2\pi}{n} \quad \text{or} \quad \Delta t = \frac{2\pi}{n \cdot \Delta\omega} = \frac{2\pi}{\Omega} \qquad (3.39)$$

The choice of Ω depends on the problem on hand [116].
Therefore, once a value is chosen for Ω, then Δt is
fixed by virtue of equation (3.39). If we are interested in
computing f(t) at intervals of (2. Δt) only, then we would
be unnecessarily calculating double the number of values of
f(t). On the other hand, if we use equation (3.26) directly
for the computation of f(t), then we can choose any conve-
nient and necessary value of Δt.

3.7.2 Numerical Example and Results

For the sake of comparison, a numerical example is
worked out, with the aid of the digital computer DEC
System 1090 at I.I.T., Kanpur, to determine separately the

time required for the computation of the frequency-
domain values and that required for the computation of
time-domain values when equation (3.26) is used (direct
method), and when equations (3.37) and (3.38) are used
(FFT method). For this purpose, a 200 Km, 3-phase, single-
circuit, 400 KV, quad-conductor transmission line, inter-
connecting two large power networks, is considered. The
tower configuration, conductor spacings and other basic
data of the line are given in Fig. 3.7 and Appendix B.
The earth resistivity is assumed as equal to 100 ohm-m.
The sending and receiving end source networks are assumed
as resistive, having resistances equal to 1/9th and 1/4th
respectively of the real part of the appropriate modal
surge impedances. The frequency dependency of the line
parameters and the untransposed nature of the line are not
disregarded. For a single-line-to-ground fault on phase 'a'
at the receiving end of the line with the assumption that the
prefault peak voltage at the fault point is 1.0 p.u., the
frequency-domain values of the fault-generated components
of all the phase voltages and line currents at the sending
end of the line for various desired frequencies are computed,
multiplied with the sigma factor and stored. Then, the time-
domain values are computed for various conditions, using the
following data.

$$n = 512,1024; \quad \Omega = 62831.8 \text{ rad/s}; \quad a = 750$$

$$m = 32,64,128,256,512,1024$$

and number of functions evaluated $=1,3,6$.

The computation time taken has been determined by running the programmes on the DEC System 1090 computer at I.I.T., Kanpur, and the results are given in Tables 3.1 and 3.2.

3.7.3 Discussion on the Results

The results given in Table 3.1 show that the FFT algorithm is not as fast as it has been claimed. For example, when n = m = 1024, the theoretical value of the ratio of the computation times needed by the direct method and the FFT method would be 51 as given by Ametani, whereas it has come to be only 21.507 in this work. The reason for this difference is that Ametani has employed the complex equivalent of equation (3.26) in his studies. However, the equation (3.26), which involves only real arithmetic, can easily be rewritten in a form, suitable for the application of FFT, as described in Section 3.7.1.

From the results given in Table 3.2, it can be observed that the relative computational relief provided by the FFT algorithm would be only marginal when the number of time-domain samples required is small. Generally, either for designing or for predicting the performance of high speed and ultra high speed protective relays, the time-domain samples are not needed for more than 1 cycle. And, with a CVT of cut-off frequency of 2.5 KHz, the sampling interval should be at least 200 μs. Therefore, the sampling interval

TABLE 3.1

Comparison of computation time in seconds taken by (i) direct method (t_1) and (ii) using the FFT algorithm (t_2). No. of frequency samples = 1024

No. of time samples	Computation times	Number of functions evaluated		
		1	3	6
32	t_1	3.641	4.876	6.776
	t_2	1.957	3.332	5.465
	t_1/t_2	1.861	1.463	1.240
64	t_1	6.030	7.849	10.484
	t_2	2.083	3.619	5.785
	t_1/t_2	2.895	2.169	1.812
128	t_1	10.787	13.789	18.349
	t_2	2.144	3.779	6.290
	t_1/t_2	5.031	3.649	2.917

Table 3.1 (contd ...)

No. of time samples	Computation times	Number of functions evaluated		
		1	3	6
256	t_1	20.098	25.379	33.177
	t_2	2.430	4.156	6.796
	t_1/t_2	8.271	6.107	4.882
512	t_1	39.039	48.762	63.437
	t_2	2.743	4.737	7.544
	t_1/t_2	14.232	10.294	8.409
1024	t_1	76.697	95.553	124.105
	t_2	3.501	5.367	8.398
	t_1/t_2	21.907	17.804	14.778

TABLE 3.2

Comparison of the computation times required for the evaluation of the frequency-domain and time-domain samples

Number of functions evaluated = 6.

Frequency-domain samples		Time-domain samples		
Number	Computation time (seconds)	Number	Computation time (seconds)	
			Direct method (t_1)	Using FFT algorithm (t_2)
512	341.929	256	16.916	4.352
		512	32.302	4.925
1024	682.410	256	33.177	6.796
		512	63.437	7.544
		1024	124.105	8.398

of 100 μs, chosen in the present numerical example, is more than adequate. With this sampling rate, the number of time-domain samples (m) required for one cycle would be 200. Under such circumstances, the FFT algorithm provides only marginal relief. For example, for n = 512 and m = 256, the time required for the computation of frequency-domain samples was 341.929 seconds, whilst that required for the computation of time-domain samples was 16.916 seconds by the direct method, and 4.352 seconds by the FFT method. Thus, the overall computation time has decreased from 358.845 to 346.281 seconds only.

3.8 CONCLUSIONS

In this chapter, two new contributions have been made; the frequency-domain fault analysis of multinode power systems using bus admittance matrix, and the development of a frequency-domain Pi model for a transmission line, suitable for this analysis. The viability of the fault analysis techniques has been demonstrated by employing them to the computation of relaying-point voltages and currents in two sample power systems. Although the sample power systems considered are relatively simple, the application of these techniques to larger systems would be a matter of straightforward extension.

In the nodal method using bus impedance matrix, the bus impedance matrix has to be formed for a large number of frequencies and stored. In cases, where this imposes

restrictions on computer memory,the analysis developed
in this chapter can be employed. The computation of
relay voltages and currents is hardly needed over more
than half a cycle in developing ultra high speed relays.
Consequently, the frequency-domain method of computation,
which is most accurate, can be employed without undue
computational effort being necessary. An accurate model
for the transmission lines has been used. And, the
choice of source models has been based on the practices
available in the literature.

The application of the FFT technique to the computation
of transients, in electrical power systems under short circuit
conditions, does not provide appreciable computational relief
when the fault data is needed only for a short period. The
results of a numerical example have confirmed this fact.

CHAPTER   4

TRAVELLING WAVE RELAYING OF EHV/UHV TRANSMISSION
LINES

4.1 INTRODUCTION

The ultra high speed (u.h.s.) clearing of faults improves
the transient stability of a power system because the tran-
sient rotational kinetic energy introduced into the system
is proportional to the square of the fault clearing time
[72]. As a matter of fact, the u.h.s. clearing of faults at
any location, particularly on ehv/uhv Intertie lines and
close to large sources of generation, will reduce the system
acceleration more than any other form of dynamic control
which can be used only after the system is being accelerated.
The fault clearing time depends on the speed of both the
protective relay and the associated circuit breaker. With
the development of u.h.s. circuit breakers in the recent
past [1,2], attention is now focussed on the development
of u.h.s. protective relays. The development of u.h.s.
protective relays has been possible with the utilization of
the travelling wave phenomena.

Quite a few authors have reported about the development
of u.h.s. protective relays based on travelling wave pheno-
mena. After the occurrence of a fault, the voltage and
current at any point in a power system can be regarded as the

sum of prefault and fault-generated components. The fault-generated components manifest themselves as travelling waves during the first few milliseconds after the occurrence of a fault. The relaying schemes developed so far, utilize these travelling waves for fault detection.

Takagi et al. [80,81] and Akimoto et al. [82,83] defined a relaying signal, which is formed from the sending and receiving end voltages and currents and also, the surge impedance of the line. This relaying signal is zero if no internal fault exists, and is finite if an internal fault exists. For the protection of three-phase lines, the modal components of voltages and currents, and appropriate modal surge impedances are used. Also, three relaying signals, one for each mode, are employed. This is a differential protection scheme. Its demerit is that it requires the exchange of quantitative information between the ends of the protected line.

They have also proposed two fault location schemes. In one scheme, a discriminant, which is a function of sending end quantities at two different instants of time and also, the surge impedance of the line, is used. In the other, the discriminant is a function of both the sending and receiving end quantities. In both the schemes, the fault location involves the determination of the two time instants which would make the discriminant zero. The time interval between

these two instants is a function of travel time of the waves between the relaying and fault points. But, these schemes are too involved to be easily realisable.

Yee and Esztergalyos [72], Chamia and Liberman [73], Esztergalyos et al. [74], Matele [75] and Carter [76] have reported about the development, design, application and operational experience of an u.h.s. relaying scheme. It has been developed by ASEA, Sweden, and tested on BPA's (Bonneville Power Administration, U.S.A.) 500 KV system. It needs the exchange of only qualitative information between the ends of the protected line. Consequently, it places less demanding requirements on the communication channel. It is basically a directional comparison scheme. In this scheme, the fault-generated components of the voltage and current of the first travelling waves reaching the relaying point are used to determine the direction to the fault. These components are of opposite sign for a fault ahead of the relaying point, and are of the same sign for a fault behind. Thus, only for an internal fault, they are of opposite sign at both the ends of the protected line.

Vitins [71] has developed a method, by means of which the location of the fault can be determined through a time delay equal to twice the travel time of the travelling waves between fault and relaying points. He has elaborated the application of a correlation technique for the determination of this time delay.

Johns [77] and Johns and Aggarwal [78] have reported about the development of an u.h.s. directional comparison relaying scheme. They have employed three pairs of relaying signals, one for each propagation mode. The signals of each pair are formed from the corresponding modal components of the fault-generated components of relaying-point voltages and currents. The direction to the fault is determined by the sequence in which the relaying signals of each mode exceed a preset level. The qualitative information about the direction to the fault is exchanged through a carrier communication channel.

Vitins [85] has proposed a similar approach for determining the direction to the fault. In this scheme also, the direction to the fault is determined by the sequence in which two relaying signals exceed a threshold level. However, there are two basic differences. A geometric approach has been employed to determine the above sequence. The three-phase protection has been provided with three signal pairs as in the previous scheme. But, the signals of a pair are formed from the fault-generated components of a phase voltage and the corresponding line current, in the present case.

Ramamoorty and Verma [84] described a relaying principle in which a discriminant is used to determine the direction to the fault. The discriminant is a function of fault-

generated backward-wave voltage and current. It exceeds a preset value for an internal fault.

With a view to provide simpler and reliable alternatives, two new relaying schemes, which utilize the characteristics of the travelling waves for detecting faults, are developed. One scheme is based upon the amplitude comparison of two relaying signals. The other scheme utilizes the reflection properties of the travelling waves to provide the fault locating capability. The relaying principles, involved in these two schemes, are validated by the results obtained from the digital computer simulation of faulted sample e.h.v. power system networks.

4.2 AMPLITUDE COMPARISON RELAY SCHEME

In this section, a relaying scheme, based upon travelling wave phenomena, whose operation depends upon the amplitude comparison of two input signals, is developed. The results of the digital simulation of faults in a 4-bus system, which confirm the validity of the relaying principles involved, are presented.

4.2.1 Principles of Operation

The underlying principles of the relay can be best explained by reference to a single-phase transmission line interconnecting two large power systems as shown in Fig. 4.1. Their extension to three-phase lines is explained in the next section. After the occurrence of a fault, the voltage and
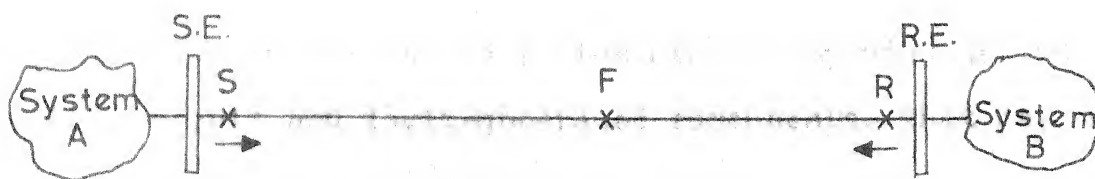
FIG·4·1 A TRANSMISSION LINE INTERCONNECTING
TWO POWER SYSTEMS
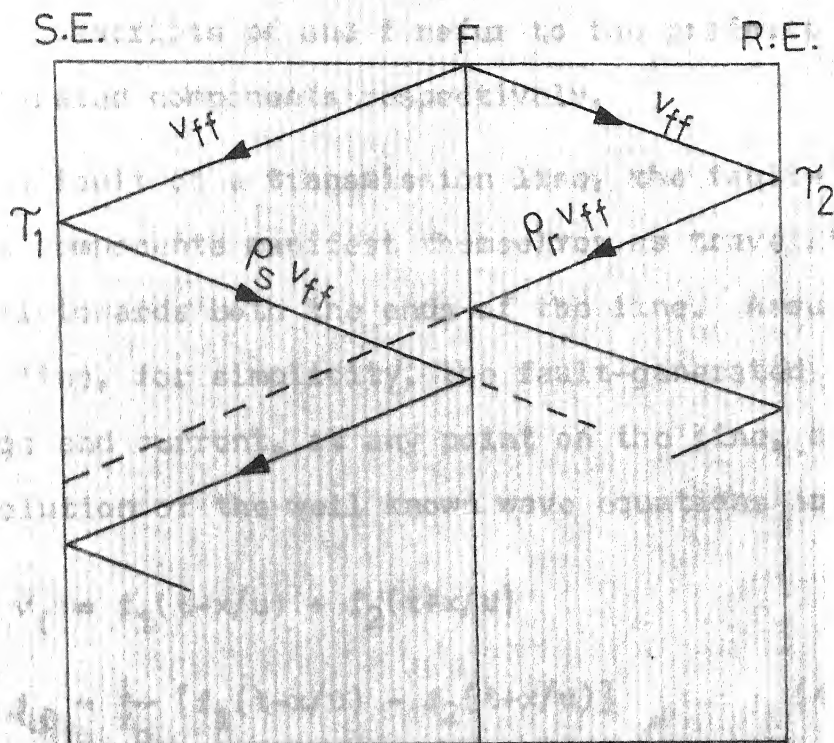
FIG·4·2 LATTICE DIAGRAM FOR AN INTERNAL
FAULT

current at any point in the system can be regarded as the
sum of prefault and fault-generated components, that is,

$$v = v_{pf} + v_f$$

and

$$i = i_{pf} + i_f \qquad (4.1)$$

where the subscripts pf and f refer to the prefault and
fault-generated components respectively.

For a fault on a transmission line, the fault-
generated components manifest themselves as travelling waves
and travel towards both the ends of the line. Assuming a
lossless line, for simplicity, the fault-generated components
of voltage and current, at any point on the line, are given
by the solution of the well known wave equations as,

$$v_f = f_1(t-x/u) + f_2(t+x/u)$$

$$i_f = \frac{1}{z_0} [f_1(t-x/u) - f_2(t+x/u)] \qquad (4.2)$$

where

f_1 and f_2 — arbitrary functions determined by the
boundary conditions

t — time from the instant of fault occurrence

u — velocity of propagation of travelling waves

z_0 — surge impedance of the line.

From the above equations (i.e. eqn. (4.2)), it can be seen that $f_1(t-x/u)$ represents a forward travelling wave and $f_2(t+x/u)$, a backward travelling wave. Also, the forward travelling waves of voltage and current are of the same sign, whilst the backward travelling waves of voltage and current are of opposite sign.

Thus, the travelling waves of the fault-generated components of voltage and current, originating at the fault point F, travel towards the ends of the line where they undergo reflection and refraction. If the voltage reflection coefficients at the sending and receiving ends are ρ_s and ρ_r respectively, these events can be depicted by means of a Lattice diagram as given in Fig. 4.2, where v_{ff} is the fault generated component of the voltage at the fault point. For example, if the fault is a bolted one, v_{ff} will be equal to the prefault voltage at the point of fault.

The proposed scheme makes use of a signal pair of the form given below for each of the relays at the ends of the protected line. For the sending end relay, the input signals (in p.u.) would be

$$S_1 = v_{fs} - R_{set} \, i_{fs}$$

and
$$S_2 = v_{fs} + R_{set} \, i_{fs} \qquad\qquad (4.3)$$

where

v_{fs}, i_{fs} - fault-generated components of voltage and
current in p.u. at the sending end

and

R_{set} - surge impedance of the line in p.u.

For a fault on the line, the values of $v_{fs}, i_{fs}, \left| S_1 \right|$ and $\left| S_2 \right|$ at various instants, deduced from the Lattice diagram and eqns. (4.3), are given in Table 4.1. τ_1 is the travel time of the waves to travel from the fault point to the sending end. Since $\left| \rho_s \right|$ is always less than 1.0, except when the sending end is on open circuit, $\left| S_1 \right| > \left| S_2 \right|$ from τ_1^- till another wave pair arrives there.

Next, consider a fault on any of the lines feeding the sending end bus. One pair of the travelling waves generated on this line travels towards the sending end bus and undergoes both reflection and refraction at the bus. Due to the refracted waves, we have

$$v_{fs} = \rho_t v_{ff} \text{ and } i_{fs} = \rho_t v_{ff}/Z_o'$$

where ρ_t is the refraction coefficient and Z_o', the surge impedance of the faulted line. Then, the relay signals are given by

$$S_1 = \rho_t \, v_{ff} - R_{set} \, \frac{\rho_t \, v_{ff}}{Z_0'} = (1 - R_{set}/Z_0') \, \rho_t \, v_{ff}$$

$$S_2 = \rho_t \, v_{ff} + R_{set} \, \frac{\rho_t \, v_{ff}}{Z_0'} = (1 + R_{set}/Z_0') \, \rho_t \, v_{ff} \qquad (4.4)$$

Therefore, it can be seen that $\left| S_1 \right| < \left| S_2 \right|$ till these waves return after reflection at the remote end of the protected line. Summarising, we have for some duration,

$\left| S_1 \right| > \left| S_2 \right|$ for a fault ahead of the relaying point

and

$\left| S_1 \right| < \left| S_2 \right|$ for a fault behind the relaying point $\qquad (4.5)$

An identical relay arrangement is provided at the receiving end. If $\left| S_1 \right| > \left| S_2 \right|$ at both the ends, an internal fault is indicated. The information about this is exchanged between the ends of the protected line through a fast communication channel. If one end of the line is on open circuit, then the relay at the other end is arranged to act independently of the communication channel information.

4.2.2 Extension of the Principles to the Protection of 3-Phase Lines

A distributed-parameter 3-phase transmission line can be described in the frequency domain by a set of decoupled modal differential equations given below [vide Appendix A]

$$\frac{d^2 \overline{V}^{(m)}}{dx^2} = \gamma_m^2 \, \overline{V}^{(m)}$$

$$\frac{d^2 \overline{I}^{(m)}}{dx^2} = \gamma_m^2 \, \overline{I}^{(m)}, \quad m = 1,2,3 \qquad (4.6)$$

where

$$\overline{V}^{(m)}, \overline{I}^{(m)}$$ – mth mode's components of phase voltage

and line current transforms

$$\gamma_m$$ – propagation constant of mth mode.

These equations show that the wave propagation in a 3-phase line can be considered in terms of three separate and independent components, each possessing its own propagation constant and surge impedance. The three separate and independent components are called modal components, and are obtained by modal transformation, using the voltage and current modal transformation matrices S and Q, defined in Appendix A.

It has been the practice to set the protective relays with the assumption of an ideally transposed line. With this assumption, S and Q become equal and frequency independent. In addition, any convenient value can be chosen for them, provided that they give rise to decoupled differential equations. In this work, the Karrenbauer modal transformation matrix [118], defined below, is used.

$$S = Q = \begin{bmatrix} 1 & 1 & 1 \\ 1 & -2 & 1 \\ 1 & 1 & -2 \end{bmatrix} \tag{4.7}$$

Also, with the same assumption, the modal surge impedances of the line are given by,

$$\overline{Z}_0^{(1)} = \left\{ (\overline{Z}_s + 2\overline{Z}_m)/(\overline{Y}_s - 2\overline{Y}_m) \right\}^{\frac{1}{2}} \quad \text{for mode 1}$$

and

$$\overline{Z}_0^{(2)} = \overline{Z}_0^{(3)} = \left\{ (\overline{Z}_s - \overline{Z}_m)/(\overline{Y}_s + \overline{Y}_m) \right\}^{\frac{1}{2}} \quad \text{for modes 2 and 3}$$

$$(4.8)$$

where

$\overline{Z}_s, \overline{Z}_m$ - self and mutual series impedance transforms of the line

$\overline{Y}_s, \overline{Y}_m$ - self and mutual shunt admittance transforms of the line.

The results of Section 4.2.1 apply equally well to each of the three modes of propagation of travelling waves described above. Accordingly, three pairs of signals, one for each mode, are employed. For the sending end relay, these are given by

$$S_1^{(m)} = v_{fs}^{(m)} - R_{set}^{(m)} i_{fs}^{(m)}$$

and

$$S_2^{(m)} = v_{fs}^{(m)} + R_{set}^{(m)} i_{fs}^{(m)}, \quad m = 1,2,3 \qquad (4.9)$$

where

$v_{fs}^{(m)}, i_{fs}^{(m)}$ - modal components of the fault-generated components of the sending end phase voltages and line currents, determined by using the modal transformation matrix given in eqn. (4.7)

$$R_{set}^{(1)} = \text{Re } [\overline{Z}_0^{(1)}]$$

and,

$$R_{set}^{(2)} = R_{set}^{(3)} = \text{Re}[\overline{Z}_0^{(2)}] = \text{Re}[\overline{Z}_0^{(3)}]$$

The amplitude comparison described in Section 4.2.1 is applied to each signal pair. A tripping or blocking signal is issued by the first positive outcome of any one of the comparisons. Summarising, the tripping and blocking criteria are given by

$$\left| S_1^{(m)} \right| > \left| S_2^{(m)} \right| \quad \text{i.e.,} \quad \left| S_1^{(m)} \right| - \left| S_2^{(m)} \right| > 0.0 \text{ for faults}$$
ahead

and,

$$\left| S_1^{(m)} \right| < \left| S_2^{(m)} \right| \quad \text{i.e.,} \quad \left| S_1^{(m)} \right| - \left| S_2^{(m)} \right| < 0.0 \text{ for faults}$$
behind, $m = 1,2,3$

$$(4.10)$$

An identical relay arrangement is provided at the receiving end.

4.2.3 Testing of the Relaying Principles by Digital Computer Simulation

The viability of the new amplitude comparison techniques, described in earlier sections, is tested by considering the 4-Bus system described in Chapter 3. In this system, all the lines are 128 Km in length. Frequency dependency of all the line and earth parameters is simulated in order to produce a realistic indication of the validity of the relaying principles.

An earth resistivity of 100 ohm-m is assumed. Each equivalent source, representing the fault level at that bus, is assumed to have a ratio of zero sequence impedance to positive sequence impedance equal to 0.5 at power frequency. A phase sequence of a,b,c is assumed.

The performance of the relay, assumed to be situated near bus 1 and affording protection to the line connected between buses 1 and 2, is studied for three-phase and one-phase-to-ground faults. For this purpose, the signal difference, viz., $\left| S_1 \right| - \left| S_2 \right|$, is computed for all the modes, and for the following locations of the fault.

i) The remote end (marked F_1) of the protected line; a distant internal fault

ii) A point, 25.6 Km from the relaying point, on the protected line; a close-in internal fault

iii) The remote end (marked F_2) of the line connected between buses 1 and 3; a distant external fault.

In each case, fault resistances of 0,50,100,150 and 200 ohms, and fault initiation angles of 0 and 90 degrees are considered. The signal difference for mode 1, in the case of 3-phase faults, has been found to be negligible. Therefore, $(\left| S_1 \right| - \left| S_2 \right|)$ for modes 2 and 3 in the case of 3-phase faults, and for all the modes in the case of one-phase-to-ground faults are plotted as a function of time. The plots are given in Figs. 4.3 to 4.32.
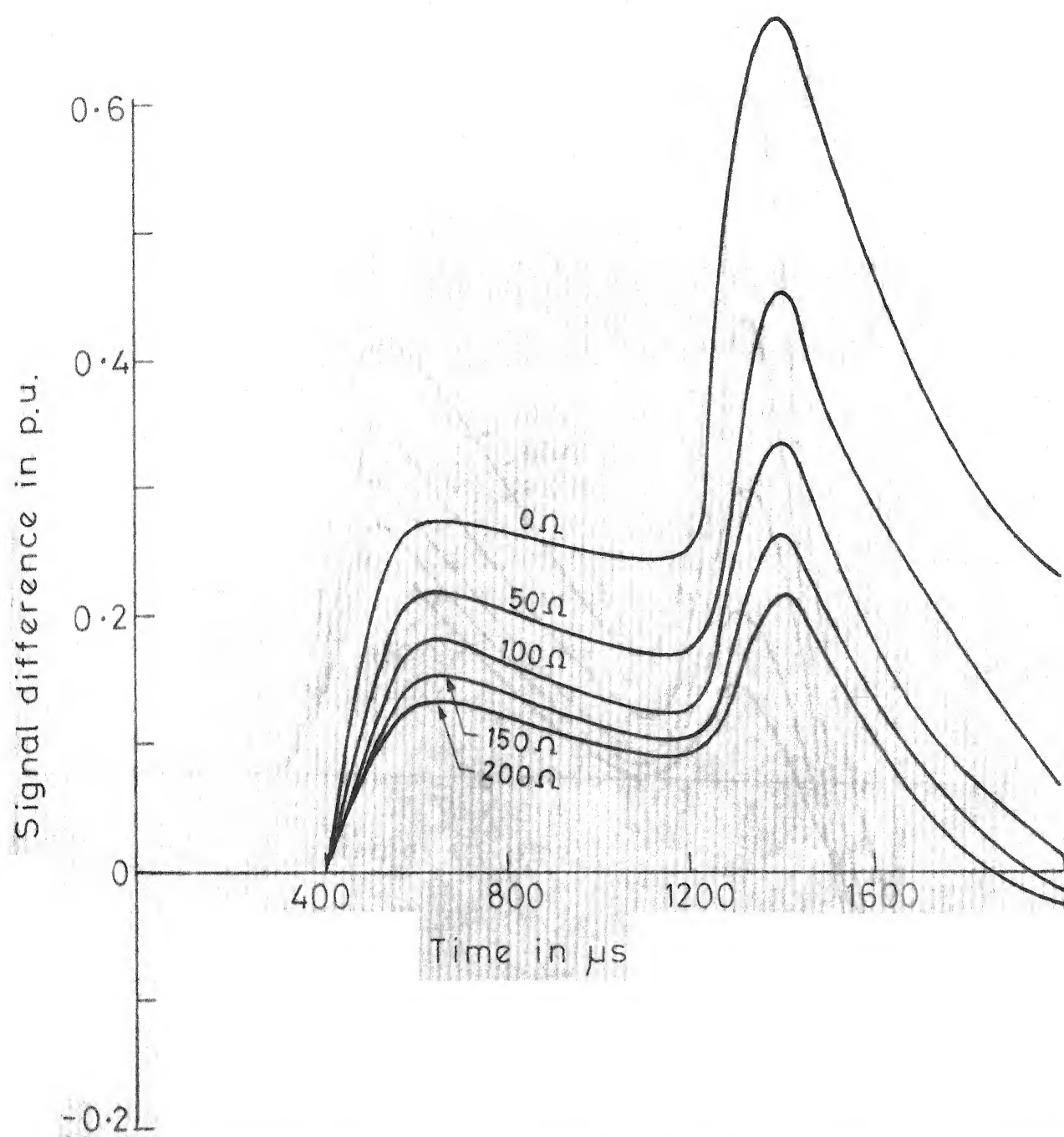
FIG.43 VARIATION OF MODE 2 SIGNAL DIFFERENCE FOR A DISTANT INTERNAL 3-PHASE FAULT: $\phi_0 = 0°$
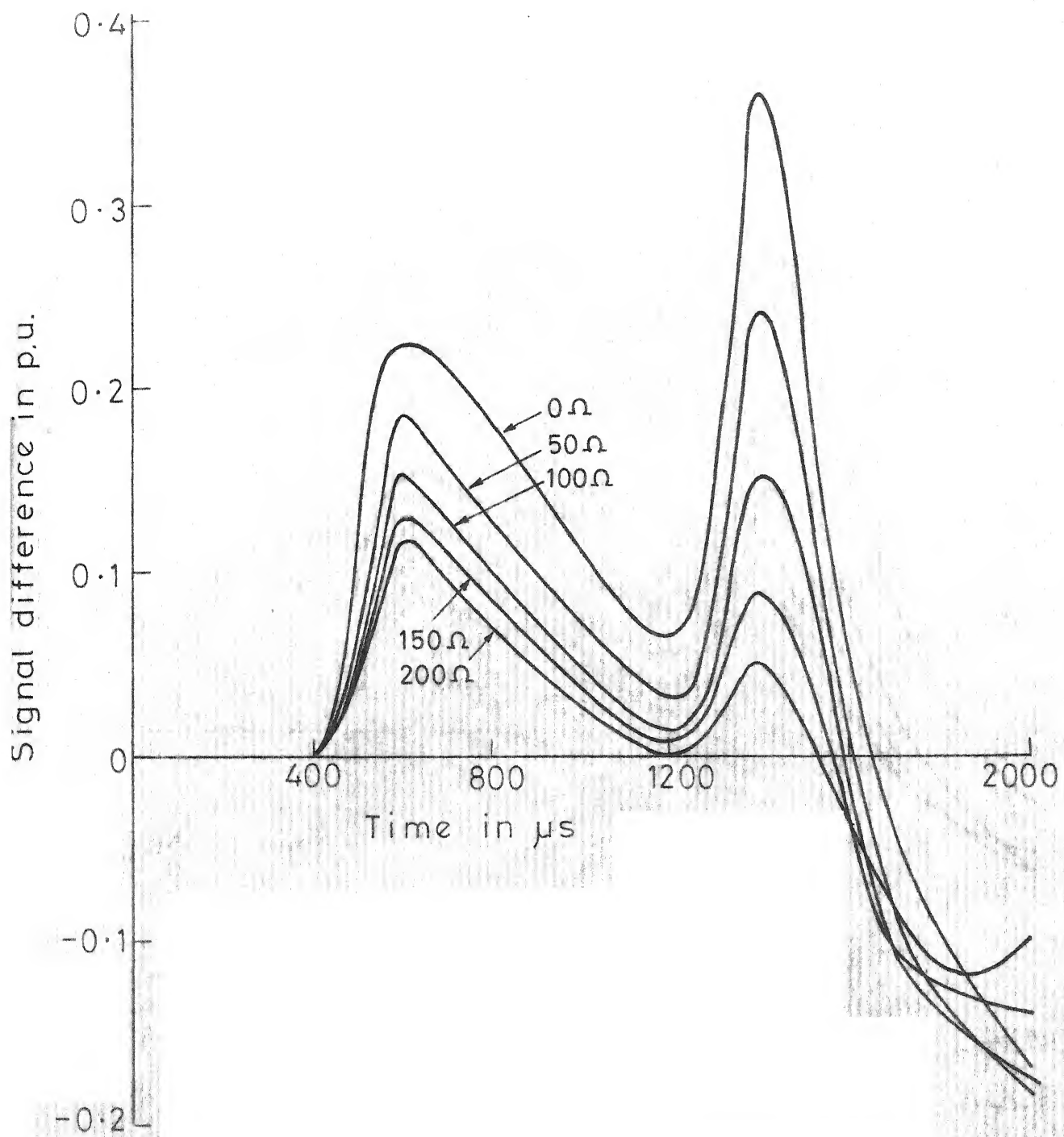
FIG·4·4 VARIATION OF MODE 3 SIGNAL DIFFERENCE
FOR A DISTANT INTERNAL 3-PHASE FAULT:
$\phi_0 = 0°$
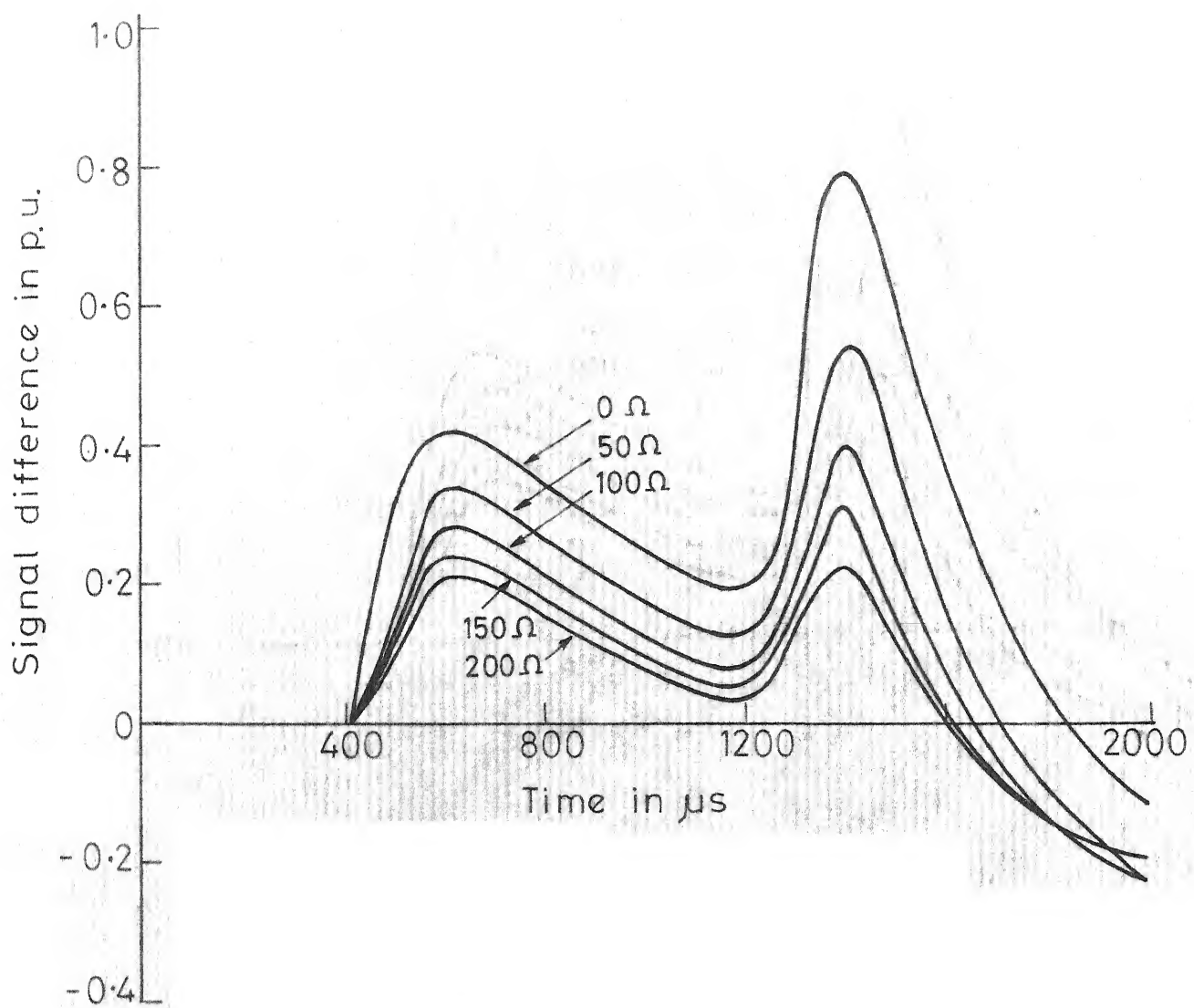
FIG·4·5 VARIATION OF MODE 2 SIGNAL DIFFERENCE
FOR A DISTANT INTERNAL 3-PHASE FAULT:
$\phi_o = 90°$
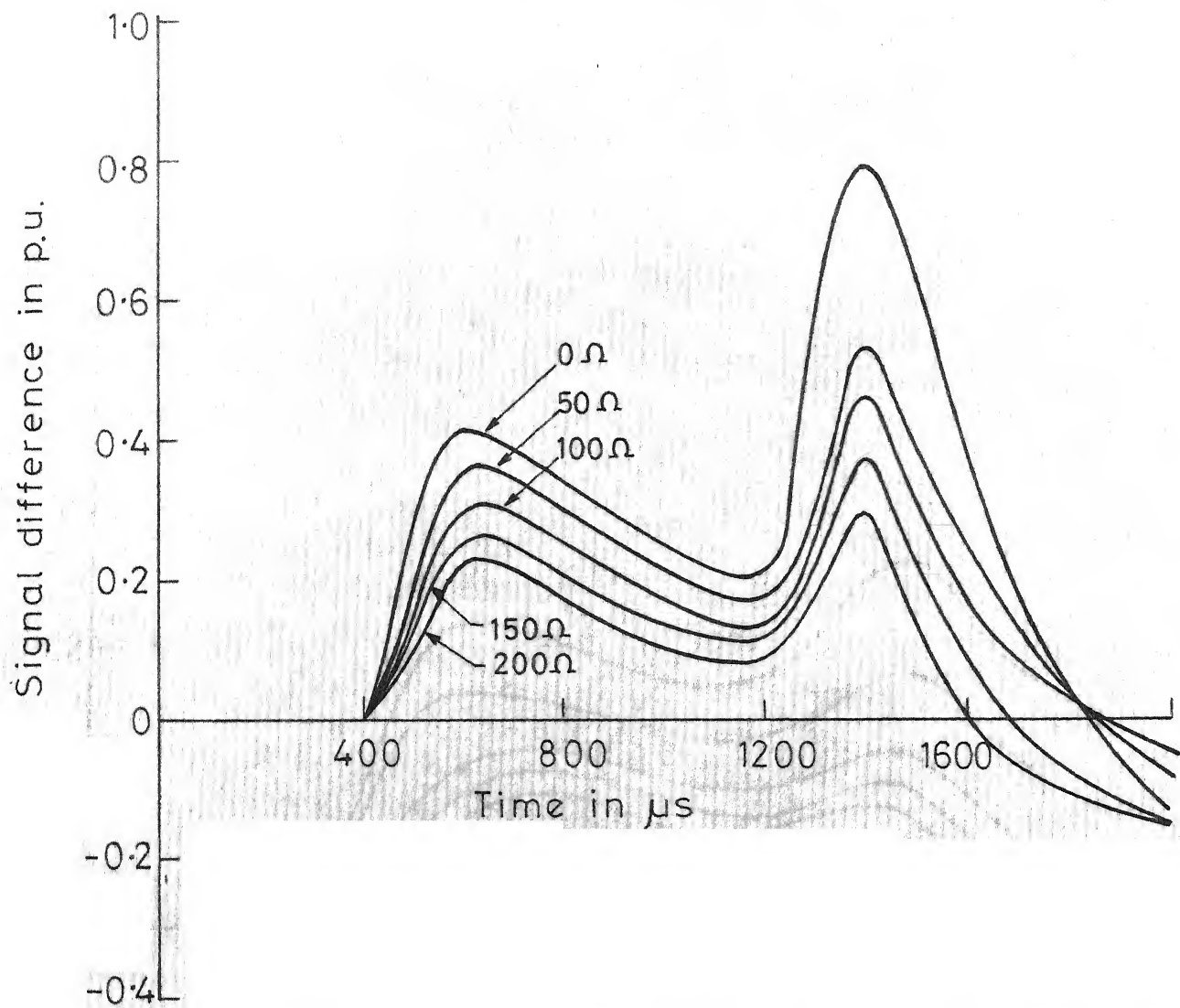
FIG. 4·6 VARIATION OF MODE 3 SIGNAL DIFFERENCE
FOR A DISTANT INTERNAL 3-PHASE FAULT:
$\phi_o = 90°$
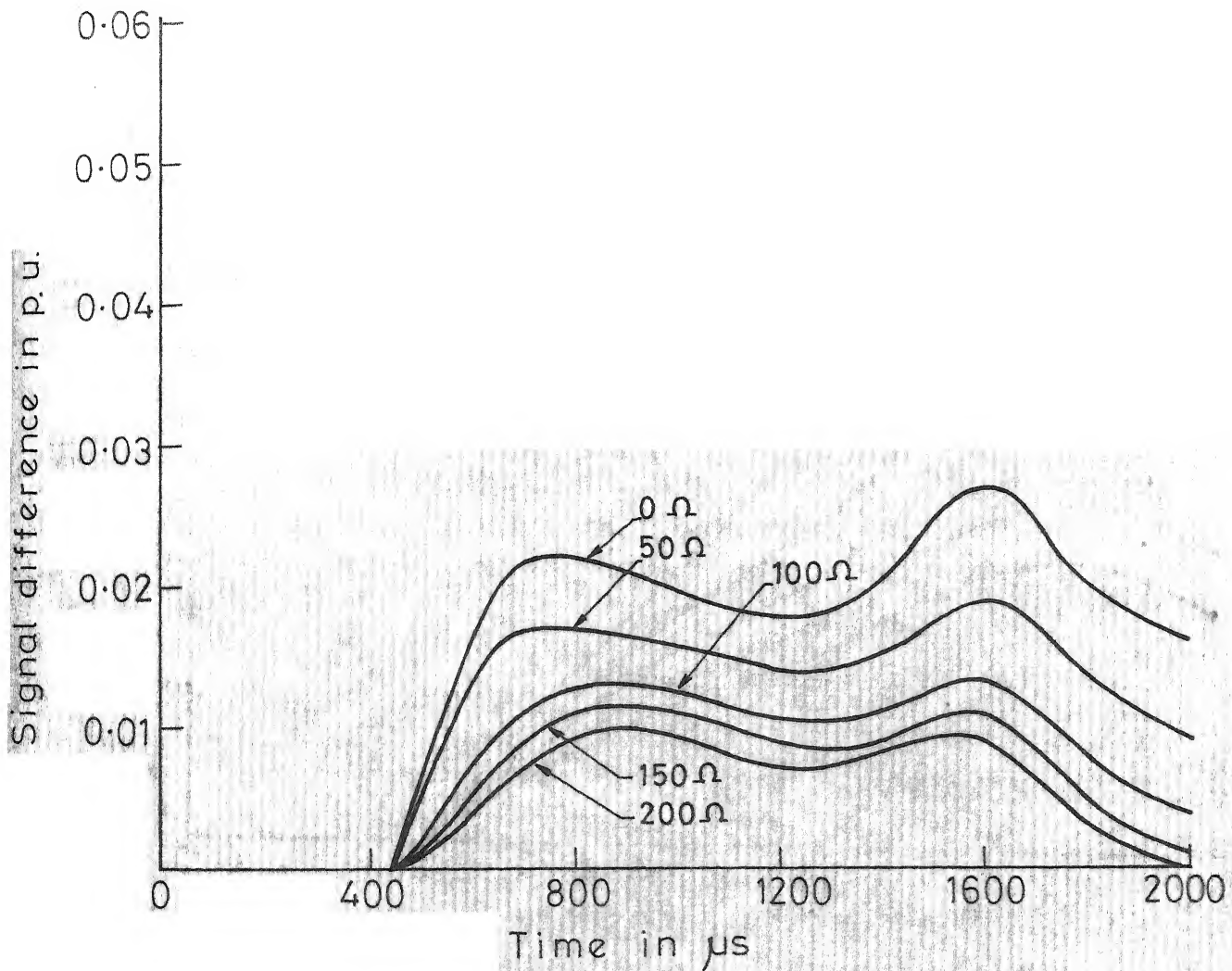
FIG. 4·7 VARIATION OF MODE 1 SIGNAL DIFFERENCE FOR A DISTANT INTERNAL ONE PHASE TO GROUND FAULT ON PHASE 'A' : $\phi_0 = 0°$
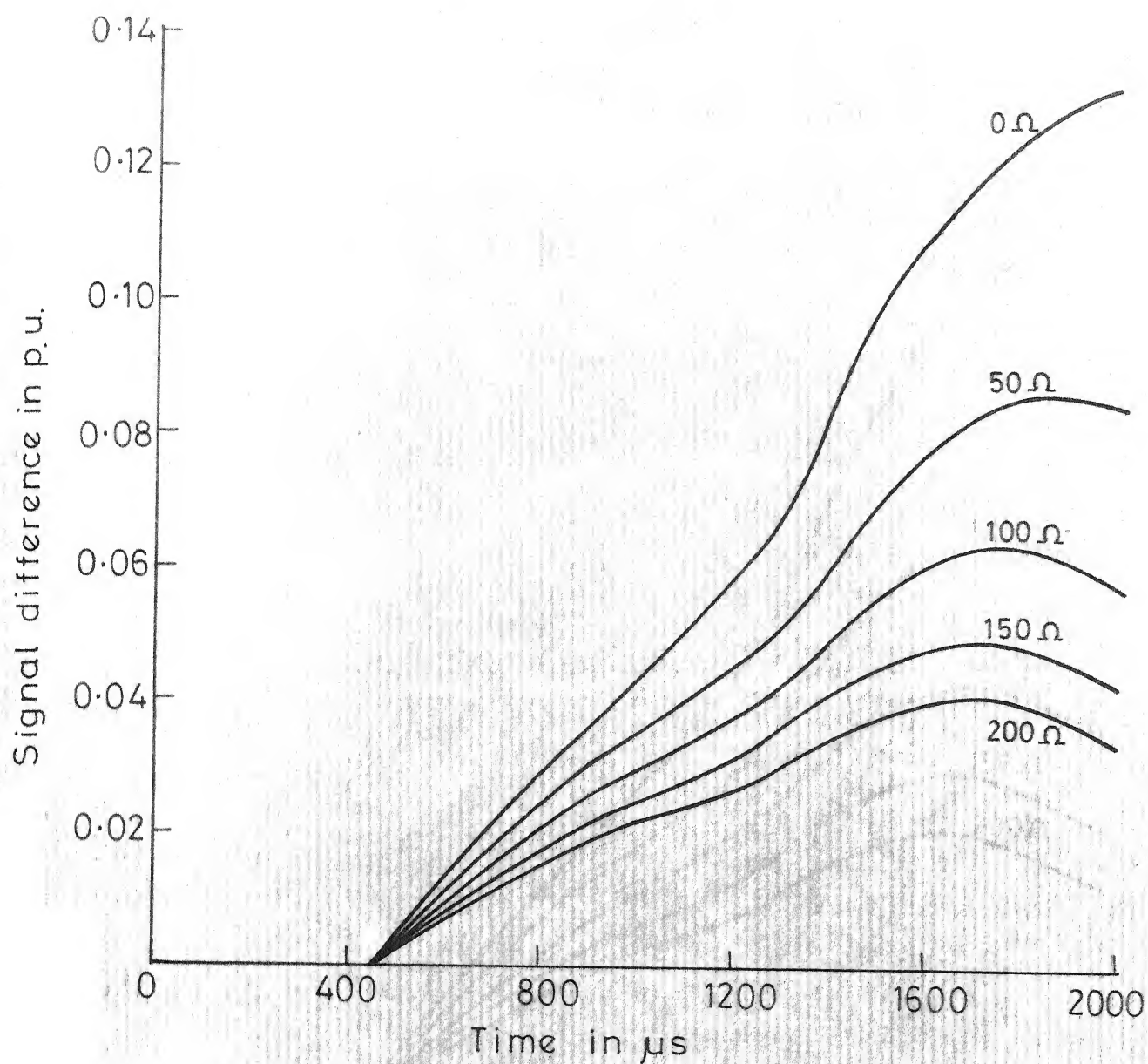
FIG.4.8 VARIATION OF MODE 2 SIGNAL DIFFERENCE
FOR A DISTANT INTERNAL ONE PHASE TO
GROUND FAULT ON PHASE 'A': $\phi_o = 0°$
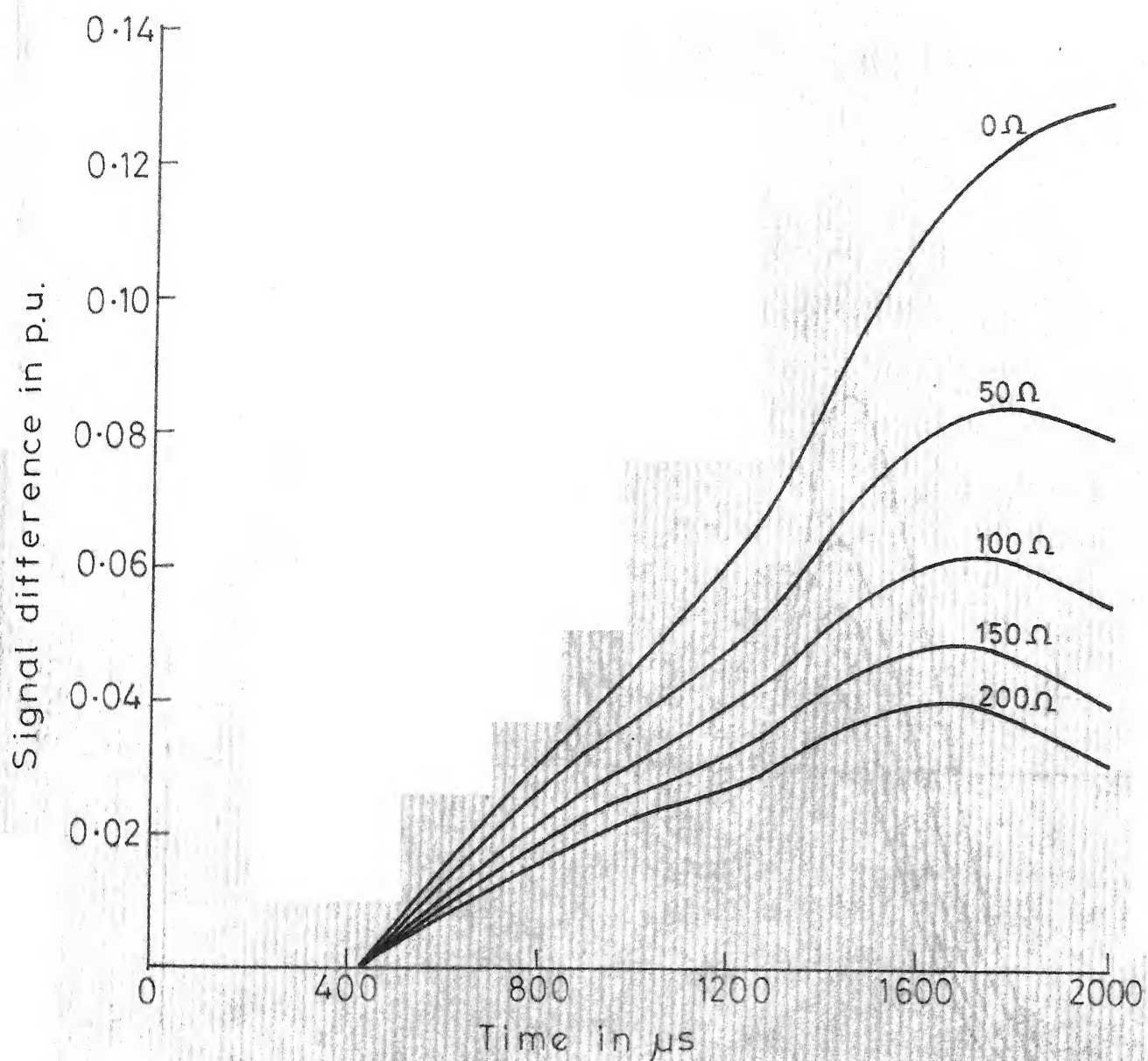
FIG. 4.9 VARIATION OF MODE 3 SIGNAL DIFFERENCE FOR A DISTANT INTERNAL ONE PHASE TO GROUND FAULT ON PHASE 'A' : $\phi_o = 0°$
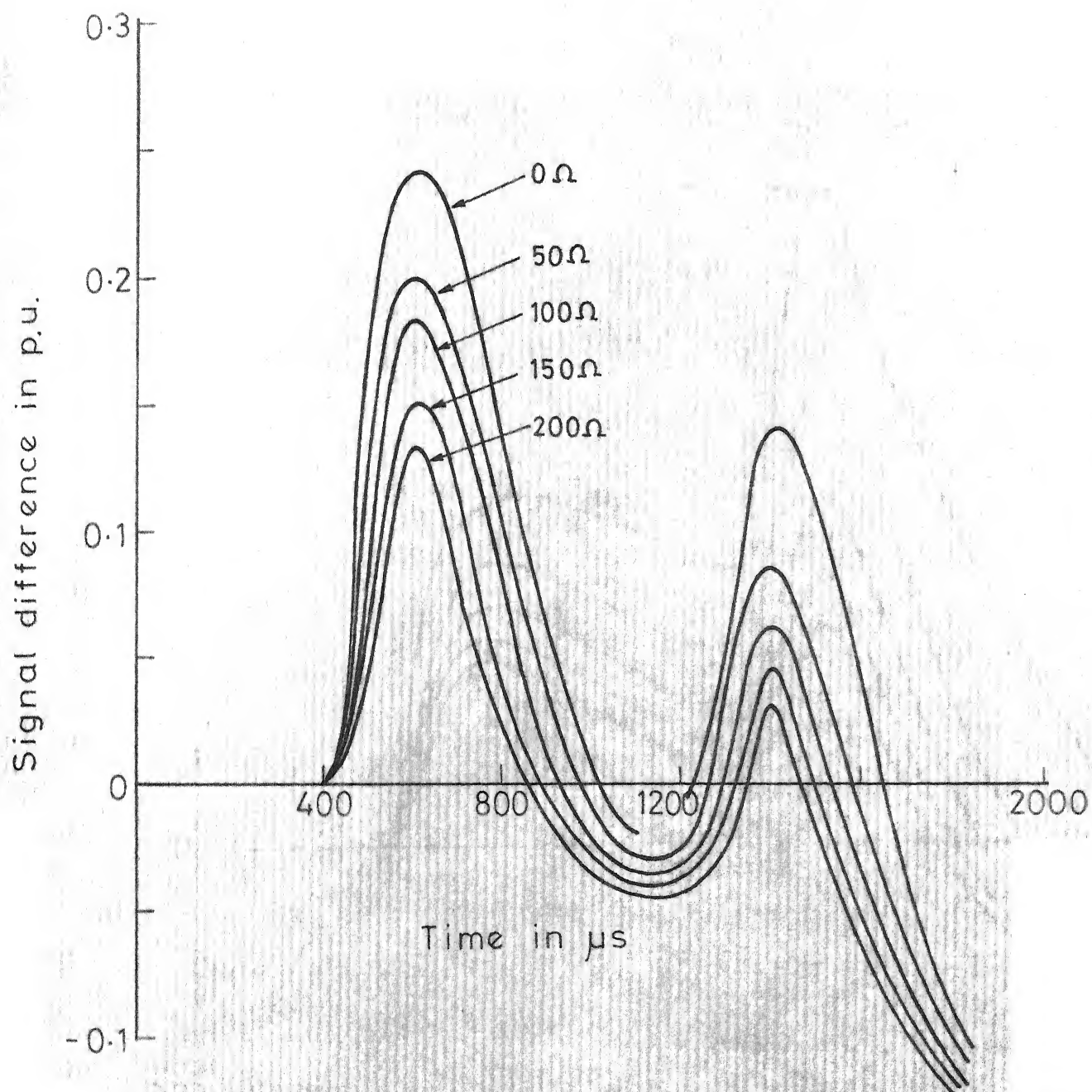
FIG.4.10 VARIATION OF MODE 1 SIGNAL DIFFERENCE FOR A DISTANT INTERNAL ONE PHASE TO GROUND FAULT ON PHASE 'A': $\phi_0 = 90°$
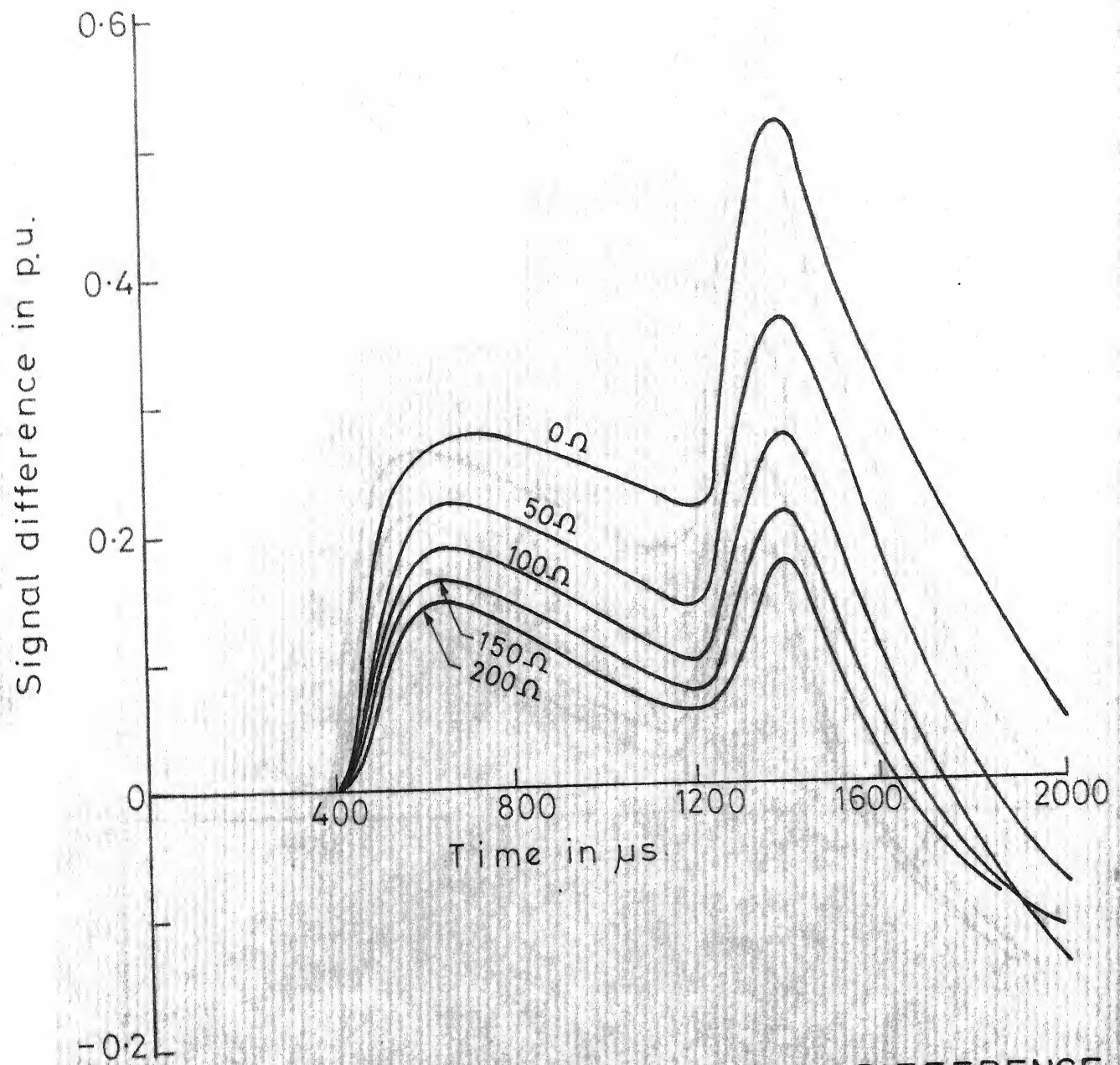
FIG.4·11 VARIATION OF MODE 2 SIGNAL DIFFERENCE FOR A DISTANT INTERNAL ONE PHASE TO GROUND FAULT ON PHASE 'A' : $\phi_0 = 90°$
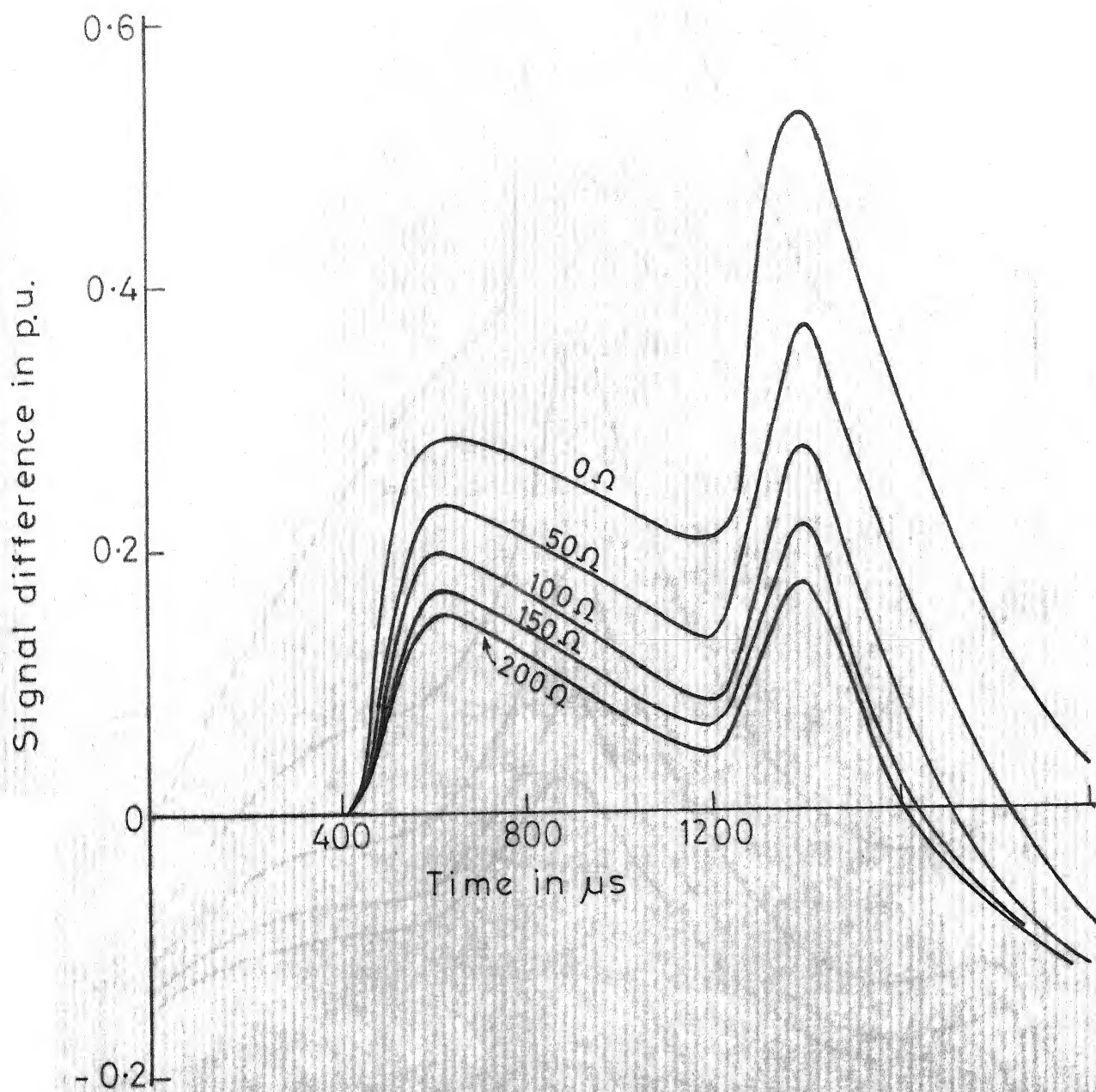
FIG.4·12 VARIATION OF MODE 3 SIGNAL DIFFERENCE FOR A DISTANT INTERNAL ONE PHASE TO GROUND FAULT ON PHASE 'A' : $\phi_0=90°$
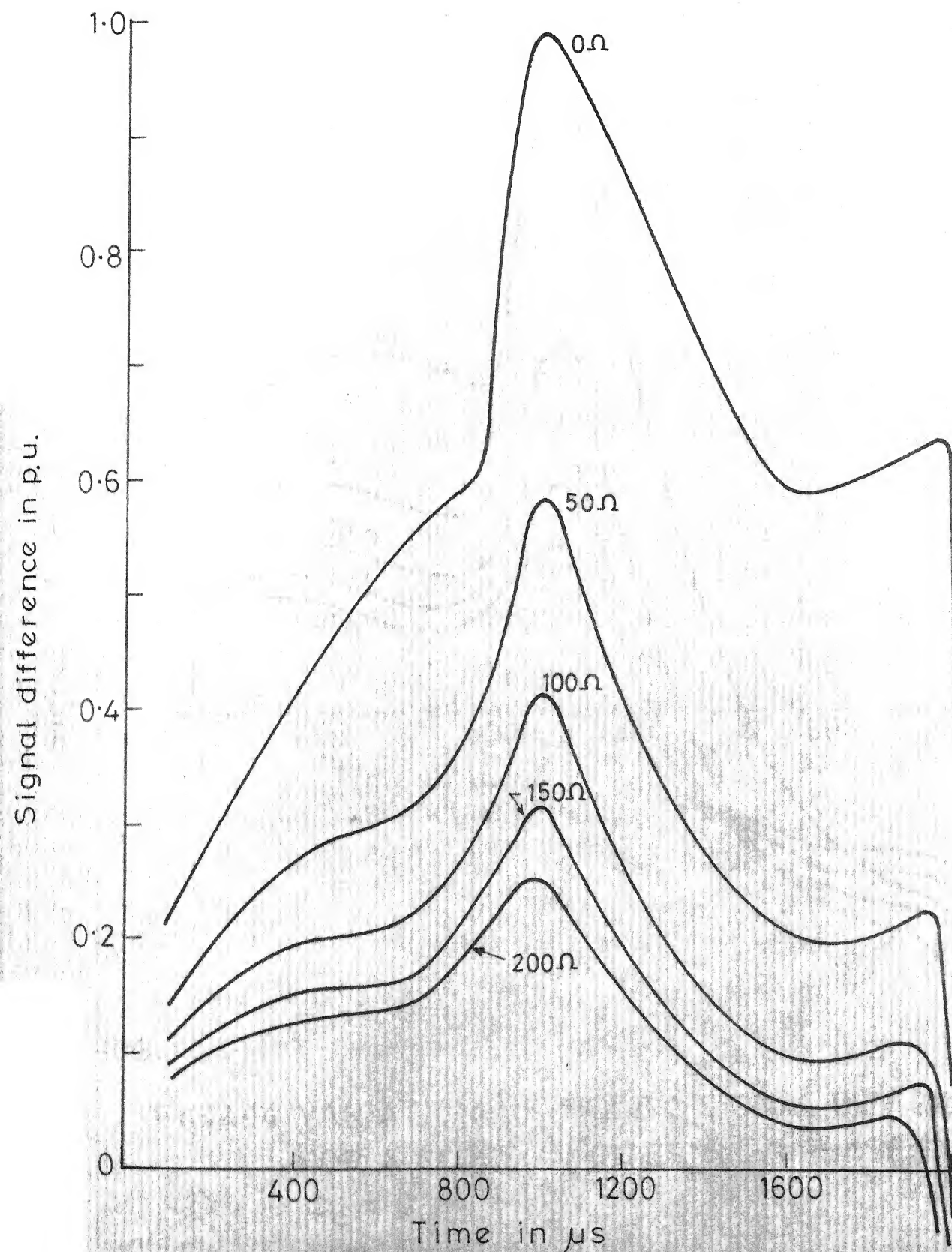
FIG. 4·13 VARIATION OF MODE 2 SIGNAL DIFFERENCE FOR A CLOSE IN INTERNAL 3-PHASE FAULT: $\Phi_o = 0°$
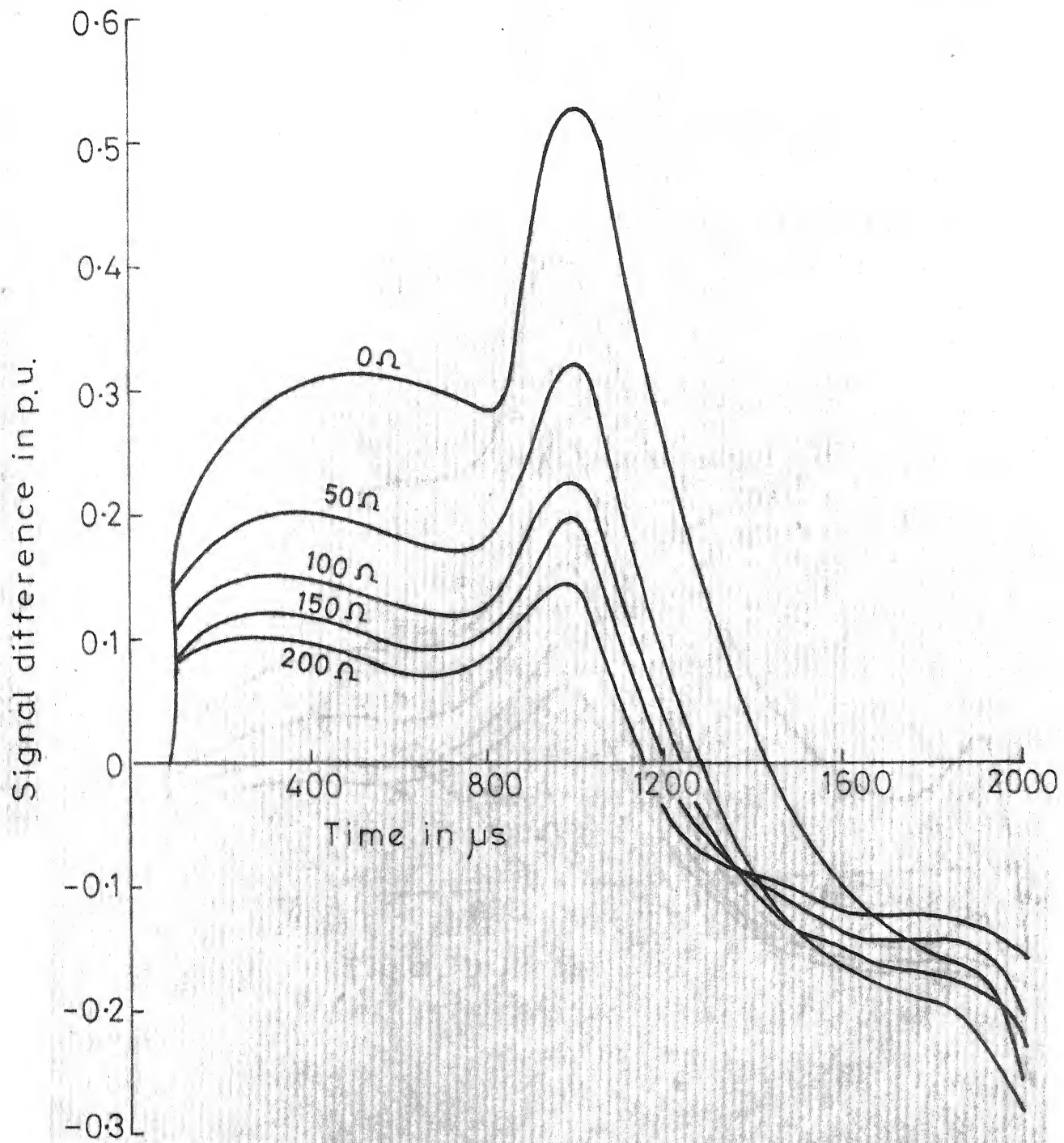
FIG·4·14 VARIATION OF MODE 3 SIGNAL DIFFERENCE FOR A CLOSE IN INTERNAL 3-PHASE FAULT: $\phi_o = 0°$
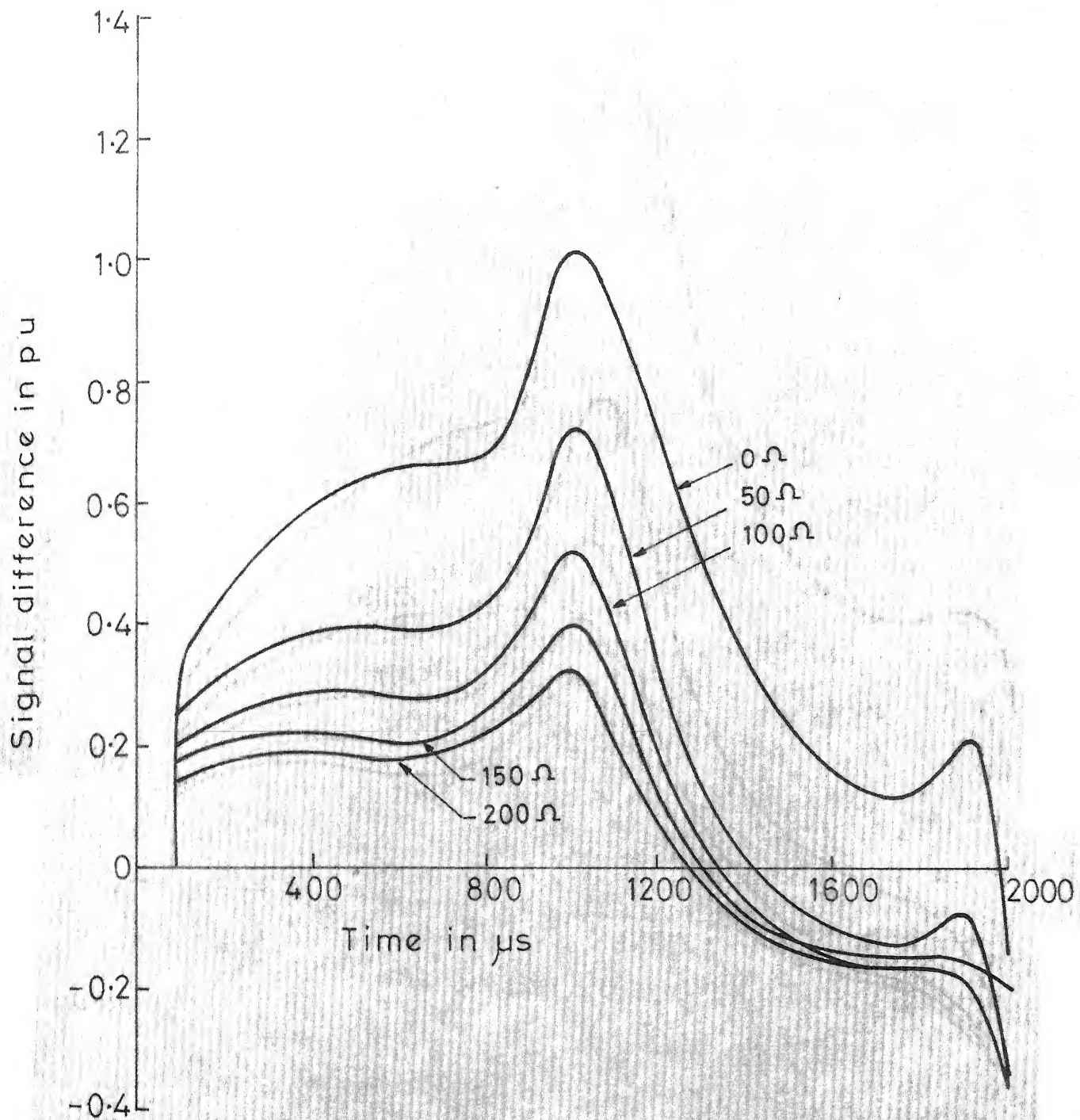
FIG. 4·15 VARIATION OF MODE 2 SIGNAL DIFFERENCE FOR A CLOSE-IN INTERNAL 3-PHASE FAULT: $\phi_0 = 90°$
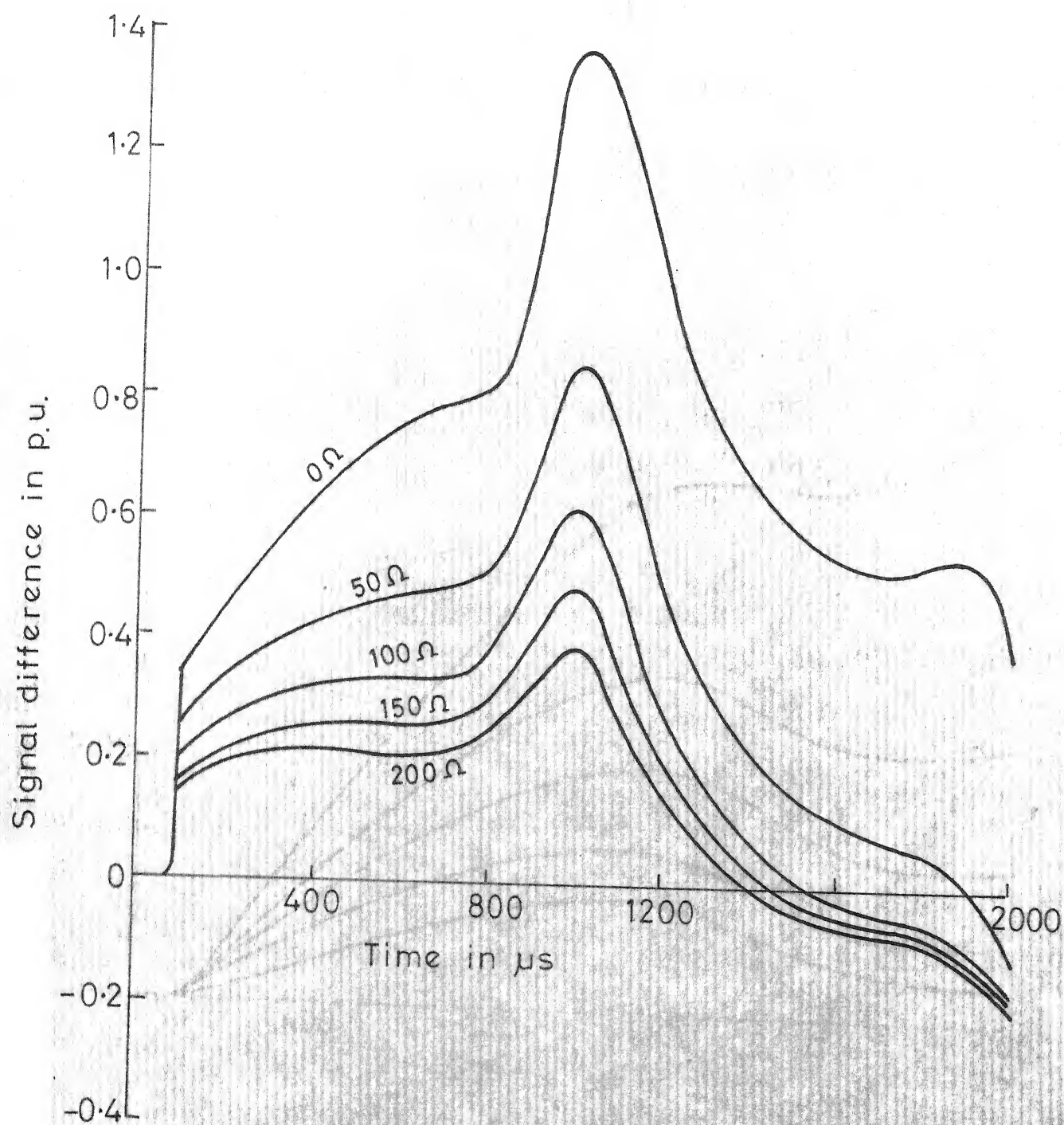
FIG. 4·16 VARIATION OF MODE 3 SIGNAL DIFFERENCE FOR A CLOSE IN INTERNAL 3-PHASE FAULT : $\phi_0 = 90°$
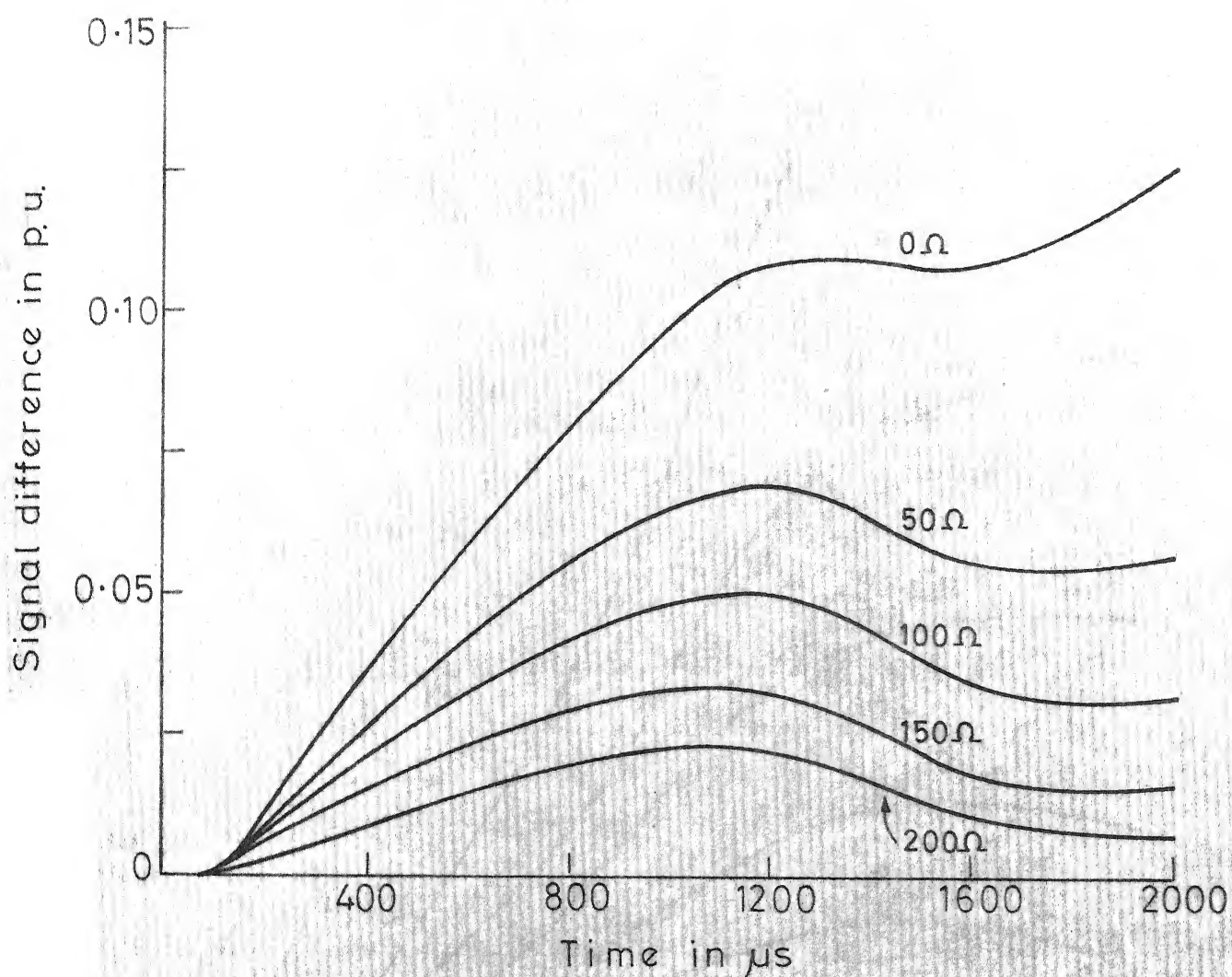
FIG. 4·17 VARIATION OF MODE 1 SIGNAL DIFFERENCE FOR A CLOSE-IN INTERNAL ONE PHASE TO GROUND FAULT ON PHASE 'A': $\phi_o = 0°$
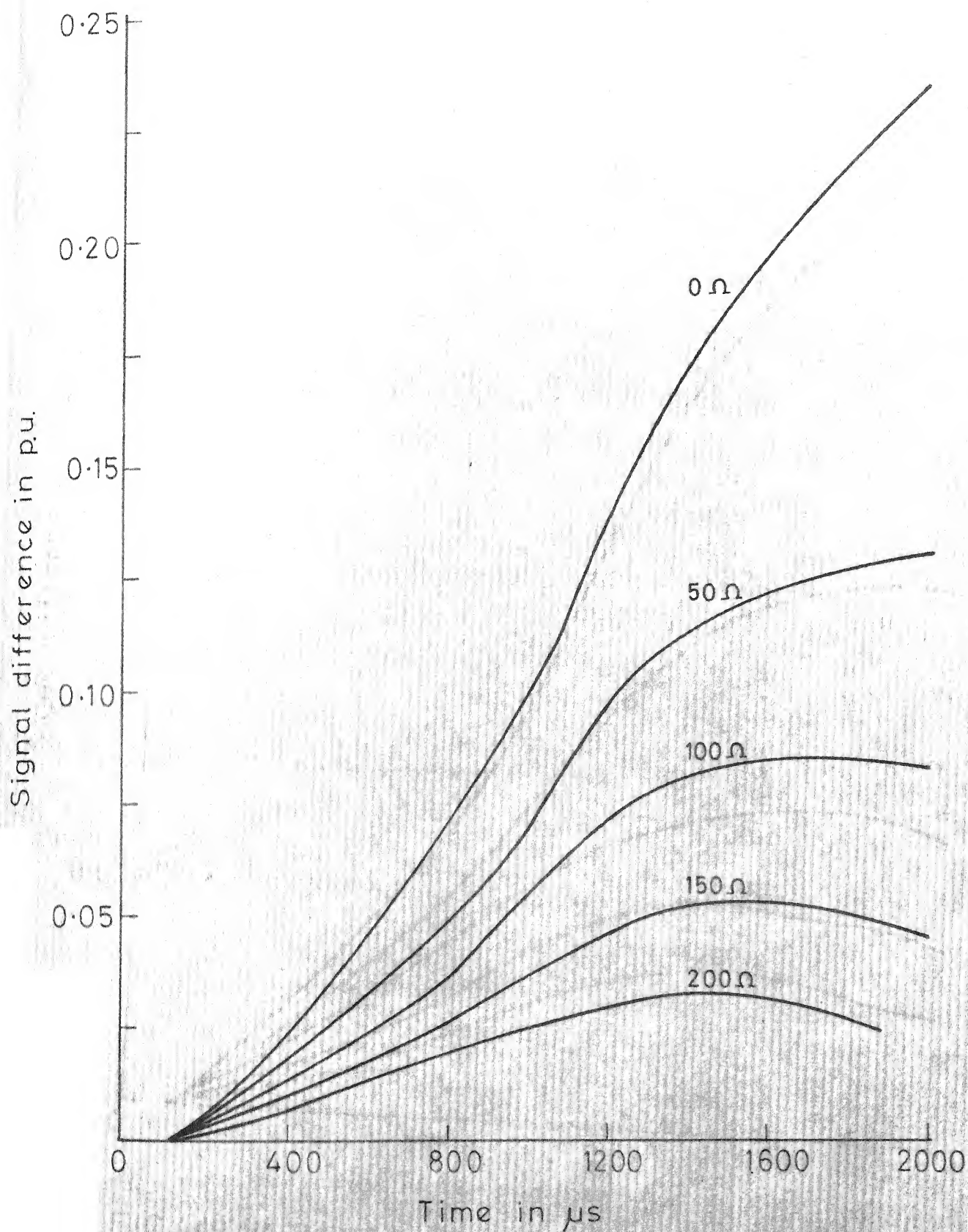
FIG.4-18 VARIATION OF MODE 2 SIGNAL DIFFERENCE FOR A CLOSE-IN INTERNAL ONE PHASE TO GROUND FAULT ON PHASE 'A' : $\phi_0=0°$
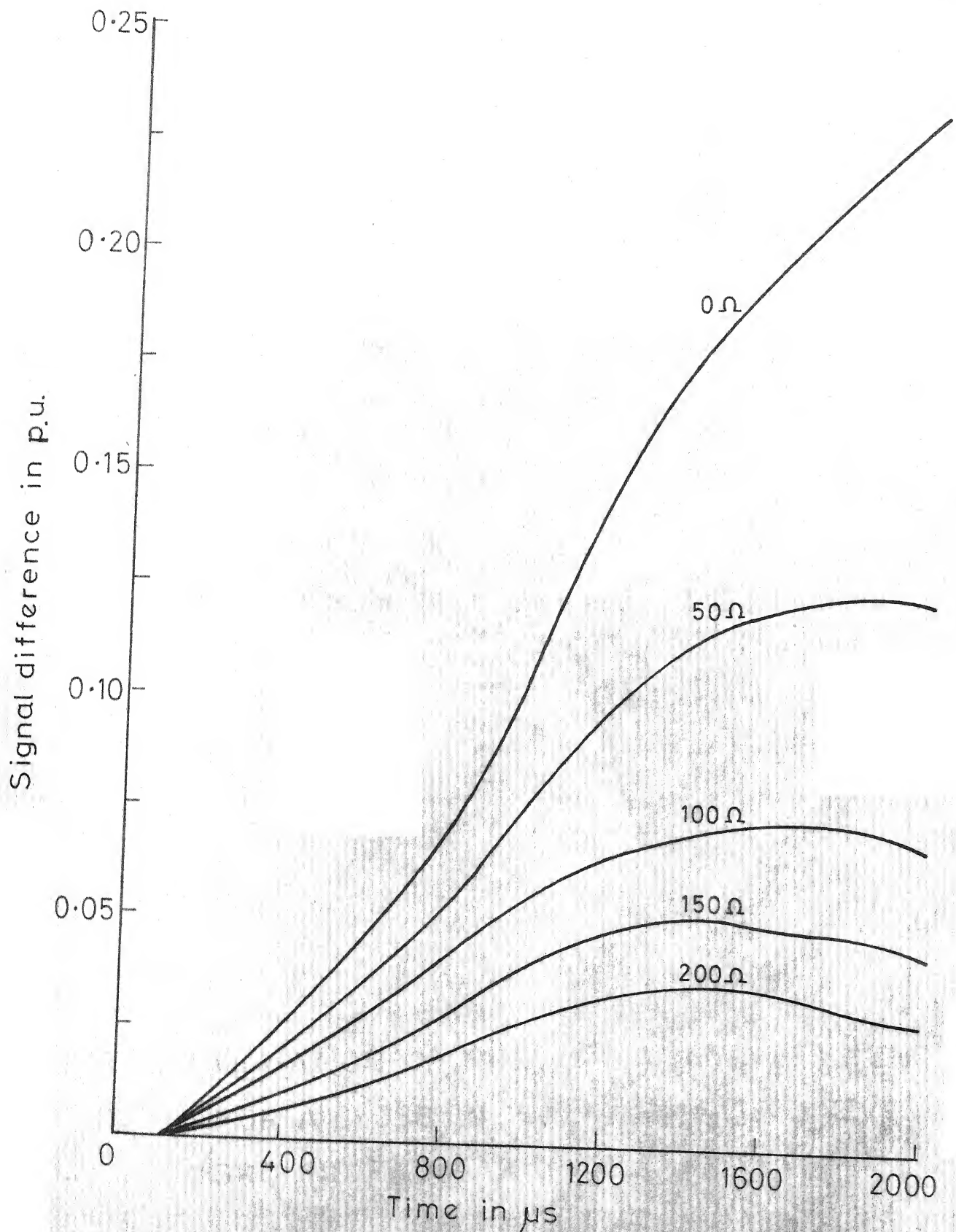
FIG.4·19 VARIATION OF MODE 3 SIGNAL DIFFERENCE
FOR A CLOSE-IN INTERNAL ONE PHASE TO
GROUND FAULT ON PHASE 'A' : $\phi_o = 0°$
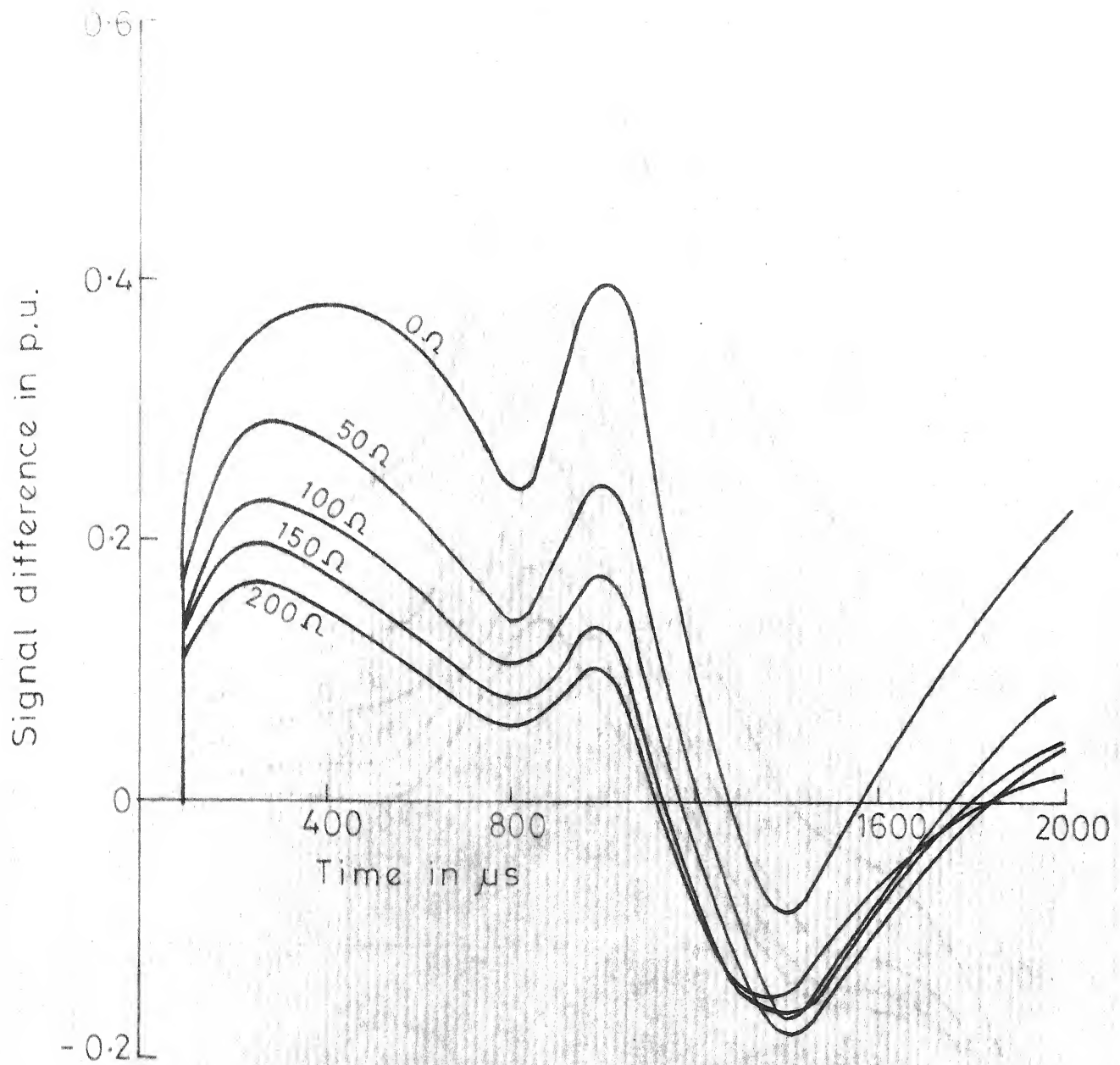
FIG·4·20 VARIATION OF MODE 1 SIGNAL DIFFERENCE FOR A CLOSE IN INTERNAL ONE PHASE TO GROUND FAULT ON PHASE A : $\phi_o = 90°$
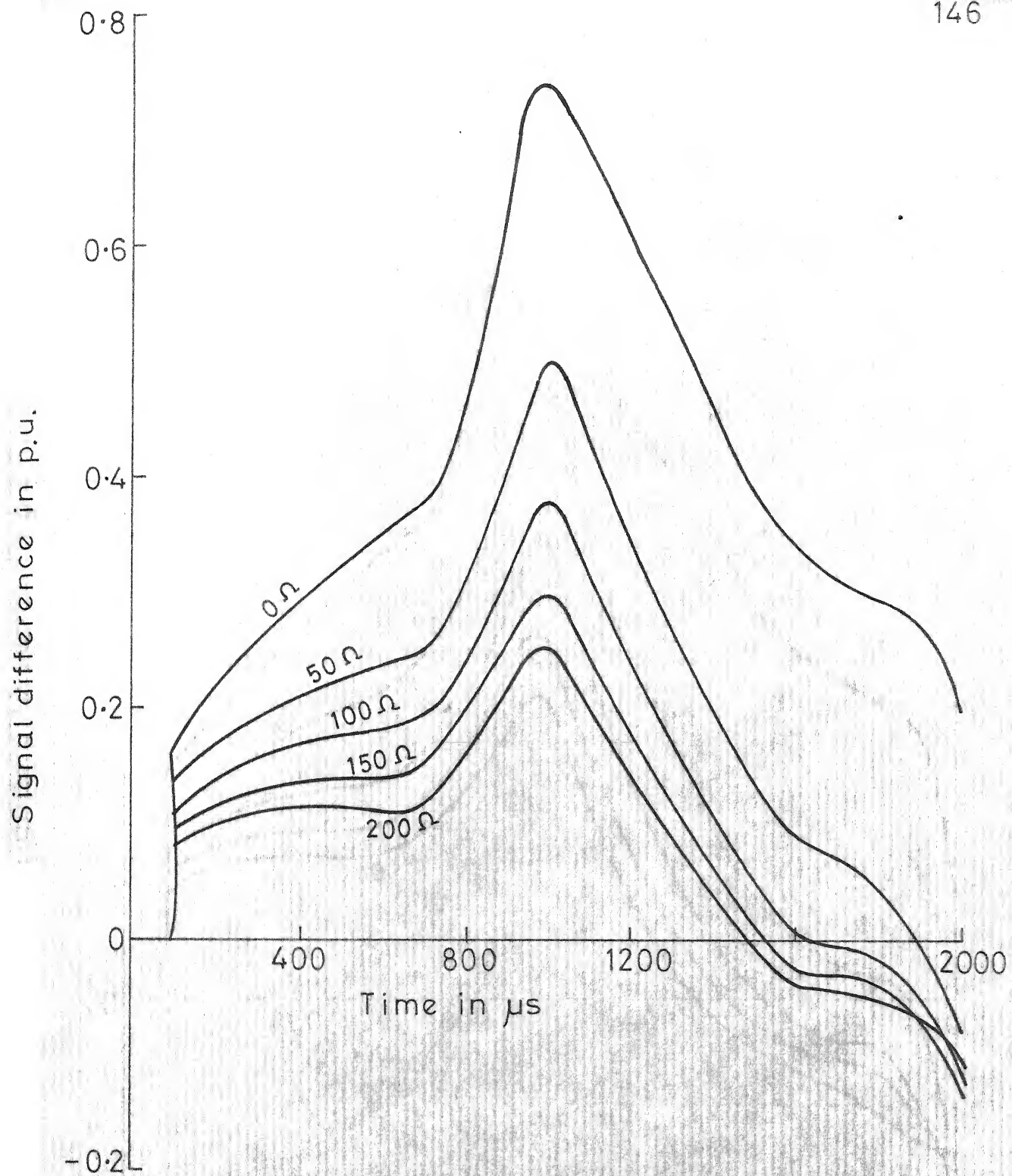
FIG. 4.21 VARIATION OF MODE 2 SIGNAL DIFFERENCE
FOR A CLOSE IN INTERNAL ONE PHASE
TO GROUND FAULT ON PHASE 'A' : $\phi_0 = 90°$
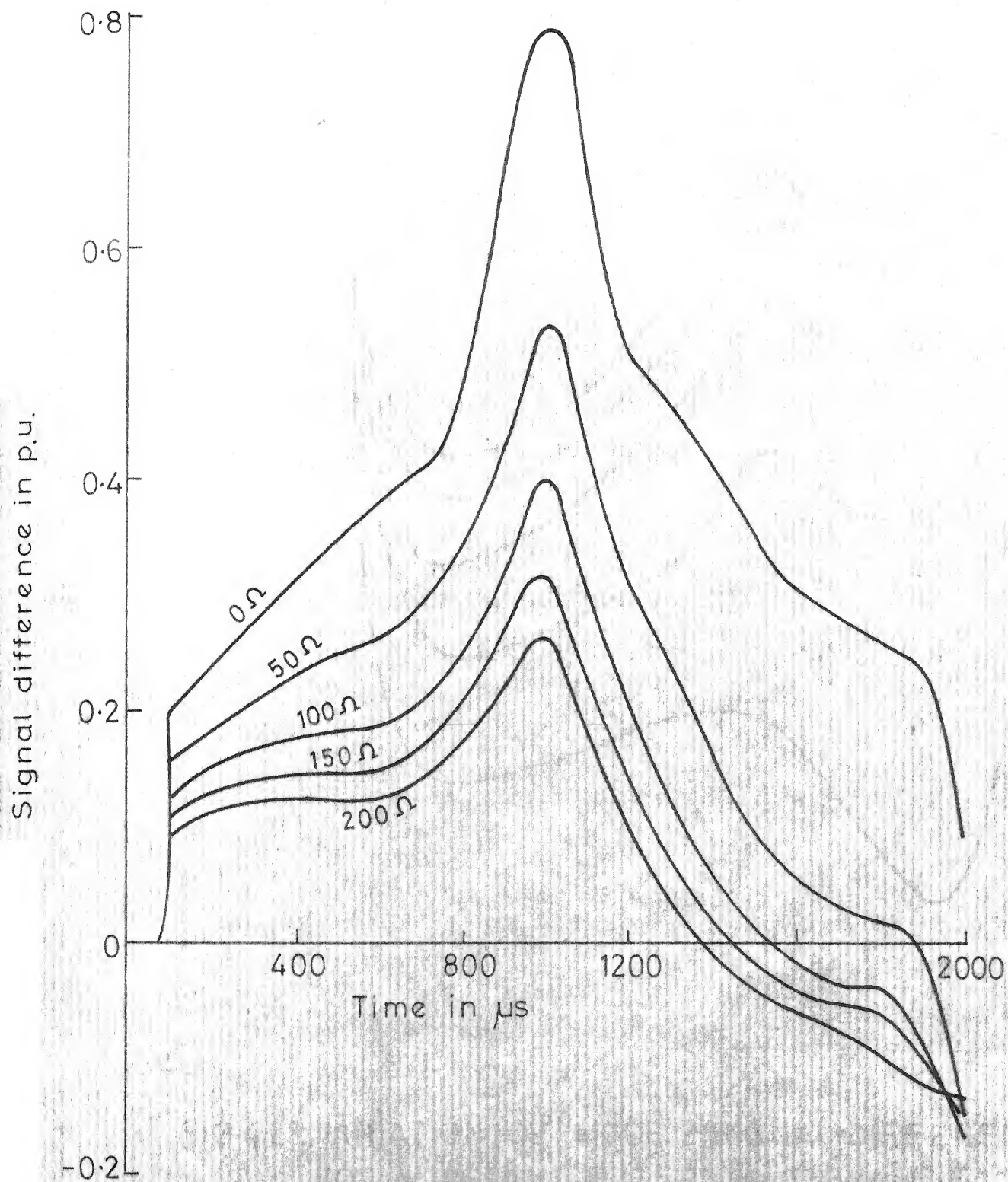
FIG. 4·22 VARIATION OF MODE 3 SIGNAL DIFFERENCE FOR A CLOSE IN INTERNAL PHASE TO GROUND FAULT ON PHASE 'A' : $\phi_0 = 90°$
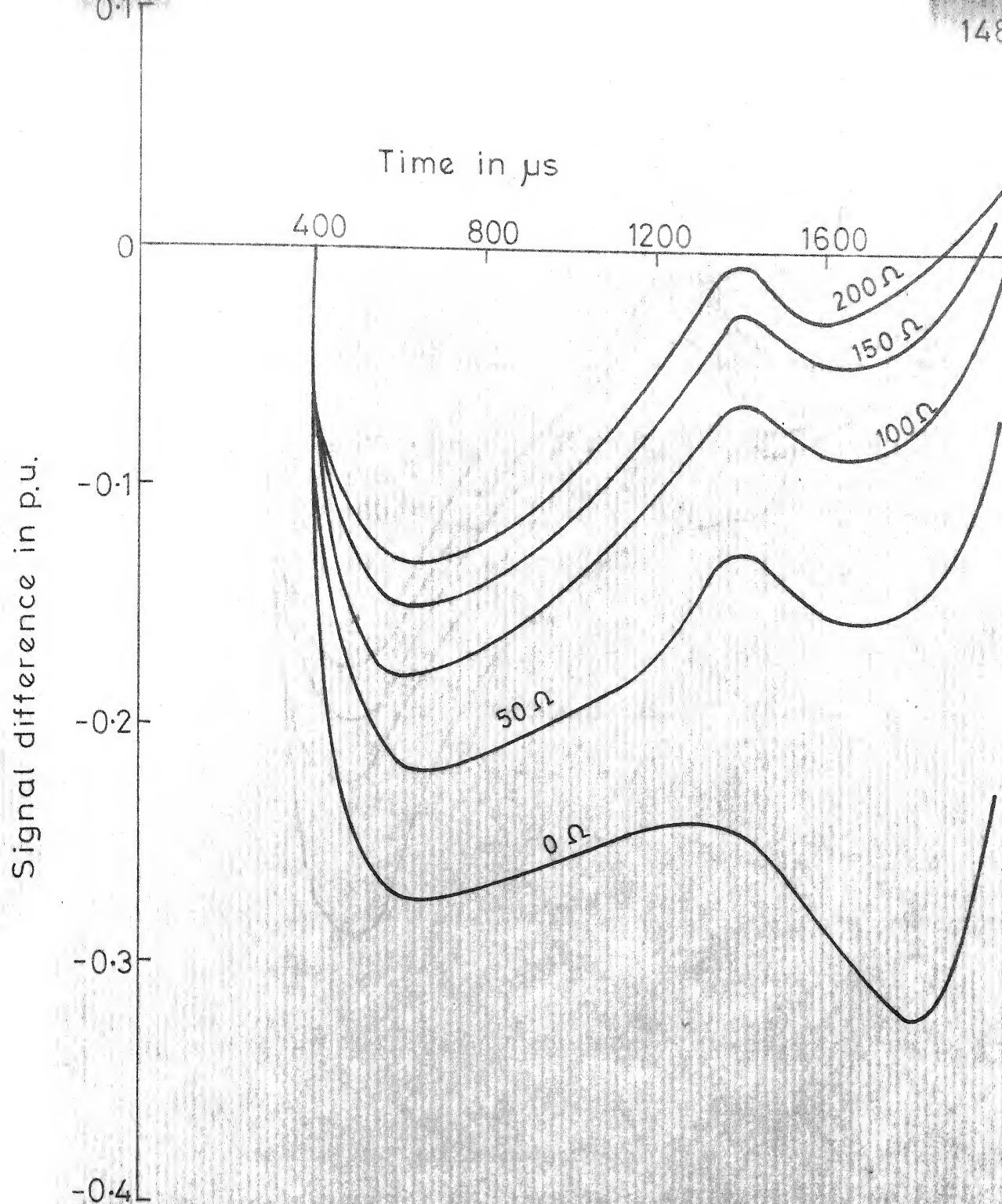
FIG.4.23 VARIATION OF MODE 2 SIGNAL DIFFERENCE FOR A DISTANT EXTERNAL 3-PHASE FAULT : $\phi_0=0°$
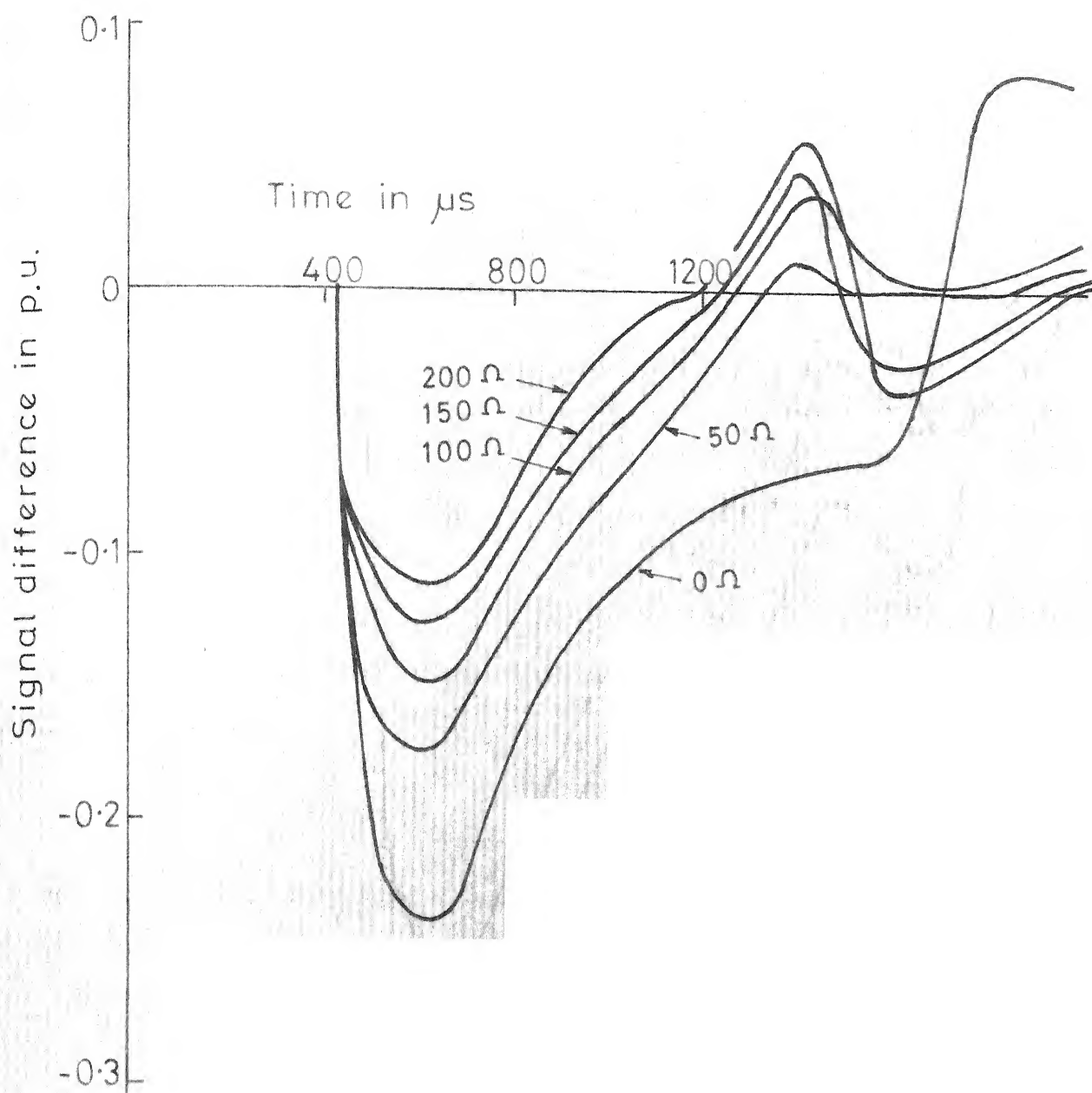
FIG. 4·24 VARIATION OF MODE 3 SIGNAL DIFFERENCE
FOR A DISTANT EXTERNAL 3-PHASE
FAULT: $\phi_0 = 0°$
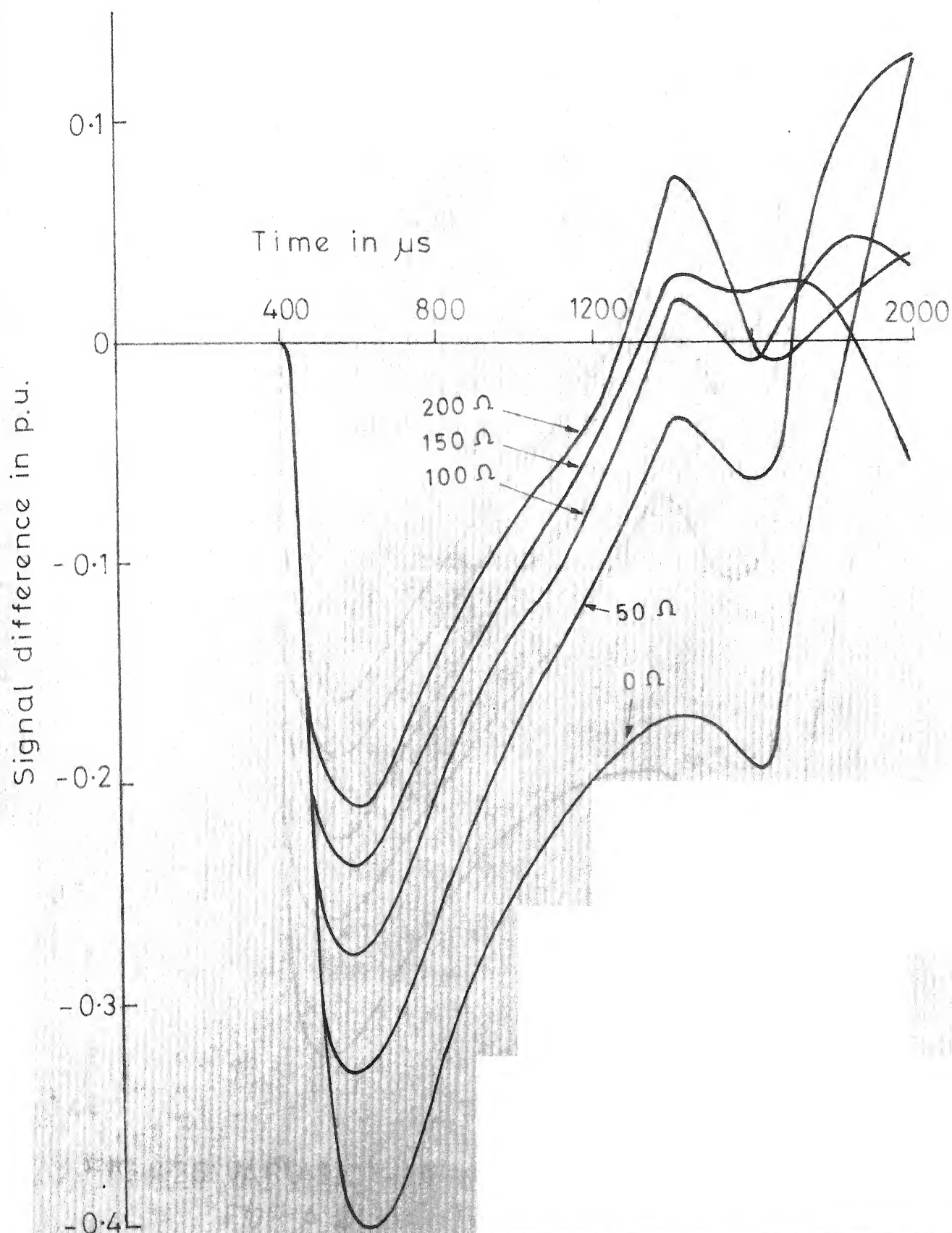
FIG.4.25 VARIATION OF MODE 2 SIGNAL DIFFERENCE FOR A DISTANT EXTERNAL 3-PHASE FAULT: $\phi_0 = 90°$
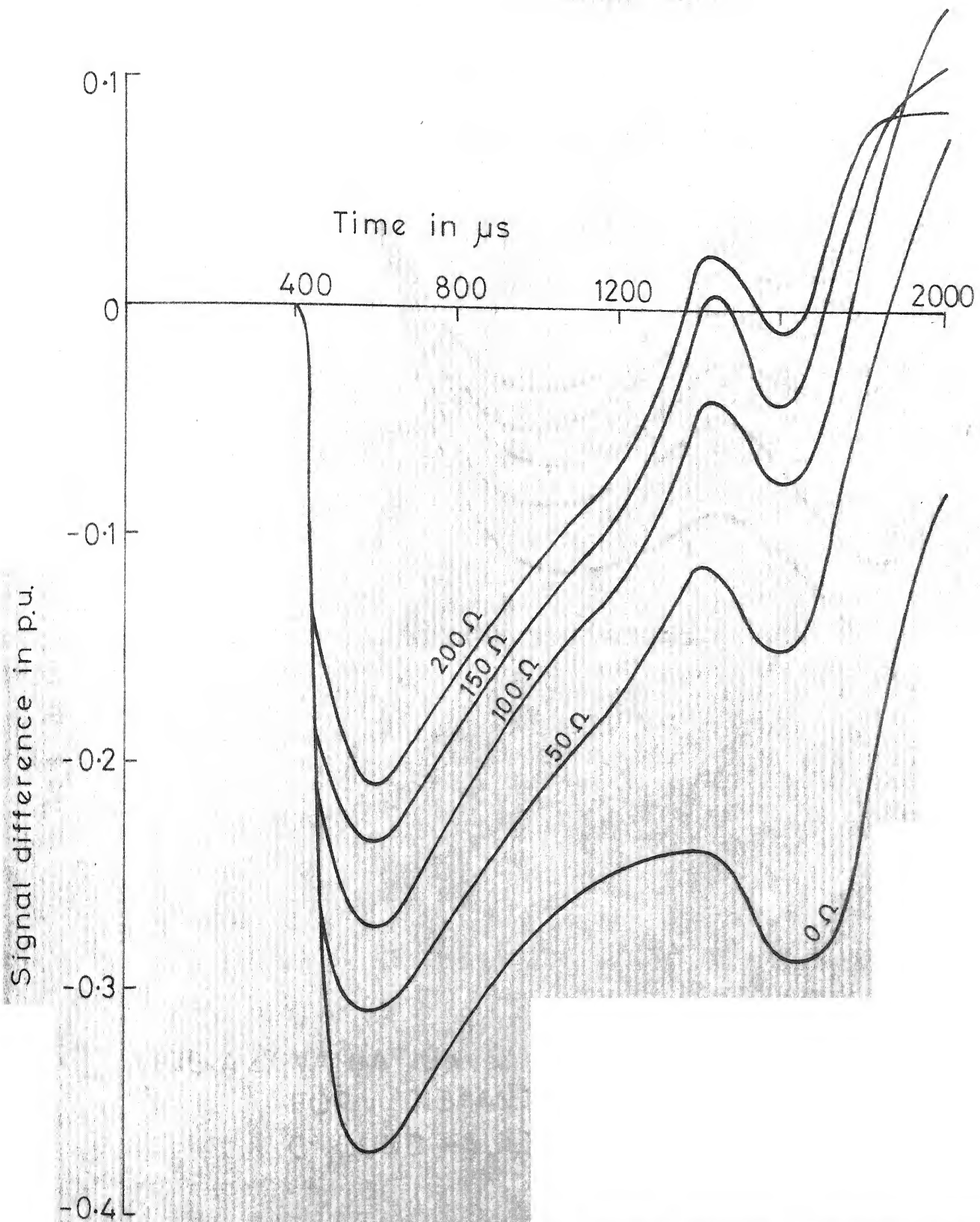
FIG·4·26 VARIATION OF MODE 3 SIGNAL DIFFERENCE FOR A DISTANT EXTERNAL 3-PHASE FAULT: $\phi_o = 90°$
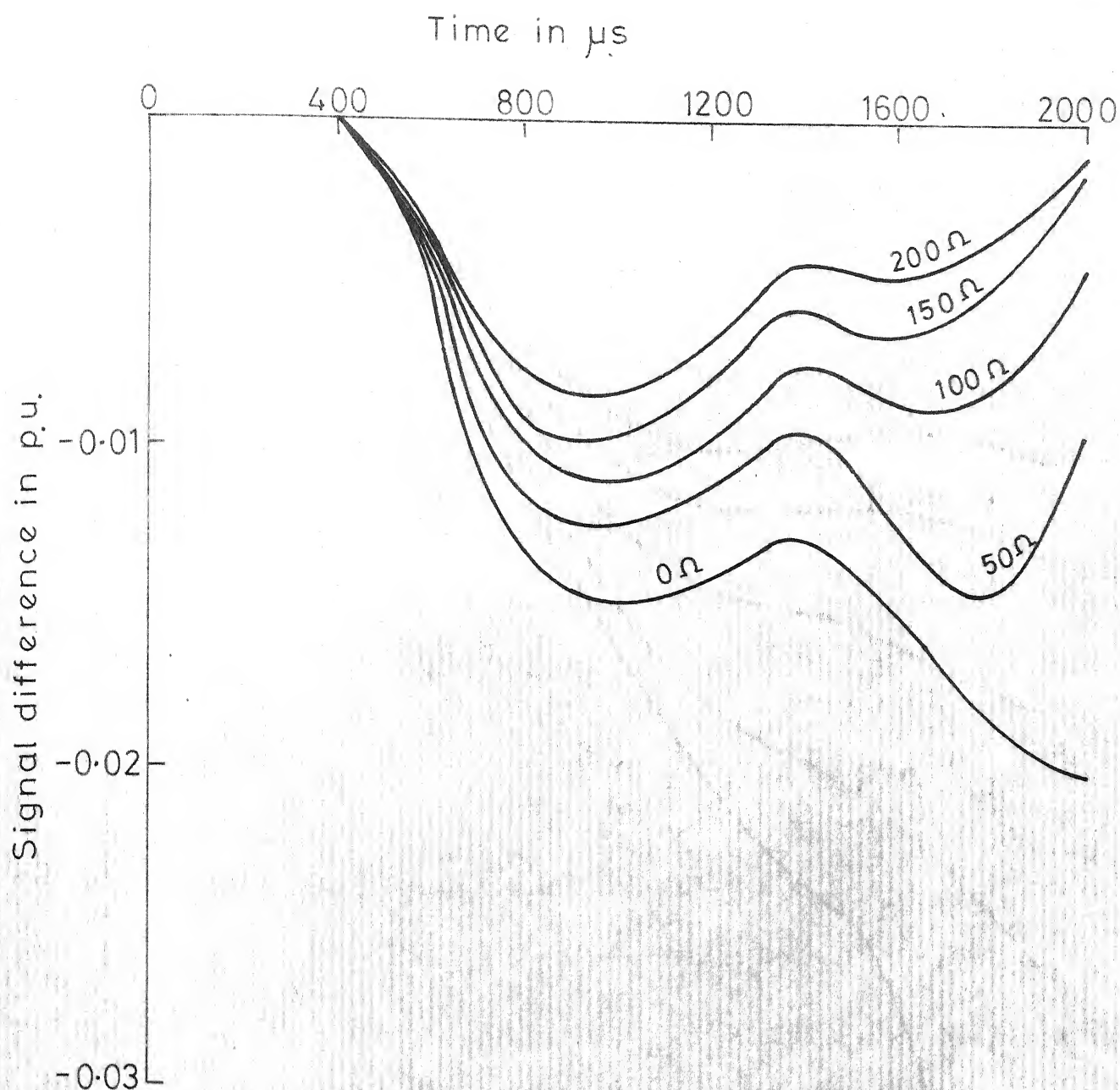
FIG. 4·27 VARIATION OF MODE 1 SIGNAL DIFFERENCE
FOR A DISTANT EXTERNAL ONE PHASE TO
GROUND FAULT ON PHASE 'A': $\phi_0 = 0°$
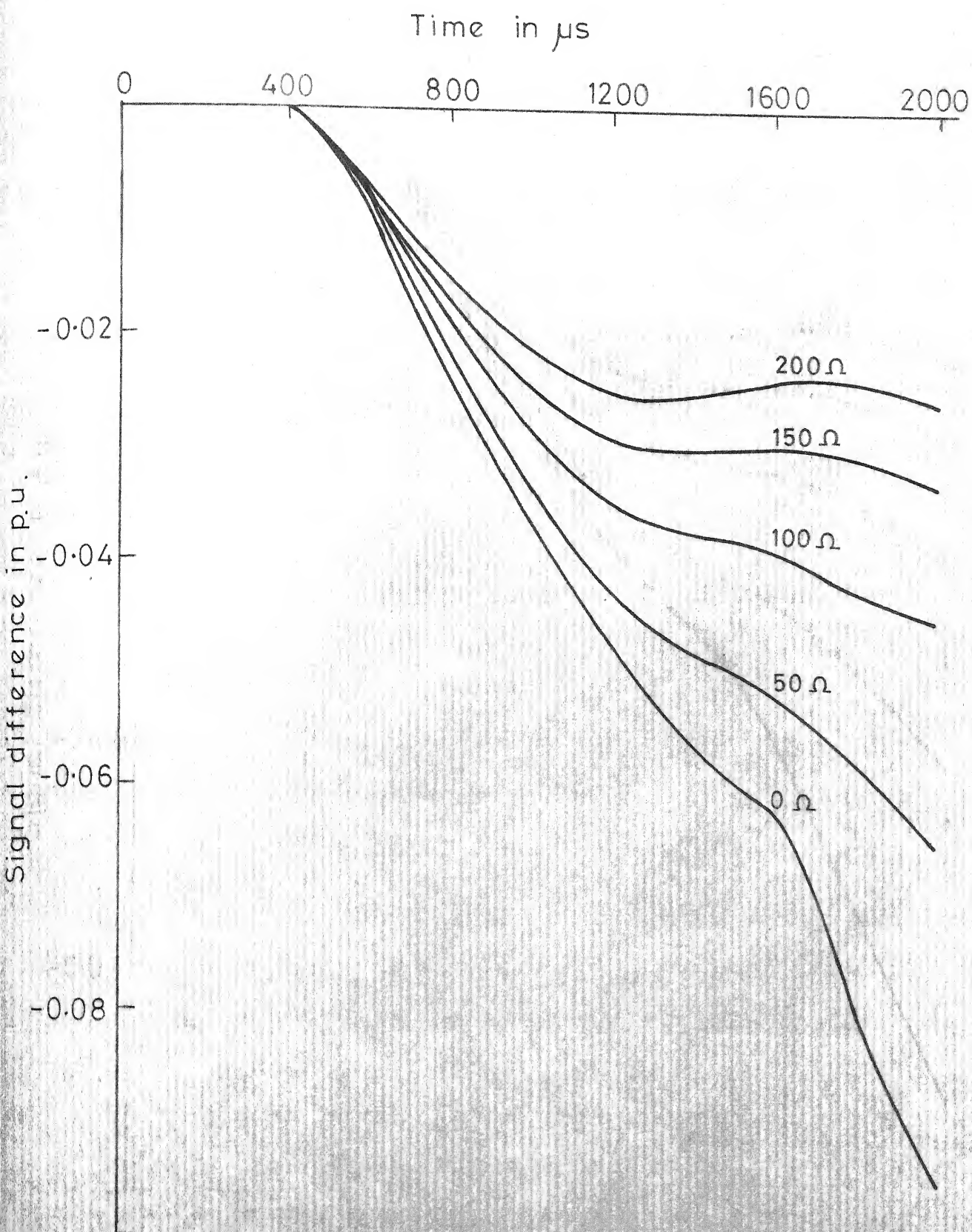
FIG. 4.28 VARIATION OF MODE 2 SIGNAL DIFFERENCE FOR A DISTANT EXTERNAL ONE PHASE TO GROUND FAULT ON PHASE 'A': $\phi_o = 0°$
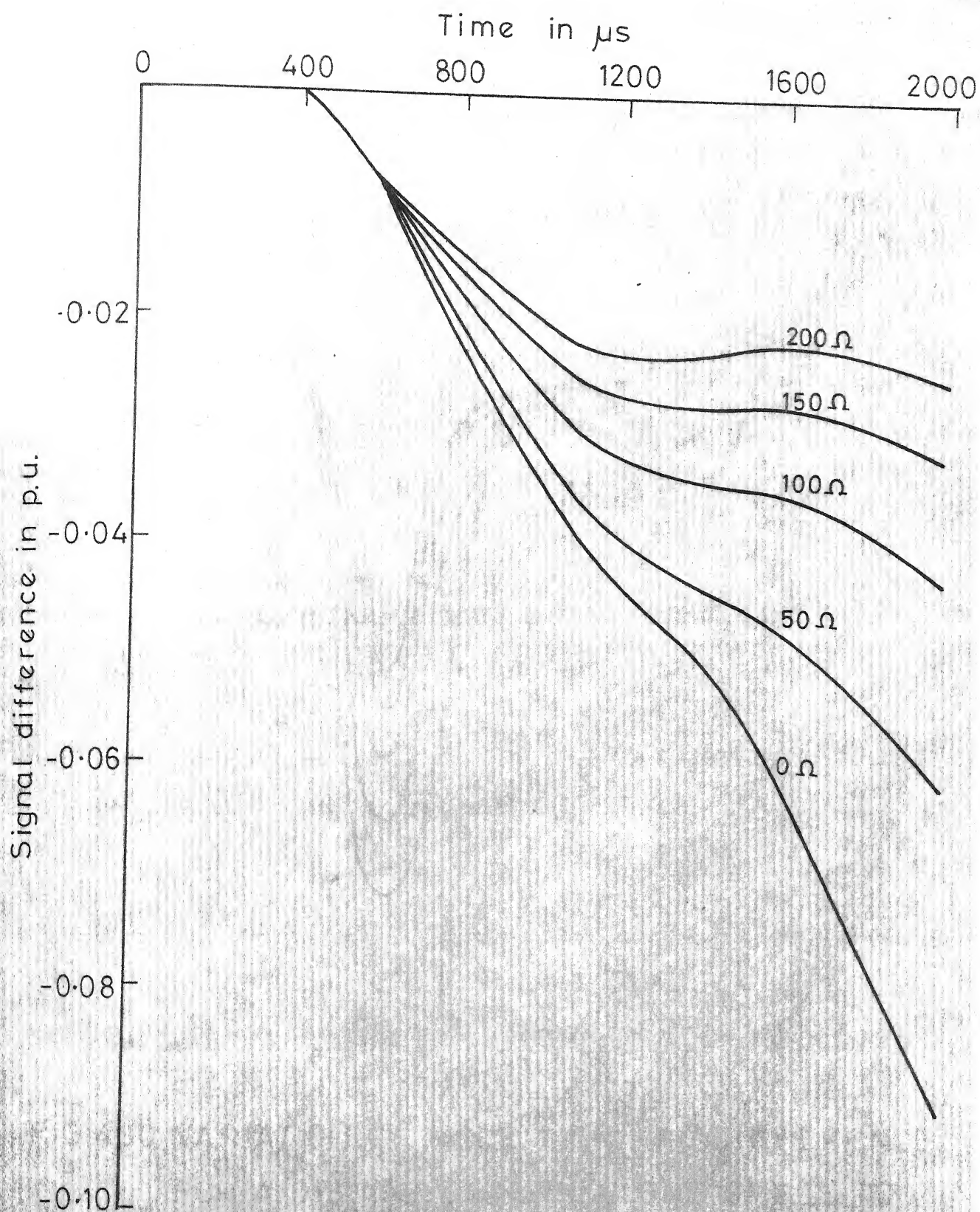
FIG.4·29 VARIATION OF MODE 3 SIGNAL DIFFERENCE FOR A DISTANT EXTERNAL ONE PHASE TO GROUND FAULT ON PHASE 'A' : $\phi_0 = 0°$
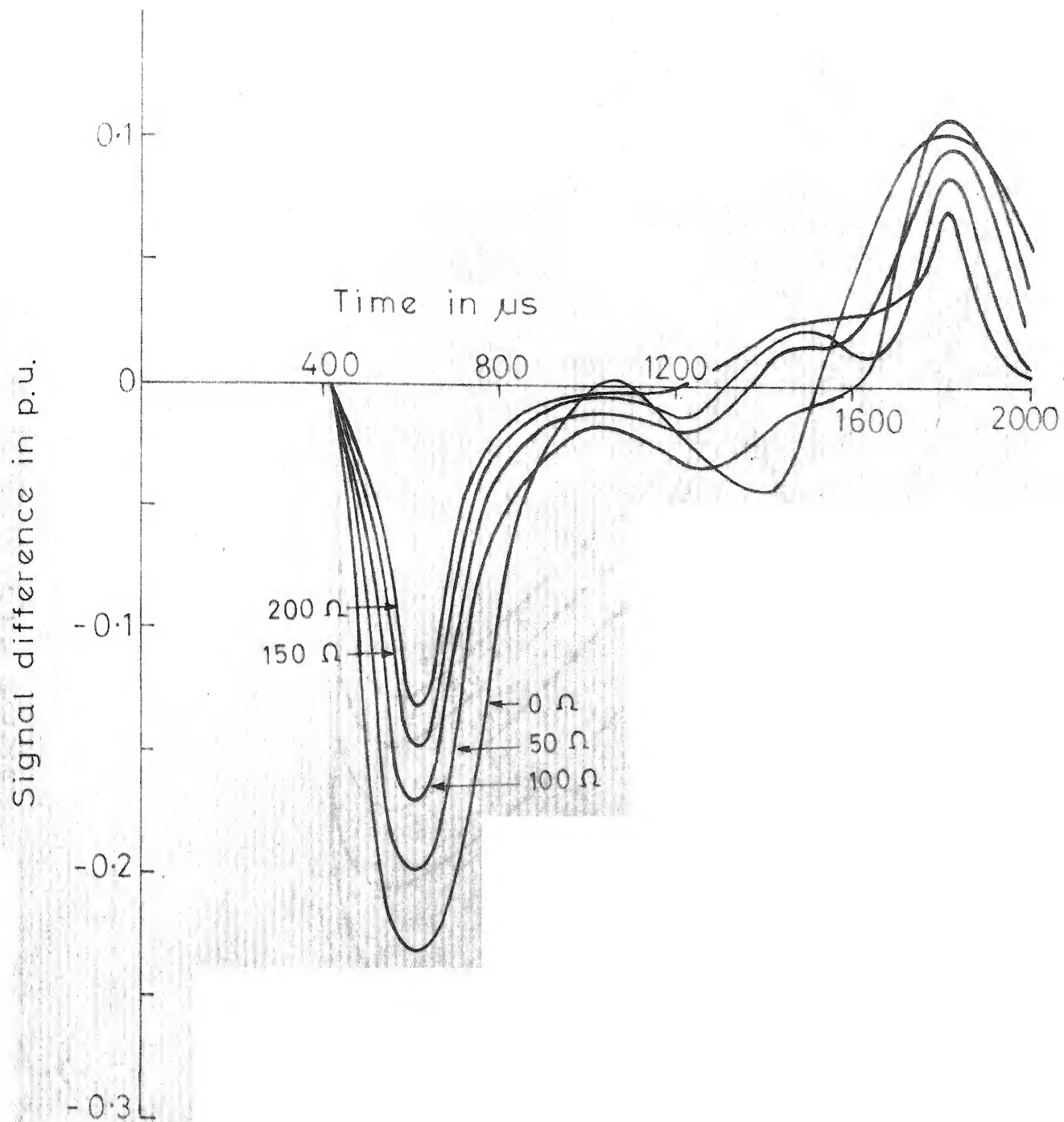
FIG·4·30 VARIATION OF MODE 1 SIGNAL DIFFERENCE FOR A DISTANT EXTERNAL ONE PHASE TO GROUND FAULT ON PHASE A : $\phi_o = 90°$
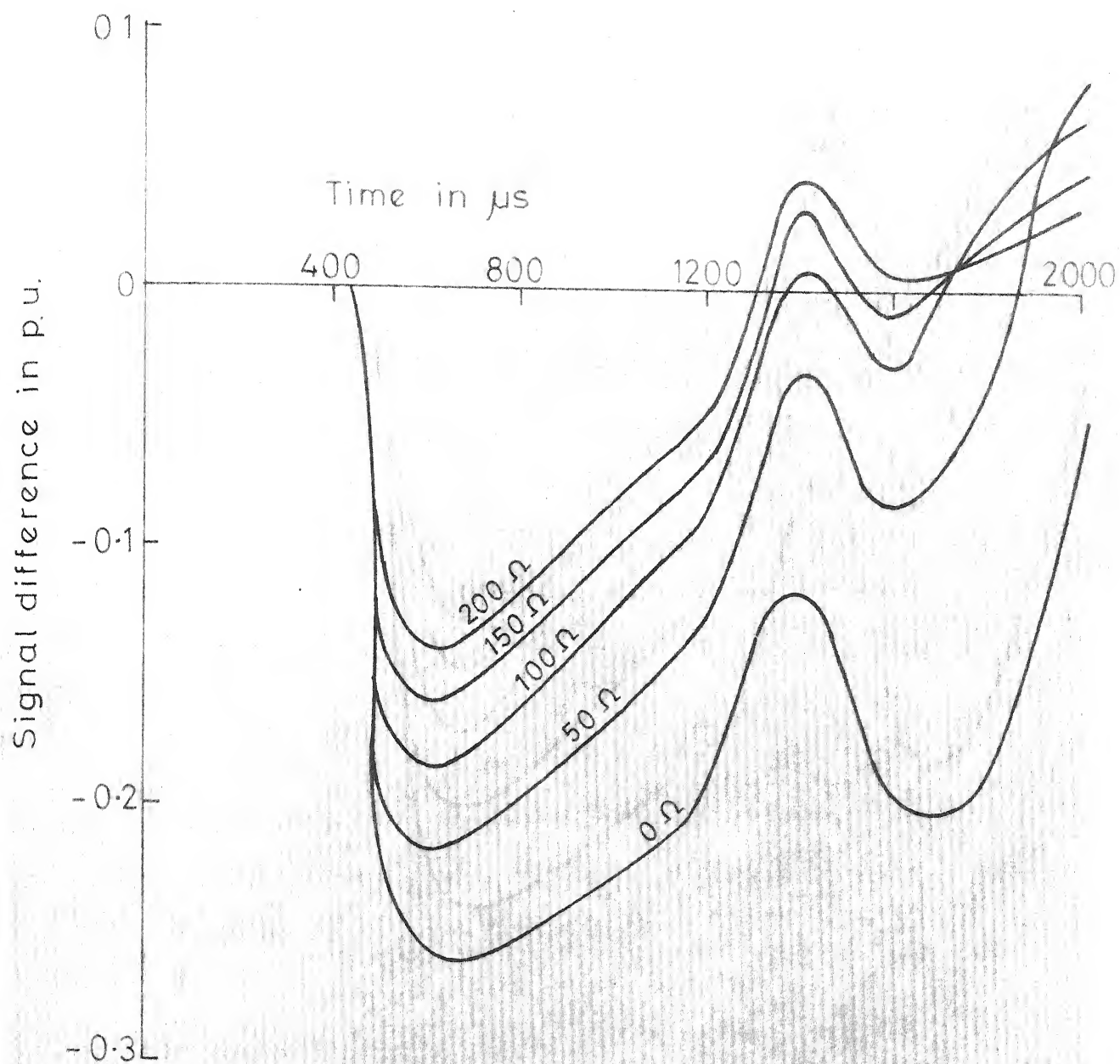
FIG. 4·31 VARIATION OF MODE 2 SIGNAL DIFFERENCE
FOR A DISTANT EXTERNAL ONE PHASE TO
GROUND FAULT ON PHASE 'A' $\phi_0 = 90°$
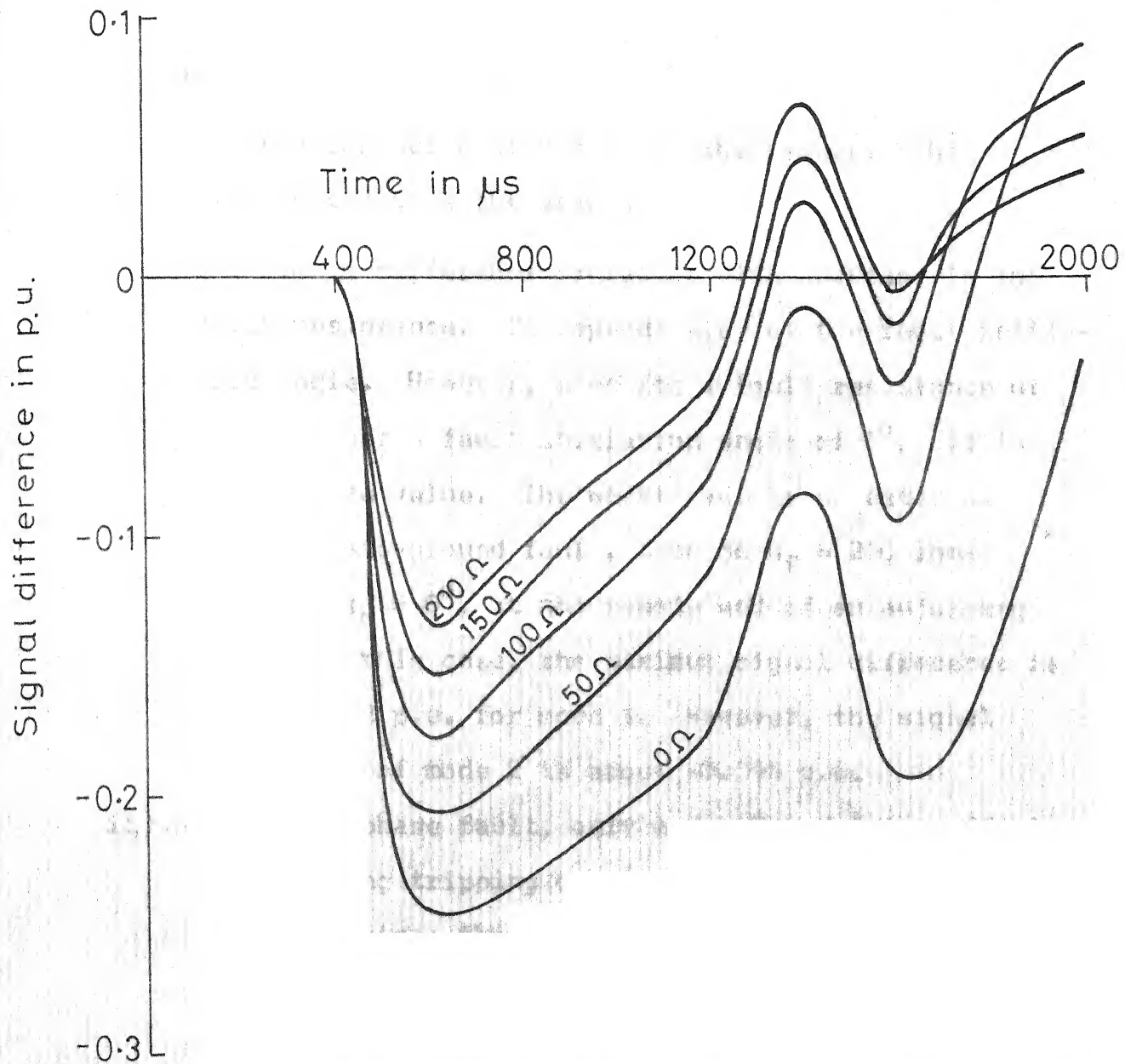
FIG. 4·32 VARIATION OF MODE 3 SIGNAL DIFFERENCE
FOR A DISTANT EXTERNAL ONE PHASE TO
GROUND FAULT ON PHASE 'A': $\phi_o = 90°$

4.2.4 Discussion on the Results

After a careful examination of the results, the following conclusions are drawn.

i) The signal difference decreases with increase in the fault resistance. It depends also on the fault initiation angle. However, even for a fault resistance of 200 ohms and a fault initiation angle of 0°, it is of adequate value. The worst case is an external one-phase-to-ground fault, through $R_f = 200$ ohms and with $\varphi_0 = 0^o$, at the remote end of an adjoining line. In this case, the maximum signal difference is about -0.02 p.u. for mode 1. However, the signal difference of mode 2 is about -0.095 p.u.

ii) For the 3-phase fault, only modes 2 and 3 are effective in producing tripping or blocking signals. This is as expected, since the mode 1 voltages and currents would be of negligible value by the very choice of the modal transformation matrix given in eqn. (4.7).

iii) The results quite clearly confirm the viability of this simple relaying technique.

4.3 FAULT LOCATING RELAY SCHEME

This is the second UHS relay scheme, which is developed in this section, and which, in addition to giving a tripping signal for internal faults, also gives the distance of the

fault. This scheme has the following special features.
The tripping on internal faults takes place without the
aid of communication channel. The communication channel
is used only for blocking purposes in the event of external
faults. Therefore, the operating time of the communication
carrier equipments does not come into picture in the case
of internal faults. The scheme makes use of the reflection
properties of the travelling waves to determine the location
of the fault. In this section, the theory and principles of
operation of the scheme, and also digital simulation results,
that confirm the viability of the scheme, are presented.

4.3.1 Theory and Principles of Operation

With regard to this scheme also, the underlying
principles are explained by considering a lossless 1-phase
transmission line, which interconnects two large power
systems, as shown in Fig. 4.1. Two identical relay schemes,
located at S and R, and with reference directions as shown,
are employed for the protection of the line. The dis-
cussion is centred on the relay scheme at S. It applies
equally well to that at R.

The input signal pair to the relay at S is the same
as in the previous scheme, and is given by eqns. (4.3).
However, in the present scheme, S_2 is used only to detect
the reverse faults (i.e. faults behind the relay) whilst
S_1 is used not only to detect but also to locate an internal

fault. These are explained below.

(i) Reverse faults

Upon the occurrence of a fault on any of the other lines connected to the sending end bus, travelling waves of voltage and current are generated. One pair of them travels towards the sending end bus where the waves undergo both reflection and refraction. Due to the refracted waves, $|S_2|$ increases from zero to $|(1+R_{set}/Z_0')\ \rho_t\ v_{ff}|$, as given by the second part of eqns. (4.4), where Z_0' is the surge impedance of the faulted line. If $Z_0' = Z_0$, as is usually the case, then $|(1+R_{set}/Z_0')\ \rho_t\ v_{ff}| = 2.0|\rho_t\ v_{ff}|$. Therefore, if $|S_2| > 0$, a reverse fault is indicated. However, there may be measurement and/or other types of errors. Accordingly, the following criterion is adopted for detecting a reverse fault,

$$|S_2| > \text{a preset level} \qquad\qquad (4.11)$$

If $|S_2|$ exceeds the preset level, a transmitter is started after a short time delay Td_1. The purpose of this time delay is explained later. In addition, issue of a trip signal at the local end, by the backward waves coming from the remote end after reflection, is blocked. The remote-end receiver, upon the receipt of the transmitter signal, blocks the issue of a trip signal there.

(ii) Forward faults

Consider a fault at the point F (Fig. 4.1) on the protected line. The travelling waves, generated at the fault point, travel between this point and the ends of the line, for some time, due to multiple reflections and refractions. These events are depicted in Figs. 4.33 to 4.38, by means of Lattice diagrams, for different conditions.

The first travelling wave pair reaching S will be backward and will cause the value of $\left|S_1\right|$ to increase suddenly from zero to $2\left|v_{ff}\right|$ at this moment as given in Table 4.1. These waves will also cause $\left|S_2\right|$ to increase to $2\left|\rho_s\, v_{ff}\right|$ immediately thereafter. This may result in the transmitter being started. However, the starting of the transmitter is delayed by a short interval of time Td_1, and meanwhile, the former event is used to block the starting of the transmitter.

After a time interval of $2\tau_1$, there will be a second sudden increase in $\left|S_1\right|$ due to the backward reflected waves coming from the fault point. The time interval between the first two sudden increases in $\left|S_1\right|$ is measured. This time interval is equal to twice the travel time of the waves between the fault and relay points. Hence, it gives the location of the fault.

However, if the fault occurs at a voltage zero, there will not be any sudden increases in $\left|S_1\right|$. This fact is
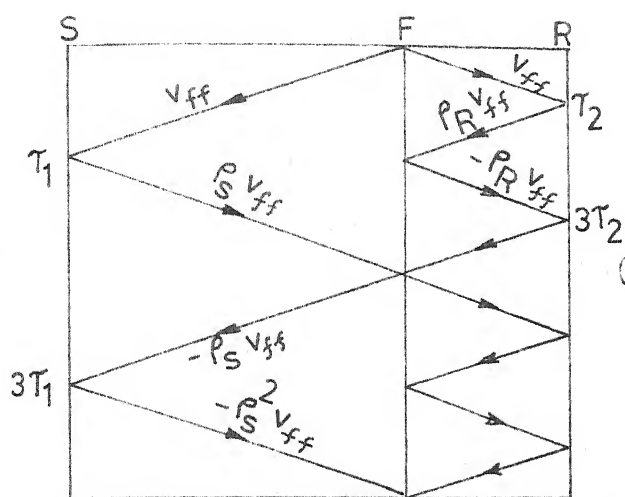
FIG·4·33 LATTICE DIAGRAM FOR
A BOLTED FAULT
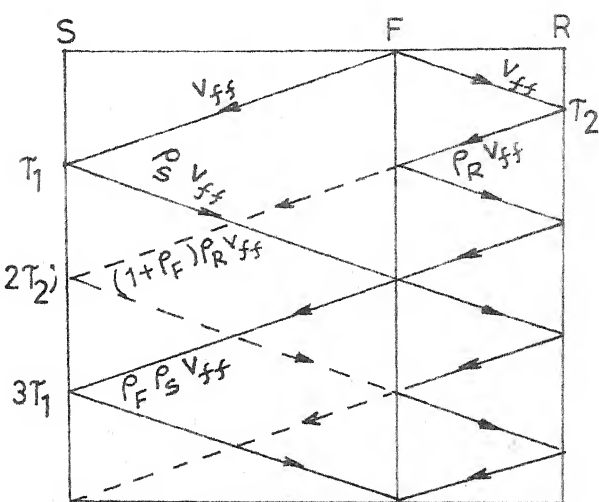
FIG·4·34 LATTICE DIAGRAM
FOR A FAULT
THROUGH R_f
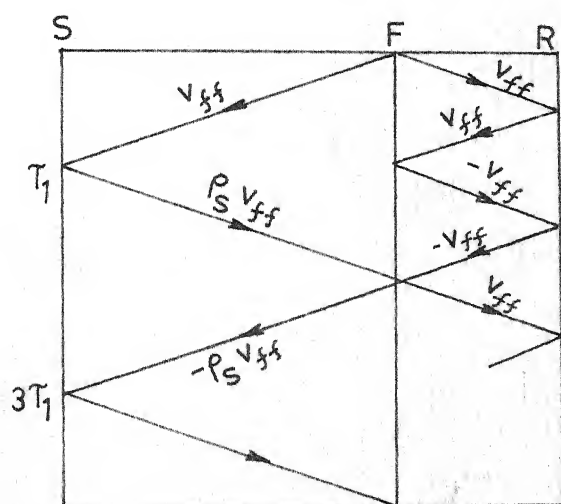
FIG·4·35 LATTICE DIAGRAM FOR
A BOLTED FAULT WHEN
R.E. IS ON OPEN CIRCUIT
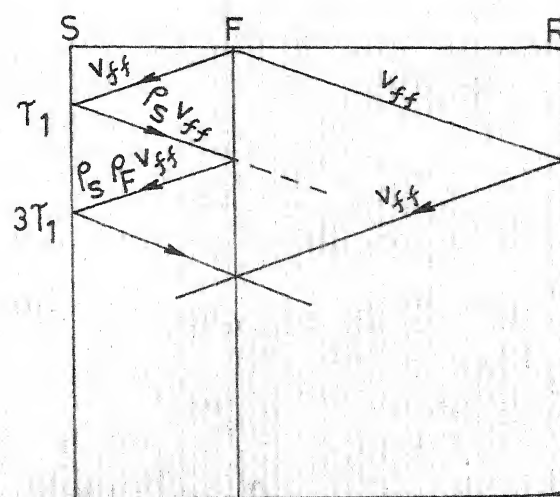
FIG·4·36 LATTICE DIAGRAM
FOR A FAULT
THROUGH R_f WITH
R.E. ON OPEN CIRCUIT
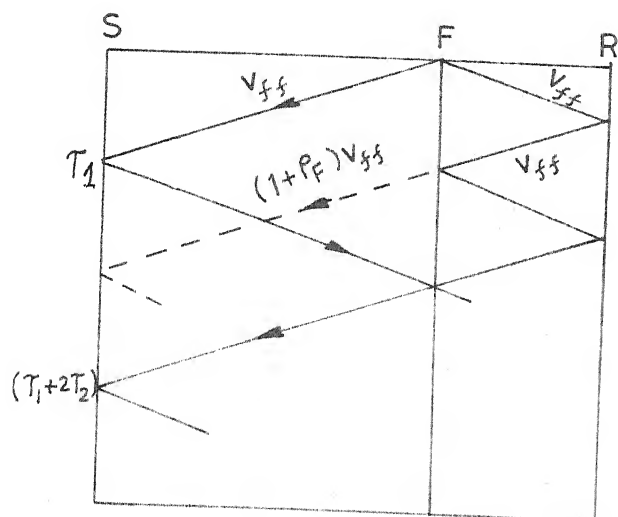
FIG·4·37 LATTICE DIAGRAM
FOR A FAULT THROUGH
R_f WITH R.E. ON OPEN
CIRCUIT
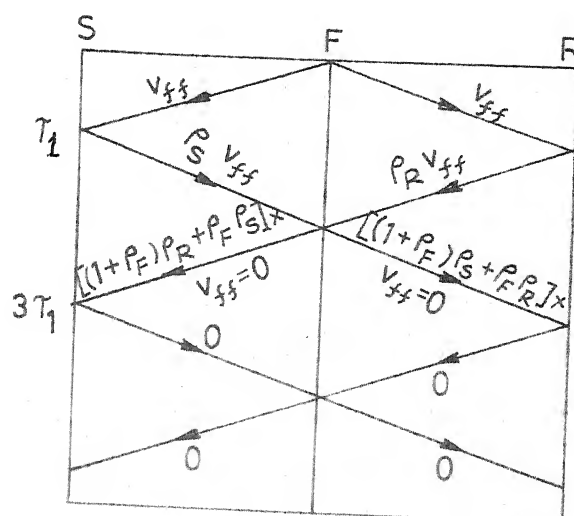
FIG·4·38 LATTICE DIAGRAM
FOR A FAULT AT
THE MIDDLE OF THE
LINE

$2(1+\rho_S\rho_F)V_{ff\,max}\sin(\omega_0 t-3\tau_1)$

$2V_{ff\,max}\sin(\omega_0 t-\tau_1)$
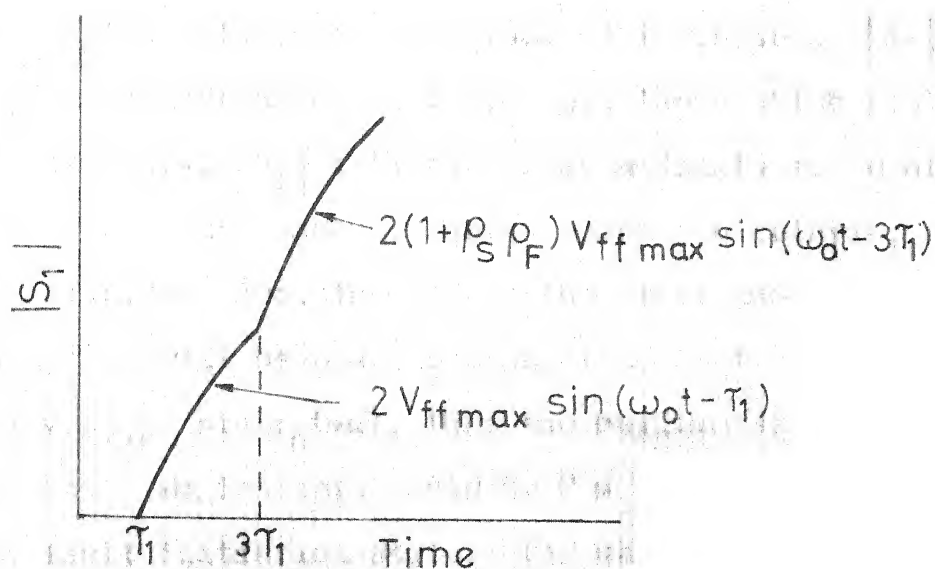
FIG·4·39 VARIATION OF $|S_1|$ WHEN $\phi_0=0°$ (not to scale)

illustrated in Fig. 4.39 where the time variation of $|S_1|$ is shown for this case. This difficulty is surmounted by using sudden increase in $d|S_1|/dt$ in addition to those in $|S_1|$ for locating the fault.

For a close- in fault, $|S_1|$ or $d|S_1|/dt$ builds up rapidly and almost continuously. If the rapid and continuous building up takes place over a certain preset time period, then tripping is initiated, and the fault is located as nearby.

4.3.2 Relay settings

In actual practice, the increases in either $|S_1|$ or $d|S_1|/dt$ will not be quite sudden, but will be only rapid. This is due to the attenuation caused by the losses in the line and earth. Also, the magnitude of increase in $|S_1|$ or $d|S_1|/dt$ depends upon the fault resistance which reduces v_{ff}. Accordingly, $|S_1|$ will have only a finite slope at the instant when the backward waves reach the relaying point, and not infinite. And, in between the first two rapid increases, $|S_1|$ will have a slope equal to that of $2|v_f|$. If $v_{ff} = V_{ffmax} \sin(\omega_0 t + \alpha)$, then the maximum slope of $|S_1|$ between these two instants could be $2\omega_0 V_{ffmax}$ depending upon the fault initiation angle. The maximum value of v_{ff} will be for a bolted fault. Then, v_{ff} will be equal to (v_{pff}), the prefault voltage at the fault. And, the maximum slope of $|S_1|$ would be equal to $2\omega_0 V_{pffmax}$. When

the rapid increase in $\left|S_1\right|$ is detected by measuring its slope, the following criterion needs adoption so that no wrong detection of fault occurs, when the slope of $\left|S_1\right|$ is maximum or close to it, during the time interval between the two rapid increases in $\left|S_1\right|$,

$$\text{i.e. } d\left|S_1\right|/dt > 2\omega_o V_{pffmax} \qquad (4.12a)$$

At the instant of second rapid increase in $\left|S_1\right|$, v_{ff} gets reduced to $\rho_s v_{ff}$. Hence, the following criterion is adopted for detecting the second rapid increase in $\left|S_1\right|$.

$$d\left|S_1\right|/dt > 2\rho_s\omega_o V_{pffmax} \qquad (4.12b)$$

In a similar way, the following criteria are adopted to detect the first and second rapid increases in $d\left|S_1\right|/dt$.

$$d^2\left|S_1\right|/dt^2 > 2\omega_o^2 V_{pffmax}$$

and

$$d^2\left|S_1\right|/dt^2 > 2\rho_s\omega_o^2 V_{pffmax} \qquad (4.13)$$

For very high fault resistances, the second rapid increase may not be appreciable. (This becomes evident when digital simulation results are observed). Under such circumstances, tripping may not ensue. This is avoided by the following procedure. A trip signal is issued after a fixed time delay of T_{d2} seconds from the moment of detection of the first rapid increase either in $\left|S_1\right|$ or in $d\left|S_1\right|/dt$, provided

that no blocking signal is received from the other end. Of course, in such a case, fault location will not take place.

The value of T_{d2} should be such that the following operations are not interfered with. In the event of an external fault beyond the remote end, the issue of a trip signal by the local relay should be blocked by the blocking signal received from the other end. For no interference with this operation, T_{d2} should be greater than the time taken by the communication equipment to produce the signal plus the response time of the blocking relay. In the event of an internal fault at the remote end of the protected line, the detection of second rapid increase in $\left|S_1\right|$ or $d\left|S_1\right|/dt$ takes place after a time lapse, equal to twice the travel time of the entire line 2τ, when reckoned from the moment of detection of first rapid increase. For no interference with this operation, $T_{d2} > 2\tau$.

4.3.3 Typical cases

Four typical cases of an internal fault are considered in this section in order to illustrate the applicability of the basic principles explained in Section 4.3.1.

(i) Bolted faults

The Lattice diagram for this case is given in Fig. 4.33. It can be observed that $\left|S_1\right|$ increases suddenly from zero to

to $2\left|v_{pff}\right|$ at τ_1, from $2\left|v_{pff}\right|$ to $2(1-\rho_s)\left|v_{pff}\right|$ at $3\tau_1$, and so on. After sensing the first two sudden increases in $\left|S_1\right|$ at τ_1 and $3\tau_1$, a trip signal is issued. The time interval between these gives the location of the fault. The time of operation would be maximum for a fault at the remote end of the protected line, and would be equal to 3τ. It obviously depends upon the length of the line. It would be equal to about 2 ms for a 200 Km line, and would be equal to 5 ms (i.e., one-fourth of a cycle on 50 Hz frequency base) for a 500 Km line.

(ii) Faults through resistance

For this case, the Lattice diagram is given in Fig. 4.34. An examination of the diagram reveals that, additional sudden changes in $\left|S_1\right|$ are produced by the transmitted (refracted) waves. The propagation of the transmitted waves is represented by broken lines on the diagram. However, these changes are normally decrements since ρ_f, the voltage reflection coefficient at the fault point, is always negative, and ρ_s and ρ_r are normally negative. Since only sudden increases in $\left|S_1\right|$ are sensed, these additional sudden changes do not affect the operation.

(iii) Faults on an open-circuited line

Let the receiving end be an open circuit. Then, the Lattice diagrams for (a) a bolted fault, (b) a fault through R_f

closer to the sending end, and (c) a fault through R_f
closer to the receiving end would be as given in Figs. 4.35,
4.36 and 4.37 respectively. It can be observed that normal
operation takes place in the first two cases. In the third
case, the sudden change at $(\tau_1+2\tau_2)$ would be an increment.
Consequently, the relay operates faster. But, the fault
point can be located only at the second attempt as explained
below. The fault is located first as at a distance of
$u\tau_2$ from the sending end, where u is the velocity of propa-
gation of travelling waves. If the fault is not found there,
then it is taken to be at a distance of $u\tau_2$ from the receiv-
ing end.

(iv) Faults at the middle of the line

For a fault at the middle of the line, there will not
be a second or subsequent sudden increases in $\left| S_1 \right|$, if
$\rho_s = \rho_r$ and $R_f = Z_0/2$ as explained below.

For this fault, the Lattice diagram will be as given
in Fig. 4.38. When $R_f = Z_0/2$,

$$\rho_f = \left[\frac{R_f Z_0}{(R_f+Z_0)} - Z_0 \right] / [R_f Z_0/(R_f+Z_0) + Z_0]$$

$$= -0.5.$$

From the Lattice diagram, it may be observed that, the
second sudden increase at the sending end is given by,

$$2[(1+\rho_f)\,\rho_r + \rho_f\rho_s] \left| v_{ff} \right|$$

With $\rho_s = \rho_r$ and $\rho_f = -0.5$, the above quantity vanishes. That is, there will not be a second sudden increase.

However, in the case of a 3-phase line, this will not pose any problem due to the following reason. The surge impedance of mode 1 and those of modes 2 and 3 have widely different values. And, if $R_f = Z_0^{(1)}/2$, then $R_f \neq Z_0^{(2)}/2$ or $Z_0^{(3)}/2$ and vice versa. And hence, there will be at least one mode available for producing the desired operation.

4.3.4 Extension of the Principles to the Protection of 3-Phase Lines

The extension of the relaying principles to the protection of a 3-phase transmission line is based on the modal decomposition of the 3-phase line into three decoupled fictitious 1-phase lines, each having its own propagation constant and surge impedance, as discussed in Section 4.2.2. Consequently, the relaying principles described in Sections 4.3.1 and 4.3.2 apply also to each of these fictitious 1-phase lines. Therefore, in this scheme also, three signal pairs, one for each mode, are employed. For the sending end relay, they are given by eqns. (4.9). The blocking and other criteria, given in eqns. (4.11) to (4.13), would get modified as given below in the same order.

For reverse fault detection,

$$\left| S_2^{(m)} \right| > \text{a preset level, } m = 1,2,3 \qquad (4.14)$$

For detecting the first and second rapid increase in $\left|S_1^{(m)}\right|$, $(m = 1,2,3)$, we have

$$d\left|S_1^{(m)}\right|/dt > 2\,\omega_o\,V_{ffmax}^{(m)}$$

and $\quad d\left|S_1^{(m)}\right|/dt > 2\,\rho_s\,\omega_o\,V_{ffmax}^{(m)}$ respectively; $m = 1,2,3$

$$(4.15)$$

For detecting the first and second rapid increases in $d\left|S_1^{(m)}\right|/dt$ $(m = 1,2,3)$, we have

$$d^2\left|S_1^{(m)}\right|/dt^2 > 2\omega_o^2\,V_{ffmax}^{(m)}$$

and $\quad d^2\left|S_1^{(m)}\right|/dt^2 > 2\rho_s\omega_o^2 V_{ffmax}^{(m)}$ respectively; $m = 1,2,3$

$$(4.16)$$

Here, $V_{ffmax}^{(m)}$, $m = 1,2,3$ are the modal components of the fault generated components of the phase voltages at the fault point for a bolted fault. These components have different values for different types of faults as derived in the next section, and given in Table 4.3. From the table, it can be observed that, the value of $V_{ffmax}^{(1)}$ is maximum in the case of one-phase-to-ground fault on phase 'a' and is equal to 0.5 p.u. The values of $V_{ffmax}^{(2)}$ and $V_{ffmax}^{(3)}$ are maximum for a 3-phase fault, and each of them is equal to 0.5773502 p.u. In order to provide safe settings, these maximum values are chosen for determining the settings defined in eqns. (4.14) and (4.15). $V_{ffmax}^{(1)}$ and $V_{ffmax}^{(2)}$ will have lowest values for one-phase-to-ground faults. Therefore, it is necessary

to verify that the settings chosen are not detrimental in the case of one-phase-to-ground faults. The values of the settings for the detection of the first and second rapid increases are given in Table 4.2.

TABLE 4.2

Relay settings for the detection of first and second rapid increases in first and second time derivatives of $\left|S_1^{(m)}\right|$, m = 1,2,3

Nominal angular frequency of the system
$$= 314.15926 \text{ rad/s}$$

$f_g = 0.8$

Modes (m)	Detection of the first rapid increase in		Detection of the second rapid increase in	
	first derivative of $\left|S_1^{(m)}\right|$	second derivative of $\left|S_1^{(m)}\right|$	first derivative of $\left|S_1^{(m)}\right|$	second derivative of $\left|S_1^{(m)}\right|$
1	314.16	98696.04	251.33	78956.84
2 and 3	362.76	113964.36	290.21	91171.49

4.3.5 Modal Components of the Fault-Point Voltages for Different Types of Faults

In this section, the modal components of the fault-point voltages $v_{ff}^{1,2,3}$ are determined for different types of faults,

with the following assumptions.

1. The transmission line is assumed to be perfectly transposed

2. The fault resistances are zero

The conditions prevailing at the fault point are depicted in Fig. 4.40, where

$v_{ff}^{a,b,c}$ — column vector of the fault generated components of the fault-point voltages of the phases a,b,c

$i_{ff}^{a,b,c}$ — column vector of the fault currents of the phases a,b,c

$i_{ffs}^{a,b,c}$ — component of $(-i_{ff}^{a,b,c})$ travelling towards the sending end

$i_{ffr}^{a,b,c}$ — component of $(-i_{ff}^{a,b,c})$ travelling towards the receiving end

$v_{ffs}^{a,b,c}$ — voltage of the waves travelling towards the sending end

$v_{ffr}^{a,b,c}$ — voltage of the waves travelling towards the receiving end

and

$$v_{ffs}^{a,b,c} = v_{ffr}^{a,b,c} = v_{ff}^{a,b,c}$$
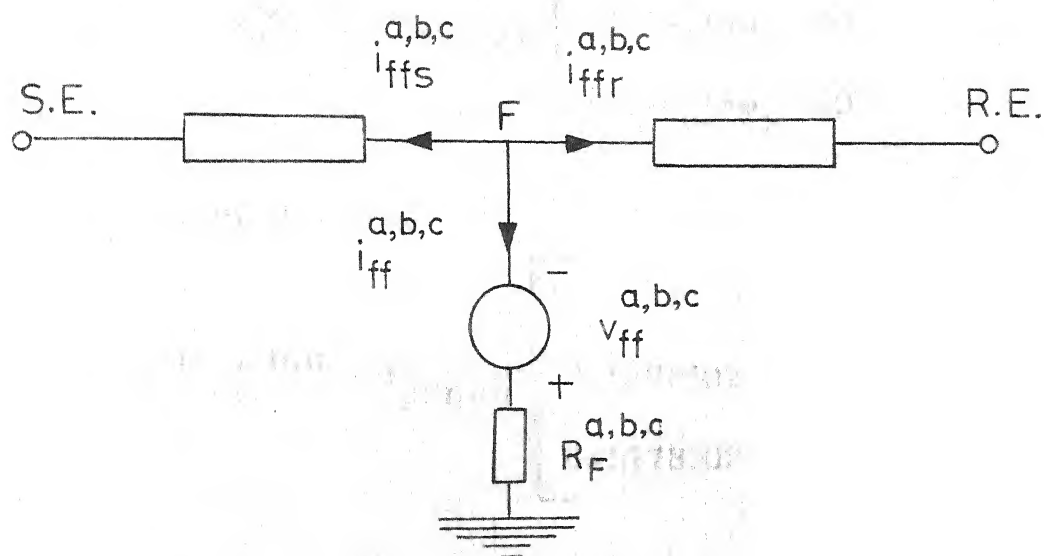
FIG·4·40 A SIMPLIFIED CIRCUIT REPRESENTING
THE CONDITIONS AT THE FAULT POINT

(i)   3-phase fault

For this fault, we have

$$v_{ff}^{a,b,c} = v_{pff}^{a,b,c} = V_{pffmax} \begin{bmatrix} \sin(\omega_o t + \varphi_o) \\ \sin(\omega_o t + \varphi_o - 120^o) \\ \sin(\omega_o t + \varphi_o + 120^o) \end{bmatrix} \qquad (4.17)$$

Therefore, we have

$$v_{ff}^{1,2,3} = S^{-1} v_{ff}^{a,b,c} = V_{pffmax} \begin{bmatrix} 0 \\ 0.5773502 \sin(\omega_o t + \varphi_o + 30^o) \\ 0.5773502 \sin(\omega_o t + \varphi_o - 30^o) \end{bmatrix}$$

$$(4.18)$$

where S is the voltage modal transformation matrix.

(ii)   One-phase-to-ground-fault on phase a.

For this fault, we have

$$v_{ff}^{a} = v_{pff}^{a} = V_{pffmax} \sin(\omega_o t + \varphi_o)$$

and

$$i_{ff}^{b} = i_{ff}^{c} = 0 \qquad (4.19)$$

Also, we know that (vide Appendix A)

$$v_{ff}^{1,2,3} = S^{-1} v_{ff}^{a,b,c}$$

and

$$i_{ff}^{1,2,3} = Q^{-1} i_{ff}^{a,b,c} \qquad (4.20)$$

Solving eqns. (4.19) and (4.20), with S and Q having values as given in eqn. (4.7), we get

$$i_{ff}^{1,2,3} = \begin{bmatrix} 1 \\ 1 \\ 1 \end{bmatrix} i_{ff}^a/3 \quad i.e., \quad i_{ff}^{(1)} = i_{ff}^{(2)} = i_{ff}^{(3)} \qquad (4.21)$$

and $[1 \quad 1 \quad 1] \, v_{ff}^{1,2,3} = v_{ff}^a = V_{pffmax} \, \sin(\omega_0 t + \varphi_0)$ \qquad (4.22)

Also, we have

$$i_{ff}^{a,b,c} = -(i_{ffs}^{a,b,c} + i_{ffr}^{a,b,c})$$

i.e., $i_{ff}^{1,2,3} = -(i_{ffs}^{1,2,3} + i_{ffr}^{1,2,3})$ \qquad (4.23)

and $v_{ff}^{1,2,3} = -Z_0^{1,2,3} \, i_{ffs}^{1,2,3} = -Z_0^{1,2,3} \, i_{ffr}^{1,2,3}$ \qquad (4.24)

where

$$Z_0^{1,2,3} = diag[Z_0^{(1)} \quad Z_0^{(2)} \quad Z_0^{(3)}]$$

For a perfectly transposed line, $Z_0^{(2)} = Z_0^{(3)}$, and generally,

$$Z_0^{(1)} \simeq 2Z_0^{(2)} = 2Z_0^{(3)} \qquad (4.25)$$

Solving eqns. (4.21) to (4.25), we get

$$v_{ff}^{1,2,3} = V_{pffmax} \begin{bmatrix} 0.50 \ \sin(\omega_o t + \varphi_o) \\ 0.25 \ \sin(\omega_o t + \varphi_o) \\ 0.25 \ \sin(\omega_o t + \varphi_o) \end{bmatrix} \qquad (4.26)$$

(iii) Phase-to-phase fault involving phases b and c

For this fault, we have

$$v_{ff}^{bc} = v_{pff}^{bc} = (v_{pff}^{b} - v_{pff}^{c})$$

$$= -\sqrt{3} \ V_{pffmax} \ \cos(\omega_o t + \varphi_o)$$

$$i_{ff}^{a} = 0$$

and

$$i_{ff}^{b} + i_{ff}^{c} = 0 \qquad (4.27)$$

Solving eqns. (4.27) in conjunction with eqns. (4.20) and (4.7), we get

$$[1 \quad -1] \begin{bmatrix} v_{ff}^{(2)} \\ v_{ff}^{(3)} \end{bmatrix} = \frac{v_{ff}^{bc}}{3} = \frac{V_{pffmax}}{\sqrt{3}} \ \cos(\omega_o t + \varphi_o)$$

$$i_{ff}^{(1)} = 0$$

and $[1 \quad 1] \begin{bmatrix} i_{ff}^{(2)} \\ i_{ff}^{(3)} \end{bmatrix} = 0 \qquad (4.28)$

Finally, solving eqns. (4.28), (4.23), (4.24) and (4.25), we get

$$v_{ff}^{1,2,3} = V_{pffmax} \begin{bmatrix} 0 \\ 0.2886751 \ \cos(\omega_o t + \varphi_o) \\ -0.2886751 \ \cos(\omega_o t + \varphi_o) \end{bmatrix} \tag{4.29}$$

(iv) Double-phase-to-ground fault involving phases b and c

For this fault, we have

$$v_{ff}^b = v_{pff}^b = V_{pffmax} \ \sin(\omega_o t + \varphi_o - 120^o)$$

$$v_{ff}^c = v_{pff}^c = V_{pffmax} \ \sin(\omega_o t + \varphi_o + 120^o)$$

and

$$i_{ff}^a = 0 \tag{4.30}$$

Solving eqns. (4.30), in conjunction with eqns. (4.20) and (4.7), we get

$$[-2 \quad 1 \quad 1] \ v_{ff}^{1,2,3} = V_{pffmax} \ \sin(\omega_o t + \varphi_o)$$

and $[1 \quad 1 \quad 1] \ i_{ff}^{1,2,3} = 0 \tag{4.31}$

Finally, solving eqns. (4.31), in conjunction with eqns. (4.23) to (4.25), we get

$$v_{ff}^{1,2,3} = -V_{pffmax} \begin{bmatrix} 0.400 \ \sin(\omega_o t + \varphi_o) \\ 0.3055 \ \sin(\omega_o t + \varphi_o - 109.1^\circ) \\ 0.3055 \ \sin(\omega_o t + \varphi_o + 109.1^\circ) \end{bmatrix} \qquad (4.32)$$

The peak values of $v_{ff}^{1,2,3}$ for the above faults, as obtained from eqns. (4.18), (4.26), (4.29) and (4.32), are tabulated in Table 4.3.

Table 4.3

Values of $V_{ffmax}^{(m)}$ (m = 1,2,3), for different types of bolted faults, expressed as a fraction of V_{pffmax}

Type of fault	$V_{ffmax}^{(1)}$	$V_{ffmax}^{(2)}$	$V_{ffmax}^{(3)}$
Three-phase	0.00	0.5773502	0.5773502
One-phase-to-ground	0.50	0.25	0.25
Phase-to-Phase	0.00	0.2886751	0.2886751
Double-phase-to-ground	0.40	0.3055	0.3055

4.3.6 Testing of the Relaying Principles by Digital Computer Simulation

The viability of the relaying techniques, described in earlier sections, is tested by considering a 200 Km, 3-phase,

400 KV quad-conductor, single-circuit transmission line interconnecting two large power systems, similar to that shown in Fig. 4.1. The tower configuration and conductor spacings of the line are given in Fig. 3.7 and the basic data, in Appendix B. An earth resistivity of 20 ohm-m is assumed. The performance of the relay located near the sending end bus is studied for 3-phase and one-phase-to-ground faults. For simplicity, the following assumptions are made.

i)   The sending end and receiving end buses are fed exclusively by other lines and cables. Accordingly, the sending end and receiving end source networks are considered as purely resistive.

ii) The resistances of the sending end and receiving end source networks are respectively equal to 1/9th and 1/4th of the real part of the appropriate modal surge impedance.

iii) The transmission line is assumed to be perfectly transposed.

iv) The parameters of the line are frequency invariant. The following values evaluated at the natural frequency of the line, viz., 4,500 rad/s, are considered.

Self and mutual series resistance/Km = 0.3992 and
0.3476 ohms respectively

Self and mutual series inductances/Km = 1.3215 and

0.4198 mH respectively

Self and mutual shunt capacitances/Km = 0.011299 and

0.00187 μF respectively.

(v) The prefault peak voltage at the fault point is 1.0 p.u.

By virtue of the assumption (iii) above, the relay signal $S_1^{(1)}$ would be zero for 3-phase faults and the signals $S_1^{(2)}$ and $S_1^{(3)}$ would be identical for one-phase-to-ground faults. Accordingly, the signals, $S_1^{(2)}$ and $S_1^{(3)}$ for 3-phase faults, and $S_1^{(1)}$ and $S_1^{(2)}$ (= $S_1^{(3)}$) for one-phase-to-ground faults, are computed for the following locations of the faults.

(i) At 50 Km from the sending end,

and

(ii) at the receiving end.

In each of the above two cases, fault resistances of 0,100,132,200 and 263 ohms and fault initiation angles of 0° and 90° are considered. The results are plotted in Figs. 4.41 to 4.56. In Figs. 4.49, 4.50, 4.53 and 4.54, the broken lines indicate the points where the slope of the curve has changed abruptly.

Also, the values of $d|S_1|/dt$ are computed for all the cases of the 3-phase fault, and for those cases of one-phase-to-ground faults having a fault initiation angle of 90°. The
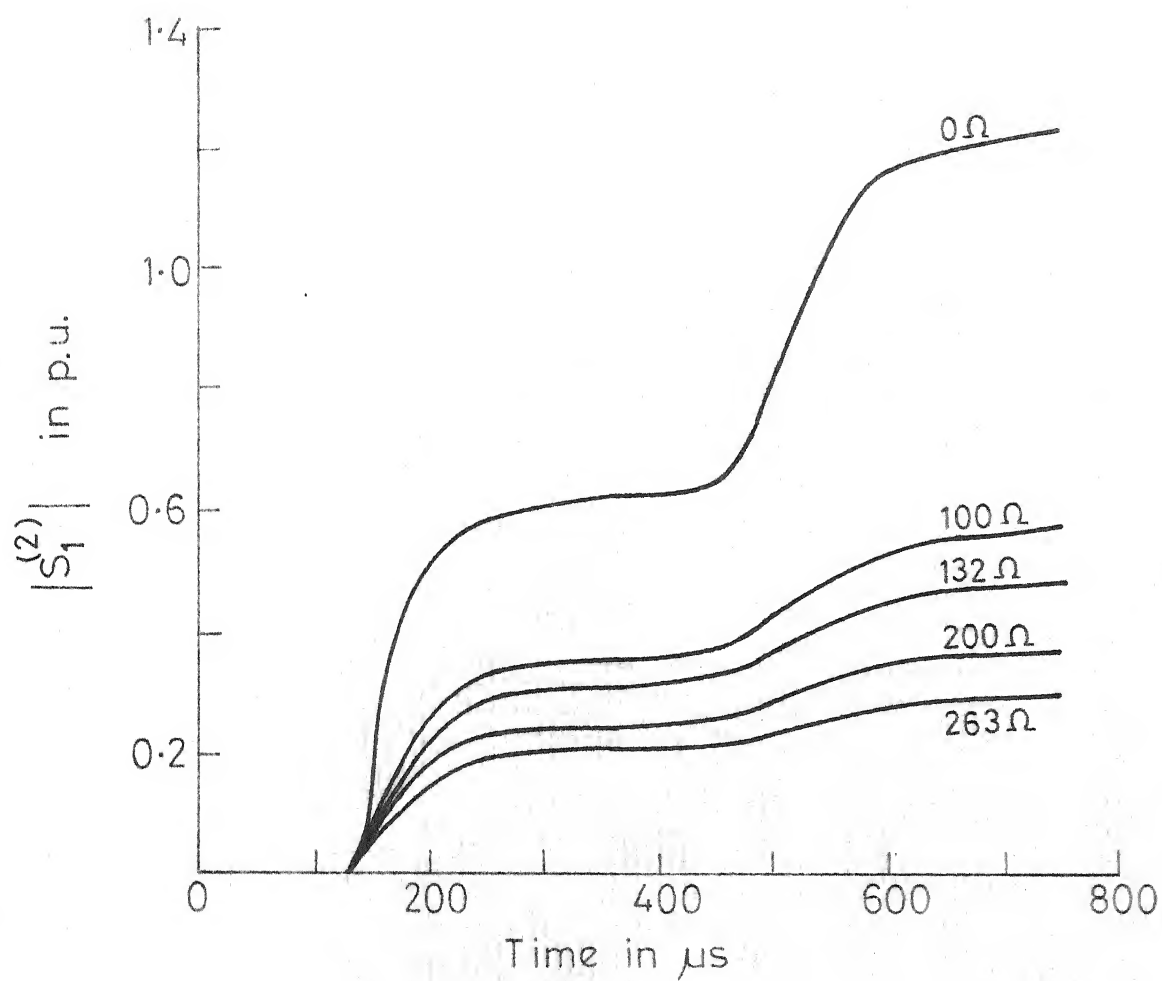
FIG.4·41 VARIATION OF $\left|S_1^{(2)}\right|$ FOR A 3-PHASE FAULT AT 50 km FROM S.E. AND $\phi_0 = 0°$
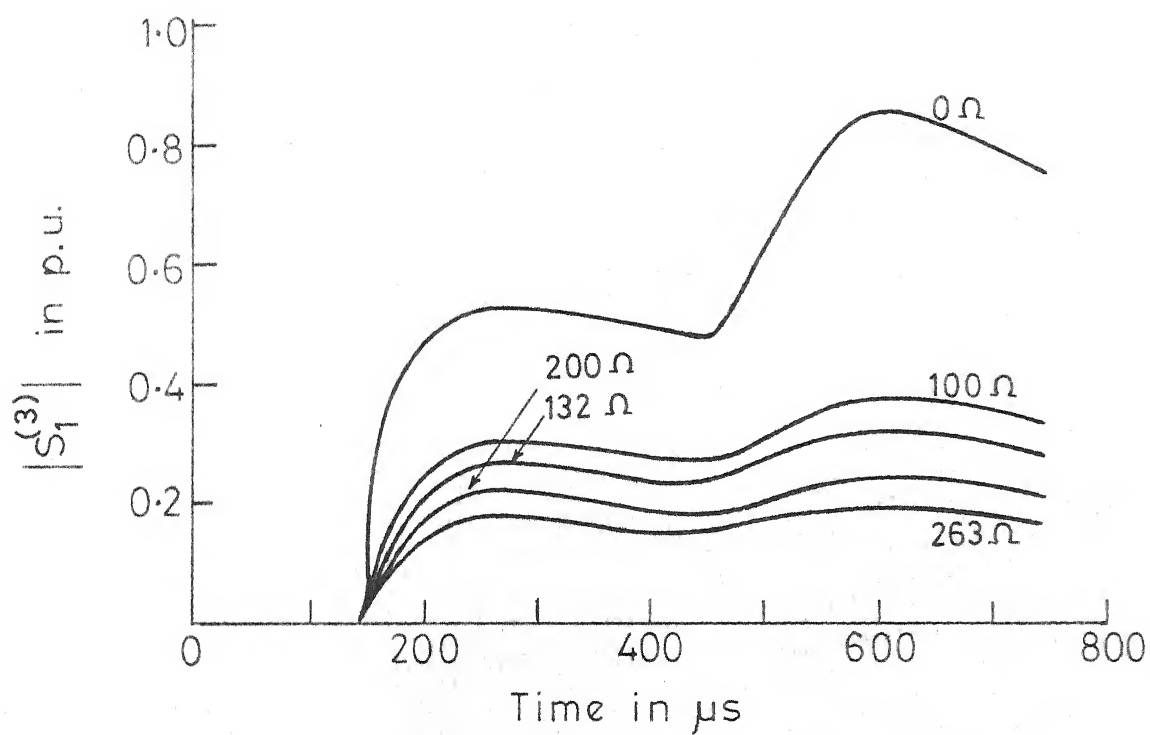
FIG·4·42 VARIATION OF $|S_1^{(3)}|$ FOR A 3-PHASE FAULT AT 50km AND $\phi_0 = 0°$
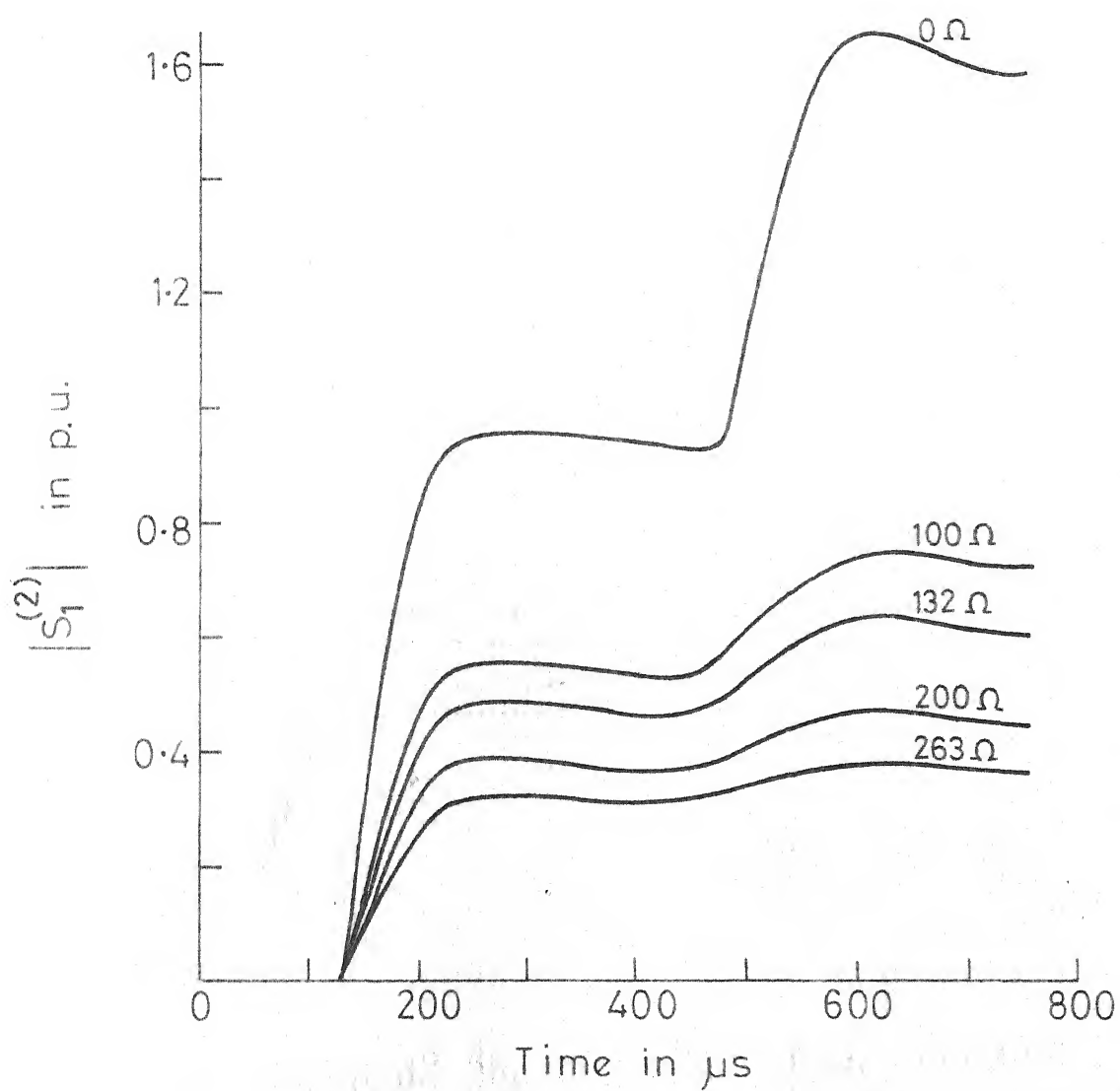
FIG. 4·43 VARIATION OF $\left|S_1^{(2)}\right|$ FOR A 3-PHASE FAULT AT 50 km FROM S.E. AND $\phi_0 = 90^\circ$
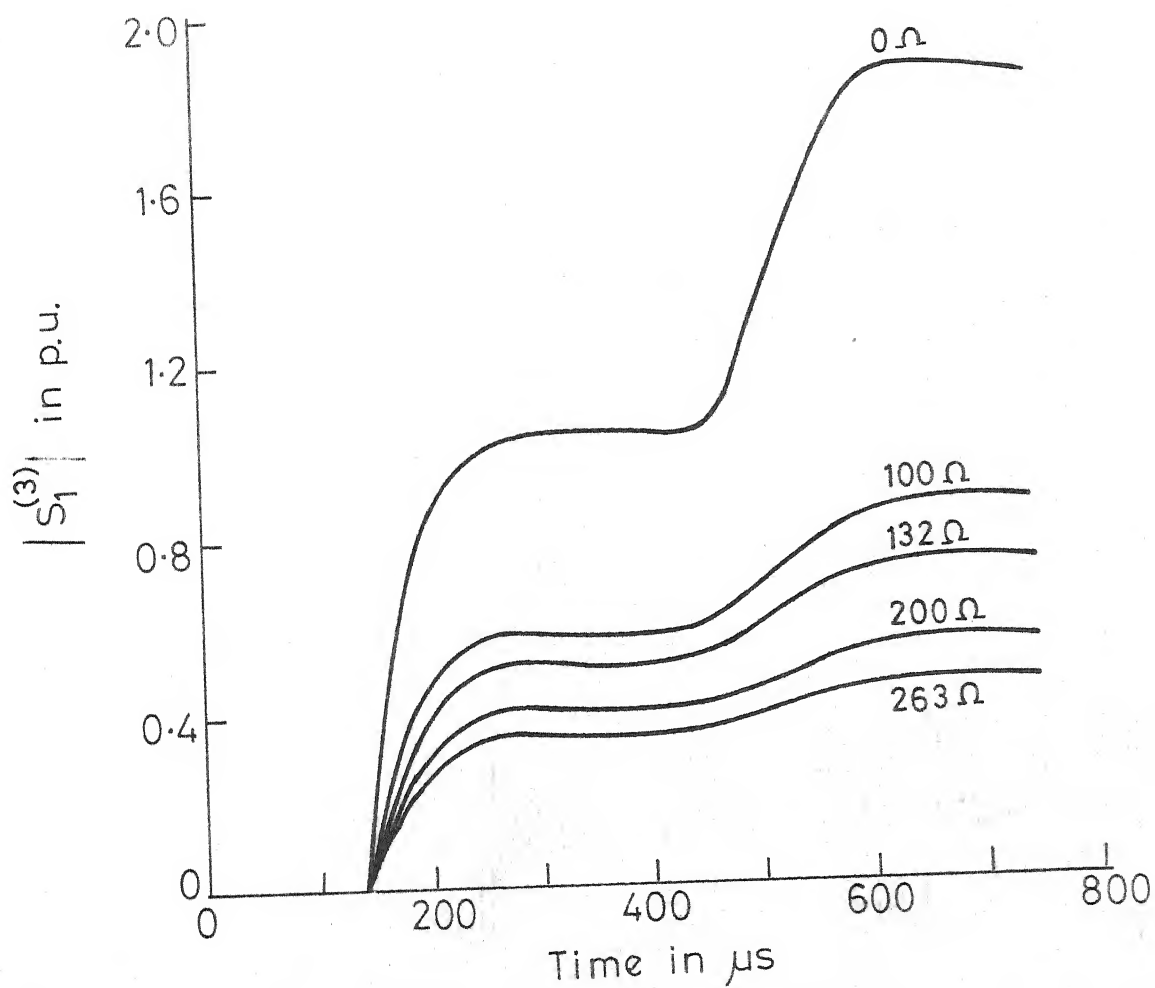
FIG. 4·44 VARIATION OF $|S_1^{(3)}|$ FOR A 3-PHASE FAULT AT 50 km AND $\phi_0 = 90°$
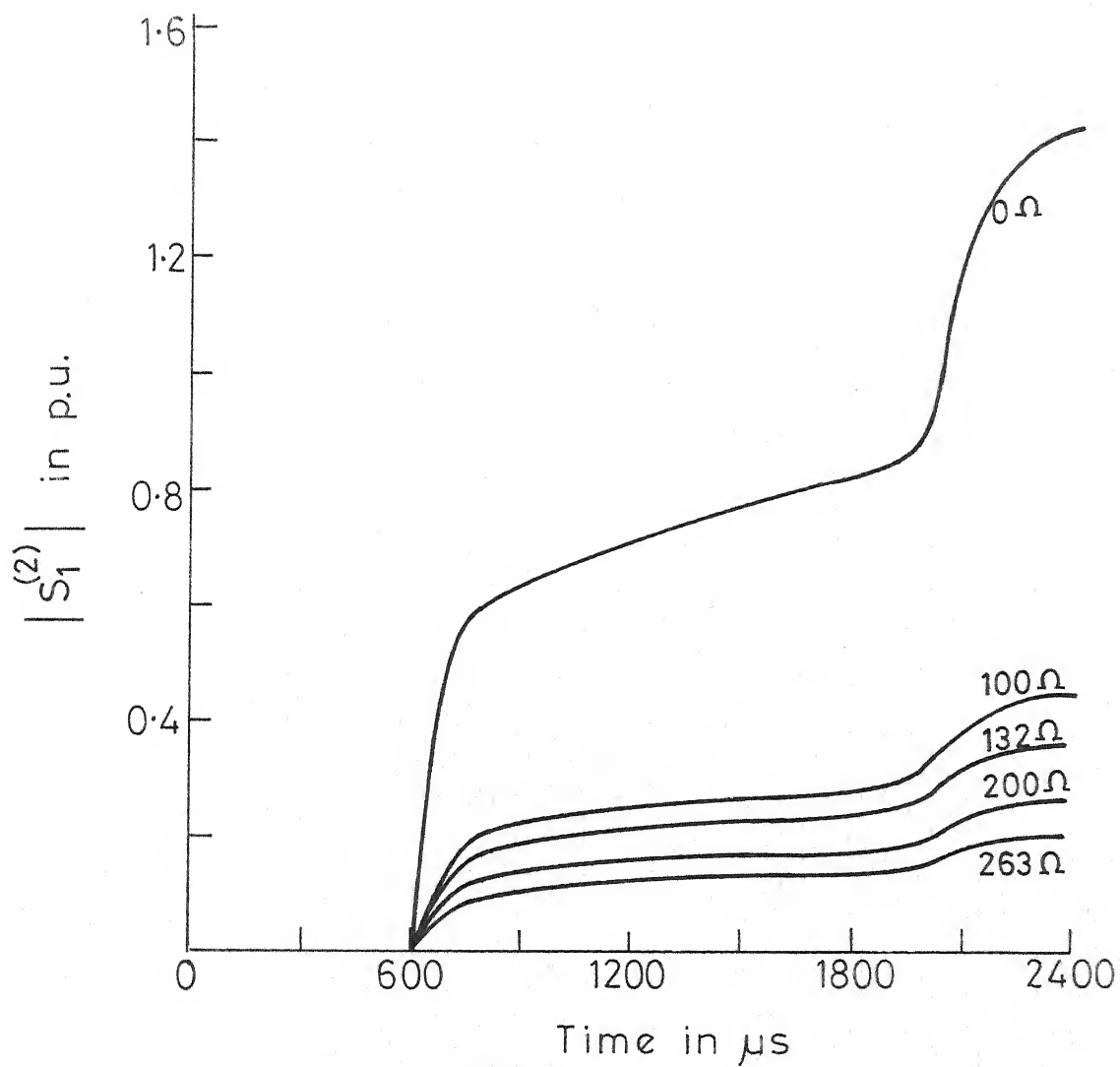
FIG.4.45 VARIATION OF $|S_1^{(2)}|$ FOR A 3-PHASE FAULT AT THE R.E. AND $\phi_o = 0^{\circ}$
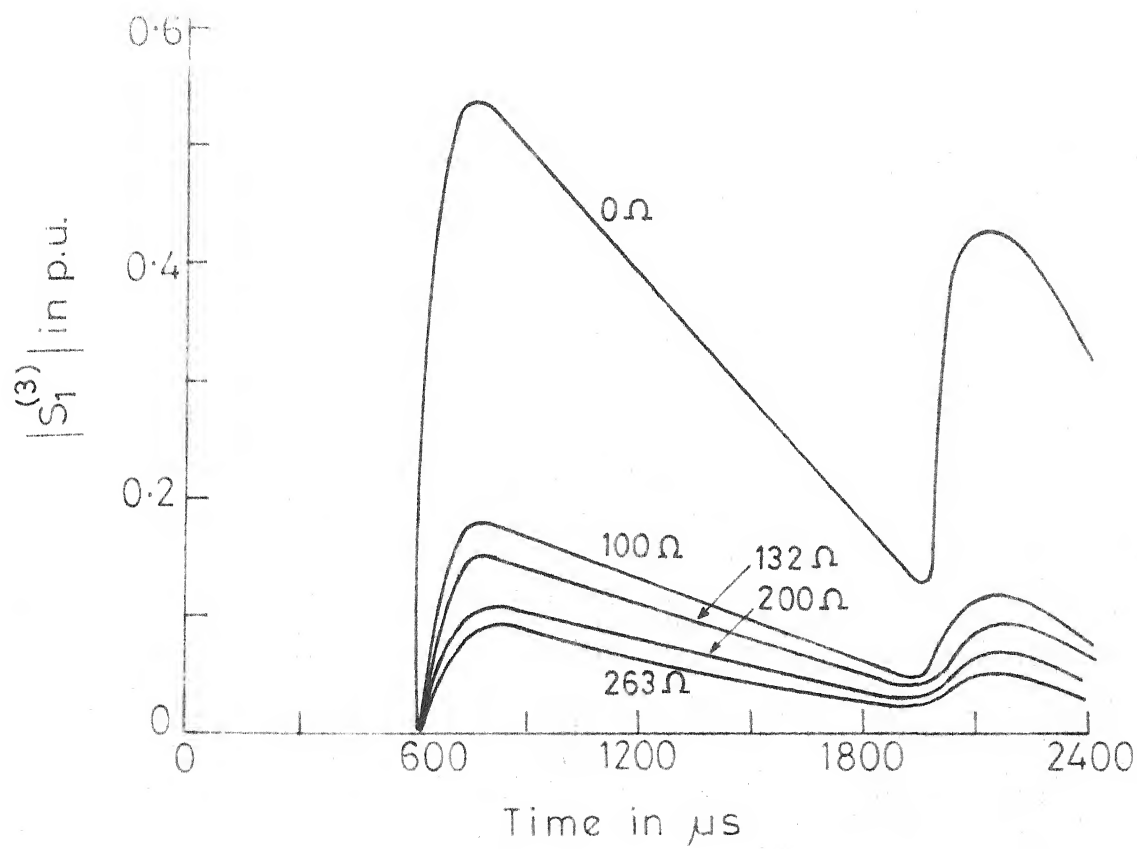
FIG. 4·46 VARIATION OF $\left|S_1^{(3)}\right|$ FOR A 3-PHASE FAULT
AT THE R.E. AND $\phi_0 = 0°$
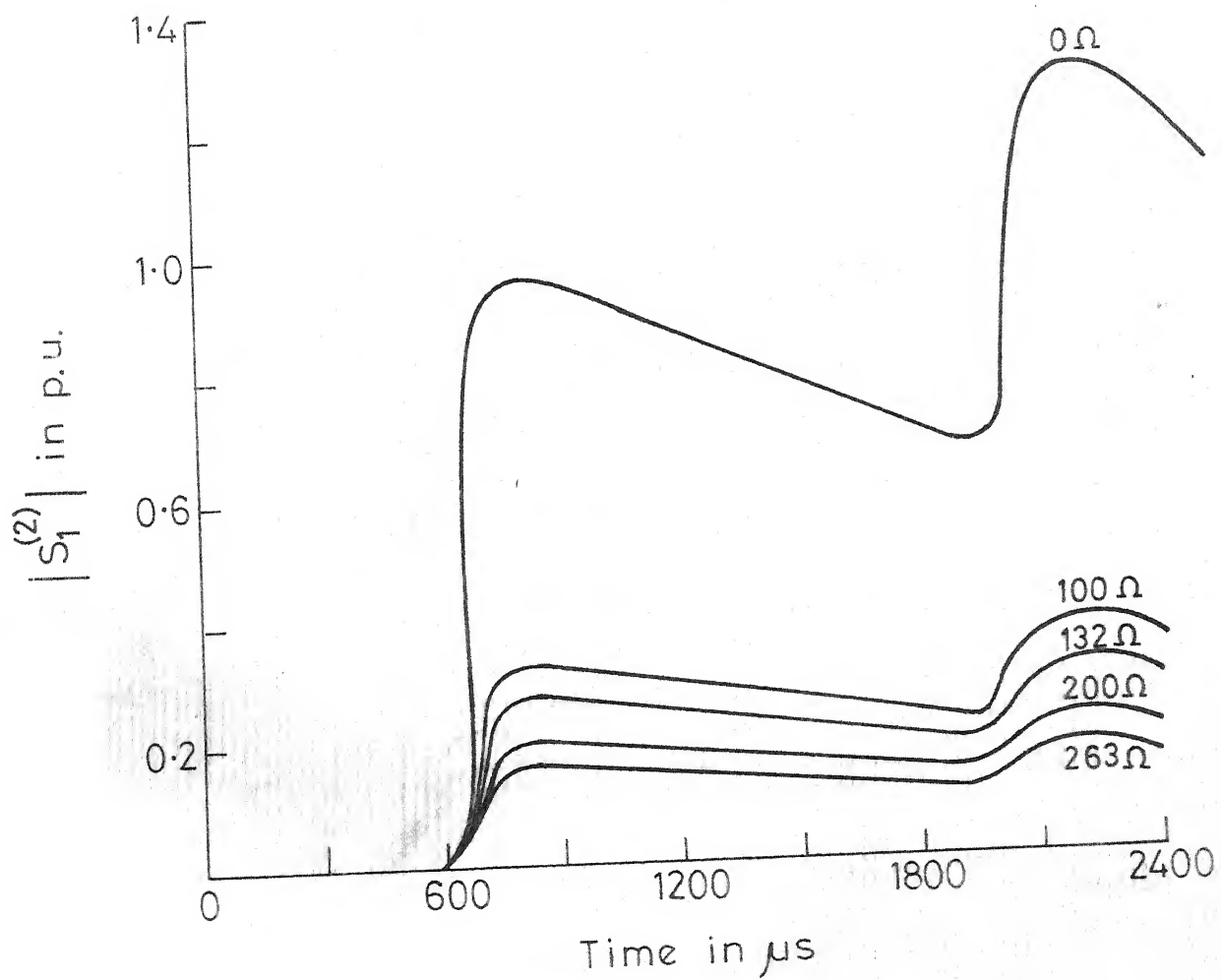
FIG.4·47 VARIATION OF $|S_1^{(2)}|$ FOR A 3-PHASE FAULT AT R.E. AND $\phi_0 = 90°$
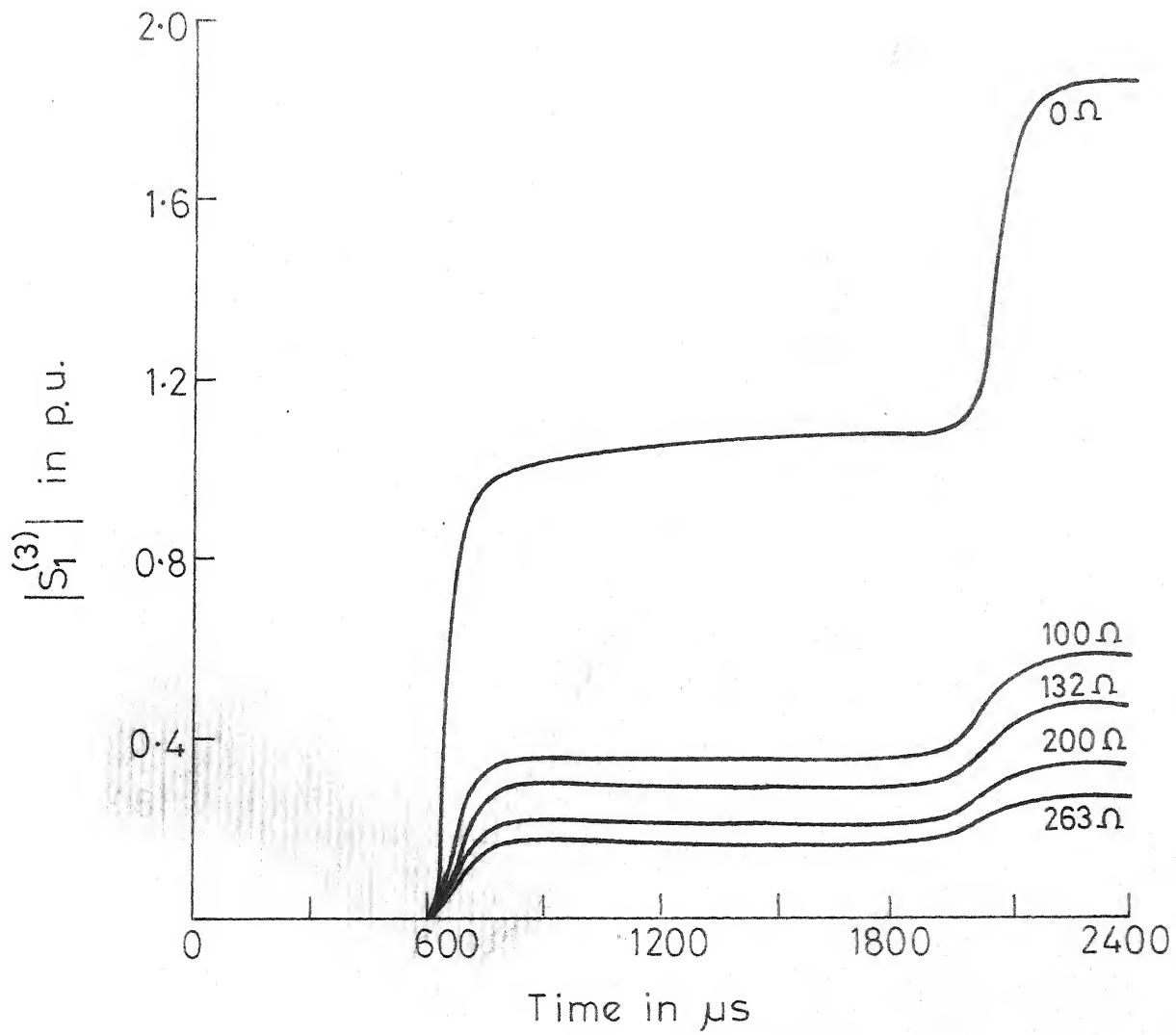
Fig.4·48 VARIATION OF $|S_1^{(3)}|$ FOR A 3 PHASE FAULT AT THE R.E. AND $\phi_0=90°$
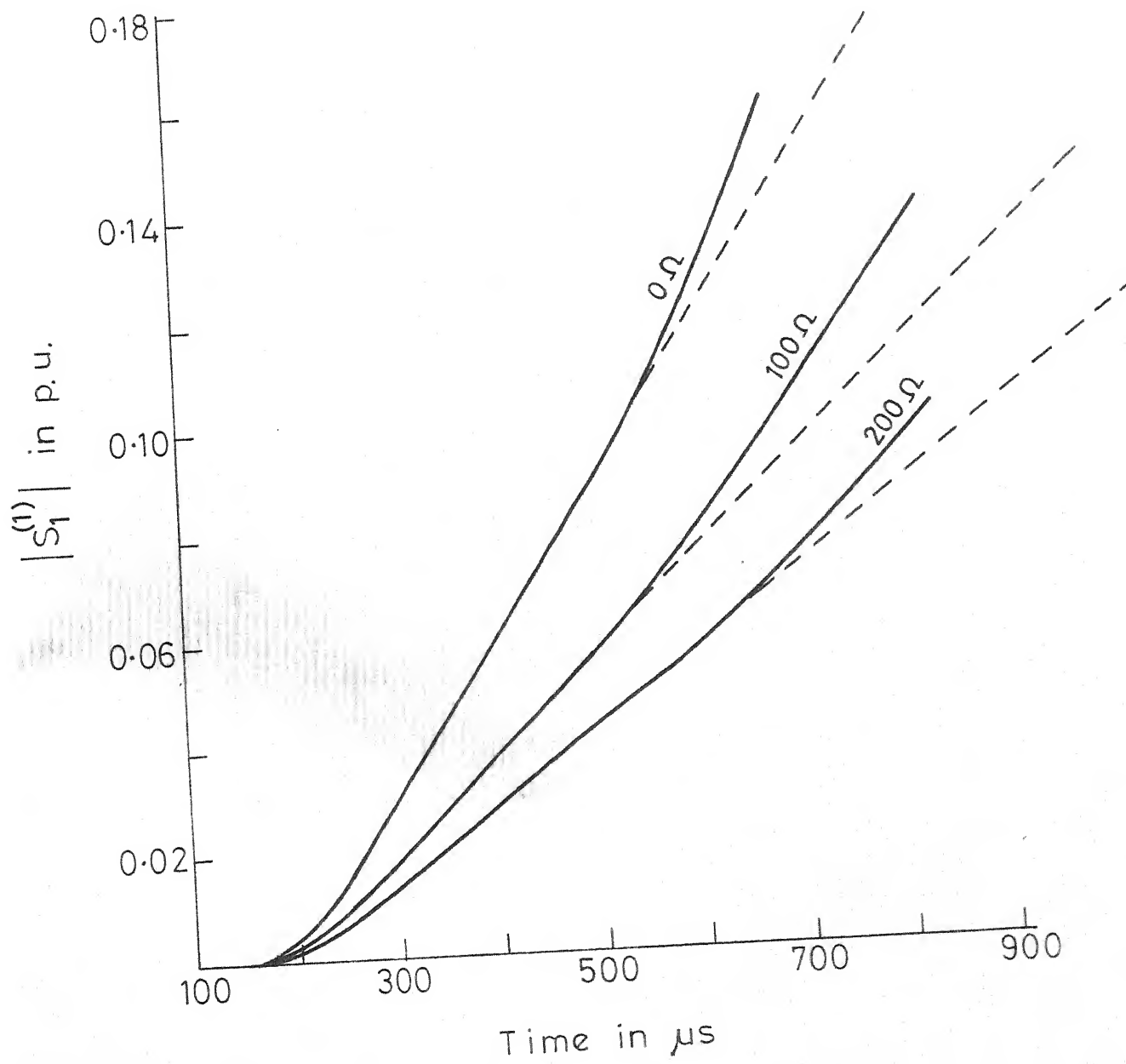
FIG.4·49 VARIATION OF $|S_1^{(1)}|$ FOR AN SLG FAULT AT 50 km FROM S.E. AND $\phi_0 = 0°$
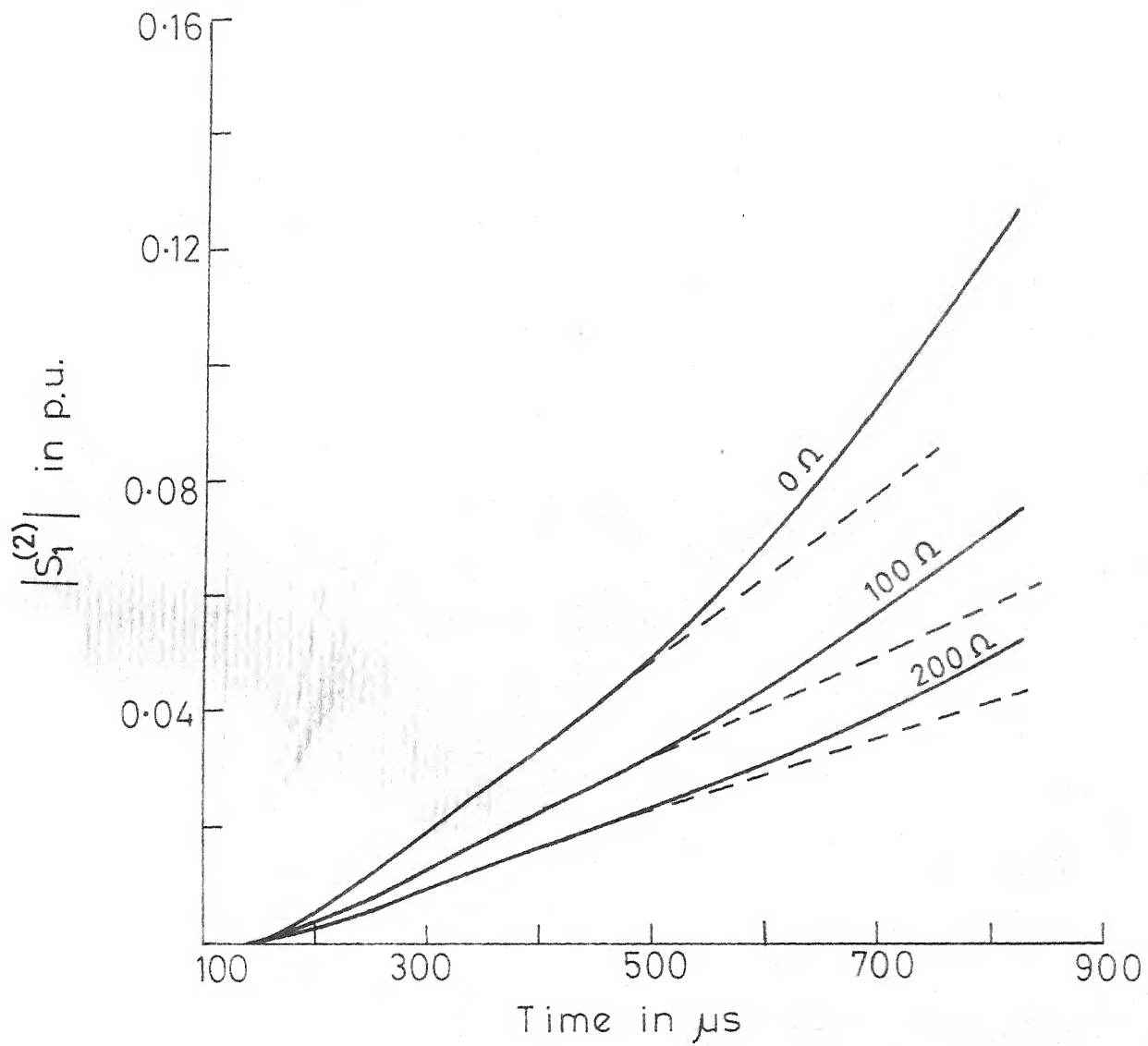
FIG.4·50 VARIATION OF $\left|S_1^{(2)}\right|$ FOR AN SLG FAULT AT 50 km FROM S.E. AND $\phi_0 = 0°$
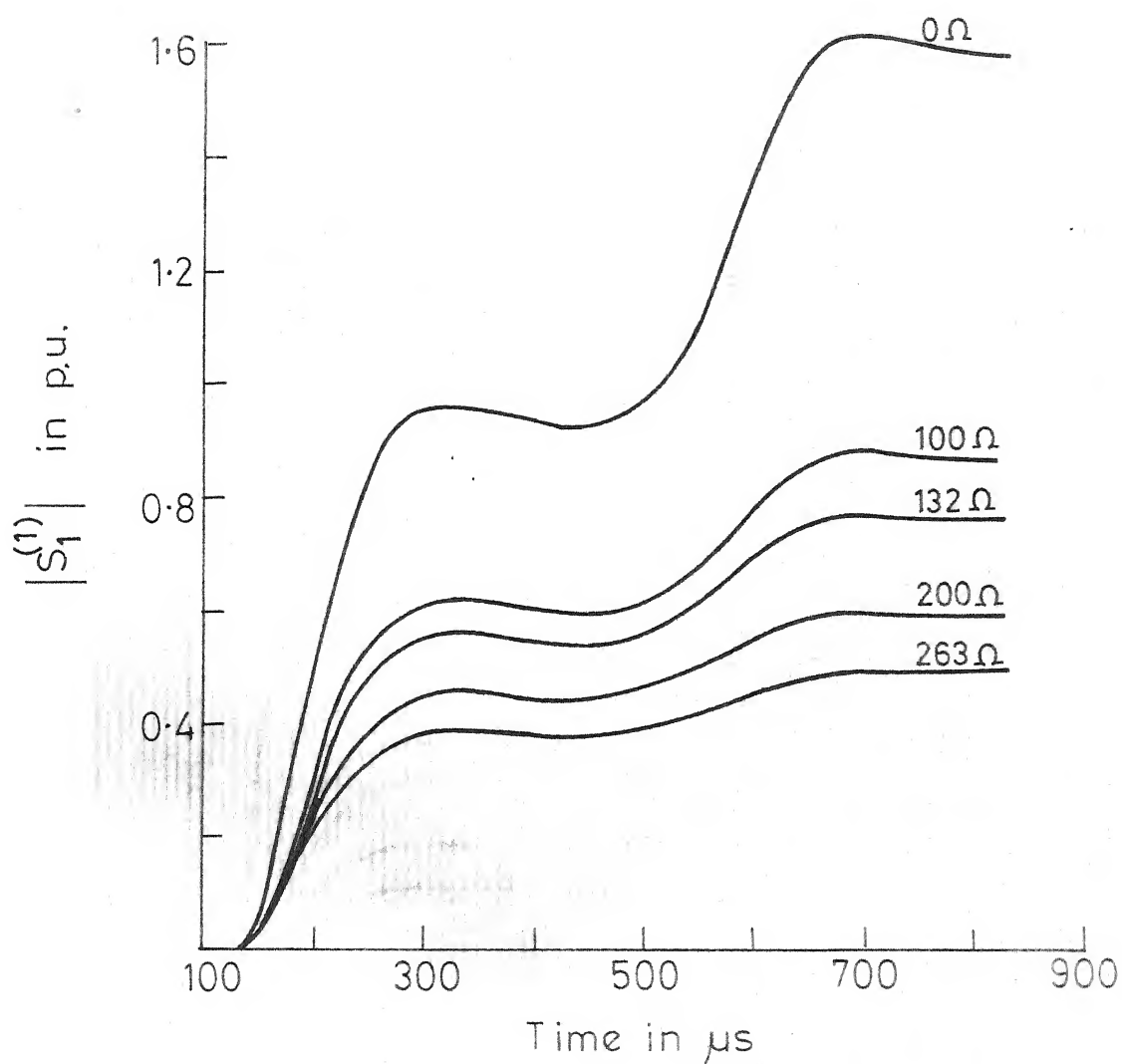
FIG·4·51 VARIATION OF $\left|S_1^{(1)}\right|$ FOR AN SLG FAULT AT 50 km FROM S.E. AND $\phi_0 = 90°$
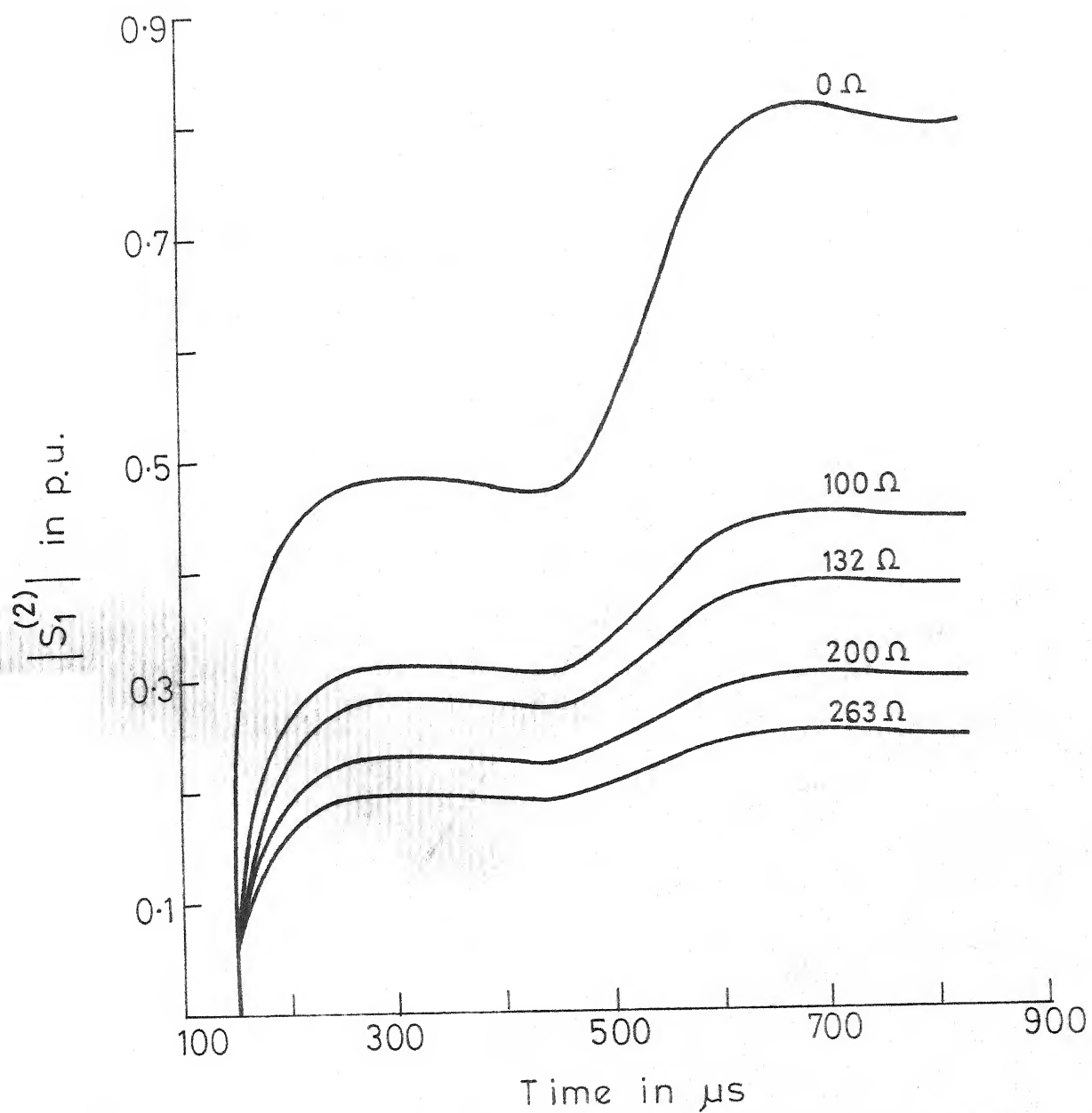
FIG.4·52 VARIATION OF $|S_1^{(2)}|$ FOR AN SLG FAULT AT 50km FROM S.E. AND $\phi_0=90°$
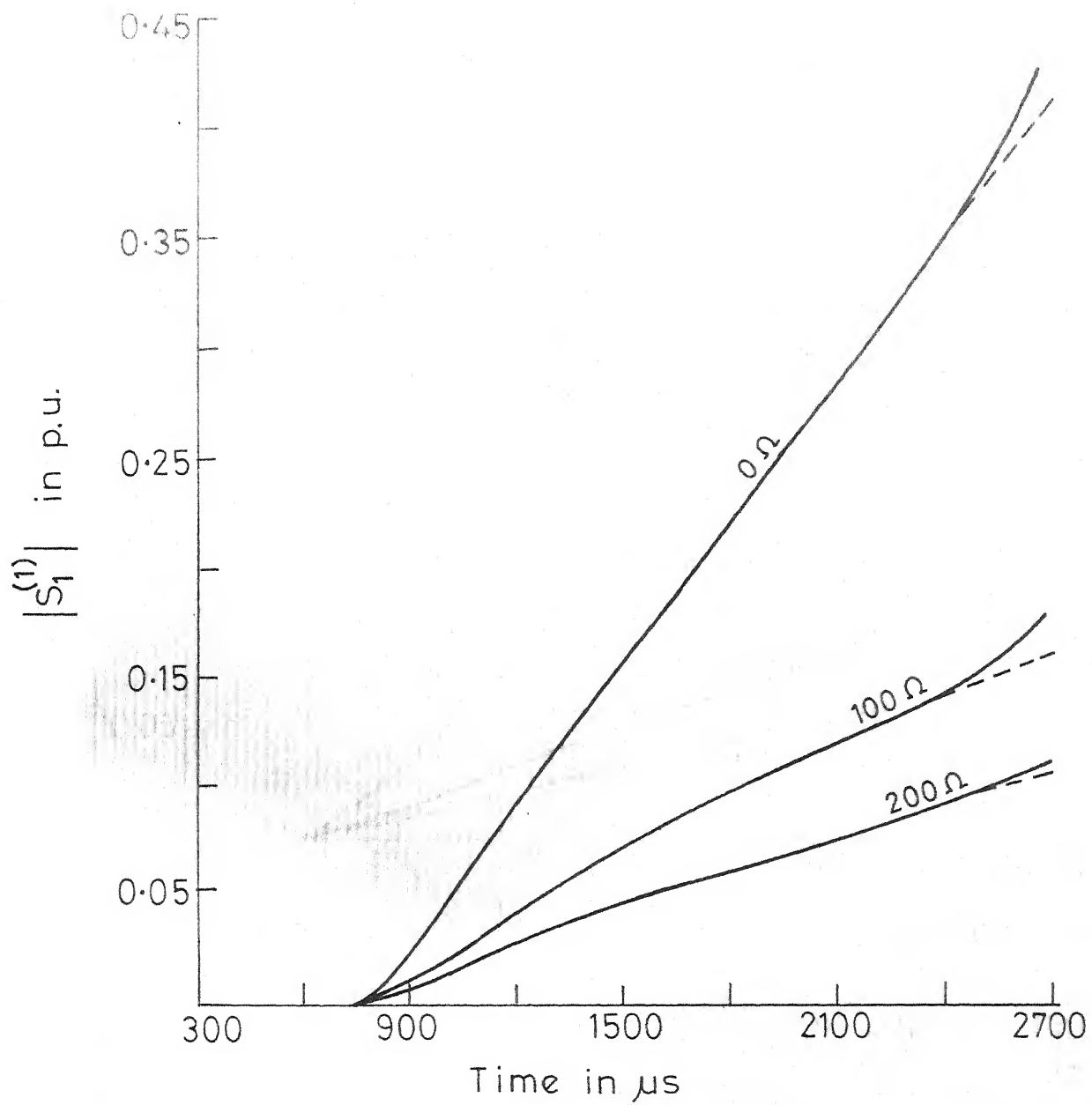
FIG·4·53 VARIATION OF $\left|S_1^{(1)}\right|$ FOR AN SLG FAULT AT THE R.E. AND $\phi_0 = 0°$
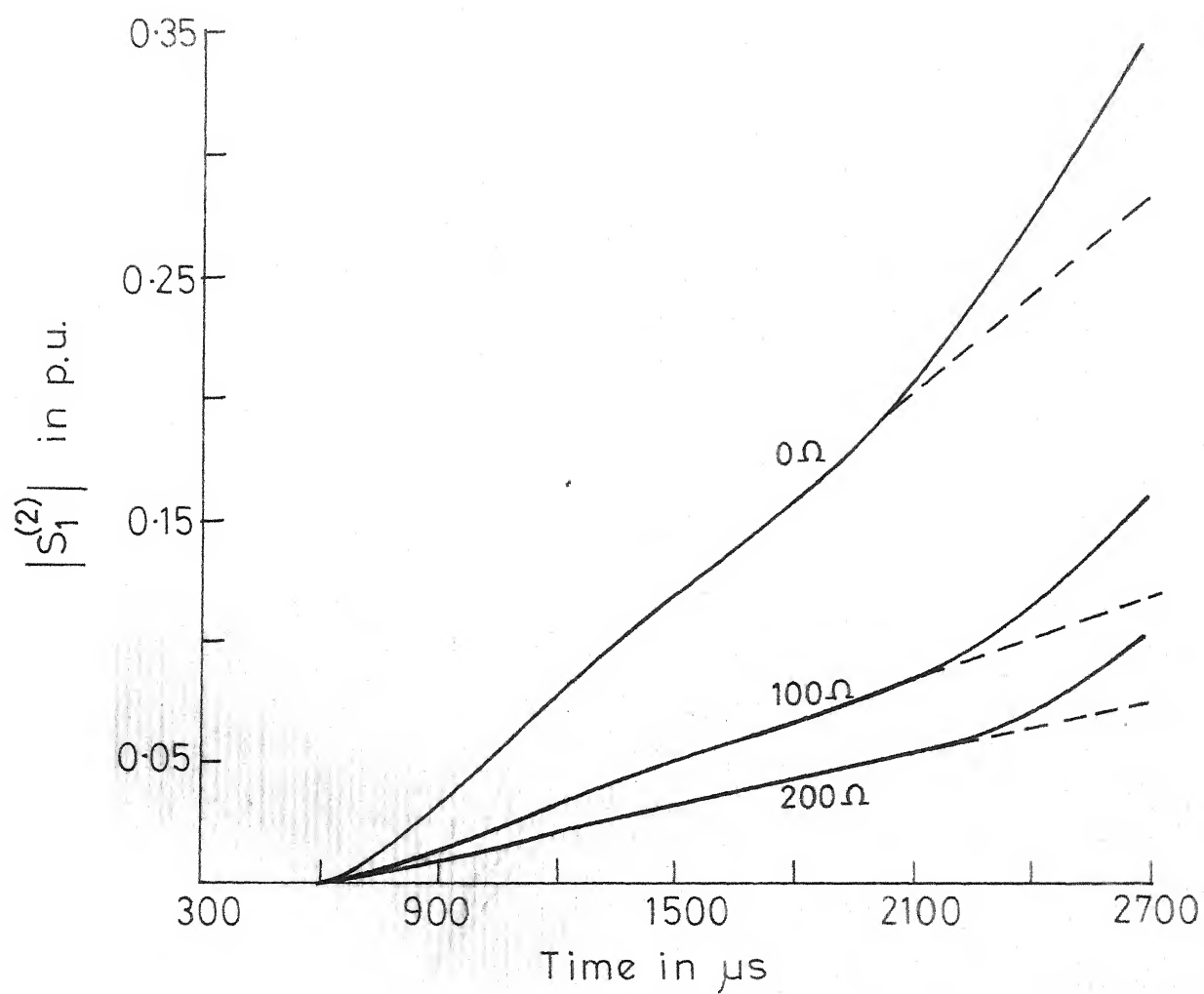
FIG.4·54 VARIATION OF $|S_1^{(2)}|$ FOR AN SLG FAULT AT THE R.E. AND $\phi_0 = 0°$
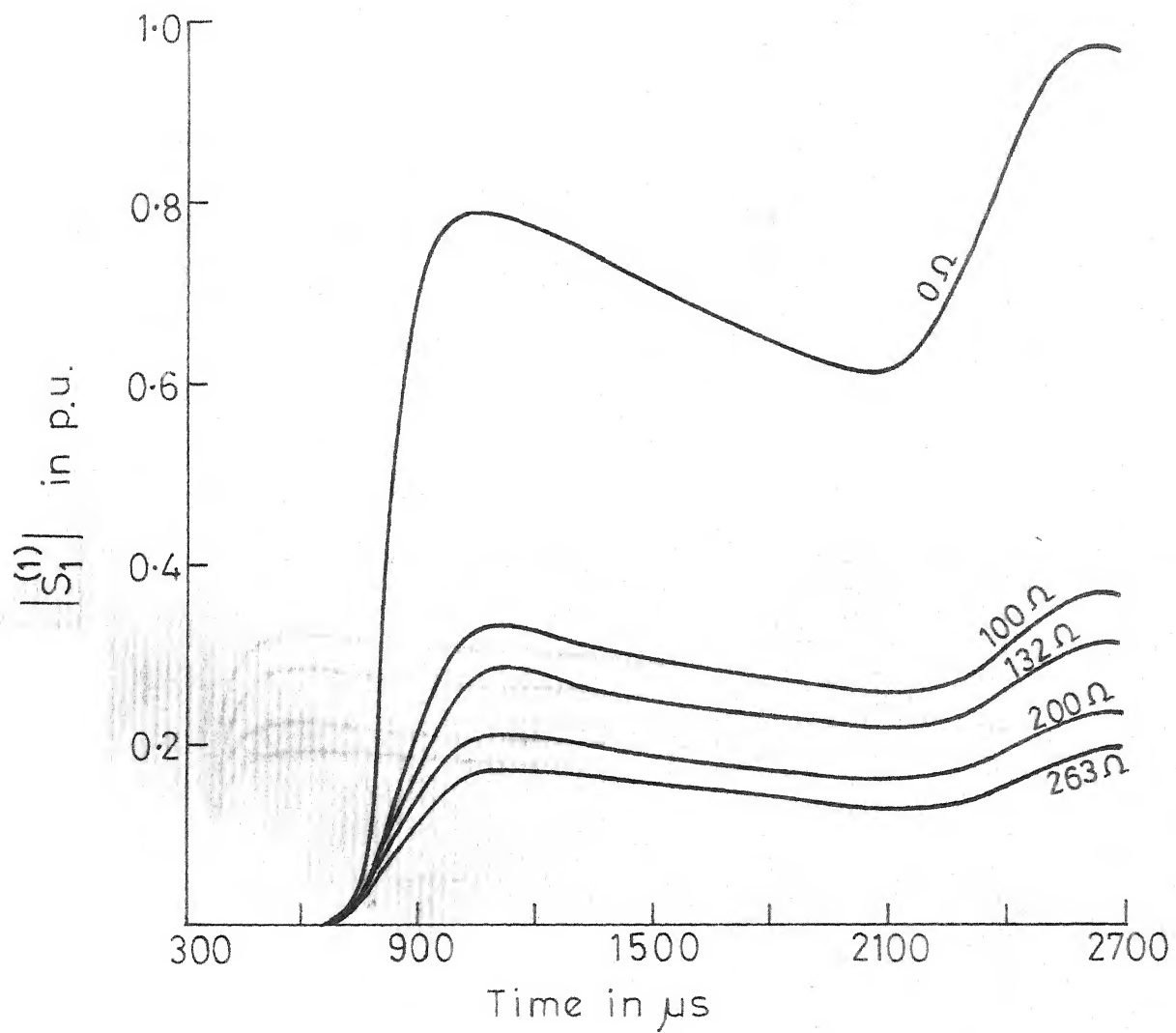
FIG·4·55 VARIATION OF $|S_1^{(1)}|$ FOR AN SLG FAULT AT THE R.E. AND $\phi_0 = 90°$
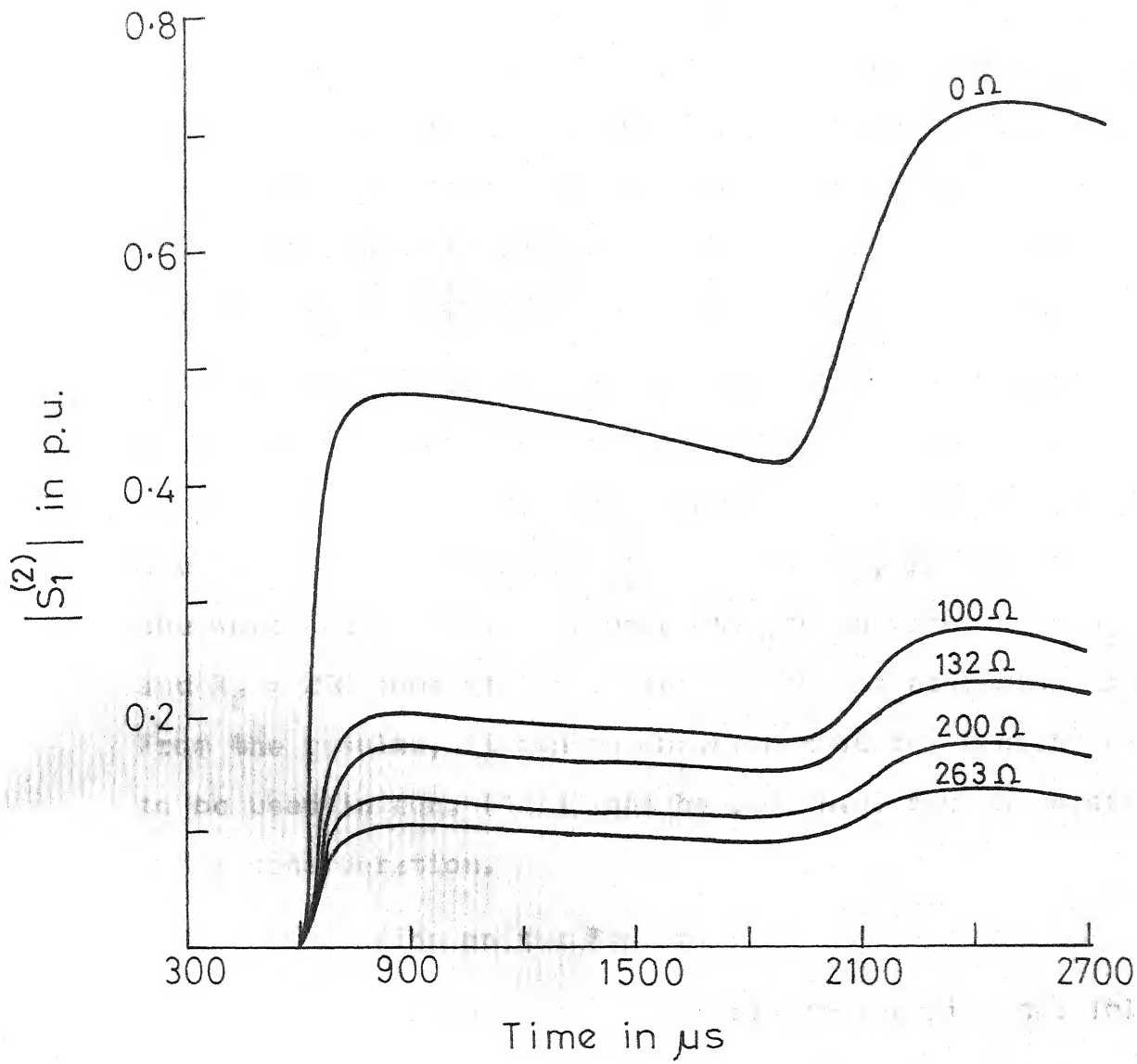
FIG. 4.56 VARIATION OF $\left|S_1^{(2)}\right|$ FOR AN SLG FAULT AT THE R.E. AND $\phi_0 = 90°$
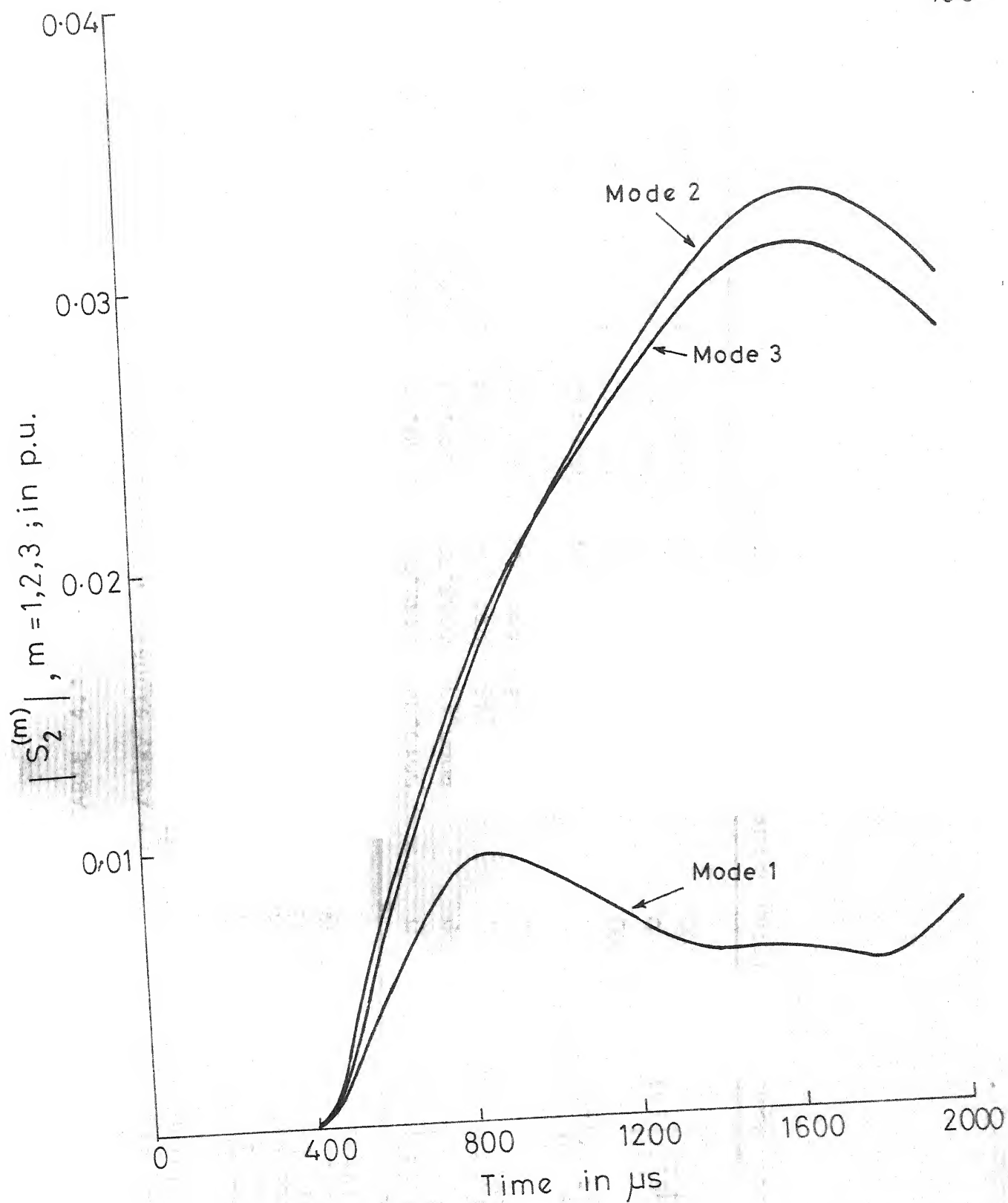
FIG. 4·57 VARIATION OF $|S_2^{(m)}|$, m=1,2,3 FOR A DISTANT ONE PHASE TO GROUND FAULT ON PHASE 'A' : $\phi_0 = 0°$

TABLE 4.4

First time derivatives of the relay signals in p.u./second at the
first rapid increase for a 3-phase fault

Distance of the fault from S.E.(Km)	First derivative of the relay signal	Fault initiation angle (Degrees)	R_f(ohms)				
			0.0	100.0	132.0	200.0	263.0
50	$d\|S_1^{(2)}\|/dt$	0	5519.32	3132.06	2740.31	2186.41	1834.99
		90	9090.13	5163.70	4540.92	3604.71	3025.35
	$d\|S_1^{(3)}\|/dt$	0	5120.46	2919.38	2555.44	2028.58	1702.55
		90	9329.46	5294.30	4655.78	3695.85	3101.83
200	$d\|S_1^{(2)}\|/dt$	0	3859.28	1326.19	1097.72	800.67	639.84
		90	6400.13	2199.34	1820.45	1327.81	517.86
	$d\|S_1^{(3)}\|/dt$	0	3613.07	1241.60	1027.70	749.59	599.03
		90	6542.31	2248.19	1860.88	1357.31	592.05

All these are above the setting value of 362.76 p.u./second.

TABLE 4.5

First time derivatives of the relay signals in p.u./second at the second rapid increase for a 3-phase fault

Distance of the fault from S.E. (Km)	First derivative of the relay signal	Fault inception angle (Degrees)	R_f(ohms)				
			0.0	100.0	132.0	200.00	263.0
50	$d|S_1^{(2)}|/dt$	0	3283.71	1298.00	1020.41	665.68	483.79
		90	5780.36	1800.92	1378.33	849.24	585.66
	$d|S_1^{(3)}|/dt$	0	3094.12	910.06	683.47	402.63	265.30*
		90	6201.62	2024.57	1572.87	1001.17	711.80
200	$d|S_1^{(2)}|/dt$	0	2621.68	682.44	548.57	384.65	300.70
		90	3790.35	934.17	745.74	517.86	402.56
	$d|S_1^{(3)}|/dt$	0	1971.72	467.80	371.55	256.16*	198.28*
		90	4165.62	1058.09	847.94	592.05	461.69

*Only these values are below the setting value of 290.21 p.u./second.

TABLE 4.6

First/Second time derivatives of the relay signals in p.u./second at the first rapid increase for one phase to ground fault on phase 'a'

Distance of the fault from S.E. (Km)	First/Second derivative of the relay signals	Fault initiation angle (degrees)	R_f(ohms)				
			0.0	100.0	132.0	200.0	263.0
50	$d^2|s_1^{(1)}|/dt^2$	0	2348604.40	1505440.00	1351608.80	1107768.80	948426.66
	$d|s_1^{(1)}|/dt$	90	8783.75	5616.22	5039.91	4127.72	3533.67
	$d^2|s_1^{(2)}|/dt^2$	0	1193831.10	763395.55	685031.11	561031.11	480320.00
	$d|s_1^{(2)}|/dt$	90	4524.93	2898.05	2601.46	2131.64	1825.43
200	$d^2|s_1^{(1)}|/dt^2$	0	4158702.20	1721671.10	1451786.60	1085457.70	879360.00
	$d|s_1^{(1)}|/dt$	90	10656.63	4414.56	3723.05	2783.91	2255.45
	$d^2|s_1^{(2)}|/dt^2$	0	8900320.00	1003786.60	846186.66	632888.88	512835.55
	$d|s_1^{(2)}|/dt$	90	6392.95	2646.93	2232.17	1668.97	1352.10

TABLE 4.7

First/Second time derivatives of the relay signals in p.u./second at the second rapid increase for one phase to ground fault on phase 'a'

Distance of the fault from S.E. (Km)	First/Second derivatives of the relay signals	Fault initiation angle (degrees)	R_f(ohms)				
			0.0	100.0	132.0	200.0	263.0
	$d^2\lvert S_1^{(1)}\rvert/dt^2$	0	1065884.40	434595.55	349706.66	234186.66	171395.55
	$d\lvert S_1^{(1)}\rvert/dt$	90	5329.56	2182.84	1758.59	1180.55	865.76
50	$d^2\lvert S_1^{(2)}\rvert/dt^2$	0	758720.00	3095457.77	248960.00	166666.67	121884.44
	$d\lvert S_1^{(2)}\rvert/dt$	90	2655.35	1087.80	876.05	587.44	430.24
	$d^2\lvert S_1^{(1)}\rvert/dt^2$	0	760764.44	267484.44	221102.22	160800.00	128195.55
	$d\lvert S_1^{(1)}\rvert/dt$	90	3089.10	1088.07	900.07	654.81	522.20
200	$d^2\lvert S_1^{(2)}\rvert/dt^2$	0	466168.88	161617.77	133386.66	96746.67	77048.89*
	$d\lvert S_1^{(2)}\rvert/dt$	90	3095.38	1089.84	901.18	655.66	522.90

*Only this value is below the setting.

only in a very few cases. For the system studied, there is at least one unaffected relay signal, in these cases, to provide tripping. For example, in the case of a 3-phase fault at the receiving end and with $\varphi_0 = 0^O$, and with $R_f = 200$ and 263 ohms, the second rapid changes in $\left| S_1^{(3)} \right|$ are less than the settings. However, in these cases, the second rapid changes in $\left| S_1^{(2)} \right|$ are above the settings, and hence, the relay operates to give a trip signal.

ii) The second rapid increases in the relay signals are low in the cases where $\varphi_0 = 0^O$, and may fall below the relay settings for very high fault resistances. However, the occurrence of a fault at $\varphi_0 = 0^O$ is relatively rare. In addition, the relay can still operate after a delay of T_{d2} seconds from the moment of detection of the first rapid increase, as explained in Section 4.3.2. Thus, this feature prevents the failure of the relay to operate under such relatively rare conditions.

iii) The determination of the distance of the fault is illustrated with reference to Fig. 4.41. It can be observed that the time interval between the first two sudden increases in $\left| S_1 \right|$ is about 325 μs. Therefore, the distance of the fault from the relay location is given by

$$(3 \times 10^5) \times (325 \times 10^{-6}) \simeq 48.75 \text{ km}$$

where 3×10^5 is the velocity of the waves in km/s.

(iv)   From the results given in Fig. 4.57, it can be observed that the relay would operate quite satisfactorily to give blocking signal for reverse faults.

4.4   CONCLUSIONS

In this chapter, two new relay schemes, based upon travelling wave phenomena, have been presented. The first scheme, which embodies the amplitude comparison of two relay signals, is simple and viable. The second scheme involves the use of the first or second time derivatives of a relay signal to determine the distance of the fault from the relaying point. In addition, the detection of an internal fault takes place without the aid of a communication channel. This eliminates the time delays associated with the communication equipment. The determination of the distance of the fault, and the detection of internal faults without the necessity of communication between the ends of the protected line, are the two beneficial features of the second scheme.

The viability of both the relay schemes, under various conditions, has been tested using digital simulation techniques, described in Chapter 3. The results obtained confirm their viability.

The relaying schemes, based on travelling wave phenomena, are immune to power swings since power swings are comparatively slow transients, and in addition, these are seen as an external

disturbance. With these schemes, the detection of faults takes place before the current transformers (c.t.s) saturate and hence, the protection problems associated with the c.t. saturation are eliminated. Also, these relays operate before the protective gaps, across the series capacitors of the series-compensated transmission lines, flash over and thus, the protection problems associated with this occurrence are absent.

The lightning strokes will have harmonic content in the MHz range [72]. Therefore, either the conventional transducers with a cut-off frequency of a few KHz eliminate them, or a simple low-pass filter can be provided to eliminate them. The switching surges produced by switching operations, except those on the protected line, would be seen as produced by external faults. If the voltage transformers are placed on the line side of the circuit breakers, as has been the current practice on EHV systems, then the switching operations, on the protected line also, are seen by the relays as external faults. In this case, the circuit breaker closure onto an existing fault on the protected line would be seen as an external fault. This difficulty can be overcome by a simple circuitry or logic as described in the reference [72].

CHAPTER 5

DIGITAL PROTECTION OF TRANSMISSION LINES USING TRAVELLING
WAVE PHENOMENA

5.1 INTRODUCTION

With the emergence of inexpensive, fast and reliable mini-
computers and microprocessors, the digital protection of trans-
mission lines is going to be a reality in the near future. The
digital protection of transmission lines provides an improved
performance in terms of speed of operation as well as flexi-
bility of obtaining, with ease, any desired relay characteri-
stics. With suitable software logic, the protection schemes
can be made self-checking against hardware failures. Also, the
sequence of software events, which occurs in the processor in
event of a fault, can be stored during the fault and output to
a data link afterwards.

A considerable amount of work in the field of digital
protection of transmission lines has been reported since late
1960's. The development has been confined mainly to different
types of algorithms which compute the fundamental frequency
impedance. The algorithms proposed uptill now can be broadly
classified into two groups : (1) distance (i.e. impedance)
relay algorithms and (2) travelling wave relay algorithms.

The post-fault waveforms, during the first one or two cycles following the occurrence of a fault, comprise of a power frequency fundamental, an exponentially decaying d.c. component and high frequency transients. They also contain subtransient and transient power frequency components, if the line fault is near a generating source. The first group of algorithms involve in computing the power frequency impedance between the relaying and fault points from the fundamental components of the voltage and current obtained by suppressing other components through analog and/or digital filters and line modelling. The accuracy, with which the fundamental components of voltage and current can be determined, depends upon the extent of filtering, and the extent and nature of filtering needed depends on the rigour of line modelling, both of which introduce longer time delays. Consequently, the speed and accuracy have been conflicting requirements. On the other hand, the algorithms, based on travelling wave phenomena, make use of the complex post-fault waveforms with just one simple digital filtering to obtain the fault-generated components. Therefore, these algorithms would be accurate as well as fast.

In this chapter, an overview of the distance relay algorithms is given first, in order to bring into focus their relative merits and inherent limitations. Next, two new travelling wave algorithms, whose viability has been tested on

a digital computer with the fault data generated by the
digital simulation of sample power systems, are presented.

5.2 AN OVERVIEW OF THE DIGITAL DISTANCE RELAY ALGORITHMS

These algorithms involve in extracting the fundamental
frequency components of voltages and currents from the
complex post-fault waveforms and then, in determining the
impedance between the fault and relaying points. Basically,
there are four digital methods of determining the impedance
from the fundamental components of voltage and current. In
the first method, the magnitude of the impedance is computed
as the ratio of the peak voltage to the peak current, and its
argument, as the difference between the phase angles of the
voltage and current. The peak values of, and the phase angle
between, the voltage and current can be determined either from
the samples of the fundamental components extracted from the
ensemble of samples collected over one full power frequency
period [88], or predicted from a much fewer number of samples
of the fundamental components by using the samples and their
time derivatives [89], or the first and second time derivatives
of the samples [91] or the samples and the sampling interval
[92].

In the second method, the fundamental components of vol-
tage and current are determined in phasor form, from which the
real and imaginary parts R and X of the pseudo impedance seen
by the relay can easily be evaluated [87,93-100,107,111,112].

In the third method, the line is modelled by differential equations, the numerical solution of which yields the values of R and X [101-106, 113]. This method has the following advantages. It is necessary to filter out only those unwanted components which are not covered by the line modelling. For example, if the line is modelled by a series R-L circuit, then there is no need to filter out the d.c. offset component. Also, this method permits the tackling, with ease, of the cases like the series compensated lines [113]. In the fourth method, the impedance is calculated directly in phasor form from the ratio of the frequency domain values of the fundamental components of the voltage and current by the finite transform method [110].

All those methods, which require samples over one full fundamental period for the computation of the pseudo impedance, do not offer any advantage in terms of speed when compared with the solid-state relays. The unwanted components of the post-fault waveforms are eliminated by employing various types of filters. Analog and digital filters, which have been proposed and/or used for this purpose, are described in the following sections.

5.2.1 Analog Filters

The mimic impedance used in the c.t. secondary plays the role of an analog filter since it filters out the d.c. offset in the current signal. Complete suppression of the d.c.offset

is, however, not possible owing to the fact that exact matching of the X/R ratios of the primary and secondary circuits is difficult to obtain because the X/R ratio of the primary circuit upto the point of fault is variable. Some algorithms [89,91,97] assumed the use of this filter.

RC low pass filters, with a suitable cutoff frequency, have been used to eliminate the high frequency components in conjunction with some of the algorithms [91,93]. The fact, that a single analog filter cannot suppress all the unwanted components and that, these filters are slower than the digital ones, led to the development and preferential use of the digital filters.

5.2.2 Digital Filters

The various types of digital filters, which have been proposed so far, are described below.

5.2.2.1 Notch Filters

Two orthogonal notch filters with sine characteristics have been used to extract the fundamental components after the high frequency components are eliminated by an analog low pass filter [93].

5.2.2.2 Selected Harmonic Filter

While the differential equations of the transmission line are being solved by numerical integration, the integration is carried out over a certain number of overlapping subintervals

with appropriate limits [105]. This leads to the elimination of certain harmonics and their multiples.

5.2.2.3   Least Square Error Filters

In one type, the deficiency in the modelling of the line by differential equations is treated as an error, and solution for the parameters of the model is obtained subject to the minimisation of the mean of the squares of this error over the data window [102,103]. In another type, a polynomial fit (for example, a straight line fit over three points, a quadratic fit over five points or a cubic fit over seven points) is determined subject to the least square error criterion [89,97]. Differentiating this polynomial, the necessary time derivatives can be found. In yet another type, a waveform containing a decaying d.c. offset, the fundamental and a desired number of harmonic components is assumed, and the least square error criterion is applied to determine the unknown parameters of the fundamental component [107-109]. All these filters are rather slow and their accuracy depends on the data window as well as number of samples per cycle [119].

5.2.2.4   Orthogonal Transform Filters

Of these, the Fourier transform filter is the most widely used one, and utilizes sine and cosine functions as an orthogonal set [87,88,94-99]. This filter suppresses all the unwanted components, and therefore, offers the best

accuracy. But, it requires a data window of one full fundamental period. However, filters employing half-a-cycle and less than half-a-cycle data windows with tolerable errors have been proposed [97,99]. Filters using odd and even square waves [94], Walsh functions [100],sample values and their derivatives [89] and the first and second derivatives of the samples [91] as orthogonal functions have also been proposed.

5.2.2.5 Finite Transform Filter

The fundamental frequency impedance is determined by carrying out the filtering process in the frequency domain through the use of finite transform spectral analysis techniques [110]. Acceptable accuracy limits could be achieved only with a speed of three-fourth of a cycle [110].

5.2.2.6 Kalman Filters [111,112]

The nonfundamental components such as harmonics and d.c. components in the voltage and current waveforms are considered as noise signals. The noise signal in the voltage waveform is considered as a white noise sequence with a decreasing variance while that in the current waveform as an exponential process plus a white noise sequence with a decreasing variance. Then, a two-state Kalman filter is used to extract the fundamental voltage phasor and a three-state Kalman filter to extract the fundamental current phasor.

The error in these filtering processes has been reported to be less than 1 percent after half-a-cycle [111].

The filtering schemes, described so far, suppress the harmonics as well as d.c. offset from the post-fault current and voltage waveforms. However, in the case of ultra high speed relays, based on the travelling wave techniques, the transient components, such as high frequency harmonics and d.c. offset present in the post-fault current and voltage waveforms, are utilized for detecting the faults. As a consequence, these relays are faster and more reliable in operation. Hence, the filters, described above, will not be useful in the case of travelling wave relays. The cycle-to-cycle comparison scheme, proposed by Mann and Morrison [90], is adapted, in this work, as a digital filter for deriving the fault-generated components, which are used for forming suitable relay signals using the travelling wave principles.

5.3 DIGITAL TRAVELLING WAVE RELAY ALGORITHMS

This group of algorithms uses the fault-generated components of the relaying point phase voltages and line currents, obtained from the complex post-fault waveforms by means of a very simple digital filter and makes relaying decisions through the application of travelling wave techniques. This group offers two distinct advantages, which lead to a high speed of operation. First, there is no need for either analog or elaborate digital filters. Consequently, the time

delays associated with them are eliminated. Secondly, a very short data window can be employed. In fact, the sampling interval should be small enough to avoid the aliassing errors. That is, the sampling frequency should be atleast twice as great as the cutoff frequency of the transducers in order to avoid the aliassing errors. Thus, with a CVT of cutoff frequency of 2.5 KHz, the sampling frequency should be atleast 5 KHz, and therefore, the sampling interval, 200 μs. Also, the number of samples needed to detect a fault would be small as explained later.

With the high speed analog to digital conversion equipment and computers available at present, the above short intersampling period would be adequate to derive and store the six digital samples of the phase voltages and line currents, and to carry out the simple fault detection algorithm described in the next section.

Very few algorithms of this category have been proposed so far [71,114], most probably, due to the fact that the travelling wave relaying concept is relatively new. Two new algorithms of this category are presented in this chapter. One is based on the amplitude comparison relay and the other, on the fault locating relay, both described in Chapter 4. Each algorithm can be split into two parts, fault detection and relaying. The fault detection algorithm is common to both and, therefore, is described first.

5.4   FAULT DETECTION ALGORITHM

This algorithm is similar to that proposed by Mann and Morrison [90]. One counter is provided for each phase voltage. The difference between the currently sampled instantaneous voltage of each phase and the corresponding one in the previous cycle (which has been stored) is computed and stored. These differences, upto one cycle after the occurrence of a fault, would be the fault-generated components and are used in the relaying algorithms described later. If this difference is greater than a preset value, for any phase, then the counter of this phase is incremented by 1. Otherwise, the concerned counter is decremented by 1, provided that it is not already zero. The latter ensures that no maloperation takes place due to spurious spikes. When the counter of any phase reaches a preset value, the fault is assumed to have occurred. Then, the sampling is suspended, the transmitter is switched off, and the relaying programme is executed.

The setting, for the difference of instantaneous voltages one cycle apart, is chosen as 0.05 p.u. for both the relays. It is based on the assumption that load fluctuations do not lead to voltage variations of more than 0.05 p.u. Actual value for this setting can be determined by conducting digital simulation tests on the power system. The setting of each phase counter is taken as 5 for the amplitude comparison

relay, and as 10 for the fault locating relay. Higher setting for the latter is necessary to collect adequate number of samples of fault-generated components of voltages needed for executing its relay algorithm. At any time, one full cycle of samples of voltages and currents are stored. As and when a new sample set arrives, the earliest set is deleted and the ensemble of sample sets is updated.

It can be observed that this algorithm is quite simple, and therefore, can easily be carried out within an inter-sampling period. The flow chart of this algorithm is given in Fig. 5.1.

5.5 AMPLITUDE COMPARISON RELAY SCHEME

The theory and principles of operation of this scheme have been described in Chapter 4. The relaying-point phase voltages and line currents need sampling and then conversion to the digital form before they are supplied to the digital computer, in actual hardware implementation. From these, the fault-generated components are computed by using the cycle-to-cycle comparison method described by Mann and Morrison [90], and are used for relaying. The criteria, given in eqns. (4.10), are employed for detecting a fault ahead of and a fault behind the relaying point respectively. The computer application of this scheme, along with an algorithm, is described in the next section.
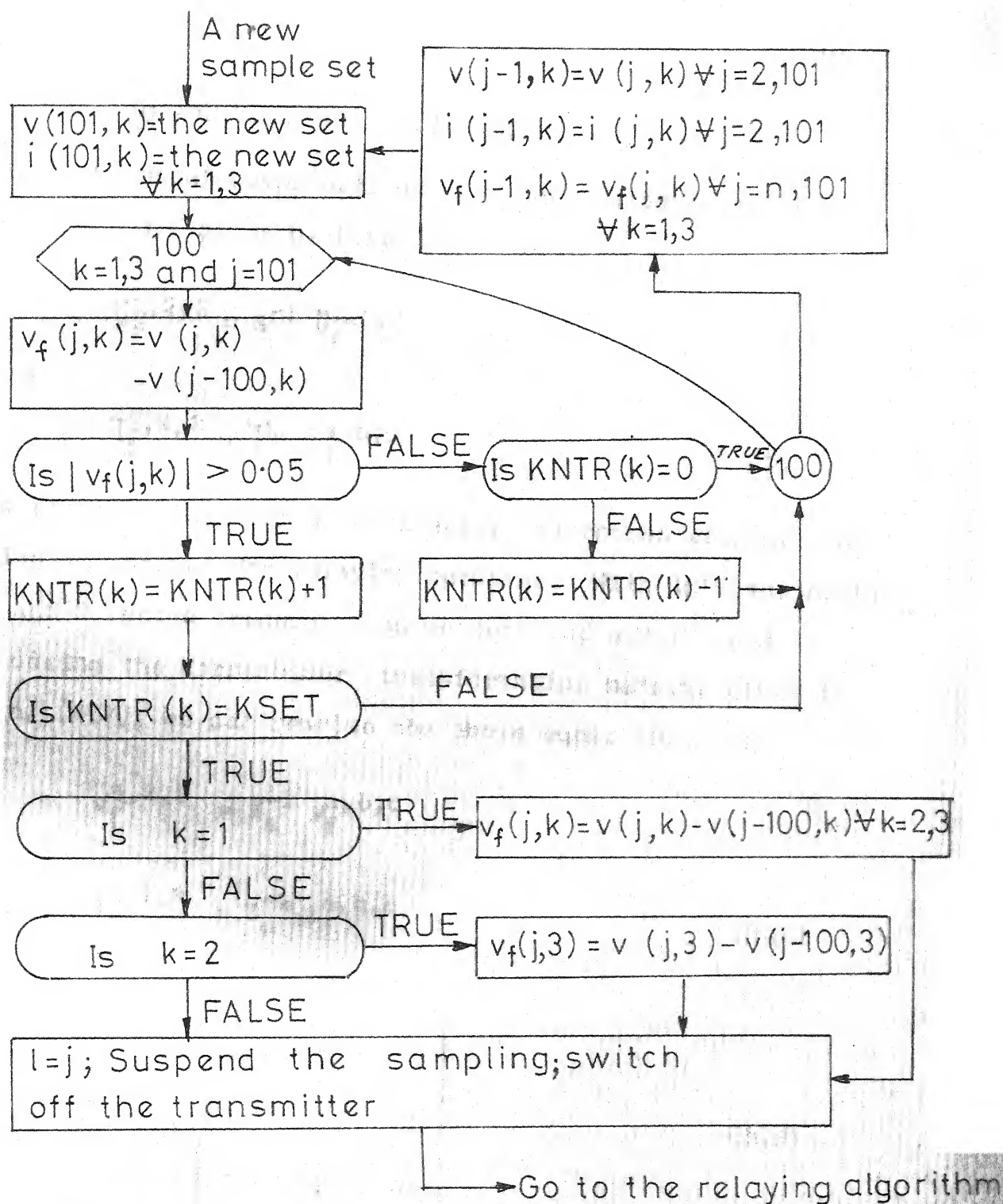
j - Sample set counter; k - Phase counter

KSET = 5 & n=98 for amplitude-comparison relay

KSET = 10 & n=91 for fault-locating relay

FIG. 5·1 FLOW CHART OF THE FAULT DETECTION
ALGORITHM

5.5.1 Digital Computer Application

The modal components of the phase voltages and line currents are given by (vide Appendix A)

$$\bar{v}_f^{1,2,3} = S^{-1} \bar{v}_f^{a,b,c}$$

and

$$\bar{i}_f^{1,2,3} = \bar{Q}^1 \bar{i}_f^{a,b,c} \tag{5.1}$$

As stated in Chapter 4, an ideally transposed transmission line is assumed for relaying purposes. With this assumption, S and Q become frequency independent and equal. And, choosing the Karrenbauer transformation matrix, given in eqn. (4.7), we can rewrite the above eqns. (5.1) as

$$v_f^{1,2,3} = T_m^{-1} v_f^{a,b,c}$$

and

$$i_f^{1,2,3} = T_m^{-1} i_f^{a,b,c} \tag{5.2}$$

where

$$T_m^{-1} = \frac{1}{3} \begin{bmatrix} 1 & 1 & 1 \\ 1 & -1 & 0 \\ 1 & 0 & -1 \end{bmatrix} \tag{5.3}$$

The computational effort is reduced by computing the modal components without division by 3, and these are called the modified modal components in the present work. Consequently,

the fault detection criteria get modified as given below.

$$\left|S_1'^{(m)}\right| > \left|S_2'^{(m)}\right| \quad \text{for faults ahead of the relaying point}$$

and

$$\left|S_1'^{(m)}\right| < \left|S_2'^{(m)}\right| \quad \text{for faults behind the relaying point;}$$

$$m = 1,2,3 \qquad\qquad (5.4)$$

where $S_1'^{(m)}$ and $S_2'^{(m)}$ are the modified relay inputs evaluated with the modified modal components of voltages and currents. With this modification incorporated, the relaying algorithm would be as follows.

Step 1 : Calculate, by the cycle-to-cycle comparison method, the fault-generated components of all the line currents for five sample sets backwards from the set at which the fault detection algorithm has yielded a logical 'yes' output.

Step 2 : Calculate the modified modal components of the fault-generated components of the phase voltages and line currents. At the first instance, the earliest sample set is considered.

Step 3 : Execute the Steps 4 to 6 for each mode, i.e.,
$$m = 1,2,3$$

Step 4 : Calculate the modified relay inputs

Step 5 : Check if $\left|S_1'^{(m)}\right| > \left|S_2'^{(m)}\right|$

If so, a fault ahead of the relaying point has

has occurred. Then, start the transmitter. Also, if a carrier signal is received from the other end, trip the circuit breaker. If not, proceed to the next step.

Step 6 : Check if $\left|S_1^{(m)}\right| < \left|S_2^{(m)}\right|$.

If so, a fault behind the relaying point has occurred. Therefore, block the possible starting of the transmitter subsequently by the backward waves coming after reflection at the remote end of the line. If not, go to the next step.

Step 7 : Take the next sample set and go to Step 2.

The flow chart of the algorithm is given in Fig. 5.2. It can be seen that this algorithm is simple and straight-forward and therefore, can be implemented even with a microprocessor system.

5.6 FAULT LOCATING RELAY SCHEME

The theory and the principles of operation of this relaying scheme have been described in Chapter 4. The fault-generated components of the relaying-point phase voltages and line currents are used for relaying purpose as in the previous scheme. With the modification explained in the next section, the criterion given in eqn. (4.14) is used for detecting the reverse faults, and those given in eqns. (4.15) and (4.16) are used for detecting and locating internal faults. The computer application of this scheme, along with an algorithm, is described in the next section.

From fault detection algorithm

$$i(j,k) = i(j,k) - i(j-100,k)$$
$$\forall \, j = (l-4), i \text{ and } k = 1,3$$

200
$$j = (l-4), l$$

200
$$m = 1,3$$

Is $m = 1$

TRUE →
$$v_f^{'(m)} = v_f(j,1) + v_f(j,2) + v_f(j,3)$$
$$i_f^{'(m)} = i_f(j,1) + i_f(j,2) + i_f(j,3)$$

FALSE

Is $m = 2$

TRUE →
$$v_f^{'(m)} = v_f(j,1) - v_f(j,2)$$
$$i_f^{'(m)} = i_f(j,1) - i_f(j,2)$$

FALSE

$$v_f^{'(m)} = v_f(j,1) - v_f(j,3)$$
$$i_f^{'(m)} = i_f(j,1) - i_f(j,3)$$

$$RI^{(m)} = R_{set} * i_f^{'(m)}$$
$$S_1^{'(m)} = v_f^{'(m)} - RI^{(m)}$$
$$S_2^{'(m)} = v_f^{'(m)} + RI^{(m)}$$

Is $|S_1^{'(m)}| > |S_2^{'(m)}|$

TRUE → A fault ahead has occurred start the transmitter

FALSE

Is $|S_1^{'(m)}| < |S_2^{'(m)}|$

TRUE → Reverse fault has occurred block the possible starting of the transmitter later.

FALSE

200

No fault detected restart sampling
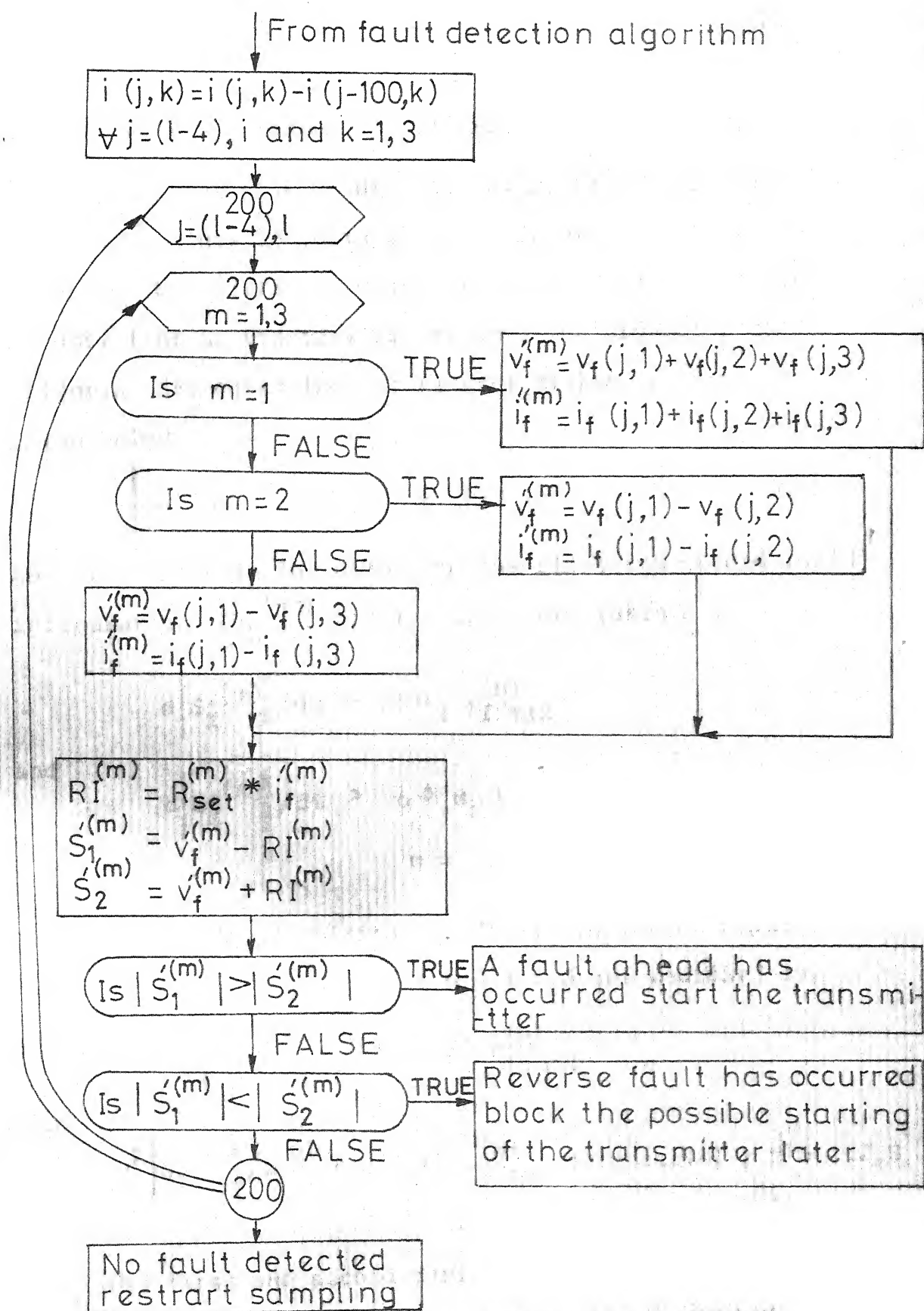
FIG·5·2 FLOW CHART OF THE AMPLITUDE COMPARISON RELAY ALGORITHM

5.6.1 Digital Computer Application

The computation of division by 3, in evaluating the modal components of voltages and currents, is eliminated by using the modified components and the modified relay inputs, like in the previous scheme. Accordingly, the criterion for detecting the reverse faults is taken as given below.

$$\left| S_2'^{(m)} \right| > 0.09 \text{ p.u.}; \quad m = 1,2,3 \tag{5.5}$$

And, the criteria for detecting the first and second rapid increases in $\left| S_1'^{(m)} \right|$ for $m = 1,2,3$ are taken as,

$$d\left| S_1'^{(m)} \right|/dt > 6 \omega_o V_{ffmax}^{(m)}$$

and

$$d\left| S_1'^{(m)} \right|/dt > 6 \rho_s \omega_o V_{ffmax}^{(m)} \text{ respectively;}$$

$$m = 1,2,3 \tag{5.6}$$

The criteria for detecting the first and second rapid increases in $d\left| S_1'^{(m)} \right|/dt$ for $m = 1,2,3$ get modified as,

$$d^2\left| S_1'^{(m)} \right|/dt^2 > 6 \omega_o^2 V_{ffmax}^{(m)}$$

and

$$d^2\left| S_1'^{(m)} \right|/dt^2 > 6 \rho_s \omega_o^2 V_{ffmax}^{(m)} \text{ respectively; } m = 1,2,3 \tag{5.7}$$

The first and second derivatives of $\left| S_1'^{(m)} \right|$, for $m = 1,2,3$, at any sampling instant t_i, are computed using

the following numerical differentiation formulae [120]

$$d\left[\left|S_1^{(m)}\right|/dt\right]_{t=t_i} = \left\{\left|S_{1,i+1}^{(m)}\right| - \left|S_{1,i}^{(m)}\right|\right\}/\Delta t$$

$$= \Delta S'^{(m)}_{1,1}/\Delta t, \text{ say; } m = 1,2,3 \qquad (5.8)$$

and

$$d^2\left[\left|S_1^{(m)}\right|/dt^2\right]_{t=t_i} = \left\{\left|S_{1,i+1}^{(m)}\right| -2\left|S_{1,i}^{(m)}\right| + \left|S_{1,i-1}^{(m)}\right|\right\}/(\Delta t)^2$$

$$= \Delta S'^{(m)}_{1,2}/(\Delta t)^2, \text{ say; } m = 1,2,3 \qquad (5.9)$$

where $S'^{(m)}_{1,i+1}$, $S'^{(m)}_{1,i}$ and $S'^{(m)}_{1,i-1}$ are the modified relay inputs computed from (i+1)th, ith and (i-1)th sample sets of voltages and currents, and Δt is the sampling interval.

The first and, if necessary, the second derivatives are to be computed repetitively and hence, it is imperative that the computational effort be reduced. This is accomplished by modifying the criteria, used to detect the first and second rapid increases in $\left|S_1^{(m)}\right|$, as follows.

$$\Delta S'^{(m)}_{1,1} > 6\,\omega_o\,V^{(m)}_{ffmax}\,\Delta t$$

and

$$\Delta S'^{(m)}_{1,1} > 6\rho_s\omega_o\,V^{(m)}_{ffmax}\,\Delta t \text{ respectively; } m = 1,2,3$$

$$(5.10)$$

Similarly, the criteria, used to detect the first and second

rapid increases in $d\left|S_1'^{(m)}\right|/dt$, are modified as given below.

$$\Delta S_{1,2}'^{(m)} > 6\omega_o^2 V_{ffmax}^{(m)} (\Delta t)^2$$

and

$$\Delta S_{1,2}'^{(m)} > 6\rho_s \omega_o^2 V_{ffmax}^{(m)} (\Delta t)^2 \text{ respectively; } m = 1,2,3$$

$$(5.11)$$

As explained in Section 4.3.4, maximum values of $V_{ffmax}^{(m)}$ for $m = 1,2,3$ are chosen in the above settings.

A rapid increase in $\left|S_1'^{(m)}\right|$ or $d\left|S_1'^{(m)}\right|/dt$ may span over two or three consecutive sampling intervals, in which case the fault-location computation may go wrong. This difficulty is overcome by a suitable logic, as described in the algorithm given below. With the above features incorporated, the relaying algorithm would be as follows.

Step 1 : Calculate, by the cycle-to-cycle comparison method, the fault-generated components of all the line currents for twelve sample sets backwards from the sample set at which the fault detection algorithm has yielded the logical 'yes' output. The two extra sample sets are used to partly cover the interval immediately preceding the arrival of waves at the relaying point in order to facilitate the computation of the second derivatives correctly.

Step 2 : Calculate the modified modal components of the fault-generated components of voltages and currents.

Step 3 : Calculate modified relay inputs for all the modes and for all the sample sets.

Step 4 : Check   if $\left|S_2^{!(m)}\right|$ > 0.09 p.u. for m = 1,2,3.

If so for any m, stop executing the relaying programme further at this end and start the transmitter, after a time delay of Td_1 (defined in Section 4.3.1 of Chapter 4), which sends information to the other end to stop executing the relaying programme there also and to block tripping. If not, proceed further. At the start, this step is executed for the first sample set.

Step 5 : Calculate $\Delta S_{1,1}^{!(m)}$ and check if $\Delta S_{1,1}^{!(m)}$ > $6\omega_0 \cdot V_{ffmax}^{(m)} \Delta t$ for m = 1,2,3. If not, take the next set of modified inputs and go to the Step 4. If satisfied, do not go to Step 4 any further. Block the possible starting of the transmitter and set the time counter to the value of the time corresponding to this sample set. The time counter setting and the rapid-increase-detection criterion remain the same if the above condition is satisfied over consecutive sampling intervals. If this happens for four consecutive sampling sets, an indication, that the fault is close-in, is given as

output. Otherwise, change the setting of the rapid-increase-detection criterion to $6\rho_s\omega_o \, V_{ffmax}^{(m)} \, \Delta t$. When the changed criterion is satisfied for any m, indicating a second rapid increase, set the time counter to the current time minus the previous setting. Stop further execution of the algorithm, compute the distance of the fault and output this value as well as a logical 'yes' for tripping. When this step yields no result, go to the next step.

Step 6 : Repeat the algorithmic procedure of Step 5 with the second derivatives of $\left|S_1^{(m)}\right|$ for m = 1,2,3, using the rapid-increase-detection criteria given in eqns. (5.11). If this step also fails to yield any result, go to the next step.

Step 7 : Under these conditions, the second rapid increase detection must have failed. Then, a trip signal is issued after a time delay of Td_2, which is defined in Section 4.3.2 of Chapter 4.

The flow chart of the algorithm is given in Fig. 5.3.

5.7 DIGITAL SIMULATION AND RESULTS

5.7.1 Testing

For testing the proposed algorithms, fault data are generated for a desired type of fault for two cycles,

FIG. FLOW CHART OF THE FAULT LOCATING RELAY ALGORITHM

one prefault and one post-fault, by employing the digital simulation techniques described in Chapter 3. The amplitude comparison relay algorithms are tested by using the fault data computed for an internal fault at the remote end (marked F_1) of the protected line and for an external fault (marked F_2) at the remote end of the adjoining line in the 4-bus system shown in Fig. 3.11. Each source is represented by an equivalent lumped-parameter model with phase inductances calculated from the fault level specified and the neutral impedance, from an assumed ratio of Z_o/Z_1 of 0.5 at power frequency, as explained in Appendix D. A three-phase fault through a resistance of 100 ohms per phase and with a fault initiation angle of 0° is assumed.

The fault locating relay algorithms are tested by using the fault data evaluated for a single line to ground fault on phase 'a' at the remote end of the protected line of 200 Km length in the power system shown in Fig. 4.1. In this case, the sending - and receiving-end sources are considered as composed solely of transmission lines and cables, and as having net modal surge impedances respectively equal to 1/9th and 1/4th of the appropriate modal surge impedances of the line. A fault resistance of 100 ohms per phase and a fault initiation angle of 90° are considered.

In both the sample power systems, each 3-phase transmission line is a typical 400 KV quad-conductor untransposed single-circuit line. An earth resistivity of 100 ohm-m is assumed and the frequency dependency of all the line and earth parameters is taken into consideration. The remaining data of each line are given in Fig. 3.7 and Appendix B. The sampling interval is taken as 200 μs and the peak value of the prefault voltage at the point of fault is assumed as 1.0 p.u.

Using the realistic fault data, generated as described above, the fault detection and relaying programmes are run on the DEC System 1090 computer at I.I.T., Kanpur.

5.7.2 Results

In both the cases, the CPU time has been found to be less than 1 ms for the execution of the entire programme, consisting of fault detection and relaying. However, eight sample sets in the first scheme and fourteen in the second were required for detecting the internal fault. Hence, the total time of operation would be about 8x0.2+1 = 2.6 ms in the first scheme, and it would be about 14x0.2+1 = 3.8 ms in the second scheme. The second scheme takes more time primarily on account of the fault locating feature. Also, in the second scheme, the distance of the fault has been computed as 210.0 Km, the actual value being 200 Km. Thus, this scheme can locate the faults only approximately.

5.7.3 Discussion

Summarising, the digital travelling wave algorithms, developed in this chapter, have been tested in the following manner. The fault data are generated for a sample power system by employing realistic models for the transmission lines, and the accurate frequency-domain method. Using these data as input, the programmes of the relay algorithms are executed on the digital computer, DEC System 1090 at the I.I.T., Kanpur, for testing the viability of the above algorithms. Since the object has been only to test the viability of the algorithms, only one faulted condition is considered in each case.

However, in actual hardware implementation, that is, in the on-line digital computer application, the three phase fault voltages and currents, derived from the system through transducers, have to be sampled simultaneously at the desired sampling frequency, converted to the digital form, and transferred to a digital processor, by means of an analog subsystem. The currents are monitored as voltage drops across resistors on the secondaries of the interposing current transformers. A typical analog subsystem, for this purpose, may consist of six buffer amplifiers, six sample-and-hold circuits, a multiplexer and an analog-to-digital converter (ADC). The purpose of the buffer amplifiers is to trim the input signals. The digital output from the ADC is transferred

to the digital processor, that is, the computer, through a direct memory access (DMA) channel. All the components of the analog subsystem would have to be of high-speed type. A simplified block schematic diagram of the hardware, needed in actual implementation, is given in Fig. 5.4. The hardware implementation, which would yield more realistic indication of the viability of the computer application of the travelling wave relay algorithms, could not be carried out for want of facilities.

5.8 CONCLUSIONS

The digital simulation tests, carried out on the two new digital travelling wave relay algorithms described in this chapter, have established their viability. The heart of these schemes is the fault detection algorithm, which is quite simple and straightforward. With this fault detection algorithm, not only the relaying algorithms described in this chapter but also the analog travelling wave relay schemes proposed by others [73,77,85] can be implemented digitally. There being no need for any elaborate filtering, the travelling wave relay algorithms are superior in terms of both the speed and accuracy. Therefore, these will ultimately supplant the distance algorithms in the digital protection of transmission lines.
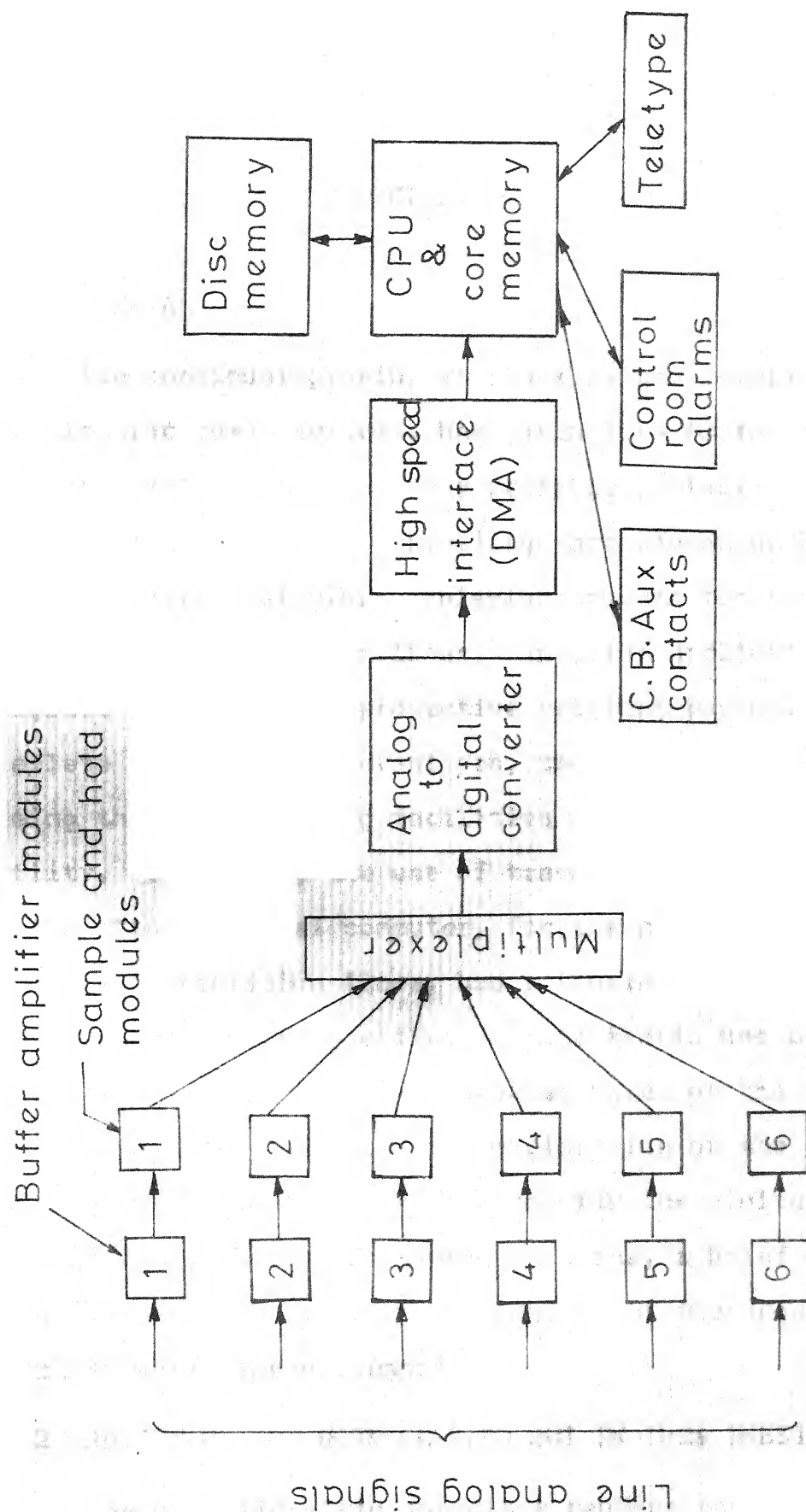
FIG.5·4 BLOCK SCHEMATIC DIAGRAM OF ON LINE
DIGITAL COMPUTER APPLICATION

CHAPTER 6

CONCLUSIONS

6.1 GENERAL

The continual growth, in the size and complexity
of electric power systems, has given rise to the need
for extremely fast and highly reliable protective schemes.
The utilization of the travelling wave phenomena has enabled
the realization of u.h.s. relaying schemes for the protection
of EHV/UHV transmission lines. And, the application of
digital computers for protective relaying purposes is
replete with several advantages,,the chief amongst them
being the self-checking facilities and the maximum flexi-
bility. Therefore, the use of travelling wave phenomena,
along with a digital computer, for the protection of
EHV/UHV transmission lines, has potential merits. Accord-
ingly, the primary objective of this thesis has been the
development of new relaying schemes based on the travelling
wave phenomena, and also, the exploration of the feasibility
of the adaptation of these schemes for the digital computer
application. In the following sections, a brief account of
the work carried out in this thesis, and the scope for
further work, are presented.

6.2 REVIEW OF THE WORK CARRIED OUT IN THIS THESIS

Use of solid-state circuitry renders the generation

of several special relay threshold characteristics, like
conic and quadrilateral etc.,easier and simpler, and
also the attainment of high speed of operation possible.
And, the use of ICs, in place of transistors and several
discrete components, results in more compact, more
reliable and economical relay units. The quadrilateral
pickup characteristic is eminently suitable for the
protection of long and heavily-loaded EHV/UHV transmission
lines. Therefore, new distance relays, employing ICs
and capable of generating a three-step quadrilateral pickup
characteristic, have been developed, fabricated and tested.
The first relay scheme demonstrates that the use of ICs
greatly simplifies the circuitry, although the input
signals used are the same as those given in reference [36].
The second relaying scheme uses less number of input
signals for generating the open quadrilateral characteristic,
and therefore, is more reliable. Also, the measurement of
the coincidence of the input signals is completed in half
a cycle, and there are no time co-ordination problems
associated with this scheme. Results of the tests
conducted on these relays closely agree with the theoretical
ones.

For designing, and for assessing the performance of,
both analog u.h.s. relay schemes and high-speed digital
computer relay algorithms, especially those based on

needed for not more than one cycle. Under such circumstances, the frequency-domain method of computation does not need undue computational effort. Also, the application of the fast Fourier transform method to the computation of time-domain values does not provide much computational relief. The results of numerical examples, worked out in this thesis, establish these facts.

Ultra high speed clearing of faults improves the transient stability. The fault clearing time depends on the speed of the protective relay as well as on that of the associated circuit breaker. With the emergence of u.h.s. circuit breakers, the need for u.h.s. protective relays has become imperative. The development of these relays has been facilitated by the use of travelling wave phenomena. However, only a few relays, based on travelling wave phenomena, have been developed so far. Consequently, new travelling-wave relay schemes, suitable for the protection of EHV/UHV transmission lines, have been developed in the present work.

In one relaying scheme, the amplitude comparison of each of the three pairs of modal relay inputs is made use of to distinguish between the reverse and forward faults. Tripping is initiated if the fault is detected as forward at both the ends of the line. The underlying relaying principles have been verified by the results obtained

through the digital simulation of a sample power system.

In the second scheme, one relay input (for each mode) is used for detecting the reverse faults, and tripping is blocked at the remote end with the aid of a carrier communication channel and also at the local end, under reverse fault conditions. By making use of the first, and if necessary the second, time derivatives of the other relay input (for each mode), the instants of first and second incidences of the backward travelling waves, at the relaying point, can be determined. This would enable the determination of the distance of the fault and hence, the detection of an internal fault. Thus, both the detection of an internal fault and the determination of the distance of the fault can be accomplished with this relaying scheme. Since carrier communication between the ends of the line is not necessary for the detection of internal faults, the operating time of the carrier communication equipment does not form a part of the operating time of the relaying scheme, unlike in the other travelling-wave relaying schemes. The applicability of the fault-locating principle has been illustrated by considering four typical cases of an internal fault. In addition, the relaying principles involved in this scheme have been validated by the results of digital simulation studies conducted on an equivalent sample power system.

The effect of fault resistances and fault initiation angle on the relay response, in both the schemes, has been studied. The response of both the relaying schemes has been found to be good, even for fault resistances as high as 200 ohms. However, the response may be poor for higher fault resistances when the fault initiation angle is zero. However, the occurrence of a fault at a voltage zero is comparatively rare. With the application of relaying principles to each of the three propagation modes, all the types of faults are taken care of in both the schemes. Therefore, these relaying schemes can be regarded as a novel type of polyphase relays.

The development of the digital protection of transmission lines has been confined mainly to the generation and improvement of different types of distance relay algorithms, which involve in the computation of the fundamental power frequency impedance from the complex post-fault current and voltage waveforms. Different types of analog and digital filters have been developed for extracting the fundamental components of voltages and currents. But, the accuracy, with which the fundamental components can be determined, depends upon the extent of filtering. On the other hand, the nature and extent of filtering needed depends upon the rigour of line modelling. Either more elaborate filtering or more rigorous line modelling would introduce longer time delays. As a

consequence, the speed and accuracy have been conflicting requirements with the digital distance algorithms. But, the digital algorithms, based on travelling wave phenomena, necessitate the filtering out of only the prefault components. Also, a fewer number of samples at shorter intervals of time are required for fault detection. Thus, these algorithms provide faster relaying.

In this thesis, the cycle-to-cycle comparison method, proposed by Mann and Morrison [90], has been adapted as a simple digital filter for filtering out the prefault components. Also, algorithms, for the digital computer application of the amplitude-comparison and fault-locating relay schemes, have been developed and presented. The viability of these algorithms has been tested on the digital computer, DEC System 1090 at I.I.T., Kanpur, by using realistic fault data obtained from the digital simulation of sample power systems. The results of these tests have demonstrated the viability of the proposed algorithms. However, there is a need for on-linedigital computer testing of these algorithms, which could not be carried out for want of facilities, to establish, more firmly, the viability of these algorithms.

6.3 SCOPE FOR FURTHER WORK

The fault data, for testing the u.h.s. protective relays developed in this thesis, have been obtained by the digital simulation of sample power systems, wherein, although the

transmission lines have been modelled with adequate details and accuracy, the sources considered are of a simple nature. Therefore, the frequency-domain representation of complex source networks incorporating generation is clearly an area in which further work needs to be done. In addition, the frequency-domain models of current and voltage transducers as well as power transformers need incorporation in the system model to include   their transient behaviour. These will facilitate in the generation of more realistic fault data.

The validity of the travelling-wave relaying principles, developed in this thesis, needs further assessment when applied to the protection of double-circuit lines, series and shunt compensated long lines and multi-terminal lines.

Actual hardware implementation of, and extensive field tests on, the travelling-wave relay schemes, proposed in this thesis, are necessary to warrant their satisfactory performance under actual conditions.

APPENDIX A

FREQUENCY DOMAIN A,B,C,D PARAMETERS OF A
TRANSMISSION LINE

A three-phase transmission line with distributed
parameters, is described in the frequency domain by the
following differential equations [116].

$$\frac{d^2 \bar{V}^{a,b,c}}{dx^2} = \bar{P}^{a,b,c} \; \bar{V}^{a,b,c}$$

and,
$$\frac{d^2 \bar{I}^{a,b,c}}{dx^2} = [\bar{P}^{a,b,c}]^t \; \bar{I}^{a,b,c} \tag{A.1}$$

where

$\bar{V}^{a,b,c}$ — column vector of the transforms of the voltages
to earth of the phases a,b,c at a point X on the
line,

$\bar{I}^{a,b,c}$ — column vector of the transforms of the line
currents, pertaining to the phases, a,b,c, at X

$\bar{P}^{a,b,c} = \bar{Z}_L^{a,b,c} \cdot \bar{Y}_L^{a,b,c}$

$\bar{Z}_L^{a,b,c}$, $\bar{Y}_L^{a,b,c}$ — transforms of the p.u. length series impedance
and shunt admittance matrices, respectively, of
the line

and, x — distance of X from S.E.

$\overline{Z}_L^{a,b,c}$ and $\overline{Y}_L^{a,b,c}$ are evaluated by taking into account the presence of earth wires, and the frequency dependency of both the resistive and inductive parameters of the line and earth. The theory of natural modes enables the above equations to be effectively decoupled by means of of voltage and current modal transformation matrices S and Q respectively. Using these transformation matrices, equations (A.1) can be rewritten as follows.

$$\frac{d^2\overline{V}^{1,2,3}}{dx^2} = S^{-1}\,\overline{P}^{a,b,c}\,S\,\overline{V}^{1,2,3}$$

and

$$\frac{d^2\overline{I}^{1,2,3}}{dx^2} = Q^{-1}\,[\overline{P}^{a,b,c}]^t\,Q\,\overline{I}^{1,2,3} \tag{A.2}$$

where

S - the matrix formed from the eigenvectors of $\overline{P}^{a,b,c}$

$Q = [S^{-1}]^t$, (i.e. the matrix formed from the eigenvectors of $[\overline{P}^{a,b,c}]^t$)

$\overline{V}^{1,2,3} = S^{-1}\,\overline{V}^{a,b,c}$, column vector of modal components of phase voltage transforms

$\overline{I}^{1,2,3} = Q^{-1}\,\overline{I}^{a,b,c}$, column vector of modal components of line current transforms

$$S^{-1} [\overline{P}^{a,b,c}] S = Q^{-1} [\overline{P}^{a,b,c}]^t Q = \text{diag.} [\lambda_1 \quad \lambda_2 \quad \lambda_3]$$

and λ_1, λ_2 and λ_3 - eigenvalues of $\overline{P}^{a,b,c}$.

The equations (A.2) can be rewritten in the decoupled form as given below.

$$\frac{d^2 \overline{V}^{(m)}}{dx^2} = \lambda_m \overline{V}^{(m)} = \gamma_m^2 \overline{V}^{(m)}$$

and,

$$\frac{d^2 \overline{I}^{(m)}}{dx^2} = \lambda_m \overline{I}^{(m)} = \gamma_m^2 \overline{I}^{(m)} \quad ; \quad m = 1,2,3 \qquad \text{(A.3)}$$

These equations show that the wave propagation in a 3-phase transmission line can be decomposed into three separate and independent components, called modal components, each possessing its own propagation constant and surge impedance.

Solving the first equation of (A.3), we get

$$\overline{V}^{(m)} = K_1 \cosh \gamma_m x + K_2 \sinh \gamma_m x; \quad m = 1,2,3 \quad \text{(A.4)}$$

where K_1 and K_2 are arbitrary constants to be determined by boundary conditions.

Also, it is known [116] that

$$\frac{d\overline{V}^{a,b,c}}{dx} = -\overline{Z}_L^{a,b,c} \overline{I}^{a,b,c}$$

Upon transformation to the modal domain, the above equation becomes

$$\frac{d\overline{V}^{1,2,3}}{dx} = -[S^{-1} \overline{Z}_L^{a,b,c} Q] \overline{I}^{1,2,3} = -\overline{Z}_M \overline{I}^{1,2,3} \qquad (A.5)$$

where

$$\overline{Z}_M = \text{diag.} [\overline{Z}^{(1)} \overline{Z}^{(2)} \overline{Z}^{(3)}]$$

The equation (A.5) can be rewritten in the decoupled form as given below.

$$\frac{d\overline{V}^{(m)}}{dx} = -\overline{Z}^{(m)} \overline{I}^{(m)} \; , \quad m = 1,2,3 \qquad (A.6)$$

Solving equations (A.4) and (A.6), we get

$$\overline{I}^{(m)} = -\frac{\gamma_m}{\overline{Z}^{(m)}} [K_1 \sinh \gamma_m x + K_2 \cosh \gamma_m x]; \quad m = 1,2,3 \qquad (A.7)$$

Now, we know that, at $x = 0$, i.e., at the S.E., $\overline{V}^{(m)} = \overline{V}_S^{(m)}$ and $\overline{I}^{(m)} = \overline{I}_S^{(m)}$ and, at $x = 1$, i.e., at the R.E., $\overline{V}^{(m)} = \overline{V}_R^{(m)}$ and $\overline{I}^{(m)} = \overline{I}_R^{(m)}$.

Using the above boundary conditions and solving eqns. (A.4) and (A.7), we get

$$\overline{V}_R^{(m)} = (\cosh \gamma_m 1) \overline{V}_S^{(m)} - \frac{\overline{Z}^{(m)}}{\gamma_m} (\sinh \gamma_m 1). \overline{I}_S^{(m)}$$

and

$$\overline{I}_R^{(m)} = -\frac{\gamma_m}{\overline{Z}^{(m)}} (\sinh \gamma_m 1) \overline{V}_S^{(m)} + (\cosh \gamma_m 1) \overline{I}_S^{(m)}; \; m = 1,2,3 \qquad (A.8)$$

Expressed in a matrix form, equations (A.8) become

$$\begin{bmatrix} \overline{V}_R^{1,2,3} \\ \\ \overline{I}_R^{1,2,3} \end{bmatrix} = \begin{bmatrix} [\cosh\gamma l] & -\overline{Z}_M[\gamma]^{-1}[\sinh\gamma l] \\ \\ -[\gamma]\overline{Z}_M^{-1}[\sinh\gamma l] & [\cosh\gamma l] \end{bmatrix} \begin{bmatrix} \overline{V}_S^{1,2,3} \\ \\ \overline{I}_S^{1,2,3} \end{bmatrix}$$

$$(A.9)$$

where

$$[\cosh\gamma l] = \text{diag.}[\cosh\gamma_1 l \quad \cosh\gamma_2 l \quad \cosh\gamma_3 l],$$

$$[\sinh\gamma l] = \text{diag.}[\sinh\gamma_1 l \quad \sinh\gamma_2 l \quad \sinh\gamma_3 l],$$

and

$$[\gamma] = \text{diag.}[\gamma_1 \quad \gamma_2 \quad \gamma_3]$$

From eqn. (A.9), the following equation can easily be derived.

$$\begin{bmatrix} \overline{V}_S^{1,2,3} \\ \\ \overline{I}_S^{1,2,3} \end{bmatrix} = \begin{bmatrix} [\cosh\gamma l] & \overline{Z}_M[\gamma]^{-1}[\sinh\gamma l] \\ \\ [\gamma]\,\overline{Z}_M^{-1}[\sinh\gamma l] & [\cosh\gamma l] \end{bmatrix} \begin{bmatrix} \overline{V}_R^{1,2,3} \\ \\ \overline{I}_R^{1,2,3} \end{bmatrix}$$

$$= \begin{bmatrix} A_m & B_m \\ \\ C_m & D_m \end{bmatrix} \begin{bmatrix} \overline{V}_R^{1,2,3} \\ \\ \overline{I}_R^{1,2,3} \end{bmatrix}, \text{ say} \qquad (A.10)$$

Performing inverse modal transformation on the above

equation, we get

$$
\begin{bmatrix} \bar{V}_S^{a,b,c} \\ \bar{I}_S^{a,b,c} \end{bmatrix} = \begin{bmatrix} S^{-1}A_mS & S^{-1}B_mQ \\ Q^{-1}C_mS & Q^{-1}D_mQ \end{bmatrix} \begin{bmatrix} \bar{V}_R^{a,b,c} \\ \bar{I}_R^{a,b,c} \end{bmatrix}
$$

$$
= \begin{bmatrix} A & B \\ C & D \end{bmatrix} \begin{bmatrix} \bar{V}_R^{a,b,c} \\ \bar{I}_R^{a,b,c} \end{bmatrix} , \text{ say} \qquad (A.11)
$$

APPENDIX B

BASIC DATA OF THE SINGLE-CIRCUIT 400 KV 3-PHASE
QUAD-CONDUCTOR TRANSMISSION LINES

Number of conductors per phase	= 4
Number of earth wires	= 1
Conductor resistivity	= 3.20×10^{-8} Ohm-m
Earth-wire resistivity	= 2.69×10^{-8} Ohm-m
Conductor strand diameter	= 0.32 cm
Earth-wire strand diameter	= 0.32 cm
Geometric mean radius of the bundle conductor	= 15.495 cm
Number of effective strands in phase conductors	= 54
Number of effective strands in the earth wire	= 54
Outer diameter of earth wire	= 2.86 cm

APPENDIX C

SOURCE DATA OF THE 3-BUS SAMPLE POWER SYSTEM

Nominal angular frequency = 314.159 rad/s

Phase sequence = a,b,c

Source impedances :

$$r_{aa} = r_{bb} = r_{cc} = 0$$

$$L_{aa} = L_{bb} = L_{cc} = 0.097615H$$

$$L_{ab} = L_{bc} = L_{ca} = -0.029709H$$

$$L_{ba} = L_{cb} = L_{ac} = -0.029709H$$

APPENDIX D

DERIVATION OF EQUIVALENT SOURCE MODELS FROM SPECIFIED FAULT LEVELS

A simplified equivalent-source model, based upon the given short-circuit level at a bus, would be as shown in Fig. D.1. The phase impedances are calculated from the fault level specified, and the neutral impedance, from a specified ratio of zero and positive sequence source impedances as outlined briefly below [115].

Let the fault level at a bus be x MVA,

the line voltage of the bus be V KV,

the ratio of the zero and positive sequence

source impedances be $Z_{s0}/Z_{s1} = k$, and

the nominal frequency of the system be ω_o rad/s.

Then, the phase impedances would be given by

$$Z_a = Z_b = Z_c = Z_{ph} = \frac{V^2}{x} \text{ ohms} \qquad (D.1)$$

It can easily be shown that,

$$Z_{s0}/Z_{s1} = \frac{Z_{ph}+3Z_n}{Z_{ph}} = 1 + \frac{3Z_n}{Z_{ph}} = k \qquad (D.2)$$

where Z_{ph} and Z_n are the phase and neutral impedances respectively.
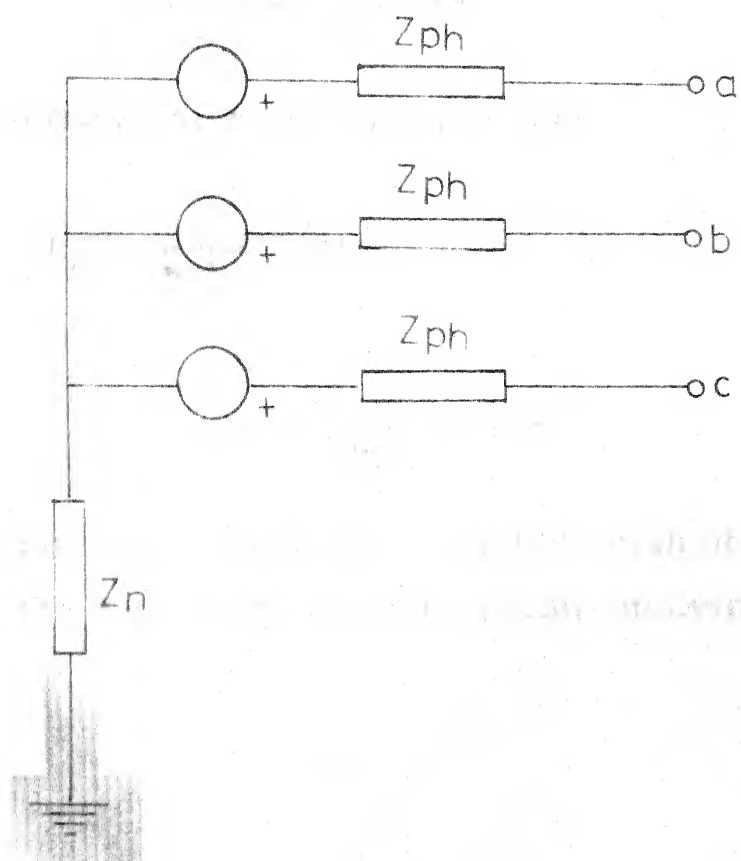
FIG. D·1 SIMPLIFIED EQUIVALENT SOURCE
MODEL

Solving equations (D.1) and (D.2), we get

$$Z_n = - \frac{(1-k)}{3} \cdot \frac{V^2}{x} \text{ ohms} \tag{D.3}$$

Neglecting resistances, we get

$$L_{ph} = \frac{V^2}{\omega_0 x} \text{ Henrys} \tag{D.4}$$

and

$$L_n = - \frac{(1-k)}{3} \cdot \frac{V^2}{\omega_0 x} \text{ Henrys} \tag{D.5}$$

Equations (D.4) and (D.5) have been used in connection with the 4-bus sample power system, employed in the thesis.

REFERENCES

1. K.L. Hicks and W.H. Butt, 'Feasibility and Economics of Ultra High Speed Fault Clearing', IEEE Transactions on Power Apparatus and Systems, vol. PAS-99, Nov./Dec. 1980, pp. 2138-2145.

2. R.O. Berglund, W.A. Mittlestadt, M.L. Shelton, P. Barkan, C.C. Dewey and K.M. Skreiner, 'One Cycle Fault Interruption at 500 KV - System Benefits and Breaker Design', IEEE Transactions on Power Apparatus and Systems, vol. PAS-93, Sept./Oct. 1974, pp.1240-1253.

3. A.T. Johns and R.K. Aggarwal, 'Digital Simulation of Faulted E.H.V. Transmission Lines with Particular Reference to Very-High-Speed Protection', Proc. IEE, vol. 123, April 1976, pp. 353-359.

4. A.R. van C. Warrington, 'Protective Relays - Their Theory and Practice', Vol. I, John Wiley and Sons Inc., New York, 1962.

5. IEEE Committee Report, 'Review of Recent Practices and Trends in Protective Relaying', IEEE Transactions on Power Apparatus and Systems, vol. PAS-100, Aug. 1981, pp. 4054-4063.

6. L.N. Crichton, 'The Distance Relay for Automatically Sectionalizing Electrical Networks', AIEE Transactions, vol. XLII, 1923, pp. 527-537.

7. H.A. McLaughlin and E.O. Erickson, 'The Impedance Relay', AIEE Transactions, vol. 47, 1928, pp. 776-782.

8. L.N. Crichton, 'High Speed Protective Relays', AIEE Transactions, vol. 49, Oct. 1930, pp. 1232-1242.

9. S.L. Goldsborough and W.A. Lewis, 'New High Speed Distance Relay', Electrical Engineering, vol. 51, March 1932, pp. 157-160.

10. S.L. Goldsborough, 'A Distance Relay with Adjustable Phase-Angle Discrimination', AIEE Transactions, vol. 63, 1944, pp. 835-838.

11. E.E. George, 'Operating Experience with Reactance-type Distance Relays', AIEE Transactions, vol. 50, 1931, pp. 288-293.

12. A.R. van C. Warrington, 'A High Speed Reactance Relay', Electrical Engineering, vol. 52, April 1933, pp. 248-252.

13. C.G. Dewey and J.R. Mc Glynn, 'A New Reactance Distance Relay', AIEE Transactions, vol. 67, Part I, 1948, pp. 743-746.

14. Warren C. New, 'Combined Phase and Ground Distance Relaying', AIEE Transactions, vol. 69, Part I, 1950, pp. 37-44.

15. A.R. van C. Warrington, 'Protective Relaying for Long Transmission Lines', AIEE Transactions, vol. 62, 1943, pp. 261-268.

16. R.E. Cordrey and A.R. van C. Warrington, 'The MHO Carrier Relaying Scheme', AIEE Transactions, vol. 63, 1944, pp. 228-235.

17. R.M. Hutchinson, 'The MHO Distance Relay', AIEE Transactions, vol. 65, June 1946, pp. 353-359.

18. J.E. Skuderna, 'A Mathematical Basis for a Protective Relay with Conic Pickup Characteristics', AIEE Transactions, vol. 81, Part III, 1962, pp. 81-88.

19. R. Wideröe, 'Thyratron Tubes in Relay Practice', AIEE Transactions, vol. 53, Oct. 1934, pp. 1347-1353.

20. R.H. Mac Pherson, A.R. van C. Warrington and A.J. Mc Connell, 'Electronic Protective Relays', AIEE Transactions, vol. 67, Part III, 1948, pp. 1702-08.

21. H.C. Barnes and R.H. Mac Pherson, 'Field Experience – Electronic Mho Distance Relay', AIEE Transactions, vol. 72, Part III, 1953, pp. 857-65.

22. James J. Loving Jr., 'Electronic Relay Developments', AIEE Transactions, vol. 68, 1949, pp. 233-242.

23. F.R. Bergseth, 'An Electronic Distance Relay Using Phase-Discrimination Principle', AIEE Transactions, vol. 73, Part III-B, 1954, pp. 1276-1279.

24. M.E. Hodges and R.H. Mac Pherson, 'All-Electronic 1-Cycle Carrier-Relaying Equipment - Relay Operating Principles', AIEE Transactions, vol. 73, Part III-A, 1954, pp. 174-186.

25. W.S. Price, R.E. Cordrcy and R.H. Mac Pherson, 'Performance Evaluation of All-Electronic 1-Cycle Carrier-Relaying Equipment', AIEE Transactions, vol.73, Part III-A, 1954, pp. 187-195.

26. H.T. Seeley and N.A. Koss, 'An All-Electronic 1-Cycle Carrier-Relaying System - Overall Operating Principles', AIEE Transactions, vol. 73, Part III-A, 1954, pp. 161-169.

27. C. Adamson and L.M. Wedepohl, 'Power System Protection with Particular Reference to the Application of Junction Transistors to Distance Relays', Proc. IEE, vol. 103-A, Aug. 1956, pp. 379-388.

28. C. Adamson and L.M. Wedepohl, 'A Dual-Comparator Mho-type Distance Relay Utilizing Transistors', Proc. IEE, vol. 103-A, Sept. 1956, pp. 509-517.

29. C. Adamson and E.A. Talkhan, 'The Application of Transistors to Phase-Comparison Carrier Protection', Proc. IEE, vol. 106, Part A, Feb. 1959, pp. 51-63.

30. C.G. Dewey and M.E. Hodges, 'Transistorized Phase-Comparison Relaying: Principles and Circuits', AIEE Transactions, vol. 79, Part III, Aug. 1960, pp. 373-380.

31. C.G. Dewey, C.A. Mathews and W.C. Morris, 'Static Mho Distance and Pilot Relaying: Principles and Circuits', IEEE Transactions on Power Apparatus and Systems, vol. PAS-82, June 1963, pp. 391-400.

32. V. Caleca, S.H. Horowitz, A.J. Mc Connell and H.T. Seeley, 'Static Mho Distance and Pilot Relaying: Application and Test Results', IEEE Transactions on Power Apparatus and Systems, vol. PAS-82, Aug. 1963, pp. 424-436.

33. C. Hahn, 'Line Protection Devices and Relays for Extremely High Voltages', Brown Boveri Review, vol. 51, Jan./Feb. 1964, pp. 93-100.

34. L.M. Wedepohl, 'Polarised Mho Distance Relay - A New Approach to the Analysis of Practical Characteristics', Proc. IEE, vol. 112, March 1965, pp. 525-535.

35. W.D. Humpage and S.P. Sabberwal, 'Developments in Phase-Comparison Techniques for Distance Protection', Proc. IEE, vol. 112, July 1965, pp. 1383-1394.

36. K. Parthasarathy, 'New Static 3-Step Distance Relay', Proc. IEE, vol. 113, April 1966, pp. 633-640.

37. K. Parthasarathy, 'Three-System and Single-System Static Distance Relays', Proc. IEE, vol. 113, April 1966, pp. 641-651.

38. Hans Hoel, W.D. Humpage and C.P. Chapman, 'Composite Polar Characteristics in Multizone Systems of Phase-Comparison Distance Protection', Proc. IEE, vol. 113, Oct. 1966, pp. 1631-1642.

39. N.M. Anil Kumar and K. Parthasarathy, 'A Mathematical Basis for Multi-Input Sine Comparators', J.I.E. (India), vol. 48, Part EL1, Oct. 1967, pp. 9-21.

40. N.M. Anil Kumar, K. Parthasarathy and K.K. Thakkar, 'A 3-Step Transistorized Distance Relay with A Quadrilateral Polar Characteristic', J.I.E. (India), vol. 48, Part EL2, Dec. 1967, pp. 189-204.

41. L. Jackson, J.B. Patrickson and L.M. Wedepohl, 'Distance Protection: Optimum Dynamic Design of Static Relay Comparators', Proc. IEE, vol. 115, Feb. 1968, pp. 280-287.

42. P.G. Mc Laren, 'Static Sampling Distance Relays', Proc. IEE, vol. 115, March 1968, pp. 418-424.

43. S.D.T. Robertson and W. Norman Meikle, 'Solid-State, High-Speed Phase Comparison Relay Based on Zero Crossings: I-Theory', IEEE Transactions on Power Apparatus and Systems, vol. PAS-87, March 1968, pp. 764-770.

44. W. Norman Meikle and S.D.T. Robertson, 'Solid-State, High-Speed Phase Comparison Relay Based on Zero Crossings: II-Design', IEEE Transactions on Power Apparatus and Systems, vol. PAS-87, March 1968, pp. 770-775.

45. A. Vitanov, 'Quadrilateral - Characteristic Transistor Distance Protection', CIGRE, Paris, 1968, Paper No. 31-03.

46. M. Ramamoorty and N.S. Wani, 'Static Distance Relay with Quadrilateral Characteristic', Presented at the IEEE Summer Power Meeting, 1970, Paper No. 70C571.

47. N.M. Anil Kumar, 'Composite Instantaneous Comparators', Proc. IEE, vol. 117, Jan. 1970, pp. 147-156.

48. H.P. Khincha, K. Parthasarathy and B.S. Ashok Kumar, 'Developments in Amplitude-Comparator Techniques for Distance Relays', Proc. IEE, vol. 117, June 1970, pp. 1118-1124.

49. H.P. Khincha, K. Parthasarathy, B.S. Ashok Kumar and C.G. Arun, 'New Possibilities in Amplitude - and Phase-Comparison Techniques for Distance Relays', Proc. IEE, vol. 117, Nov. 1970, pp. 2133-2141.

50. N.M. Anil Kumar, 'New Approach to Distance Relays with Quadrilateral Polar Characteristic for EHV Line Protection', Proc. IEE, vol. 117, Oct. 1970, pp. 1986-1992.

51. A.T. Johns, 'Generalised Phase Comparator Techniques for Distance Protection-Basis of their Operation and Design', Proc. IEE, vol. 119, July 1972, pp. 833-841.

52. A.T. Johns, 'Generalised Phase Comparator Techniques for Distance Protection-Theory and Operation of Multi-Input Devices', Proc. IEE, vol. 119, Nov. 1972, pp. 1595-1603.

53. A.T. Johns, 'Variable-Characteristic Generalised Techniques for Distance Protection: Theory and Initial Performance Studies', Proc. IEE, vol. 120, Aug. 1973, pp. 891-898.

54. A.T. Johns, 'Variable-Characteristic Generalised Techniques for Distance Protection: Double-Circuit Application Studies', Proc. IEE, vol. 121, Dec. 1974, pp. 1582-1584.

55. A.T. Johns, 'New Discriminative Distance - Protective Relays for Selective-Pole Autoreclosure Applications', Proc. IEE, vol. 126, Feb. 1979, pp. 159-161.

56. L. Jackson, 'Distance-Protection Comparator with Signal Dependent Phase-Angle Criterion', Proc. IEE, vol. 121, Aug. 1974, pp. 817-825.

57. Y.G. Paithankar and V.T. Ingole, 'New Techniques in Multi-Input Amplitude Comparators to Generate Quadrilateral Distance Relay', J.I.E. (India), vol. 54, Part EL3, Feb. 1974, pp. 79-85.

58. M. Ramamoorty and S.N. Lall, 'A Versatile Phase Comparator Relay Using Digital Circuits', J.I.E.(India), vol. 59, Part EL6, June 1979, pp. 309-314.

59. K. Parthasarathy, H.P. Khincha and B.L. Mathur, 'An Adaptive Distance Relay for the Protection of Transmission Lines', Conference Papers, vol.1, Conference on Power System Protection, Madras (India), April 16-19, 1980, Paper No.A3.

60. M. Ramamoorty and S.N. Lall, 'Digital Multi-Input Phase Comparator', Conference Papers, vol.1, Conference on Power System Protection, Madras (India), April 16-19, 1980, Paper No. A5.

61. M. Ramamoorty, M.N. Gandhi, R.J. Phansalkar and P.J. Durkal, 'Static Distance Relay with Conic Characteristics', Conference Papers, vol.1, Conference on Power System Protection, Madras (India), April 16-19, 1980, Paper No.A7.

62. Y.G. Paithankar and A.S. Thoke, 'Variable Characteristic Earth-Fault Quadrilateral Distance Relay Suitable for Double-End-Infeed Lines: A New Technique', Conference Papers, vol.1, Conference on Power System Protection, Madras (India), April 16-19, 1980, Paper No. A6.

63. G.C. Weller, A. Newbould and R.B. Miller, 'New Principles for Distance Protective Relays', Second International Conference on Developments in Power System Protection, London, June 10-12, 1980, Conference Publication No. 185, IEE, 1980, pp. 284-288.

64. A.J. Kellogg, L.P. Singh and G.K. Dubey, 'General Purpose Static Relay Using Digital Techniques', J.I.E.(India), vol. 63, Part EL2, August 1982, pp. 5-11.

65. J.L. Bräten and H. Hoël, 'A New High-Speed Distance Relay', CIGRE, Paris, vol.67, 1950, Paper No.307.

66. C. Ryder, J. Rushton and F.M. Pearce, 'A Moving-Coil Relay Applied to Modern High-Speed Protective Systems', Proc. IEE, vol.100, Part II, Feb. 1951, pp. 47-66.

67. G.G. Gimoyan, 'A Practical Method for Designing Relays with Rectifiers', Electric Technology, vol.3, 1958, pp. 196-203.

68. W.D. Humpage, K.P. Wong, M.H. Al-Dabbagh and E.S. Mukhtar, 'Dynamic Simulation of High-Speed Protection', Proc. IEE, vol. 121, June 1974, pp. 474-480.

69. G.C. Kothari, K. Parthasarathy, B.S. Ashok Kumar and H.P. Khincha, 'Digital Transient Analysis of Power System and Transducers for Relay Analysis', Presented at the IEEE Summer Meeting and EHV/UHV Conference, Vancouver,Canada, July 15-20, 1973, Paper No. C73-349-8.

70. G.C. Kothari, K. Parthasarathy, B.S. Ashok Kumar and H.P. Khincha, 'Computer-Aided Analysis of High-Speed Protective Relays', Proc. IEE, vol. 121, July 1974, pp. 687-694.

71. M. Vitins, 'A Correlation Method for Transmission Line Protection', IEEE Transactions on Power Apparatus and Systems, vol. PAS-97, Sept./Oct. 1978, pp. 1607-1616.

72. M.T. Yee and J. Esztergalyos, 'Ultra High Speed Relay for EHV/UHV Transmission Lines - Installation - Staged Fault Tests and Operational Experience', IEEE Transactions on Power Apparatus and Systems, vol. PAS-97, Sept./Oct. 1978, pp. 1814-1825.

73. M. Chamia and S. Liberman, 'Ultra High Speed Relay for EHV/UHV Transmission Lines - Development, Design and Application', IEEE Transactions on Power Apparatus and Systems, vol. PAS-97, Nov./Dec. 1978, pp. 2104-2116.

74. J. Esztergalyos, M.T. Yee, M. Chamia and S. Liberman, 'The Development and Operation of an Ultra High Speed Relaying System for EHV Transmission Lines', CIGRE, Paris, 1978, Paper No. 34-04.

75. L. Matele, 'Development, Design, Application and Field Experience of an Ultra High Speed Relaying System for EHV/UHV Transmission Lines', Conference Papers, vol.1, Conference on Power System Protection, Madras (India), April 16-19, 1980, Paper No.B3.

76. R.P. Carter, 'UHS Relay for EHV/UHV Lines Based on Directional Wave Detection Principles', Second International Conference on Developments in Power System Protection, London, June 10-12, 1980, Conference Publication No. 185, IEE, 1980, pp. 166-170.

77. A.T. Johns, 'New Ultra-High-Speed Directional Comparison Technique for the Protection of E.H.V. Transmission Lines', Proc. IEE, vol. 127, Part C, July 1980, pp. 228-239.

78. A.T. Johns and R.K. Aggarwal, 'New Ultra-High-Speed Directional Blocking Scheme for Transmission Line Protection', Second International Conference on Developments in Power System Protection, London, June 10-12, 1980, Conference Publication No. 185, IEE, 1980, pp. 141-145.

79. H.W. Dommel and J.M. Michels, 'High Speed Relaying Using Travelling Wave Transient Analysis', Presented at the IEEE PES Winter Meeting, Jan. 1978, IEEE Publication No. 78CH1295-PWR, Paper No. A78, pp 214-219.

80. T. Takagi, J. Baba, U. Katsuhiko and T. Sakaguchi, 'Fault Protection Based on Travelling Wave Theory - Part I Theory', Presented at the IEEE PES Summer Meeting, 1977, Paper No. A77-750-3.

81. T. Takagi, J. Baba, U. Katsuhiko and T. Sakaguchi, 'Fault Protection Based on Travelling Wave Theory - Part II Sensitivity Analysis and Laboratory Tests', Presented at the IEEE PES Winter Meeting, 1978, Paper No. A78-220-6.

82. Y. Akimoto, T. Yamamoto, H. Hosawaka, T. Sakaguchi, T. Yoshida and S. Nishida, 'Fault Protection Based on Travelling Wave Theory (Part I - Theory)', Electrical Engineering in Japan, vol. 98, Jan./Feb. 1978, pp 79-86.

83. Y. Akimoto, T. Yamamoto, H. Hosawaka, T. Sakaguchi, T. Yoshida and S. Nishida, 'Fault Protection Based on Travelling Wave Theory (Part II - Feasibility Study), Electrical Engineering in Japan, July/Aug. 1978, pp. 113-120.

84. M. Ramamoorty and K.N. Verma, 'A Rigorous Method for Fault Current Evaluation - Application to Relaying', Proceedings of the Symposium on EHV Engineering, Testing Equipments and Techniques, University of Roorkee, vol. I, Sept. 1980, pp 4-21 to 4-33.

85. M. Vitins, 'A Fundamental Concept for High Speed Relaying', IEEE Transactions on Power Apparatus and Systems, vol. PAS-100, Jan. 1981, pp 163-173.

86. G.D. Rockefeller, 'Fault Protection with a Digital Computer', IEEE Transactions on Power Apparatus and Systems, vol. PAS-88, April 1969, pp 438-464.

87. G.R. Slemon, S.D.T. Robertson and M. Ramamoorty, 'High Speed Protection of Power Systems Based on Improved System Models', CIGRE, Paris, 1969, Paper No. 31-09.

88. M. Ramamoorty, 'A Note on Impedance Measurement Using Digital Computers', IEE-IERE Proc. (India), vol. 9, Nov./Dec. 1971, pp 243-247.

89. B.J. Mann and I.F. Morrison, 'Digital Calculation of Impedance for Transmission Line Protection', IEEE Transactions on Power Apparatus and Systems, vol. PAS-90, Jan./Feb. 1971, pp 270-279.

90. B.J. Mann and I.F. Morrison, 'Relaying a Three-Phase Transmission Line with a Digital Computer', IEEE Transactions on Power Apparatus and Systems, vol. PAS-90, March/April 1971, pp 742-750.

91. G.B. Gilcrest, G.D. Rockefeller and E.A. Udren, 'High-Speed Distance Relaying Using a Digital Computer Part I - System Description', IEEE Transactions on Power Apparatus and Systems, vol. PAS-91, May/June 1972, pp 1235-1242.

92. J.G. Gilbert and R.J. Shovlin, 'High Speed Transmission Line Fault Impedance Calculation Using a Dedicated Minicomputer', IEEE Transactions on Power Apparatus and Systems, vol. PAS-94, May/June 1975, pp 872-883.

93. J. Carr and R.V. Jackson, 'Frequency Domain Analysis Applied to Digital Transmission Line Protection', IEEE Transactions on Power Apparatus and Systems, vol.PAS-94, July/Aug. 1975, pp 1157-1166.

94. G.S. Hope and V.S. Umamaheswaran, 'Sampling for Computer Protection of Transmission Lines', IEEE Transactions on Power Apparatus and Systems, vol. PAS-93, Sept./Oct. 1974, pp 1522-1534.

95. G.S. Hope, O.P. Malik and M.E. Rasmy, 'Digital Transmission Line Protection in Real Time', Proc. IEE, vol. 123, December 1976, pp 1349-1354.

96. G. Thirupathaiah, A. Varshney and L.P. Singh, 'On-Line Digital Protection Using a Microcomputer- A Decentralized Approach', Technical Proceedings, National Conference on Planning, Operation and Control of Large Scale Power Systems, Annamalai University, India, June 24-25, 1982, Paper No. S5.3.

97. A.G. Phadke, T. Hlibka and M. Ibrahim, 'A Digital Computer System for EHV Substations: Analysis and Field Tests', IEEE Transactions on Power Apparatus and Systems, vol. PAS-95, Jan./Feb. 1976, pp 291-301.

98. A.G. Phadke, M. Ibrahim and T. Hlibka, 'Fundamental Basis for Distance Relaying with Symmetrical Components', IEEE Transactions on Power Apparatus and Systems, vol. PAS-96, March/April 1977, pp 635-646.

99. A. Wiszniewski, 'How to Reduce Errors of Distance Fault Locating Algorithms', IEEE Transactions on Power Apparatus and Systems, vol. PAS-100, Dec. 1981, pp 4815-4820.

100. J.W. Horton, 'Walsh Functions for Digital Impedance Relaying for Power Lines', IBM Journal of Research and Development, No.10, 1976, pp 530-541.

101. A.D. Mc Innes and I.F. Morrison, 'Real Time Calculation of Resistance and Reactance for Transmission Line Protection by Digital Computer', E.E. Transactions, Institution of Engineers, Australia, EE7, No.1, 1971, pp 16-23.

102. R. Poncelet, 'The Use of Digital Computers for Network Protection', CIGRE, Paris, 1972, Paper No. 32-08.

103. P. Bornard and J.C. Bastide, 'A Prototype of Multi-processor Based Distance Relay', IEEE Transactions on Power Apparatus and Systems, vol. PAS-101, Feb. 1982, pp 491-498.

104. W.J. Smolinski, 'An algorithm for Digital Impedance Calculation Using a Single Pi Section Transmission Line', IEEE Transactions on Power Apparatus and Systems, vol. PAS-98, Sept./Oct. 1979, pp 1546-1551.

105. A.M. Ranjbar and B.J. Cory, 'An Improved Method for the Digital Protection of Transmission Lines', IEEE Transactions on Power Apparatus and Systems, vol. PAS-94, March/April 1975, pp 544-550.

106. T. Sakaguchi and K. Uemura, 'A New Directional Protection Based on Laplace Transformation with Special Reference to Computer Relaying', Second International Conference on Developments in Power System Protection, London, June 10-12, 1980, Conference Publication No. 185, IEE, London, 1980, pp 146-150.

107. M.S. Sachdev and M.A. Baribeau, 'A New Algorithm for Digital Impedance Relay', IEEE Transactions on Power Apparatus and Systems, vol. PAS-98, May/June 1979, pp 2232-2240.

108. R.G. Luckett, P.J. Munday and B.E. Murray, 'A Substation Based Computer for Control and Protection', Conference on Modern Developments in Protection, IEE, London, 1975, Publication No. 125, pp. 252-260.

109. A.W. Brooks, Jr., 'Distance Relaying Using Least-Squares Estimates of Voltage, Current and Impedance', Proceedings of the PICA Conference, IEEE Publication No. 77CH 1131-2 PWR, May 1977, pp 394-402.

110. A.T. Johns and M.A. Martin, 'Fundamental Digital Approach to the Distance Protection of E.H.V. Transmission Lines', Proc. IEE, vol. 125, May 1978, pp 377-384.

111. A.A. Girgis and R.G. Brown, 'Application of Kalman Filtering in Computer Relaying', IEEE Transactions on Power Apparatus and Systems, vol. PAS-100, July 1981, pp 3387-3395.

112. A.A. Girgis, 'A New Kalman Filtering Based Digital Distance Relay', IEEE Transactions on Power Apparatus and Systems, vol. PAS-101, Sept. 1982, pp 3471-3480.

113. J.V.H. Sanderson and A. Wright, 'Protective Scheme for Series-Compensated Transmission Lines', Proc. IEE, vol. 121, Nov. 1974, pp 1377-1384.

114. T. Takagi and Y. Yamakosi, 'Digital Differential Relaying System for Transmission Line Primary Protection Using Travelling Wave Theory - Its Theory and Field Experience', Presented at the IEEE PES Winter Meeting, 1979, Paper No. A79-096-9.

115. W.D. Humpage, K.P. Wong, T.T. Nguyen and D. Sutanto, 'Z-Transform Electromagnetic Transient Analysis in Power Systems', Proc. IEE, Part C, vol. 127, June 1980, pp 370-378.

116. J.P. Bickford, N. Mullineux and J.R. Reed, 'Computation of Power System Transients', IEE Monograph, No.18, Peter Peregrinus Limited, England, 1980.

117. R. Ch. G. Bergmann and P.J.M. Ponsioen, 'Calculation of Electrical Transients in Power Systems: Untransposed Transmission Line with Frequency-Dependent Parameters', Proc. IEE, vol. 126, August 1979, pp 764-770.

118. H. Karrenbauer, 'Ausbreitung von Wanderwellen bei Verschiedenen Anordnungen von Freileitungen bei Abstandskurzschlüssen', Doctoral Dissertation, Munich, 1967.

119. J.G. Gilbert, E.A. Udren and H. Sackin, 'The Development and Selection of Algorithms for Relaying of Transmission Lines by Digital Computers', Power System Control and Protection, Academic Press, New York, 1978, Edited by B.D. Russel and M.E. Council, pp 83-127.

120. John M. McCormick and Mario G. Salvadori, 'Numerical Methods in Fortran', Prentice-Hall of India Private Limited, New Delhi, 1979.

121. J.W. Cooley and J. Tukey, 'An Algorithm for the Machine Calculation of Complex Fourier Series', Mathematics of Computation, vol. 19, 1965, pp 297-301.

122. J.W. Cooley, P.A.W. Lewis and P.D. Welch, 'The Fast Fourier Transform and its Applications', IEEE Transactions on Education, vol. E-12, March 1969, pp 27-34.

123. A. Ametani, 'The Application of the Fast Fourier Transform to Electrical Transient Phenomena', International Journal of Electrical Engineering Education, No.10, 1972, pp 277-287.

CURRICULUM VITAE

1. Candidate's name   : KANDALA VEDANTA DESIKACHAR

2. Academic background :

Degree	Specialization	University	Year
B.E.	Electrical Engineering	Sri Venkateswara	1960
M.E.E.	Electrical Power Systems	Jadavpur	1966

3. Publications

   A. Not pertaining to the thesis

      1. 'Determination of Optimum Value of the Series Compensation of a Transmission Line and its Experimental Verification', (with Dr. G.P. Purakayastha), J.I.E. (India), vol. 47, Pt. EL4, April 1967.

   B. Pertaining to the thesis

      1. 'Protection of EHV/UHV Transmission Lines using Travelling Wave Phenomena', (with Dr. L.P. Singh). Paper presented at the National Power Systems Conference, Hyderabad, India, December 1981.

      2. 'New Relay Scheme for EHV/UHV Transmission Lines', (with Dr. L.P. Singh and Y. Asthana), J.I.E. (India), vol. 63, Pt. EL3, December 1982.

      3. 'Fault Analysis of Multinode Power Systems for Designing Ultra High Speed Protective Relays along with a Proposed Relaying Scheme', (with Dr. L.P. Singh), Electric Power Systems Research, vol.6, No.1, Mar-May, 1983, pp 13-26.